CRANFIELD UNIVERSITY

TOMAS BAUDIN LASTRA

Performance Based Diagnostics of a Twin Shaft Aeroderivative Gas Turbine: Water Wash Scheduling

SCHOOL OF ENGINEERING

MSc by Research
Academic Year: 2015

Supervisor: Dr. Panagiotis Laskaridis
Pr. Riti Singh

May 2015

CRANFIELD UNIVERSITY

SCHOOL OF ENGINEERING
MSc by Research

MSc by Research

Academic Year 2015

TOMAS BAUDIN LASTRA

Performance Based Diagnostics of a Twin Shaft Aeroderivative Gas Turbine: Water Wash Scheduling

Supervisor: Dr. Panagiotis Laskaridis
Pr. Riti Singh
May 2015

ABSTRACT

Aeroderivative gas turbines are used all over the world for different applications as Combined Heat and Power (CHP), Oil and Gas, ship propulsion and others. They combine flexibility with high efficiencies, low weight and small footprint, making them attractive where power density is paramount as off shore Oil and Gas or ship propulsion. In Western Europe they are widely used in CHP small and medium applications thanks to their maintainability and efficiency. Reliability, Availability and Performance are key parameters when considering plant operation and maintenance. The accurate diagnose of Performance is fundamental for the plant economics and maintenance planning. There has been a lot of work around units like the LM2500®, a gas generator with an aerodynamically coupled gas turbine, but nothing has been found by the author for the LM6000®.

Water wash, both on line or off line, is an important maintenance practice impacting Reliability, Availability and Performance. This Thesis aims to select and apply a suitable diagnostic technique to help establishing the schedule for off line water wash on a specific model of this engine type. After a revision of Diagnostic Methods Artificial Neural Network (ANN) has been chosen as diagnostic tool.

There was no WebEngine model available of the unit under study so the first step of setting the tool has been creating it. The last step has been testing of ANN as a suitable diagnostic tool. Several have been configured, trained and tested and one has been chosen based on its slightly better response. Finally, conclusions are discussed and recommendations for further work laid out.

Keywords:

Aeroderivative, Water Wash, Artificial Neural Network, Performance Diagnostic, Maintenance, LM6000

ACKNOWLEDGEMENTS

I would like first to express thanks to my wife Marisa and my children Tomas and Daniela. Without their support and patience, I would have never been able to complete this Thesis. I owe them many weekends and mountain trips. Also to my mother always there to help when times were difficult.

I have special gratitude to my supervisor Dr. Panagiotis Laskaridis. His patience and guidance have kept me in the right path towards finalizing this challenge. To Pr. Riti Singh whose comments during yearly reviews always put things under the right light.

I would also like to thanks Asteris Apostolidis and Suresh Sampath for their work on the WebEngine.

All my gratitude to my company General Electric Distributed Power, that supported financially and morally this research. Amongst many inside it I would like to highlight my former manager Mr. Douglas Junner who encouraged me to start this project; my current manager Dr. Michael Foerster who has always supported my efforts to finish. And of course the full Gas Turbine Product Service Engineering team in Europe. They have always been there when needed. It is an honour and a pleasure to work with such a team of great engineers and better persons.

TABLE OF CONTENTS

LIST OF FIGURES

Appendices

LIST OF TABLES

Appendices

LIST OF EQUATIONS

LIST OF ABBREVIATIONS

AANN – Auto-Associative Neural Network

AC – Alternating Current

ANN – Artificial Neural Network

ASME – The American Society of Mechanical Engineers

ASTM – ASTM International (formerly American Society for Testing and Materials)

BS – British Standards

CAPA – Corrective Action and Preventive Action

CBM – Condition Based Maintenance

CERT – Component Exchange Rate Table

CHP – Combined Heat and Power

CP – Specific Heat at Constant Pressure

CPLM – Critical Parts Life Management

CTQ – Critical To Quality

DC – Direct Current

DF – Degradation Factor

DLE – Dry Low Emissions

ECD – Electronic Chip Detectors

EFH – Effective Forced Outage Hours

ERT – Exchange Rate Table

FCM – Fault Coefficient Matrix

FFBP – Feed Forward Back-Propagation Neural Networks

FIGV – Fixed Inlet Guide Vanes

FMEA – Failure Mode and Effects Analysis

FO – Forced Outage

FOD – Foreign Object Damage

GE – General Electric Co.

GPA – Gas Path Analysis

GUI – MALTAB Graphical User Interface

HO – Hours of Operation at reduced value

HPC – High Pressure Compressor

HPT – High Pressure Turbine

HSE – Hot Section Exchange

HSRG – Heat Recovery Steam Generator

ICM – Influence Coefficient Matrix

ISO – International Organization for Standardization

LCF – Low Cycle Fatigue

LGPA – Linear Gas Path Analysis

LHV – Lower Heat Value

LM – Land and Marine

LNG – Liquefied Natural Gas

LP – Low Pressure

LPC – Low Pressure Compressor

LPT – Low Pressure Turbine

LVDT – Linear Variable Differential Transformer

MDM - Measurement Delta Matrix

MIL-PRF – Military Performance Specification

MLFFNN – Multilayer Feedforward Network

MLP – Multilayer Perceptron

MOH – Major Overhaul

MSE – Mean Square Error

NDT – Non Destructive Testing

NLGPA – Non Linear Gas Path Analysis

NOx – Oxides of Nitrogen

OBSM – Observability Matrix

OEM – Original Equipment Manufacturer

PFC – Primary Frequency Control

PM – Planned Maintenance

PR – Pressure Ratio

PT – Period Time

PTC – Performance Test Code

PTMP – Performance-based total productive maintenance

QFD – Quality Function Deployment

RE – Reliability

RBF – Radial Basis Function

RCC – Remote Charge Converter

RCFA – Root Cause Failure Analysis

RGB – Reduction Gearbox

RM&D – Remote Monitoring and Diagnostics

RMS – Root Mean Square

RTD – Resistance Temperature Detector

SAC – Single Annular Combustor

SAI – Semiannual Inspections

SLO – Synthetic Lube Oil

SOAP – Spectrometric Oil Analysis Program

SOM – Self-Organizing Map Network

STIG – Steam Injected Gas Turbine

TBC – Thermal Barrier Coating

TET – Turbine Entry Temperature

VIGV – Variable Inlet Guide Vanes

VOC – Voice of Customer

WF36DMD – Calculated fuel flow

LIST OF SYMBOLS

bar – pressure unit (a absolute, g gauge, d differential)

β – Bias or systematic error

ºC – degrees centigrade

CO – Carbon Monoxide

CO_2 – Carbon Dioxide

cos – cosine

Δ – delta, variation of a the parameter affected (i.e. Δ***z***)

η_i – Efficiency, the subscript relates to the individual component characterized

f – frequency

F – degrees Fahrenheit

FF – Fuel flow

g – acceleration unit

Γ – Flow capacity, the subscript relates to the individual component characterized

HS – Hydrogen Sulphide

H – ICM

H^{-1} – FCM

hr(s) – hour(s)

[I] – identity matrix

ips – inches per second

∞ – infinite

kg – kilograms

kg/kW-hr – kilogram/kilowatt-hours, SFC unit

kW – kilowatts

lm – Levenberg-Marquardt training algorithm

λ – eigenvalue

m – meter(s)

M^{-1} – Inverse of matrix M (for example ERT)

M^{T} – Transpose of matrix M (for example ERT)

mA – milliamperes

mV – millivolts

mV/g – millivolts per g

mV/ips – millivolt per inch per second

mm/s – millimeter per second

MW – Megawatts, used in equivalence to Power

MW_d – Gas turbine output corrected to reference conditions, including a Degradation Factor

MW_a – Maximum acceptance test corrected load or Guarantee Performance Value

MW_c – Corrected power to reference conditions

Na – Sodium

Na_2SO_4 – Sodium Sulfate

NO_x – Nitrogen oxides

O_2 – Oxygen

Ω – Ohms

P0 – Pressure before the FOD screen in the inlet, comparable to LPC inlet pressure

P2 – LPC inlet pressure

P25 – LPC exit pressure

P3 – HPC discharge total pressure

P48 – HPT exit pressure

P8 – LPT exit pressure (equivalent to exhaust pressure)

P_{amb} – Ambient pressure

pC – Pico coulombs

pC/g – Pico coulombs per unit of acceleration

pC/bar – Pico coulombs per bar

pC/psi – Pico coulombs per psi

psi – Pound per Square Inch (a absolute, g gauge, d differential)

PS3 – HPC discharge static pressure

rpm – Revolutions per minute

scg – Scaled Conjugate Gradient training algorithm

SO_2 – Sulphur Dioxide

σ – Population standard deviation

Σ – summatory

S_x – Sample standard deviation

$S_{\bar{X}}$ – Average standard deviation

sin – sine

t -- time

T2 – LPC inlet pressure

T3 – HPC discharge temperature

T48 – HPT exit pressure and LPT inlet temperature

T8 – LPT exit temperature (equivalent to exhaust temperature)

T_{amb} – Ambient Temperature

t_{95}—Student's statistical distribution with a 95% level of confidence

UHC – Unburnt Hydrocarbons

U_{ADD} – Additive Uncertainty

U_{RSS} – Root Sum Square Uncertainty

ω – angular speed

$\boldsymbol{x}$ – engine component health parameters

[X] – measurement vector matrix

XN25 – High pressure shaft speed

$\boldsymbol{z}$ – engine measurable parameters

– number

In ANN

p = the input signal

w = synaptic weight (weight of input signal)

b = neuron bias

n = induced local field or activation potential

$f(n)$ = transfer or activation function

a = neuron output

When highlighted in bold they are considered vectors and matrices (reference Chapter 9)

$\boldsymbol{n_j}$ – weighted sum of all inputs to neuron j

$\boldsymbol{a_j}$ – output of neuron j

$logsig(n_j)$ – Logistic sigmoid transfer function

$tansig(n_j)$ – Tan-sigmoid transfer function

t_i – target outputs

1 INTRODUCTION

1.1 Historical background

The gas turbine concept has been around for a long time. Already in 1791 John Barber patented an engine with all the elements of a gas turbine (compressor, combustion chamber and turbine) for “horseless carriage propulsion” [34].

Figure 1-1: Drawing of first patent for a gas turbine (Barber 1791) [32]

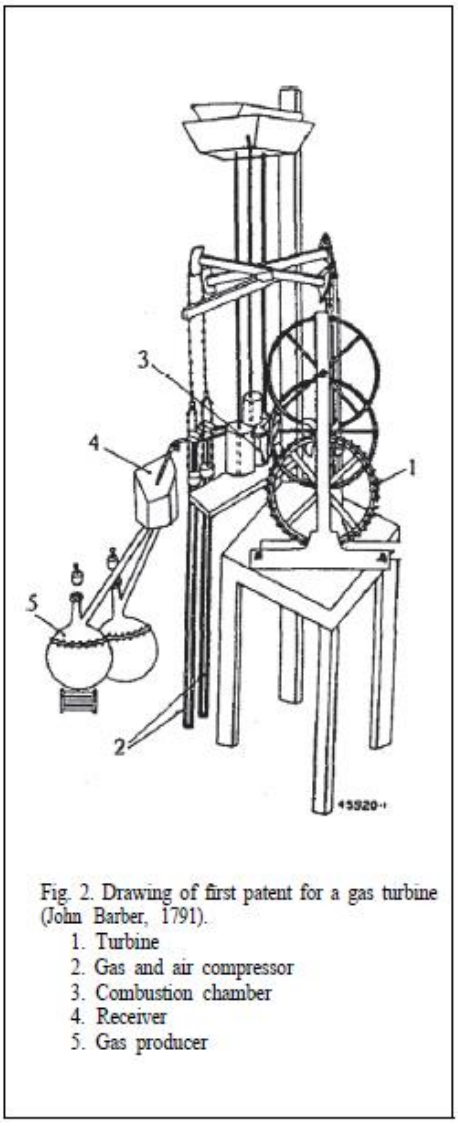

The development of viable gas turbine for aircraft propulsion happened in the Thirties mainly through the works of Sir Frank Whittle and Hans von Ohain.

From the early years the concept was also considered for land based applications as propulsion and electricity generation. The world's first industrial gas turbine set was installed in Neuchatel (Switzerland) by BBC Brown Boveri (Figure 1-2 [32]). Its layout and main figures were:

Figure 1-2: Gas Turbine standby set [32]

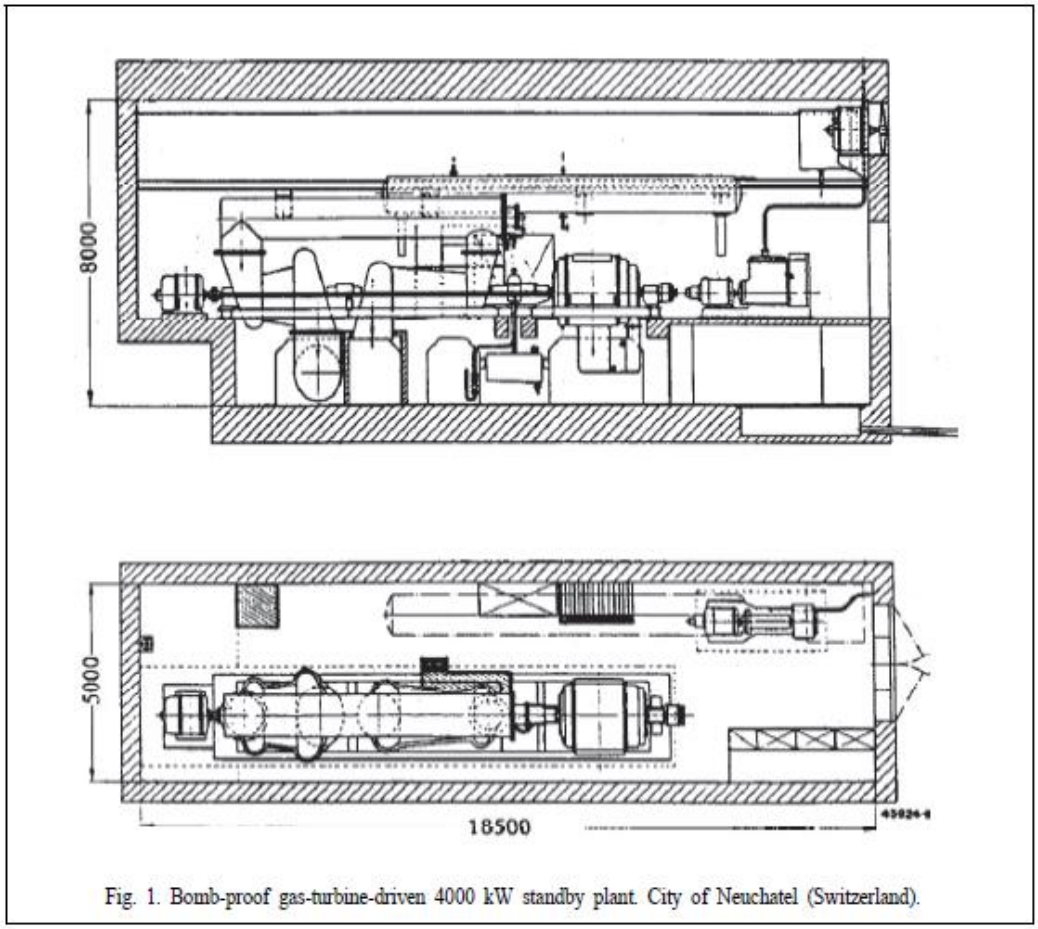

Fig. 1. Bomb-proof gas-turbine-driven 4000 kW standby plant. City of Neuchatel (Switzerland).

Power output: 4 MW

Rotating speed: 3000 rpm

Cycle efficiency: 17.4%

TET: 550ºC

PR: 4.2:1

The plant operated for 63 years (1038 to 2002) and was decommissioned due to generator damage.

After the war development of gas turbine for aircraft propulsion and industrial applications went in parallel. Reference [35] is an interesting historical summary of all applications but aircraft propulsion.

1.2 Aeroderivative Industrial Gas Turbines

Aeroderivatives are non-flying gas turbines derived from aircraft engine gas turbines. Usually they are described as stationary, but certain applications as ship or train propulsion are not truly stationary. They are used in several applications as

- Power generation
    - Cycle
        - Simple cycle
        - Combined cycle
        - Cogeneration

Figure 1-3 Aeroderivative gas turbine unit in Cogeneration application

(Courtesy of GE Distributed Power® https://www.ge-distributedpower.com/news-media/download-center)

- Location
  - Off shore
  - On shore
  - Mobile applications

Figure 1-4: Multi-unit TM2500+® Mobile application in Algeria

(Courtesy of GE Distributed Power® https://www.ge-distributedpower.com/news-media/download-center)

- Operating mode
  - Peaker
  - Mid merit
  - Base load
  - Balance of renewable energy power plants
  - Grid stability support

- Mechanical drive
  - Off shore
  - On shore

Figure 1-5: Triton FPSO with two Aeroderivative units

(Courtesy Dana Petroleum® http://www.dana-petroleum.com/Media-centre/Download-library/)

An offshore application where the small footprint is highlighted

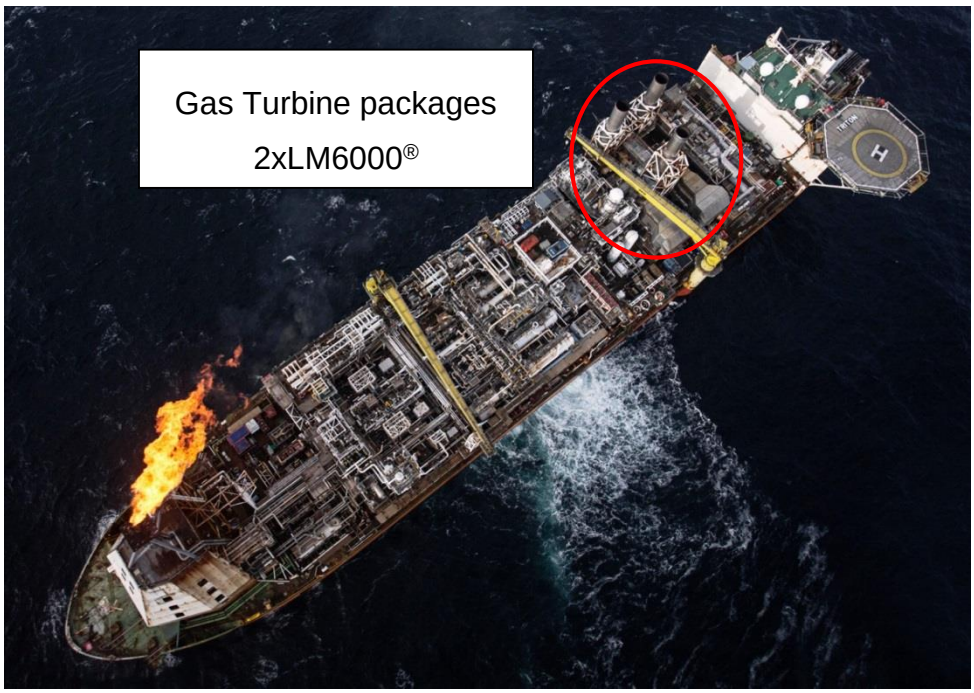

- Naval propulsion

Figure 1-6: Rolls Royce MT30® Aeroderivative for marine propulsion

(Courtesy Rolls Royce® http://www.rolls-royce.com/customers/marine/about-marine/products.aspx)

- Train propulsion, as the United Aircraft Corporation, which used a variant of the Pratt& Whitney PT6 called ST6 for propulsion. This train was used in USA and Canada.

Figure 1-7: Turbo Train

("Ann Arbor AMTK Sep 1971 5-3" by Lawrence and David Barera - Flickr: Ann Arbor AMTK Sep 1971 5-3. Licensed under CC BY-SA 2.0 via Wikimedia Commons)

The first land based power generation application was a Pratt and Whitney FT3. Since then many other aircraft engines from several manufacturers have been modified for stationary applications. Some examples are

- Rolls Royce (Olympus®, Avon®, Trent, RB211®)
- General Electric (LM1500® (J79), LM1600® (F404), LM2500® base and plus (TF39/CF6-6)), LM6000® (CF6C2/E1), LMS100® (CF6E1))
- Pratt & Whitney (FT3® (JT3), FT4® (JT4), FT8® (JT8), ST40® (PW150)

The advantages of an Aeroderivative gas turbine in such applications are:

- Flexibility:
    - Fast start capability (from cold to full power in 5 min).

    - High ramp up rate (over 50 MW/min).
    - Multiple daily starts with no maintenance penalty.
- Higher thermal efficiency both in full and partial load (i.e. LMS100® 44% @ 100% load, 36% @50% load, simple cycle).
- Excellent starting torque capacity.
- High power to weight ratio that leads to small footprint and light weight.
- Maintainability:
    - Modular maintenance, where main engine modules can be replaced on site.
    - Full engine replacement in 24 to 48 hours.
    - On condition maintenance inherited from aircraft engines, flexible maintenance with easy accessibility to replaceable units (pumps, starter).
- Wide range of fuels (Natural gas, flare gas, synthetic gas, diesel, naphtha, biodiesel, ethanol, etc…) with minimal modifications.
- High Reliability and Availability.
- Several options of emissions control configuration and level within the same product line (steam, water, Dry Low Emissions).

Some disadvantages are

- The materials required for the high pressure ratios and TET add to the base cost
- In some applications the low inertia is a disadvantage
- Heavy fuels cannot be used
- Maximum power output is limited and related to aircraft engine industry requirements

1.3 Thesis Aim and Objectives

The Project aim is the selection and application of a Gas Turbine Performance Diagnostic Technique for a Twin Shaft Aeroderivative Gas Turbine in order to determine the need of Off-Line Water wash. The project objectives are:

- Develop a computer model of the referenced gas turbine using WebEngine.

- Test the gas turbine model in on off design condition.
- Determine the optimized instrument package for diagnostic.
- Determine the most suitable diagnostic method to support off line water wash decision of the unit, both from user and OEM perspective.
- Build, validate and test such a tool using model data.
- Study the interconnection of the tool with a Remote Monitoring and Diagnostic system to provide a quick analysis tool for remote engineers.

The novelty of this thesis is first in the engine model used. Throughout the literature research the author has not found any public reference to similar work done on this type of gas turbine. The thesis project uses existing technologies to develop the basis for a tool with a practical approach towards water wash a common issue always highlighted by customers, when to water wash. Further development is needed, but the foundations are laid off.

1.4 Thesis Methodology

Figure 1-8 is a block diagram of the Thesis Methodology

Review of Maintenance philosophies

The initial chapters deal with a review of Maintenance philosophies, water wash and typical Aeroderivative instrumentation.

Review of performance diagnostics tools

A preliminary review of diagnostics tool has been done to determine the most suitable tool (Chapter 4).

Selection of Gas Turbine model

The first step is determining what type of unit will be used for this project. The LM6000® has been selected. The unit comes in many different configurations with varying degrees of complexity when it comes to modelling them (Chapter 5). The author's opinion is the most reasonable approach is to start with the simplest

configuration possible. The simplest version is a natural gas fuelled SAC unit with FIGV and no emissions control. Due to WebEngine capabilities the fuel will be liquid.

Gas Turbine WebEngine model

A model of the LM6000® gas turbine has been built using Cranfield's available tools via WebEngine. The model has been built based on public data. PhD student Asteris Apostolidis has helped building this model from data provided by the author.

Figure 1-8: Thesis Methodology block diagram

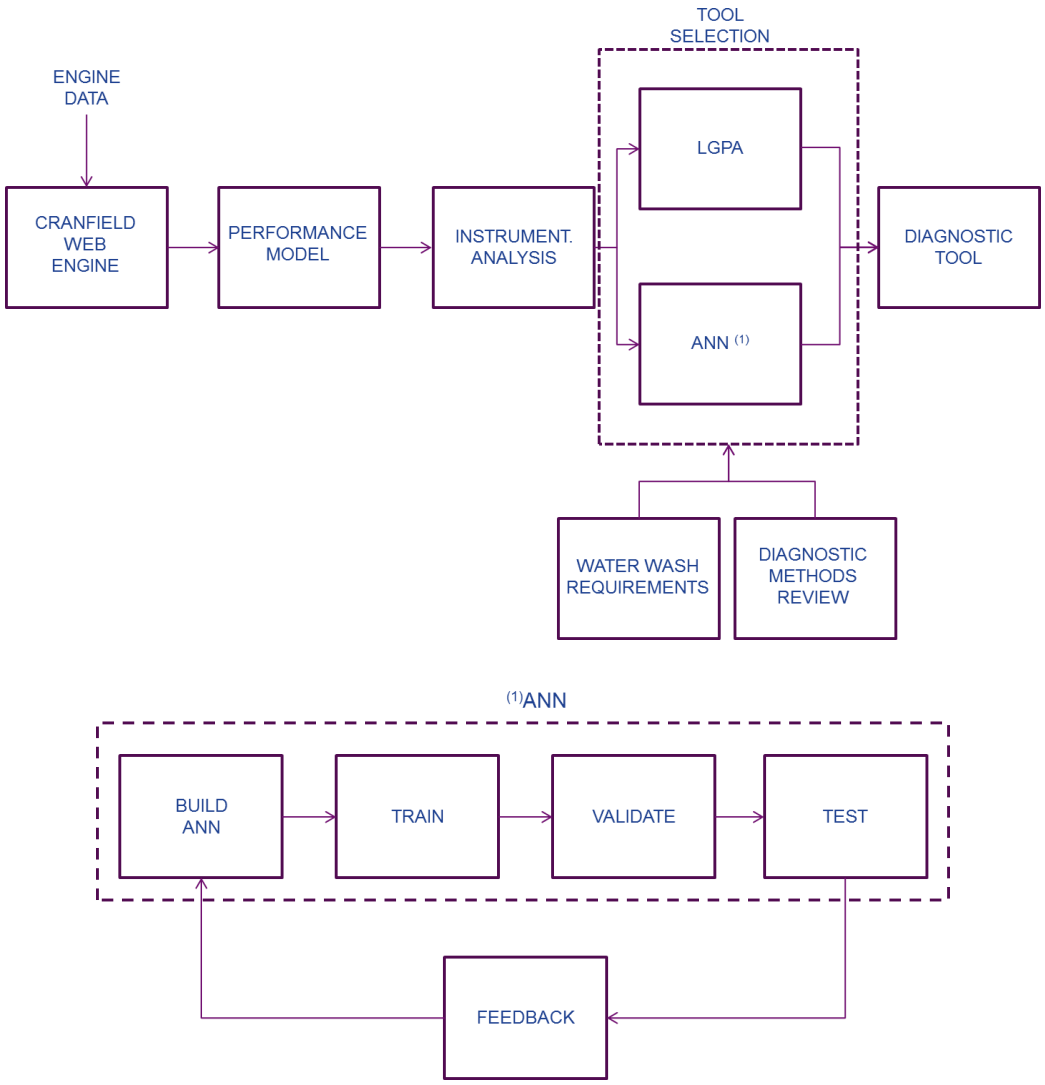

Gas Turbine Instrumentation analysis

Using the above referenced model a standard approach has been used to optimize of the unit's gas path measurement suite for diagnostic purposes (Chapter 7).

Creation and use of performance diagnostics tool

The purpose of the diagnostics tool is to identify a faulty component. As the subject is off line water wash the two degraded components considered have been considered LPC and HPC based on author's experience. An ANN tool has been created, validated and tested with model data, by implanting known degradation to gas turbine components and using the model's resulting output to train the tool. It is compared with LGPA results, obtained previously during the instrumentation optimization exercise.

Testing of the tool with real engine data

The intention was to use of real engine data to test the tool. Real engine data has not been available. The next steps are discussed in the final chapter.

1.5 Thesis Structure

The Thesis chapters will be:

1.- Introduction

This chapter contains a brief historical background, description of Aeroderivative Gas Turbines, as well as the Thesis aims and objective, methodology and structure.

2.- Gas Turbine Maintenance

Gas Turbine maintenance techniques and philosophies are reviewed in this chapter. The cost of doing maintenance is reviewed. Within the review of maintenance water wash is singularized, describing types, implications and a practical case of interest.

3.- Instrumentation and Measurement uncertainty

The typical instrumentation used in an Aeroderivative unit is summarized. The subject of Measurement Uncertainty and its consequences is also explored in this chapter.

4.- Gas Turbine Diagnostic Methods

The requirement for maintenance emphasizes the need for gas turbine diagnostics. A review of Gas Turbine Diagnostic methods with the relative merits of each one is done. The chapter includes a conclusion describing why ANN has been selected as the tool for this thesis.

5.- Gas Turbine WebEngine Model

The LM6000® details, models and ratings are discussed. The WebEngine model is introduced and both design and off design results reviewed.

6.- Degraded Performance

The causes for Gas Turbine performance degradation are discussed. The chapter finalizes with the simulation and analysis of degraded gas turbine performance in WebEngine model.

7.- Optimal measurement selection

A standard analysis technique is applied with the aim to define the optimal instrumentation suite for Diagnostics on this type of engine.

8.- Linear Gas Path Analysis Application

LGPA is used and analysed as a possible method of to determine the need for water wash.

9.- ANN tool

Neural networks are reviewed in further detail. An ANN tool is built, trained and verified in MATLAB. Its performance and comparison to LGPA are explored.

10.- Conclusions and recommendations

The Chapter will present the main conclusions from the Thesis, and future steps to create a useful tool.

2 GAS TURBINE MAINTENANCE

2.1 Introduction

Paraphrasing [33] “Maintenance describes the work required during the plant’s service life to ensure it operates safely, reliably and cost effectively”. The three concepts, Safety, Reliability (and Availability) and Cost Effectiveness are paramount to the life and economic viability of a plant.

There can be no compromise with Safety. Failure to address a potential Safety issue may end up in plant closure and legal implications. Life cycle costs are a primary factor on the design and operation of gas turbine based plants [4]. If a plant is not available when required or not reliable enough, it may be missing huge revenue opportunities in the current market set up, where being available when required is paid heftily. Maintenance needs a Cost Effective way approach if it does not want to be a burden to the economic results of a plant.

The substitution of the word engine by plant is not arbitrary. This chapter and document will concentrate on the Gas Turbine, but when considering overall plant maintenance all items need to be addressed. A lot of emphasis is made on the maintenance of the Gas Turbine, often leaving aside other major elements as the Generator or Reduction Gearbox. Improper maintenance of those items can lead to outage times far in excess those created by the Gas Turbine. A typical lead time for a new RGB wheel or pinion is well over three months, unless the manufacturer happens to have it in stock. A Generator rotor lead time is over six months, and so on. The author has seen this happening more than once in his professional career. Long gone are the days were manufacturers or operators kept such high capital cost items in stock. Only in the Oil and Gas industry, where the cost of an extended outage is enormous, are sometimes stocks of high cost long lead spare parts considered.

This chapter will review the basics of Reliability, Availability and Maintainability. Deeper description of these concepts can be found in [46] and the bibliography there listed. The next step is an historical review of Maintenance needs and

associated philosophies. The maintenance peculiarities of Aeroderivative Gas Turbines will be described paying special attention to water wash.

2.2 Availability and Reliability

2.2.1 Availability

“Availability of a gas turbine is the percent of time the gas turbine is available to generate power in any given period at its acceptance load” ([43]). It does include Planned Maintenance (PM) hours and Forced Outage (FO) hours.

If we compare this definition with the more standard one ([12]) “Probability of being available, independent of whether the unit is needed”, Boyce’s definition introduces the concept of acceptance load. “The Acceptance Load would be the net electric power generating capacity of the gas turbine at design or reference conditions established as a result of the Performance Tests conducted for acceptance of the plant” ([43]). The Acceptance Load can be calculated by correcting the power to the reference conditions. It highlights something that in the author’s experience is becoming more and more important. It is not enough to be available to generate power, but also to do at it the required level.

Eventually the Acceptance Load value does not necessarily need to be the result of plant acceptance Performance Tests as described in [43]. The author has seen this defined by Guarantee Performance Value when in contract negotiations between Operator and Service Provider.

The revenues of an Operator are greatly affected by the gas turbine output, not only because the amount of electricity sold, but also due to the potential agreements with Utilities. For example, in certain markets the Operator declares to the Utility its power producing capability based on ambient conditions, unit condition, etc… The unit is then set at part load, and the Utility takes remote control of the power setting. The Power Reserve, that is, the difference between current power setting and maximum load capability, is considered by the Utility as an emergency reserve. The unit’s output can be increased by the Utility to its maximum if needed. This type of operation is paid handsomely to the operator. Similar is the Primary Frequency Control (PFC), where the Utility uses the unit’s

excess power producing capability to stabilize grid frequency if required. Once again the Operator gets substantial additional revenues thanks to this operating scheme.

Boyce [43] introduces the concept of EFH (Effective Forced Outage Hours), defined as:

$$EFH = HO\ \frac{(MW_a - MW_d)}{MW_a}$$

Equation 2-1 Effective Forced Outage Hours

The concepts of MW_d and MW_a referenced below differ from Boyce's to take into account items described in this paragraph:

MW_d = Gas Turbine output corrected to reference conditions, including a Degradation Factor. It should be less than MW_a. If larger then EFH is considered 0, as there is no impact in the capability to produce the required level of power.

MW_a = Maximum acceptance test corrected load or Guarantee Performance Value as per above.

HO = Hours of Operation at reduced value

The formula above differs from that in reference [43], as the one there would render always a negative result, therefore a positive value in Equation 2-3 below. When rewritten as above the factor affecting the hours is a percentage of MW_a.

The Degradation Factor (DF) is a number between 0 and 1. It accounts for the fact from minute one of operation a Gas Turbine is subject to Non Recoverable Performance (reference Chapter 6). It is an additional correction factor when calculating corrected power to reference conditions.

$$MW_d = \frac{MW_c}{DF}$$

Equation 2-2 Degraded Power

Where:

MW_d = as above

MW_c = Corrected power to reference conditions

DF = Hourly based Degradation Factor

The Availability can then be calculated as:

$$A = \frac{(PT - PM - FO - EFH)}{PT}$$

Equation 2-3 Availability

Where:

A = Availability

PT = Period Time hours

PM = Planned Maintenance hours

FO = Forced Outage hours

EFH = Effective Forced Outage hours

The PT hours is typically a year (8760 hrs), but it can also be accommodated to the true operating profile, i.e. the duration of an operating season (in France it used to be 5 months 3600 hrs for CHP plants).

2.2.2 Reliability

Reference [46] defines Reliability as “the ability of an entity to perform a required function under given conditions for a given period of time”. For a Gas Turbine Reliability is the percentage of time the unit is operating with no FO. Once again, in the current definition the operation of the unit below its expected power level is taken into account. Reliability can be calculated as [43]:

$$RE = \frac{(PT - FO - EFH)}{PT}$$

Equation 2-4 Reliability

RE is Reliability. All other parameters have been defined above.

Reliability is determined by the design features of the gas turbine [12]. Elements as OEM design practices, design maturity, redundancy, etc… have a major impact on Reliability. But there are also other elements that can have major impact as the quality of fluids entering the unit (air, fuel and water), ambient conditions, operating and maintenance personnel technical capabilities, operational profile, etc.… These elements may drive the unit outside its design envelope resulting in more Planned Maintenance than expected, therefore causing a decrease in Reliability, and Availability. Some degradation mechanisms are reviewed in Chapter 6. Correct Maintenance and Operation techniques can only restore Reliability to its original level.

2.2.3 Maintainability

Maintainability is a measure of how easy it is to maintain a system. Once again it is basically a design feature. Reference [46] states “Maintainability is a characteristic of an item, expressed by the probability that a preventive maintenance or a repair of the item will be performed within a stated time interval for given procedures and resources (skill level of personnel, spare parts, test facilities, etc.)”. More details can be found in that reference. It is sufficient to say here that Maintainability is sometimes overlooked during the design phase, with major consequences once the Gas Turbine comes into Service. It is not enough to consider the turbine by itself, by its relation to other elements as Auxiliaries, Control, Enclosure, Plant layout, etc…

Maintainability is an important concept in Aeroderivatives coming from their flight ancestors, as will be discussed later in this Chapter. Things as the location of boroscope ports, instrumentation, sample points for fluids, etc… should be considered from maintenance perspective when designing a Gas Turbine and its associated plant.

2.3 Maintenance

2.3.1 Historical Perspective

Li in reference [12] describes the change in Maintenance requirements derived from the change of machinery design and associated costs. In the first

generation, spanning from XXth century 30's to mid-50's machines were simple and over designed. Also downtime did not matter much. That led to a breakdown type of maintenance.

The increasing complexity of equipment and the need to reduce downtime led to the development of preventive maintenance. Maintenance was done at scheduled intervals.

Around the 80's the increase of maintenance costs, combined with the raise of fixed capital costs that required maximization of asset's life, drove the change to predictive maintenance. The move was supported by the rapid development of affordable computer systems and electronic instrumentation, paving the way to the data acquisition and control systems existing nowadays. Figure 2-1 from [12] summarizes the change.

Figure 2-1: Growing expectations of maintenance [12]

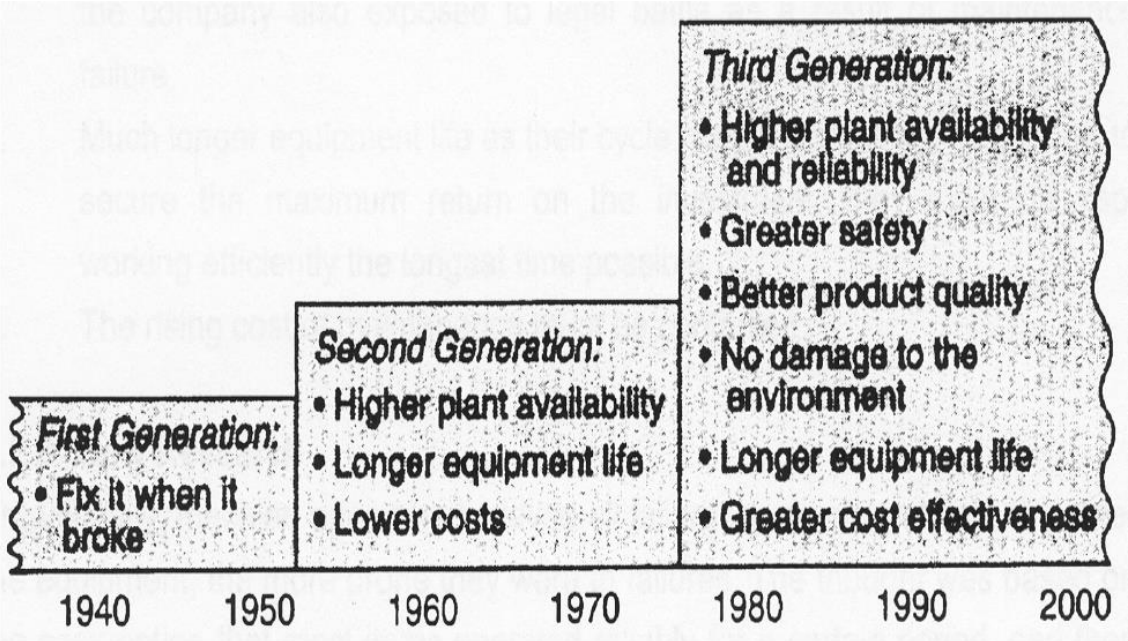

Following [43] and [44] in the 90's a proactive maintenance was introduced. It goes a step further than predictive maintenance with a comprehensive approach that encompasses not only the condition of the equipment, but the analysis of events, total quality control and total employee involvement.

Maintenance types are further explained in the next paragraph.

2.3.2 Types of Maintenance

In general, four types of maintenance approaches can be considered [44]:

- Breakdown or run to failure maintenance.
- Preventive or time-based maintenance.
- Predictive or condition-based maintenance.
- Proactive or prevention maintenance.

Figure 2-2 from reference [44] summarizes them:

Proactive maintenance maybe expected to be the standard. But in real life all four can be found when considering the maintenance of a full plant. It can be considered that cost increases as one goes down the list of maintenance types, from Breakdown to Proactive maintenance. A careful cost-benefit analysis has to be made with every element of a plant or system, as sometimes the increased expenditure of a certain type of maintenance is not justified by the increase of Reliability or Availability it brings. The evaluation and final determination of which philosophy to be applied is the subject of the Maintenance plan. This thesis will not go deeper into the subject, but more can be found in [43] under the Performance-Based Total Productive Maintenance Program (PTMP) paragraph.

Figure 2-2: Maintenance philosophies [44]

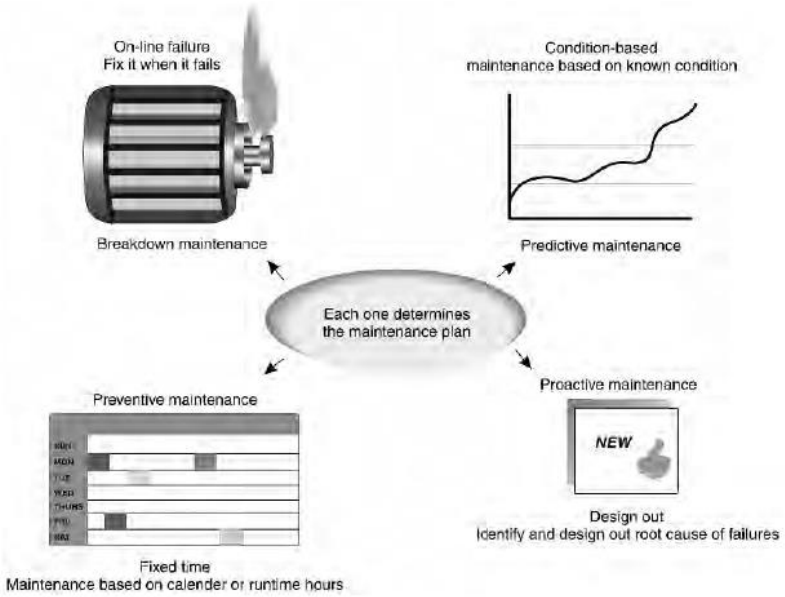

2.3.2.1 Breakdown Maintenance

Under this philosophy a unit is allowed to run until failure of a component(s), which is then replaced or repaired when the unit comes to a complete stop [44]. It is also called Run-To-Failure [12], Panic maintenance based on breakdowns [43] or Corrective maintenance [46].

It is a very inefficient way to run a complex system as a whole plant or a Gas Turbine. But within a complete Maintenance Plan some individual elements maybe determined to be subject of this type of approach. Figure 2-3 is a flow chart of this type of maintenance.

Figure 2-3: Breakdown or Corrective maintenance flow chart [46]

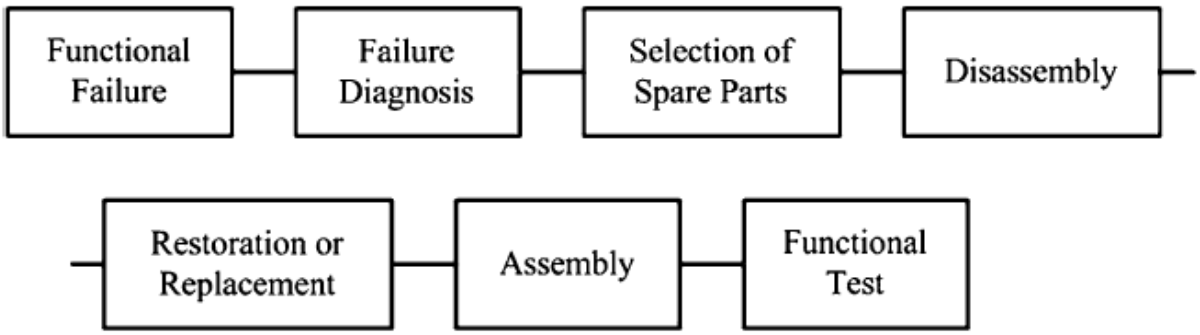

2.3.2.2 Preventive or time based maintenance

Maintenance activities are scheduled at predetermined time intervals [44]. The Gas Turbine or any other element is withdrawn from service at scheduled intervals to perform inspection or repair. It has been the classic way to operate an engine or plant in the past and even nowadays [12]. This type of maintenance may drive the replacement of elements when they still have substantial operating life left and increase the number of scheduled maintenance outages. Figure 2-4 is a flowchart of Preventive maintenance.

Gas Turbine scheduled maintenance intervals are determined by the OEM based on statistical analysis of the fleet (MTBF, MTBO, Reliability, Availability, etc…), design practices and others, as Safety considerations. A classic Aeroderivative time based maintenance schedule is described in Table 2-1.

Figure 2-4: Preventive maintenance [46]

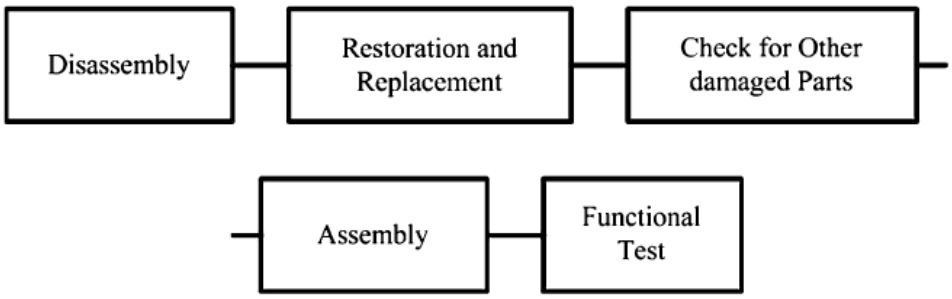

Table 2-1: Aeroderivative classic preventive maintenance schedule

Maintenance activity	Operating hours
Semiannual (including BSI)	Every 4000
Hot Section Repair (gas only)	Every 25000
MOH	Every 50000

Table 2-1 is based on units typically operating with few starts and a large number of hours per year (>6000 hrs). Some maintenance activities will be recommended based on starts (i.e. semiannual at 450 starts) or event time (annual, semiannual) for units with different operational profiles.

Figure 2-5: Engine failures and overhaul intervals [12]

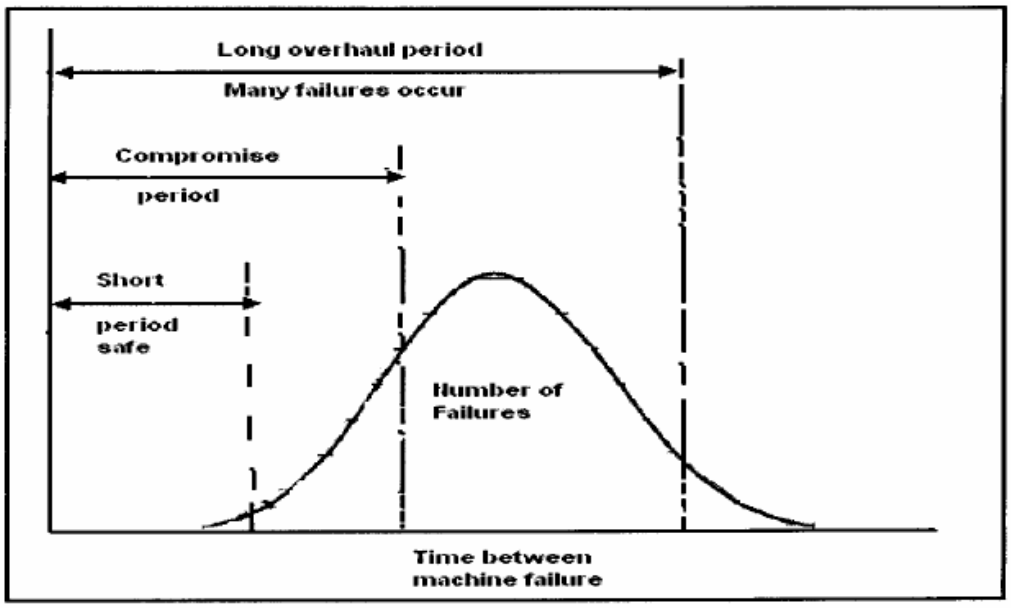

Figure 2-5 from [12] is a simplified example of how the maintenance interval is set. If the period is long a large number of events may happen. If it is too short a large amount of life is left in the engine and maintenance outages are increased. The correct number is always a compromise.

2.3.2.3 Predictive or Condition Based Maintenance

This philosophy relies in predicting component failure based on some kind of monitoring and diagnostic technique [12]. The operation and maintenance activities are then programmed to avoid the failure of that component. A summary flowchart can be found in Figure 2-6.

Condition Based Maintenance (CBM) is an example of this type of approach (references [12] and [45]). It is defined as “a maintenance program that recommends maintenance actions based on the information collected through condition monitoring. CBM attempts to avoid unnecessary maintenance tasks by taking maintenance actions only when there is evidence of abnormal behaviours of a physical asset” [45]. It can be applied to any system, but the focus in this case is a Gas Turbine.

Figure 2-6: Predictive maintenance [46]

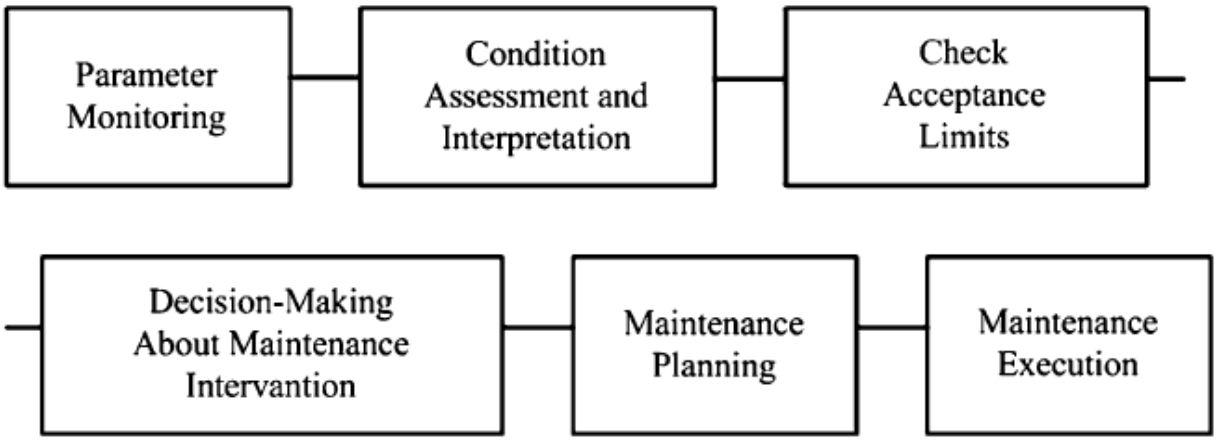

CBM requires a number of steps (combined from [12] and [45]):

- Data acquisition: obtains data from the gas turbine. Chapter 3 has further information on gas turbine instrumentation. Data can be divided into ([45]),

    - Condition monitoring data, acquired through the data acquisition and control system (i.e. pressures, rotational speeds, temperatures, vibrations, etc…).
    - Event data, manually acquired information:
        - Inspection data, as oil analysis, visual inspection, Boroscope inspection, etc…
        - Operational profile which should contain fired hours, starts, trips, load variations, etc…
        - Design information if available
        - Maintenance records
- Data processing: acquired data is validated and transformed to help decision making.
    - Diagnostic system, automated or semi-automated processing of the condition monitoring data. Diagnostic methods are more thoroughly discussed in Chapter 4.
    - Data fusion, where the results of the Diagnostic system and Event data are combined to produce conclusions about the health of the unit.
- Decision making: based on the above conclusions this step aims to provide final actions as,
    - Maintenance procedures (replacement, repair, alteration) [47].
    - Operational recommendations (derating, cycle avoidance, etc…)
    - Inspection intervals and methods (reduced schedule BSI, visual inspections, NDT, etc...).
    - Monitoring recommendations (additional slave instrumentation, modified analysis procedures, etc…).
    - Maintenance planning.

One potential disadvantage of this method is maintenance work may increase due to the wrong assessment of the machine's health. It has to be noted this approach requires specialized equipment and highly trained personnel.

2.3.2.4 Proactive or prevention maintenance

It seeks to go one step further than Predictive maintenance, understanding the root causes of failures and taking proactive measures to incorporate the lessons into the maintenance plan ([44]). It uses Root Cause Failure Analysis (RCFA) tools as Apollo®, TOPS8D®, fishbone, etc…There are many approaches like Performance-based total productive maintenance (PTMP, [43]), Reliability Centered Maintenance (RCM, [46]) or Risk-Based Inspection and Maintenance (RBIM, [47]).

The steps of a Proactive maintenance philosophy can be summarized in:

- Analysis of the plant, classifying the equipment into for example ([44])
    - Critical,
        - Failure has Health and Safety implications, including environmental.
        - Drive major production losses as complete plant stoppage
        - High capital cost equipment expensive to repair of with potential long outages. Gas Turbines are prime examples of this type of equipment.
        - “Bad actors”, elements with continuous reliability or availability problems.
        - Systems where improvement may drive major savings in production costs.
    - Essential, similar to above but with less serious economic or safety implications. The definition of “seriousness” should be part of the initial analysis. It may also include
        - Machines that fail with a known schedule.
        - Systems that drive partial plant outage.
    - General purpose,
        - No effect plant safety.
        - Not critical to plant production.
        - Machine has an installed spare or can operate on demand.
        - Secondary damage does not occur or is minimal.

Techniques as Failure Mode and Effects Analysis (FMEA) are used to understand the plant availability, reliability and maintenance costs. The outcome is a classification of equipment and processes.

- Establish Maintenance and Condition Monitoring plans for the equipment. It will include diagnose, corrective, preventive and predictive tasks based on the analysis performed above. Decisions can be made using techniques like RCM decision diagram ([46]), RIBM risk analysis ([47]) or PTPM methodology ([43])
- Proactive follow up of the established plans:
    - Operational feedback.
    - RCFA of events.
    - Corrective Action and Preventive Action (CAPA) implementation.
    - Continuous review of the Maintenance and Condition Monitoring plans.

Proactive maintenance requires the involvement of all plant personnel, from Management, Operations, Maintenance, Finance, etc... It takes time to be established. Boyce in [43] estimates it may take three years in a large plant. The training of plant personnel is a fundamental task. It may require significant capital expenditure in tools and systems; therefore a detailed cost vs benefit analysis is needed.

Figure 2-7 is an example of RCM flow chart from reference [46]. All the items discussed above can be easily identified.

2.3.3 Aeroderivative Maintenance Concepts

Aeroderivative Gas Turbines maintenance philosophy can be summarized in three concepts: On condition maintenance, maximize on-site maintenance capability and minimize downtime.

2.3.3.1 On condition maintenance

Elements of the gas turbine are repaired or replaced only when it is required. This concept is a part of Condition Based Maintenance. Techniques to monitor the condition of the gas turbine will be discussed in Chapter 4.

Figure 2-7: Reliability Centered Maintenance flow chart [46]

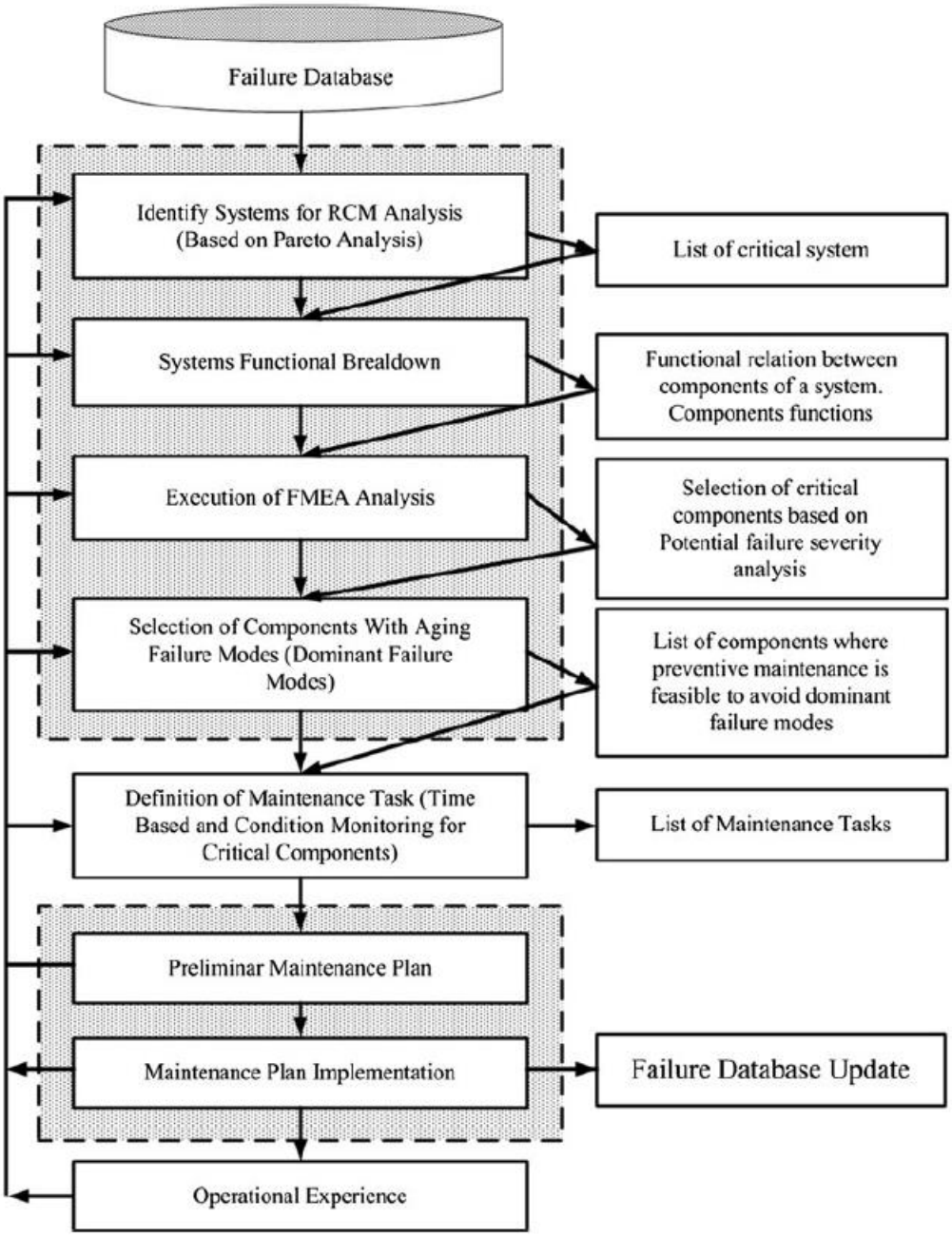

2.3.3.2 Maximize on-site maintenance capability

The design of the Aeroderivative Gas Turbines leverages from the aircraft engine to maximize on-site maintenance capability (references [48] and [49]).

- Modular design, allowing for on-site major component exchanges, like the High Pressure Turbine, without total engine disassembly. Figure 2-8 shows the modules of an Industrial Trent 60. The modules can be replaced

on site, minimizing downtime. Later the removed modules are repaired at an overhaul facility.

- Controls, accessories and sensors are externally mounted therefore easily replaceable.
- Replacement modules as the HPT are sent to site preground to required dimensions. Interchange is thus straightforward.

Compressors are typically of split design. Blades can be easily repaired and replaced on site.

2.3.3.3 Minimize downtime

The light weight Aeroderivative gas turbine design allows for fast on site exchange. When major maintenance is required the gas turbine enclosure design permits easy removal, using preinstalled crane or removal cradles ([48]). The affected unit is then replaced by a spare or lease unit. Downtime can be as low as 24 hours. Figure 2-9 shows and LM6000® being removed for MOH.

Figure 2-8: Industrial Trent 60 modules [49]

(Courtesy Siemens®)

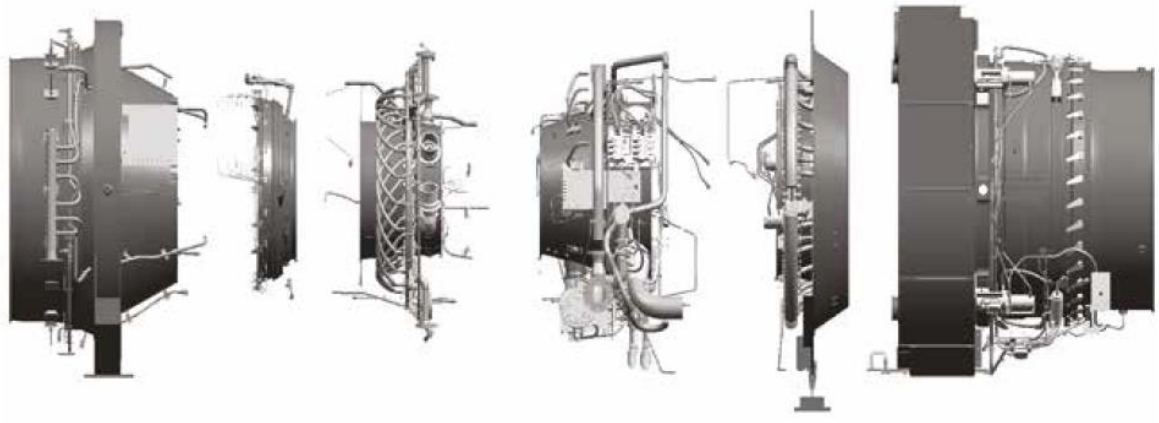

2.3.4 Water Wash

Gas turbines ingest a large quantity of air. The LM6000® ingests 125 kg/s at design point ISO conditions (reference Chapter 5). If the air is contaminated with 10 ppm foulant loading rate, a quick calculation results in approximately 80 Tons per year of contamination, in continuous operation ([17]). Inlet filtration careful design may avoid the majority of the contaminants, but there is always a quantity that passes by ([18]). Furthermore, high efficiency filtration capable of trapping small 3 µm particles may have high inlet pressure losses resulting in unacceptable performance loss ([55]).

Figure 2-9: LM6000® removal [48]

(Courtesy General Electric®)

As the compressor fouls the decrease in mass flow and efficiency has a major impact in gas turbine output and heat rate (overall efficiency), with corresponding economic losses derived from excess gas fuel consumption and loss of electrical revenue. In the Oil and Gas industry gas turbine performance loss has a big impact in the plant process capability ([36]), therefore in its final output and total revenue. Fouling and its effects are described in Chapter 6.

2.3.4.1 Compressor cleaning

Compressor fouling can be recovered by cleaning the compressor ([17], [22] and others). Three procedures are used in Aeroderivatives, off line water wash, on line water wash and hand cleaning. Which one to use will depend on the level of compressor dirtiness. There are advantages and disadvantages to each one of them (Table 2-2). The table below has been modified from reference [56]. Grit blasting is not used in Aeroderivative Gas Turbines, as it causes major hardware damage due to erosion and impact, sump contamination, hot section cooling holes clogging and coatings erosion:

Table 2-2: Relative advantages and disadvantages of wash methods

Method	Advantages	Disadvantages
Online washing	No interference with load profile Extends intervals of crank washes	Less effective Cannot replace off line washing
Offline washing	Very effective	Engine shutdown required (hours)
Hand cleaning	Very effective	Engine shutdown required Long outage (over a day)

A more detailed description of gas turbine compressor washing systems, procedures and fluids can be found in references [17], [43] and [55].

2.3.4.2 On line water wash

It is performed by injecting atomized cleaning fluid at compressor inlet during engine operation, with no significant impact for plant operation other than a variation of produced power during water wash period. Water evaporates as it travels downstream of the compressor. Therefore it is effective to remove dirt from the initial stages, but can increase fouling of later stages.

Effectiveness of on line washing is highly site dependent. Evaluating the impact of on line water wash requires a systematic plan before the optimum schedule is achieved ([43]). On line washing should start right after an off line wash or hand clean, to avoid deposit growth from the start ([55]). The type of cleaning fluid (water alone, water + detergent, type of detergent) is another variable of the investigation plan. Water has to be highly demineralized as it will go through the

unit in operation exposed to gas path temperatures. If contaminants are present, the hot section hardware may experience early degradation (Chapter 6).

Figure 2-10 ([57]) below presents the degradation rates in case of no on line wash (red line), only on line wash (blue line) and when on line and off line combined (green line). The improvement combining both methods is clear. In reality as stated above this effect is very site dependent because the kind of environmental contamination and type of gas turbine have major effect on the optimized schedule of on and off line washes ([43]).

Figure 2-10: On line and offline effect on degradation rates [57]

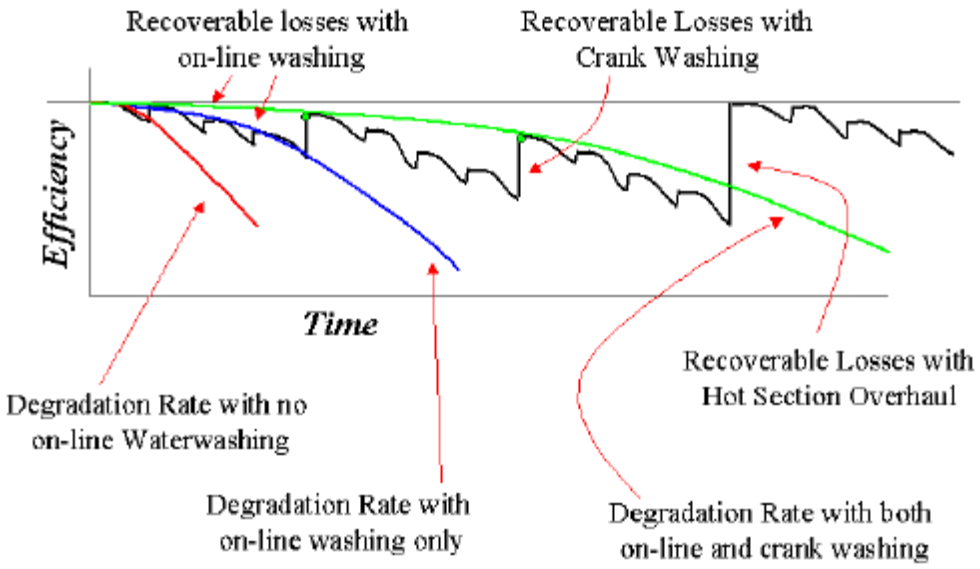

2.3.4.3 Off line water wash

Requires the unit to stop production and it is performed by injecting a water-detergent mix while unit is cranking, followed by a soaking period and finalized with several clean water rinses. The gas turbine turns driven by a hydraulic, pneumatic or electrical motor called starter.

The cleaning fluid will usually be a mixture of water and detergent. There are many types of detergents divided in water, solvent and surfactants. The type of environmental contaminants going into the gas turbine will determine which one to use. Once again it requires a systematic plan before the optimized schedule is

achieved ([43]). The outage time is a significant variable in the study as it has measurable consequences in the total revenue of the plant. The unit has to cool down below a value recommended by OEM before water was can be started. Cooling time can be reduced by forced cooling via engine crank. Then the off line water wash can be started. The total time may vary between 3 to 8 hours ([55]) depending on engine size and water wash equipment. The outage time has to be balanced against the performance loss in order to determine if outage is recommended. Another variable discussed later is the fact that over a certain level of degradation off line water wash may become ineffective. All these items should be accounted for in the water wash scheduling plan. A good performance diagnose is very important to accurately establish the proper threshold of degradation that requires an off line water wash.

Figure 2-11 shows the effect of off line water wash on ISO corrected power output of a LM6000® located in Southern Europe. The power steps before and after water washes are around 1 MW. The blue and green linear trend lines show the degradation in output through time, not recovered by off line water wash in this particular case.

Figure 2-11: Off line water wash effect on ISO corrected power

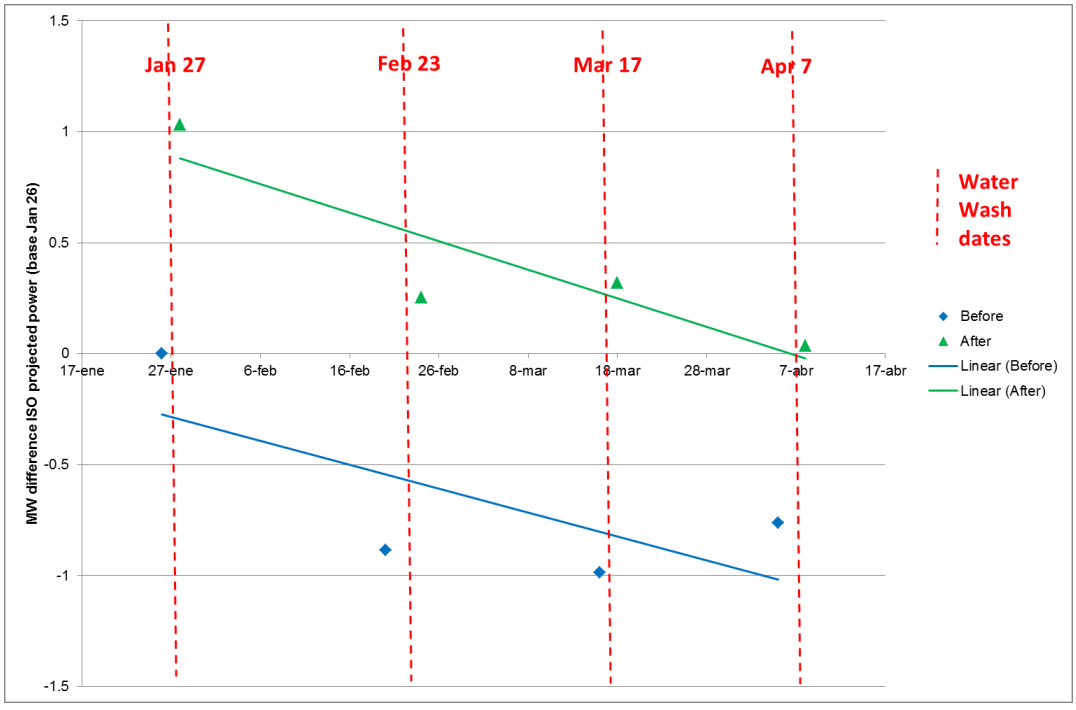

2.3.4.4 Hand cleaning

Off line water wash does not always reach the last stages of the compressor. The high temperatures in the last stages of Aeroderivative contribute to dirt “baking” into blades ([17]). Baked deposits are very difficult to remove by off line water wash, but can be removed by hand cleaning. For hand cleaning the compressor cases are removed, taking advantage of their split design, and blades and vanes are cleaned manually by hand scrubbing after applying a cleaning agent. The cleaning agents vary depending on dirt type (steam, demineralized water, slightly acidic solution, water wash detergent or even commercial oven cleaner). Thorough rinse with demineralized water is needed. Figure 2-12 are compressor vanes before and during hand cleaning. Cleaning agent foam can be observed in right hand side photograph.

Figure 2-12: Compressor vanes before and during hand cleaning

Continuing with the engine discussed in the previous paragraph Figure 2-13 describes the effect of a LPC and HPC hand cleaning on the same engine. The graph is measured power filtered for a range of T2 and P0 (ref Chapter 7 for the details of where this parameters are measured). Power increased an average of 3.5 MW after hand cleaning. Data is filtered to a range of T2 (compressor inlet pressure) and P0 (Pressure before the FOD screen in the inlet, comparable to LPC inlet pressure) to account for ambient condition variations. It will be described in next paragraph, but inlet filtration system was improved, accounting for the stable power output as compared to prior hand cleaning in Figure 2-11.

Figure 2-13: LPC and HPC Hand clean effect

66<T2<70 & 14.42<P0<14.48

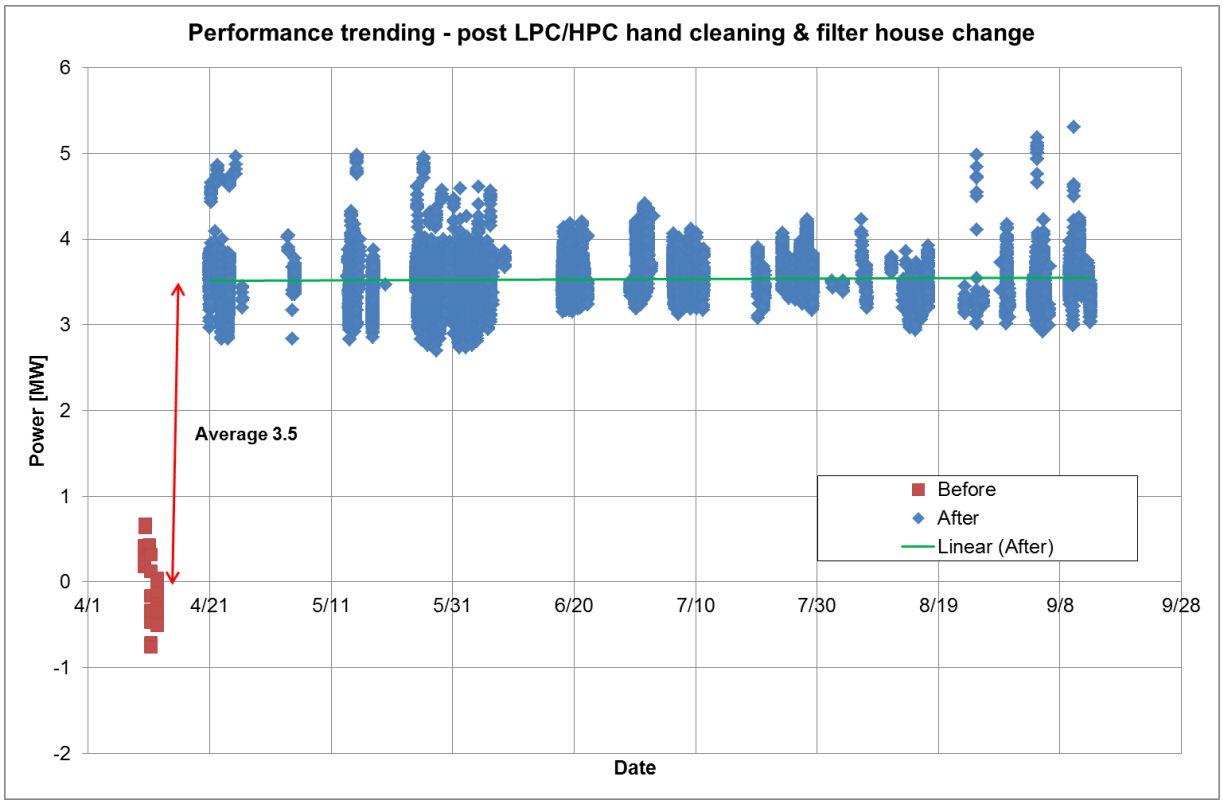

2.3.4.5 Inlet filtration, compressor fouling and water wash

Figure 2-13 is a practical example of the effect on the inlet filtration in compressor fouling and water wash ([17] & [18]). The customer improved the filter house from the original design to an upgraded F7+H10 design (for a description of filter classifications refer DIN EN-1822:2009 and reference [18]) at same time of the hand cleaning outage. The comparison of Figures 2-11 and 2-13 highlights:

- The water wash period was less than a month before the filter house upgrade.
- Non water wash recoverable power degradation was accumulated as time went by, shown by the linear power loss lines in Figure 2-11. Probably it could be diminished with a more frequent water wash, with the corresponding economic impact related to outage time. The average outage time for water wash was six hours.

- Five months of operation (approx. 3600 hrs) were accumulated without visible power degradation after the filter house upgrade. In fact, since then the customer water washes every six months at the time of periodic boroscope inspections.

The increase of inlet losses was measured around 2 inches of water, estimated to be 0.3 MW less. The details of the customer's economic calculation are not known, but in their own words the payback was estimated in "less than 2 years".

2.4 Conclusion

The present chapter has provided an overview of Maintenance philosophies, with particular focus on Aeroderivative Gas Turbines. Water wash is one of the several maintenance activities of a Gas Turbine with a big impact in the economic results of the plant because of its relation to power output and availability.

3 INSTRUMENTATION AND MEASUREMENT UNCERTAINTY

3.1 Introduction

Proactive and Predictive Maintenance require the acquisition and analysis of Condition Monitoring gas turbine data (Chapter 2). This chapter reviews typical Aeroderivative Gas Turbine instrumentation used in Data Acquisition and Control systems.

Data quality is paramount. Errors in data will drive incorrect analysis, or abnormal control actions that may risk the unit's integrity. Uncertainty Analysis and error are reviewed in this chapter, although, due to time and space constraints, this project will consider available data as healthy. Many references can be found in sensor fault diagnostics, for example [12] and [29] and the bibliography collected in them.

3.2 Aeroderivative Gas Turbine Instrumentation

Many types of sensors are used to control and monitor Aeroderivative gas turbines. Some will be described below, but it is a field of knowledge and technology in constant change, moreover with the miniaturization of electronics.

3.2.1 Temperature

Temperature sensors are used in gas path and other measurements as oil, fuel (either liquid or gas), metal (i.e. bearing metal temperatures, generator stator), ambient (atmospheric and gas turbine or generator enclosure). Temperature sensors can be of many kinds, but the most common are:

3.2.1.1 Resistance Temperature Detectors (RTD)

RTD's are temperature sensors whose electrical resistance increases with temperature. They are usually made of a platinum coil inside a housing submerged in the fluid to be measured (air, oil, fuel). Another common type is a thin metallic film stuck on the element whose temperature is of interest, as in the case of bearing metal temperatures. The RTD is connected to a power source.

Its resistance measured either by comparison with a known resistor, or by measuring voltage drops across the RTD.

RTD's are recommended for steady state measurements below 1000ºC. They require good heat transfer conditions between probe and environment ([38)].

Commonly used RTD are PT100, made of Platinum wire with a 100 Ω resistance at T = 0ºC. For this type the standard temperature coefficient is α = +0.385 Ω/ºC in the range of 0 to 100ºC. It means that both the slope and absolute values are small resistance values, so connecting wire impedance can impact measurement substantially. The usual methods to avoid this effect are 3 wire and 4 wire bridge circuits. Description of those is above the intent of this document.

Figure 3-1: 3 wire circuit RTD

(http://www.jms-se.com/rtd.php)

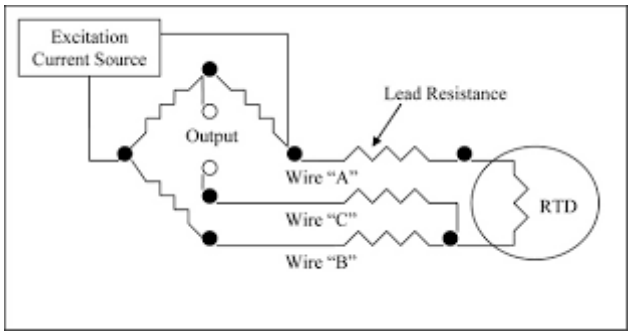

3.2.1.2 Thermocouples

Thermocouples are based on the thermoelectric effect discovered by Thomas Seebeck in 1821. Two thermoelectrically dissimilar wires are joined at one end (measurement junction). The opposite ends are connected to a voltage measuring device (reference junction). If the measurement junction has a different temperature than the reference junction, a voltage related to the temperature difference can be measured. The temperature of the reference junction needs to be accurately known. Figure 3-2 is a scheme of the thermoelectric effect.

Figure 3-2: Thermoelectric effect

(http://saba.kntu.ac.ir/eecd/ecourses/instrumentation/projects/reports/Thermocouple/myweb10/2-Fundamentals%20of%20TC's.htm)

Table 3-1 is a list of the most common thermocouple types, ranges and different international color codes (courtesy of Omega engineering Inc. ©).

Thermocouple measurement loops need to be carefully designed and installed to avoid introducing unwanted reference junctions at different temperatures that may create additional thermoelectric force. Thermocouples are commonly used to measure gas path temperatures for monitoring and control. Figure 3-3 is a sample of a thermocouple that maybe inserted inside the gas path through a gas turbine case port.

Figure 3-3: Thermocouple sample

(Courtesy of TC Medida y Control S.A. http://www.tc-sa.es/termopar/termopares.htm)

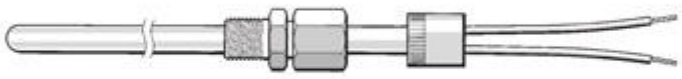

Table 3-1: 3 wire circuit RTD

(Courtesy of Omega engineering Inc.© downloaded from http://www.omega.com/techref/colorcodes.html)

Connectors										Connectors
ANSI Code	ANSI MC 96.1 Color Coding		Alloy Combination		Comments Environment Bare Wire	Maximum T/C Grade Temp. Range	EMF (mV) Over Max. Temp. Range	IEC 584-3 Color Coding		IEC Code
	Thermocouple Grade	Extension Grade	+ Lead	– Lead				Thermocouple Grade	Intrinsically Safe	
J	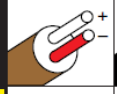	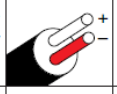	IRON Fe (magnetic)	CONSTANTAN COPPER-NICKEL Cu-Ni	Reducing, Vacuum, Inert. Limited Use in Oxidizing at High Temperatures. Not Recommended for Low Temperatures.	–210 to 1200°C –346 to 2193°F	–8.095 to 69.553	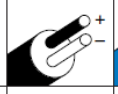	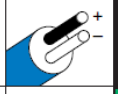	J
K	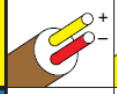	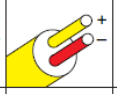	CHROMEGA® NICKEL-CHROMIUM Ni-Cr	ALOMEGA® NICKEL-ALUMINUM Ni-Al (magnetic)	Clean Oxidizing and Inert. Limited Use in Vacuum or Reducing. Wide Temperature Range, Most Popular Calibration	–270 to 1372°C –454 to 2501°F	–6.458 to 54.886	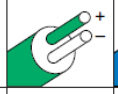	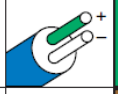	K
T	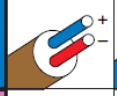	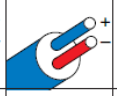	COPPER Cu	CONSTANTAN COPPER-NICKEL Cu–Ni	Mild Oxidizing, Reducing Vacuum or Inert. Good Where Moisture Is Present. Low Temperature & Cryogenic Applications	–270 to 400°C –454 to 752°F	–6.258 to 20.872	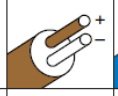	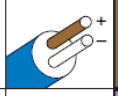	T
E	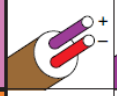	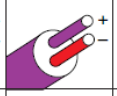	CHROMEGA® NICKEL-CHROMIUM Ni-Cr	CONSTANTAN COPPER-NICKEL Cu-Ni	Oxidizing or Inert. Limited Use in Vacuum or Reducing. Highest EMF Change Per Degree	–270 to 1000°C –454 to 1832°F	–9.835 to 76.373	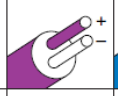	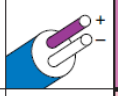	E
N	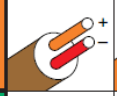	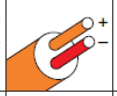	OMEGA-P® NICROSIL Ni-Cr-Si	OMEGA-N® NISIL Ni-Si-Mg	Alternative to Type K. More Stable at High Temps	–270 to 1300°C –450 to 2372°F	–4.345 to 47.513	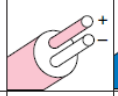	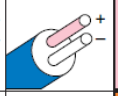	N
R	NONE ESTABLISHED	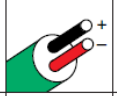	PLATINUM-13% RHODIUM Pt-13% Rh	PLATINUM Pt	Oxidizing or Inert. Do Not Insert in Metal Tubes. Beware of Contamination. High Temperature	–50 to 1768°C –58 to 3214°F	–0.226 to 21.101	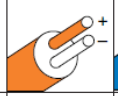		R
S	NONE ESTABLISHED	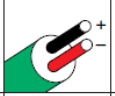	PLATINUM-10% RHODIUM Pt-10% Rh	PLATINUM Pt	Oxidizing or Inert. Do Not Insert in Metal Tubes. Beware of Contamination. High Temperature	–50 to 1768°C –58 to 3214°F	–0.236 to 18.693	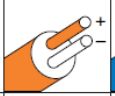	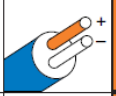	S
U	NONE ESTABLISHED		COPPER Cu	COPPER-LOW NICKEL Cu-Ni	Extension Grade Connecting Wire for R & S Thermocouples. Also Known as RX & SX Extension Wire.			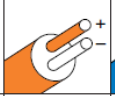	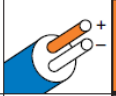	U
B	NONE ESTABLISHED		PLATINUM-30% RHODIUM Pt-30% Rh	PLATINUM-6% RHODIUM Pt-6% Rh	Oxidizing or Inert. Do Not Insert in Metal Tubes. Beware of Contamination. High Temp. Common Use in Glass Industry	0 to 1820°C 32 to 3308°F	0 to 13.820	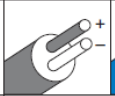		B
G* (W)	NONE ESTABLISHED		TUNGSTEN W	TUNGSTEN-26% RHENIUM W-26% Re	Vacuum, Inert, Hydrogen. Beware of Embrittlement. Not Practical Below 399°C (750°F). Not for Oxidizing Atmosphere	0 to 2320°C 32 to 4208°F	0 to 38.564	NO STANDARD USE ANSI COLOR CODE		G (W)
C* (W5)	NONE ESTABLISHED	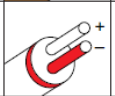	TUNGSTEN-5% RHENIUM W-5% Re	TUNGSTEN-26% RHENIUM W-26% Re	Vacuum, Inert, Hydrogen. Beware of Embrittlement. Not Practical Below 399°C (750°F) Not for Oxidizing Atmosphere	0 to 2320°C 32 to 4208°F	0 to 37.066	NO STANDARD USE ANSI COLOR CODE		C (W5)
D* (W3)	NONE ESTABLISHED	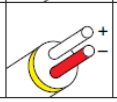	TUNGSTEN-3% RHENIUM W-3% Re	TUNGSTEN-25% RHENIUM W-25% Re	Vacuum, Inert, Hydrogen. Beware of Embrittlement. Not Practical Below 399°C (750°F)–Not for Oxidizing Atmosphere	0 to 2320°C 32 to 4208°F	0 to 39.506	NO STANDARD USE ANSI COLOR CODE		D (W3)

** Not official symbol or standard designation*

† JIS color code also available.

3.2.2 Pressure

There are many pressure measurements in an Aeroderivative Gas Turbine and its associated systems. Gas path pressures are measured from the inlet to the

exit of the gas turbine in several stations (inlet pressure drop, compressor inlet and outlet, turbine inlet and outlet, exhaust pressure). The configuration of the particular machine and its control will determine the number of measurements required. The filters differential pressures, whether air, oil or fuel, are of interest for maintenance intervals and diagnostic of the system condition. Oil pressures are needed for the monitoring and health of critical components as bearings. Measured fuel pressures are used for example to determine fuel flow and protect the engine against too high or too low fuel pressure.

Pressure transducers require a reference pressure. The measurement unit (psi, bar, etc…) is qualified to indicate the zero pressure reference:

Gage (psig, barg) – The reference pressure is the atmospheric pressure. When exposed to atmospheric pressure it will measure 0.

Absolute (psia, bara) – The transducer measures with respect to a vacuum. Its interior is evacuated and hermetically sealed. When exposed to atmospheric pressure it will measure atmospheric pressure.

Differential pressure (psid, bard) – For this kind of measurement the transducer has two pressure ports, whereas the others above have only one. Pressures are applied to both sides of the transducer and the output is the difference between them. The accuracy is much better than the difference between individual pressure measurements when measuring small pressure differences at high pressures.

Pressure measurement is based on the distortion of a deformable element subject to pressure. There are many types but the most commonly used in Gas Turbine and its associated installation are bourdon tube and piezoelectric.

Bourdon tube transducers are based on the deformation of a Bourdon tube. It can be connected to several kinds of displacement measurement devices as potentiometers, LVDT, and other but the usual is a simple needle type indicator. They are commonly used for non-critical field measurements of auxiliary systems as oil pressures, etc… Figure 3-4 is a Bourdon type pressure indicator.

Figure 3-4: Bourdon type pressure indicator

(Courtesy WIKA® http://www.wika.us/21X_53_en_us.WIKA)

Piezoelectric pressure transducers use piezoelectric effect sensing elements. When a force is applied to a piezoelectric element a charge is generated. The charge signal is converted to voltage by signal conditioners. These transducers are used for the Gas Path measurements due to their capability to withstand high pressures and temperatures. The development of electronics has made them the most commonly used in industrial installations. They can be easily connected to data acquisition and control systems. The typical outputs are voltage or current (4-20 mA). An image can be found in Figure 3-5.

Figure 3-5: Piezoelectric pressure transducer

(Courtesy of GE Measurement and Control®
https://www.gemeasurement.com/sensors-probes-and-transducers)

3.2.3 Rotating speeds

There are two main types of speed sensors used to measure gas turbine shaft speeds:

- Tachogenerator, an electromagnetic generator that produces an output voltage proportional to the rotational speed of the shaft that drives it.
- Variable reluctance speed sensor as in Figure 3-6. It is made of a ferromagnetic pole, a permanent magnet and coil around the pole. The complete system requires a gear or toothed wheel. The pole is magnetized and will be very close to the gear teeth. When the gear moves the magnetic flux across the changes with the passing teeth. Flux variation with time generates a voltage in the coil. The passing gear generates a sine wave in the coils, with voltage proportional to gear speed. By electronic means the sine wave can be converted to digital pulses. The numbers of pulses per unit are proportional to the gear speed and teeth number thus can be easily translated into shaft rotational speed (rpm).

Figure 3-6: Variable reluctance speed sensor

(Courtesy of Flight Systems Inc.®
http://www.flightsystems.com/images/products/industrial-sensors/magnetic-pickup-rpm-sensor-graph.jpg)

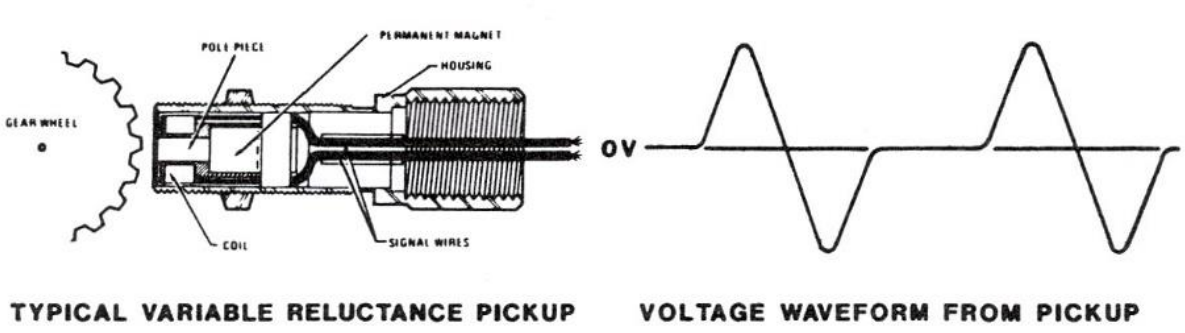

3.2.4 Flow

There are several flows that may need to be measured in a gas turbine installation

- Fuel flow, either gas or liquid.
- Water flow for power augmentation or emissions control.
- Steam flow for power augmentation or emissions control.
- Airflow for performance test.

The usual system for compressible fluids is to measure flow through the fluid control valve position (Fuel metering valve, Steam metering valve), pressure measurement before and after the valve and fluid temperature. The valve comes together with a laboratory generated throat area vs position calibration table. The information is loaded in the control system. Combining known throat area, pressure loss and temperature the flow can be accurately estimated.

Turbine flow meters are used for water and liquid flow measurement (i.e. fuel). The fluid passes through a rotor in the flow meter, causing it to turn with an angular velocity proportional to the fluid linear velocity, thus to the volumetric flow rate. The rotor speed is gathered with a variable reluctance speed sensor similar to the one described above. Flow indication can be instantaneous or totalized. The turbine flow meter should operate in its linear range to deliver an accurate output.

3.2.5 Vibration

Vibration measurement is done for monitoring and engine health diagnostic purposes. Aeroderivative Gas Turbines have seismic type piezoelectric accelerometers mounted on the gas turbine case (Figure 3-7). The principle of operation is the same to that described in the pressure paragraph for piezoelectric transducers. The motion of the associated seismic mass distorts the piezoelectric crystal, creating a charge output (pC) proportional to the magnitude and frequency of engine vibrations. This varying charge value can be conditioned to a more rugged mV signal and integrated as required to display velocity or displacement. These sensors are very sensitive, have a very good signal to noise ratio and are quite insensible to electrostatic noise. They have no moving parts and can withstand high temperatures.

Other types of vibration sensors used around an Aeroderivative Gas Turbine plant are:

- Proximity probes: used for generator vibrations
- Velocity pickups: used in RGB, fans, pumps, etc...

A detailed description of these sensors can be found in references [43] and [44].

Figure 3-7: Triaxial piezoelectric accelerometer

(Courtesy of Endevco® https://www.endevco.com/2280-2/)

3.2.6 Dynamic Pressure measurements

Dynamic pressure measurements are done in the combustion chamber of the gas turbine and are typically related to emissions control needs. The control of nitrogen oxides (NOx) emissions in gas turbines is achieved by controlling combustion flame temperatures through two methods ([43]):

- Wet: Injection of steam or water into the combustor
- Dry: Control of airflow and fuel flow into the combustor to maintain a lean cold flame (i.e. DLE)

Both methods may drive combustion instabilities manifested in pressure pulsations within the combustor that eventually could damage the hardware. Frequently they occur within audible range, and are commonly called “acoustic”, “humming” or “rumble”.

“Acoustics” are measured by using a dynamic pressure transducer (Figure 3-8). They are piezoelectric transducers with micro second response times that can measure rapidly changing pressure over a wide range of amplitudes and frequencies. They are prepared for very high temperature applications because they are usually mounted close to the combustor area. Their output is a charge signal with a certain sensitivity expressed in pC/psi (or pC/bar). The measurement is used in the control scheduling air and fuel flow to contain fluctuations within an acceptable range.

Figure 3-8: Dynamic Pressure transducer

(Courtesy Vibro-Meter® http://energycatalog.vibro-meter.com/index.php?option=com_mtree&task=viewlink&link_id=48&Itemid=56)

3.2.7 Position

Position indication is fundamental to gas turbine operation. It is used to monitor and control the position of variable geometry actuators, fuel metering valves and bleed valves. It can be linear or rotary position.

The simplest is a DC potentiometer. It was common in the past, but its constructive characteristics make it sensitive to electrical noise and mechanical failure.

These days the most popular position indication sensors are Linear (or Rotary) Variable Differential Transformers (LVDT / RVDT). The principle is the same for both but LVDT measures a linear position and RVDT an angular one.

In a LVDT three wire coils are wound around an insulating material. The primary coil is excited by a known AC voltage. The principle of mutual inductance requires that an AC voltage of the same frequency is created in the secondary cores. A movable ferromagnetic core is centered in between the two secondary coils. In that case the voltage across the two secondary coils is the same. But if the core moves i.e. towards one coil, the voltage across that coil will be greater. By measuring the relationship between secondary coils voltages the position of the core can be deduced. LVDT schematic and operation is summarized in Figure 3-9.

LVDT has advantages like friction free operation as there is no mechanical contact between core and coils, mechanical robustness, insensitive to cross axis movements, and almost infinite resolution.

Figure 3-9: LVDT schematic and operation

(Courtesy of sensorsland.com http://www.sensorland.com/HowPage095.html)

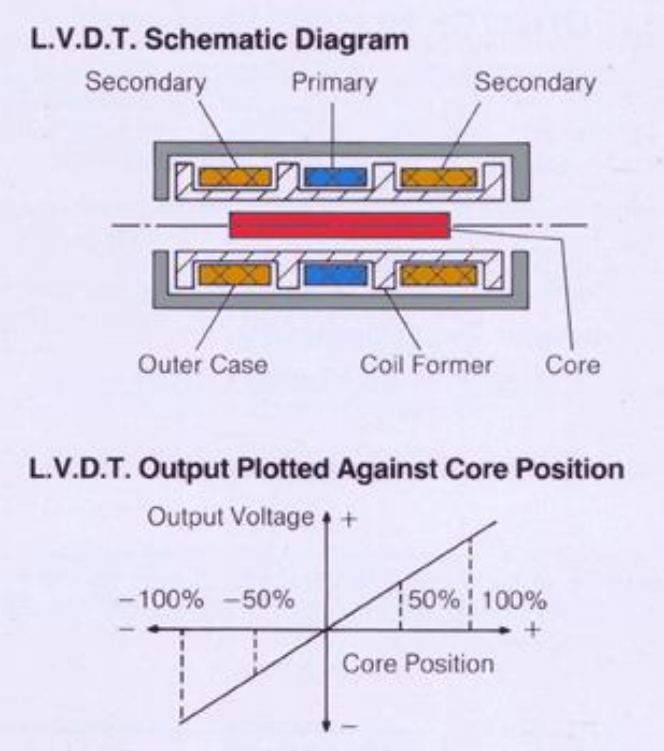

3.2.8 Electronic Chip Detectors

Electronic Chip Detectors (ECD) are magnets submerged in the bearing sumps scavenge oil flow, before the filters, that capture magnetic debris particles generated by bearings during operation. Debris particles bridge a gap between two electrodes, acting as a switch for circuit closure. The signal is read by the Data Acquisition and Control system and used for health diagnostic (i.e. alarm). Figure 3-10 shows a schematic circuit and 3-11 is an ECD with debris.

Figure 3-10: ECD circuit and sample ECD

(Courtesy Eaton® http://www.tedecoindustrial.com/electric.htm)

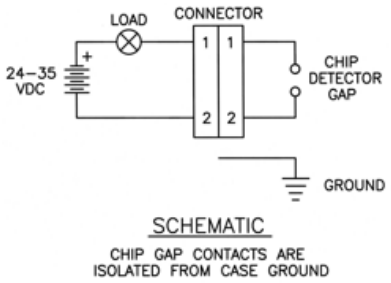

Figure 3-11: ECD and strainer with bearing debris

3.2.9 Emissions

Emissions are measured for regulatory and control reasons. A sensing probe is introduced inside the exhaust gas flow through an exhaust port. The sensing probe has a number of sensing ports to ensure gas is not sampled at a single location, but averaged across the exhaust flow. The sample gas is cooled and dehydrated prior to the analyser. The number of sensors in the analyser is dependent on the components to be analysed. Each component requires its individual sensor. Typical components are Oxygen (O_2), Carbon Monoxide (CO), Carbon Dioxide (CO_2), Sulphur Dioxide (SO_2), Hydrogen Sulphide (HS) and Unburnt Hydrocarbons (UHC).

Each component has specific sensor techniques suitable for different expected concentration ranges and accuracies. The description is outside the scope of this Thesis. Reference [53] is a good starting point for this topic.

3.3 Measurement Uncertainty

The purpose of measurements is to numerically characterize the state or performance of a physical process ([39]). The data gathered can be used for analysis, diagnostic, control or any other need. Understanding the quality of the data is crucial. This can be achieved by measurement uncertainty analysis. It is not the subject of this Thesis such analysis. The intention of this paragraph is to highlight its importance and introduce the subject.

3.3.1 Measurement error

Error is the difference between the measurement and the true value ([7], [39]). Every measurement ever made has had an error. Errors come from several sources like:

- Probe location (i.e. spatial effect of the location in gas path)
- Probe design (i.e. pressure probes)
- Transducer characteristics (i.e. range, sensitivity, calibration)
- Measurement loop
- Data acquisition system characteristics (i.e. Analog to Digital conversion, electronics)

Every measurement should come together with its uncertainty analysis, so the quality of the data can be understood. The uncertainty limits are typically set by OEM, Standards Bodies (ASME, ISO) or customer. These limits are different depending on the use of the data. Data used for equipment control may have larger uncertainty limits that that used for contract performance testing. Tables 3-2 and 3-3 show ASME PTC22-2005 [40] and BS ISO 2314:2009 [41] requirements.

Table 3-2: ASME PCT22-2005 Uncertainty limits [40]

Table 4-1 Maximum Allowable Measurement Uncertainties

Parameter or Variable	Uncertainty
AC power (RSS of VTs, CTs and meters)	0.25%
Auxiliary power	5%
DC power	0.5%
Torque	1.5%
Speed	0.1%
Time	0.05%
Inlet temperature	1°F or 0.6°C
Barometric pressure	0.075%
Humidity: Wet bulb, or	2°F or 1.1°C
RH from meter	2%
Extraction/injection flows (Water, steam, N_2, rotor cool)	2%
Extraction/injection temperature	5°F or 2.8°C
Gas fuel heat input	
Orifice factors (orifice meter)	0.4%
Mass flow (turbine meter)	0.5%
% volume of constituents	0.33%
Oil fuel heat input	
Mass flow	0.5%
Heat value	0.4%
Gas fuel temperature (for sensible heat calculation)	5°F or 2.8°C
Oil fuel temperature (for sensible heat calculation)	5°F or 2.8°C
Inlet total pressure drop	10%
Exhaust static pressure drop	10%
Exhaust temperature (Appendix A)	10°F or 5.6°C

Table 3-3: BS ISO 2314:2009 Uncertainty limits [41]

Table 3 – Maximum permissible uncertainties

Individual instrument or parameter	Max. uncertainty	Remarks
Barometric pressure	± 0.05 %	Instrument uncertainty
Air inlet temperature	± 0.2 K	Instrument uncertainty
Relative humidity	± 2 %	Instrument uncertainty
Electrical power metering	± 0.2 %	Instrument uncertainty
Current transformer	± 0.2 %	Equivalent to accuracy class 0.2S
Voltage transformer	± 0.2 %	Equivalent to accuracy class 0.2S
Mechanical power (torque)	± 1.0 %	Instrument uncertainty
Frequency / Shaft speed	± 0.25 %	Instrument uncertainty
Gas fuel pressure	± 0.25 %	Instrument uncertainty
Gas fuel temperature	± 0.2 K	Instrument uncertainty
Gas fuel heating value	± 0.5 %	Combined uncertainty of gas composition
Gas fuel mass flow	± 0.5 %	Combined uncertainty of temperature, pressure, volumetric flow and gas composition
Oil fuel temperature	± 0.2 K	Instrument uncertainty
Oil fuel heating value	± 1.0 %	Combined uncertainty of laboratory analysis
Oil fuel mass flow	± 0.5 %	Combined uncertainty of volumetric flow and temperature
Turbine exhaust temperature	± 3 K	Instrument uncertainty
Inlet pressure loss	± 50 Pa	Instrument uncertainty
Exhaust pressure loss	± 50 Pa	Instrument uncertainty

3.3.2 Types of errors

The classic way of classifying errors ([7], [39] and [40]) describes two types

- Random
- Systematic or bias

Reference [42] has the most recent approach, classifying errors by the method of evaluation

- Type A, evaluated by statistical analysis
- Type B, evaluated by other means than statistical analysis

This document will follow the classic way. Latest ISO standards as [41] refer to the most recent approach.

3.3.2.1 Precision or random error

This error comes from the non-repeatability of the measurement system. It can be calculated using the population standard deviation σ. In reality there are a limited number of measurements, a sample, so S_x, the sample standard deviation is used. It is improved by increasing readings and instruments.

It is calculated using the Standard Deviation of the average of a sample for a certain measurement.

$$S_X = \sqrt{\frac{\sum_1^N (X_k - \bar{X})^2}{N-1}}$$

Equation 3-1: Standard deviation of a sample

$$S_{\bar{X}} = \frac{S_X}{\sqrt{N}}$$

Equation 3-2: Standard deviation of the average

Where:

S_X standard deviation of the sample

N number of readings

(N-1) degrees of freedom

X_k individual reading

$\bar{X}$ average of readings

$S_{\bar{X}}$ Standard deviation of the average $\bar{X}$

Assuming a normal distribution for the measurand, therefore of the measurements and using Student's t_{95} distribution, the interval $\bar{X} \pm t_{95} S_{\bar{X}}$ will contain 95% of the data sample. $\pm t_{95} S_{\bar{X}}$ is also called the Precision Error Index. When there are more than 31 data points (30 degrees of freedom) $t_{95} = 2$, so the error index becomes:

$$\pm 2 S_{\bar{X}}$$

Equation 3-3: Error index for 30 degrees of freedom

3.3.2.2 Systematic error or Bias

Systematic error or bias β is a constant error that affects every measurement of a variable by the same amount and not observable in the test data ([39]). It is never known, so it should be estimated. B is the estimator of the limits of β.

$$-B \leq \beta \leq +B$$

Following reference [39] five types of systematic errors can be described (Table 3-4).

Table 3-4: Types of Bias errors [39]

Size	Known sign and magnitude	Unknown magnitude
Large	1 - Calibrated out	3 - Assumed eliminated
Small	2 - Negligible	4 - Unknown sign 5 - Known sign

1. Large errors known to exist typically calibrated out (i.e. instrument calibration).
2. Existing errors considered negligible and not used in uncertainty analysis.
3. Large errors that are engineered out of the measurement (i.e. errors due to the improper position of a pressure tap in the shadow of a beam).

4. Included in uncertainty analysis, may need to include a $-B^-$ and $+B^+$ if not symmetrical.
5. Included in uncertainty analysis through B.

These errors are typically evaluated by comparing to national standards, using several independent methods to measure the same parameter, careful evaluation of spatial variation, engineering assessment and, last but not least, experience of the engineers involved.

3.3.2.3 Calculation of Uncertainty

Measurement uncertainty is defined as the combination of bias and precision errors. The following methods of calculation consider symmetrical bias. Reference [39] describes two methods. The choice of method is driven by user and should be clearly stated when reporting uncertainty.

- Additive Uncertainty

$$U_{ADD} = \pm(B + t_{95}S)$$

  U_{ADD} provides an interval around the test average that will contain the true measurement 99% of the time.

- Root Sum Square Uncertainty

$$U_{RSS} = \pm[B^2 + (t_{95}S)^2]^{1/2}$$

  U_{RSS} provides an interval around the test average that will contain the true measurement 95% of the time.

3.4 Measurement faults

Measurement faults must not be confused with measurement errors. Measurement errors can be identified and evaluated as explained above. Measurement faults occur when something goes wrong in the measurement chain. They cannot be evaluated a priori. They need to be detected if the measurement has to be used either for control or diagnostic. Some examples of measurement faults are:

- Sensor faults
- Leaks on pressure taps and lines
- Electrical noise

- Faulty connections

Measurement faults would have a big impact on the results of a diagnostic. The first step for a diagnostic tool would be the analysis of measurements to detect these faults. Redundancy can be used ([7]):

- Hardware redundancy uses multiple instruments to measure the same engine parameter. Measurements are compared and a voting system is used to select the right one.
- Analytical redundancy uses a model of the engine and information from dissimilar sensors to provide an estimate of the measured parameter.
- Temporal redundancy uses redundant information in successive samples of a measurement. Examples are range and rate checks.

Most of the gas turbine parameters have redundant sensors, and in some cases sensor taps in the engine. OEM's data acquisition and control systems do have redundancy checks as described above. An example on the gas turbine under study is PS3, where two sensors are provided, although from the same engine tap. The two measurements are range checked and compared against each other. If a sensor is out of range it is discarded. In case of both drifting apart above a certain value the highest is selected (conservative approach). These situations are alarmed in the HMI screen. If both sensors pass the checks then the measurement will be the average of both sensor outputs.

Even with redundancy checks it is possible that a measurement drifts significantly over time undetected. Several schemes have been tested as ANN and Genetic algorithms ([7]).

The diagnostic tool of this thesis does not include measurement fault checks. Part of the development of a practical tool would be the inclusion of fault checks. It could be done by an Auto-associative ANN as described in references [7] and [12], embedded in a Nested Neural Network with other ANN. Figure 3-12 is an example from [12]. The first NN is an AANN for measurement fault detection.

Figure 3-12: Nested Neural Network with Measurement fault detection step [12]

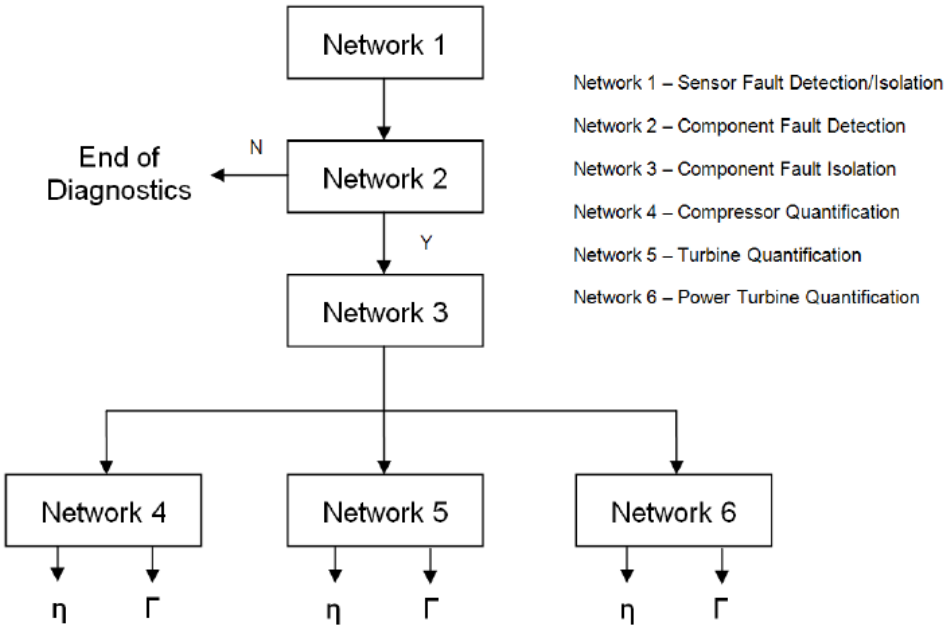

3.5 Conclusion

Instrumentation and accuracy have been reviewed, so the next step will be the use of data within Diagnostic Methods. Once again it is emphasized this report will consider data as accurate. The subject of error detection has been briefly shown above. Further work on the subject is needed for a completely viable Diagnostic tool.

4 GAS TURBINE DIAGNOSTIC METHODS

4.1 Introduction

The review in Chapter 2 of Maintenance philosophies highlighted the importance of accurate diagnostic tools that can help in proactive and preventive maintenance.

The aim of Diagnostics is to detect the presence and identify the kind of faults appearing in a machine ([4]). A healthy engine is an engine free of faults. As the engine operates the degradation of the engine gas path components result in the degradation of Gas Turbine performance, compared to that of the healthy engine. The change in the condition of a part of an engine will produce a corresponding change in the parameters that describe its functioning. Measurement of the changes of parameter values from their values for “healthy” operation can in principle lead to the diagnostic of the alterations in the parts that caused this change ([4]).

Complete engine health diagnostics is a combination of many techniques for the analysis of Event Data and Condition Monitoring Data used for Predictive Maintenance in Condition monitoring data and event data (reference Chapter 2, [45]). Event data gathering and analysis techniques are dealt with in this chapter. Condition monitoring data instrumentation and accuracy was the subject of previous chapter. A brief review of Vibration Analysis is done as well.

Condition monitoring data comprises several types of data like vibration, thermodynamic cycle data, exhaust emissions, fuel properties, ambient data, etc… The total analysis and diagnostic of a gas turbine requires the blend of all this data ([43]). The rest of the chapter will be dedicated to the analysis Condition Monitoring data gathered. Vibration data analysis will be briefly discussed as it is a critical topic for health monitoring, but not the subject of this Thesis. Finally several Performance Analysis Based Diagnostic Methods will be reviewed, their advantages and drawbacks compared, and the reason for ANN choice explained.

4.2 Event data gathering and analysis

Romesis and Li in reference [45] highlight the importance of Event Data for a successful CBM program. Any Predictive or Proactive maintenance program has to include this type of data in it.

4.2.1 Boroscope Inspections

The internal of the gas turbine are inspected using a flexible probe optic fibre Boroscope (Figure 4-1). Current models allow 3-D or 2-D measurement of defects, plus high quality digital video and still images; and remote connectivity. The measurement is then compared with established OEM limits and used in conjunction with other available data to determine path ahead (operation, repair, replace, etc…). Some equipment have the possibility of using different types of Boroscope tips, including boroblending, the capability to repair minor damages by using a tip with a mini grinding tool.

Figure 4-1: Flexible Boroscope [50]

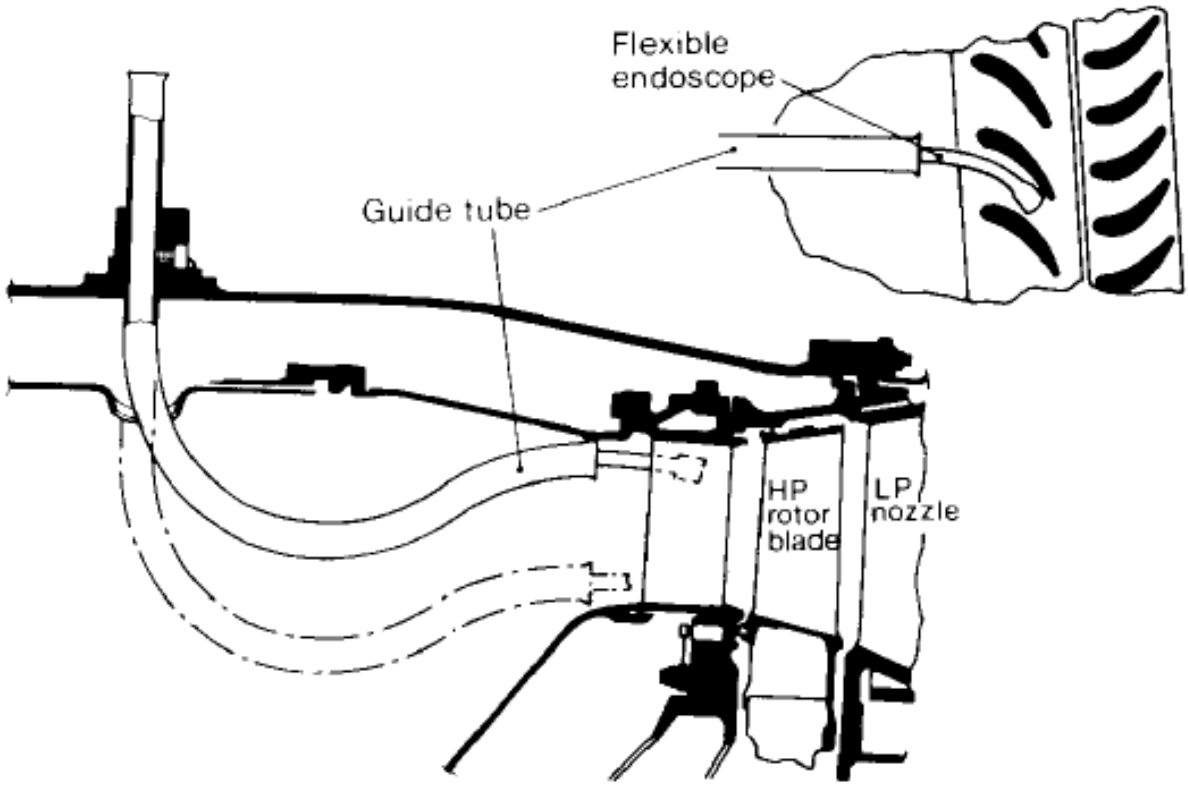

Figure 4-2: Tip shroud damage measurement via Boroscope

(Courtesy of Combined Cycle Journal http://www.ccj-online.com/)

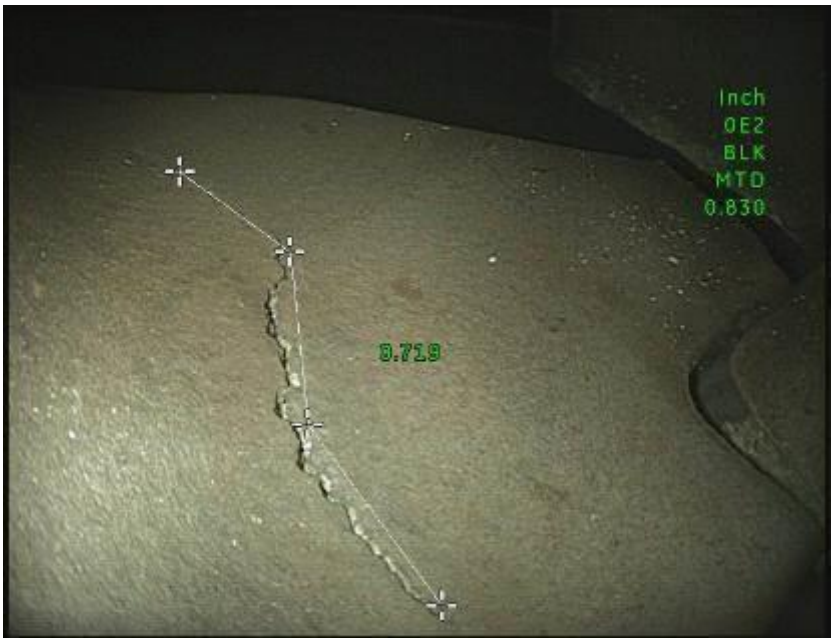

4.2.2 Oil analysis

Oil analysis is a powerful tool for the monitoring and health diagnostic of the gas turbine. Aeroderivative Gas Turbines usually have anti-friction bearings (roller or ball bearings). Oil is used to cool, lubricate and clean the bearings; but also to drive control mechanisms as actuators, etc… Due to the temperature inside the bearing sumps commonly SLO (Synthetic Lube Oil) is used. The SLO must be compliant with recognized standards as:

- SAE AS5780 - Specification for Aero and Aero-Derived Gas Turbine Engine Lubricants
- MIL-PRF-23699 - Lubricating Oil, Aircraft Turbine Engines, Synthetic Base

The condition of the oil is regularly assessed by standard tests ([50]), which can loosely be divided into three categories. Categories are listed below with a recognized standard test included. These tests may change in between countries. Limits change with engine OEM and product line.

- Physical and chemical properties as
    - Total Acid Number (TAN) measures the oil's acidity. Oil degradation creates organic acids that can drive bearing corrosion or the

creation of varnishes, etc. ASTM D664-58 - Standard Test Method for Acid Number of Petroleum Products by Potentiometric Titration.

  - Viscosity (Kinematic). Measures the resistance to flow of oil at a certain temperature. Large shifts in viscosity may be caused by mixing with other oils, excessive oxidation or thermal cracking. ASTM D445-65 - Standard Method of Test for Viscosity of Transparent and Opaque Liquids (Kinematic and Dynamic Viscosities).

- Contaminants
  - Particle count measures the quantity of particles in the oil. The results are reported as the number of particles greater than 4 microns/6 microns/14 microns per ml of fluid in the standard ISO 4406:1999 - Hydraulic fluid power -- Fluids -- Method for coding the level of contamination by solid particles. Portable counters are available.
  - Water, if excessive drives early oil degradation and hardware corrosion. A daily visual test is easy. A cloudy or hazy appearance indicates that water may be present. ASTM D1744 - Standard Test Method for Determination of Water in Liquid Petroleum Products by Karl Fischer Reagent.
  - Color. It is used to measure insoluble materials in the oil that may lead to varnishes and detect oil degradation and contaminant presence. Changes in oil color are the one of the first and easiest method to determine the degradation of the oil. Aside from the standard analysis listed a regular simple comparison with new fresh oil is good practice. ASTM D1500 - Standard Test Method for ASTM Color of Petroleum Products (ASTM Color Scale).
- Wear metals. Spectrometric Oil Analysis Program (SOAP), either by Atomic Absorption or Emission methods is used to detect the presence of metal particles of small size that indicate wear in the sump (seals, cases) or bearing area (rollers, balls, cages or races).

In the past years on line monitoring of oil has been developed. Scavenge oil is circulated through on line sensors that detect the presence of Ferrous and Non Ferrous particles. The analysis of the data can help determining the health of the sumps. An example is GasTOPS Ltd. MetalSCAN®. Figures 4-3 and 4-4 are from the on line available literature.

Figure 4-3: MetalSCAN® schematic

(Courtesy GasTOPS Ltd. http://www.gastops.com/metalscan.php)

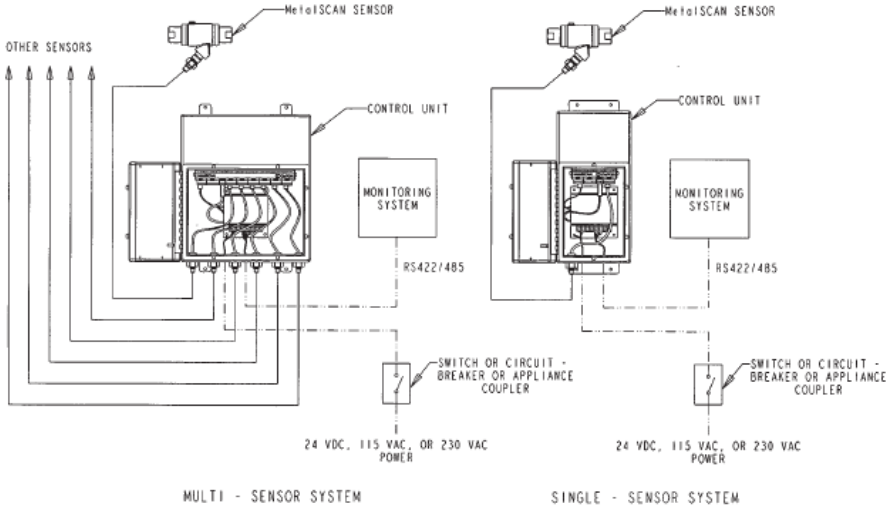

4.2.3 Operational profile

It contains data as total fired hours, starts, trips, load changes bigger than a certain value (usually defined by OEM), etc… Information is used to determine the remaining life of gas turbine components and schedule maintenance activities.

Initially Aeroderivative Gas Turbine maintenance scheduling in land or offshore based applications was done through fired hour count (reference Chapter 2). Electricity market changes now drive more complex application operational profiles that base load operation, as load following, PFC, start and stop peaking, reserve power, etc… They require more frequent starts and stops and load changes, so cycle counting as in aircraft engine or marine applications is necessary. It is sometimes called Critical Parts Life Management (CPLM) and related to Low Cycle Fatigue (LCF) life of components.

Figure 4-4: LM6000® Application

(Courtesy GasTOPS Ltd. http://www.gastops.com/metalscan.php)

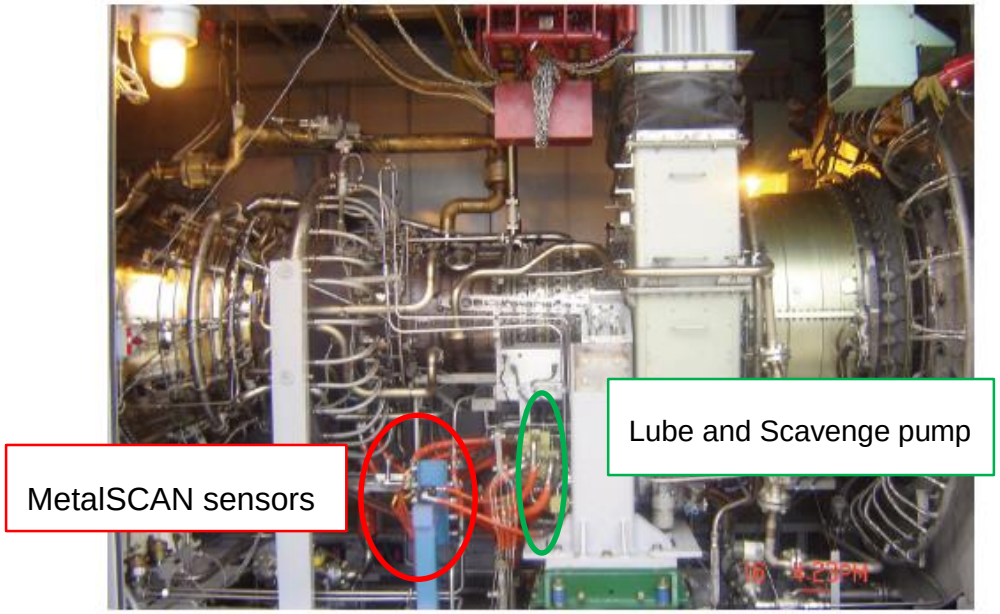

Creep mode life can be estimated by Larson Miller equation ([52]). In those applications where the unit runs at lower than rated temperature it is important to determine remaining life, so the unit is removed from service only when needed. Offshore application is a classic case of this.

4.2.4 External Visual Inspection

It is the simplest form of inspection but it is an extremely powerful tool. It helps detect heat distressed areas (i.e. via discoloration), leaks, lose or worn parts, etc… No data gathering should be considered full without an external visual inspection. Figure 4-5 shows a distressed fuel hose found during a visual inspection. Its complete rupture could have led to a prolonged outage.

4.3 Vibration monitoring and analysis

As with any other complex rotating machine vibration is a fundamental part of gas turbine diagnostics. Shafts and seals rotate at high speed with rotor parts attached (spools, blades, retainers, etc…), and supported by bearings. Distress in any of these parts changes the vibration signature of the gas turbine.

Figure 4-5: Heat distressed fuel hose

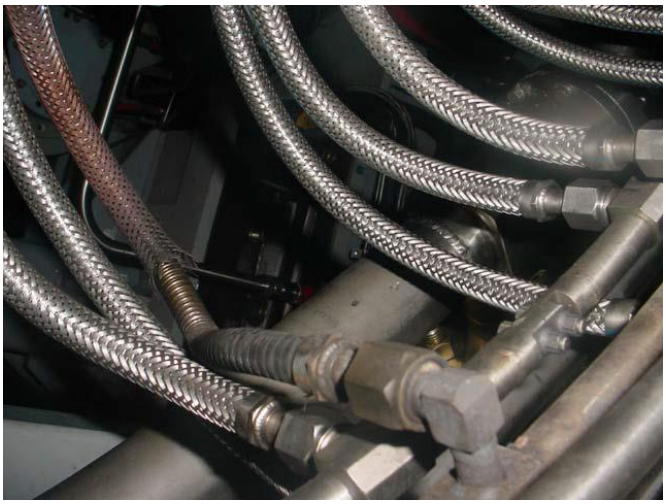

4.3.1 Vibration monitoring

The gas turbine will have several accelerometers installed. Figure 4-6 is a schematic of the monitoring system of one the accelerometers for a two shaft machine as the one considered in this thesis. The accelerometer signal (pC/g) is amplified and converted to mV in the Remote Charge Converter (RCC). The output is usually a velocity signal in mV per inch per second (ips, or mm/s). This signal goes through a band pass filter where low frequencies, most likely from structural interferences, and high frequencies are filtered out, within a workable range. That filtered signal is called “wideband signal” although it does not contain all the frequency components. The wideband signal goes into the Control and Monitoring system.

The output of the band pass filter is also sent to two tracking filters. Tracking filters monitor vibration in a window of frequencies centered on a reference frequency. In this gas turbine there are two tracking frequencies, HP and LP shaft speeds. The output of the tracking filters is sent to the Control and Monitoring system. Together with wideband the three signals are checked and usually have Alarm and Trip ranges. They are also transferred to the Diagnostic system.

Figure 4-6: Aeroderivative Gas Turbine vibration monitoring schematic

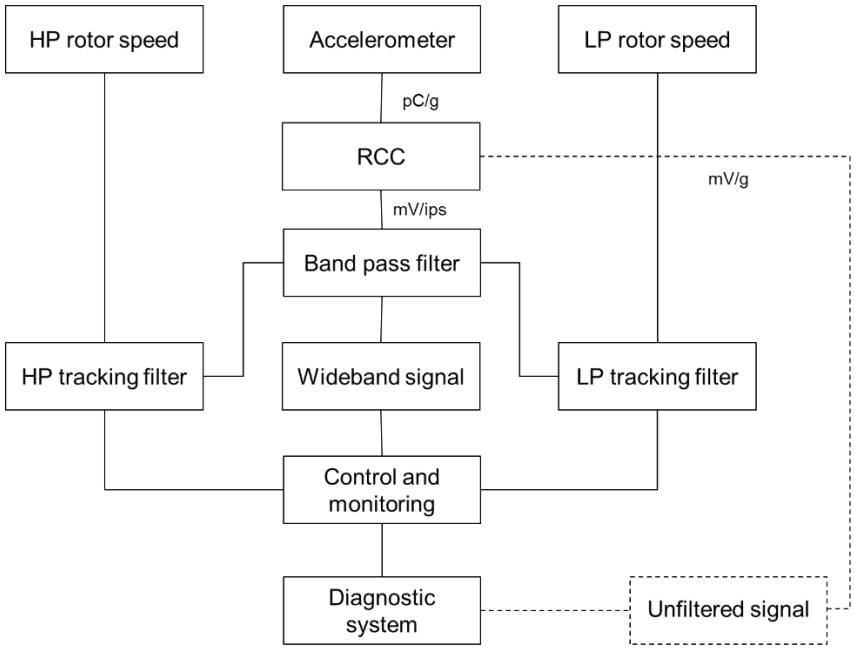

In some cases there is an additional completely unfiltered acceleration signal in mV/g that is connected to the Diagnostic system. This signal allows for wider Diagnostic capability if required, as no frequency components are lost.

4.3.2 Vibration diagnostics

Vibration signals from a gas turbine are very complex time based signals generated by several forces. The signal can be modelled as the summation of many “pure” tones represented by sinusoidal waveforms of constant frequency. The analysis consists in the decomposing the signal into its frequency components. This is done through the Fast Fourier Transform (FFT).

Through Fourier analysis a function of time is decomposed in the summation of a series of sine waves each one with a characteristic frequency (Figure 4-7 [44]).

$$F(t) = \frac{a_0}{2} + \sum_{n=1}^{\infty} (a_n \cos n\omega t + b_n \sin n\omega t)$$

Equation 4-1: Fast Fourier Transform

Where a_n and b_n are the amplitudes of the oscillatory functions *cos(nωt)* and *sin(nωt)* and

$$\omega = 2\pi f$$

Equation 4-2: Angular speed

f is the frequency of the related sinusoidal wave and *ω* the angular speed.

Figure 4-7: Fourier Transform [44]

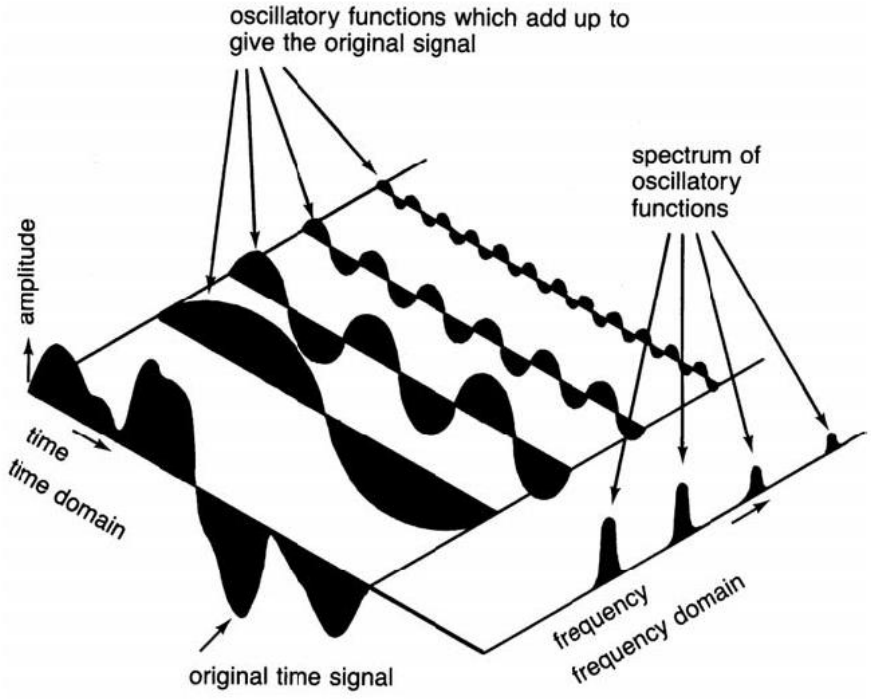

The frequency based information is then represented in several ways to help diagnose potential issues. The most frequent is spectrum where individual frequencies and their associated amplitudes are represented. Waterfall adds time as third axis. Figures 4-8 and 4-9 are the spectrum and waterfall plot of a gas turbine with oil inside the rotor in a hung start up consequence of massive rubbing driven by the oil in rotor presence.

Figure 4-8: Spectrum of a gas turbine with oil in rotor

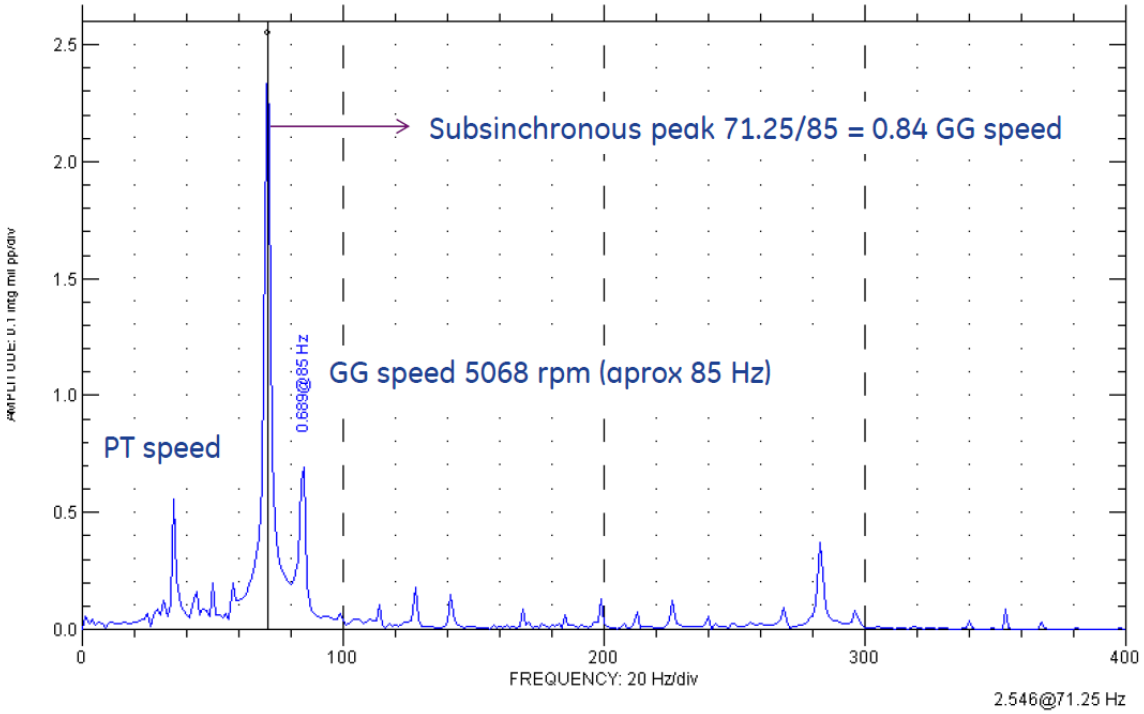

Figure 4-9: Waterfall of the same machine from Figure 4-8

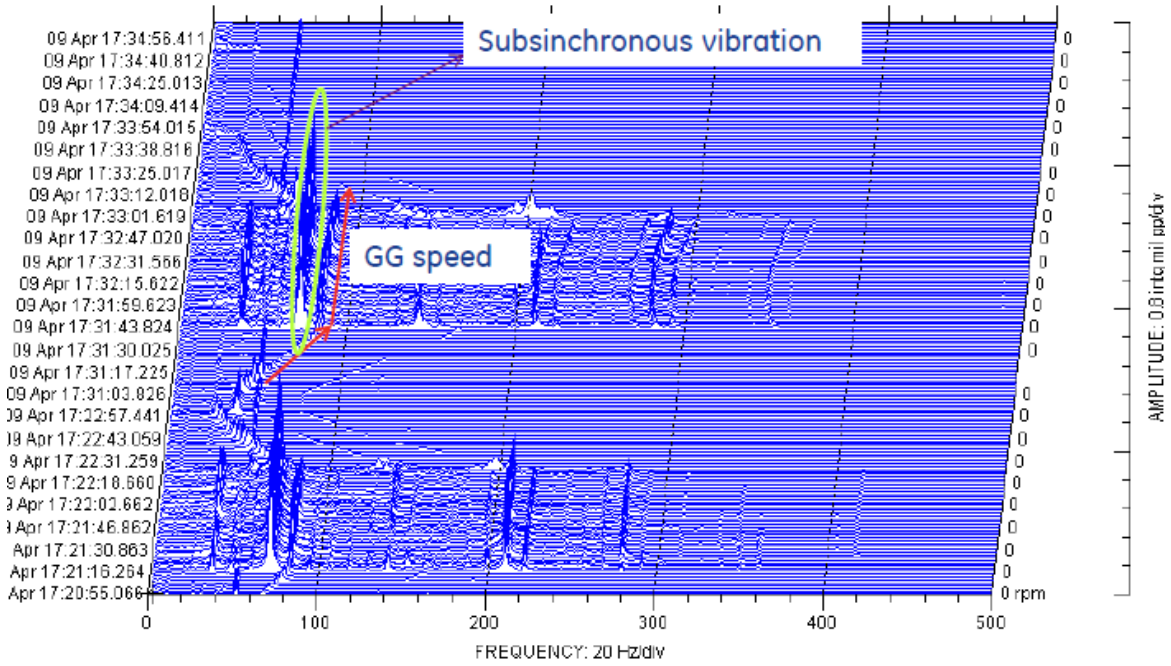

The best practice in vibration analysis is to gather a baseline set of data during initial machine start up. Diagnostic is a lot easier afterwards by continued data gathering and comparison with the initial baseline. In the author's experience diagnostics engineers are much savvier when analysing changes and their potential reasons. Figures 4-10 and 4-11 show the change in signature of a gearbox accelerometer signal. After detecting the change an inspection was recommended and severe pitting found on the gears.

Figure 4-10: Baseline spectrum

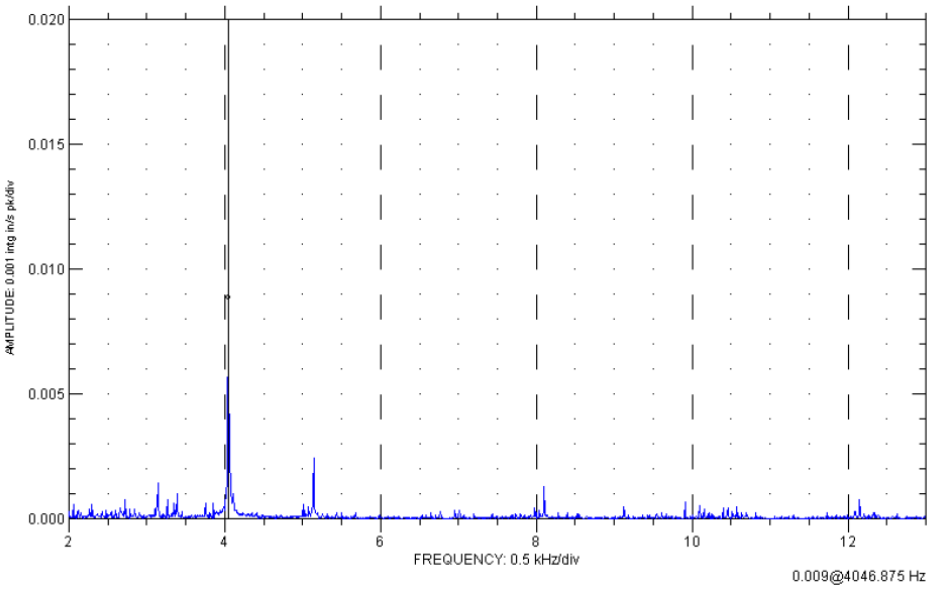

Figure 4-11: Distressed spectrum highlighting changes

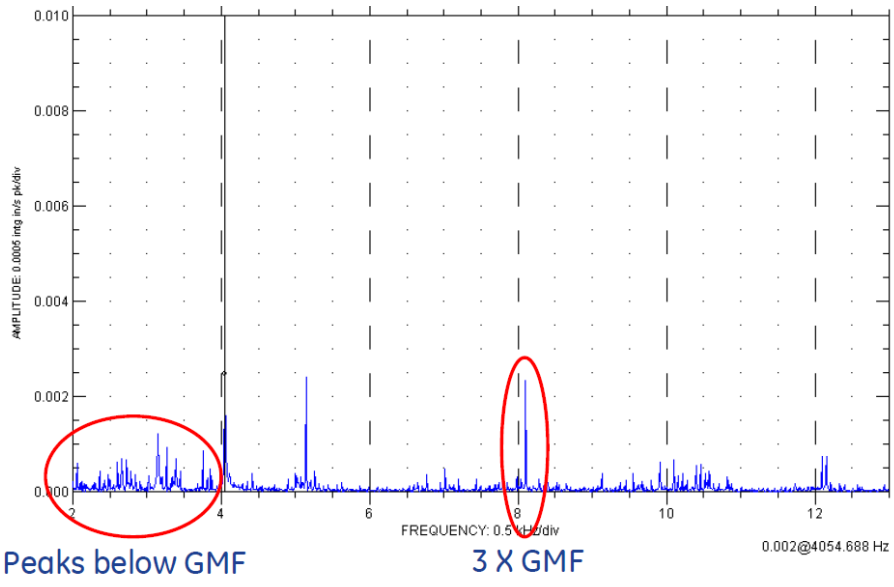

Vibration analysis is a highly specialized subject. It has to be incorporated into plant maintenance and follow up, but requires specific equipment and costly personnel training. Therefore a cost benefit analysis should be carefully made for small plants, avoiding a large investment with too long return.

4.4 Performance Analysis Based Diagnostic Methods

Two types of parameters are considered in performance analysis:

- Gas turbine health parameters, the efficiencies (η) and flow capacities (Γ) of each component. They cannot be measured directly so they are also called non measurable parameters.
- Measurable parameters as pressures, speeds, temperatures, etc…

The degradation of the performance of a gas turbine can be described by the variation of its component health parameters as mass flow capacity and efficiency. The variation of health parameters impacts the measurable parameters of the engine as the engine operating point is affected. Performance analysis task tries to understand the variation of engine health parameters by analysing the variation of measurement parameters. There are many Performance Analysis Based Diagnostic Methods and the rest of the chapter will discuss some of the most usual.

Figure 4-12: Sample fault tree [7]

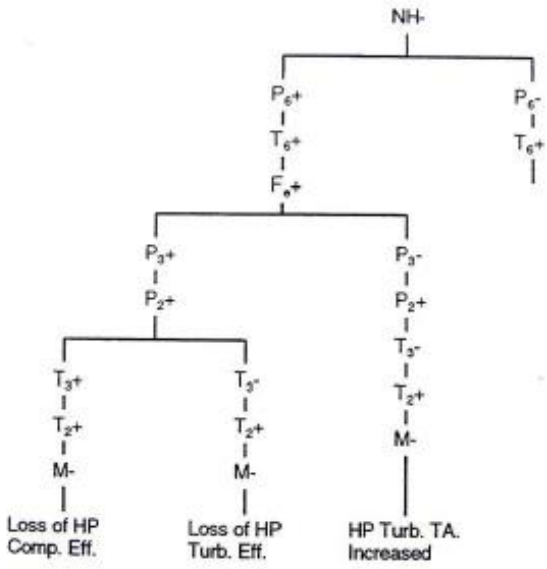

4.4.1 Fault Tree

A gas turbine fault tree examines the increase or decrease of the measurable parameters and, through a decision tree, determines a probable fault at the end of the path. Figure 4-12 is a sample fault tree.

4.4.2 Fault Matrix

The variation of the measurable parameters is observed and compared with tables showing deviations of the parameters for potential engine faults. The tables help determine the most probable fault (Figure 4-13 [7]).

Figure 4-13: Fault Matrix example [7]

Type	Fault	TIT	SHP	m_1	CPR	Vibration	Indication
Turbine (Generator)	Rotor Damage	↑	↑	↑	↑	Yes	η_t Low
	Nozzle Erosion	↑	↑	↑	↓	No	$m\sqrt{T_3}/P_3$ High
Turbine (Power)	Rotor Damage	0	↓	0	0	Yes	η_t Low, EGT High
	Nozzle Erosion	↓	↓	↓	↓	No	$m\sqrt{T_4}/P_4$ High
Compressor	F.O.D.	↑	↓	↑	↓	Yes	η_c Low, m_1 Low
	Dirty	↓	↓	↓	↓	No	η_c Low

Fault Tree and fault matrix only allow the detection of a single fault and cannot be used when two or more components have a fault. They are qualitative techniques.

4.4.3 Gas Path Analysis

The relationship between various engine measurable parameter deltas and non-measurable component health parameter deltas at certain engine operating conditions is expressed with a linear Influence Coefficient Matrix (ICM) ([7], [9] and [10]):

$$\Delta \boldsymbol{z} = H \times \Delta \boldsymbol{x}$$

Equation 4-3: Measurable parameter deltas

The deviation of engine component health parameters can be calculated with a Fault Coefficient Matrix (FCM) (or diagnostic matrix), which is the inverse of the influence coefficient matrix:

$$\Delta \boldsymbol{x} = H^{-1} \times \Delta \boldsymbol{z}$$

Equation 4-4: Health parameter deltas

Fault coefficients are generated implanting known degradation values to component characteristics.

LGPA advantages are

- Idealistically simple
- Provides quick solutions to gas turbine diagnostics
- Fault isolation and quantification
- Multiple fault diagnostics.

LPGPA main disadvantage is it requires not easily achievable conditions:

- Accurate influence coefficient matrix to describe the engine performance
- Fault and noise free sensors
- Uncorrelated measurements
- Correct choice of measurement locations

4.4.4 Nonlinear GPA (NLGPA) methods

Engine behaviour is highly nonlinear, so to account for this nonlinear model based diagnostic methods were introduced. These methods solve the nonlinear relationship between dependent and independent parameters using an iterative method.

From the LGPA the relationship between dependent and independent parameters is expressed as:

$$\Delta \boldsymbol{x} = H^{-1} \times \Delta \boldsymbol{z}$$

Using a Newton-Ralphson iterative method it can be written:

$$\boldsymbol{x}_{NEW} = \boldsymbol{x}_{OLD} + \Delta\boldsymbol{x}$$

The changes in $\Delta\boldsymbol{x}$ can be as small as required, overcoming the non-linearity problem with LGPA. Each performance change is added to the previous, iterating until convergence happens. Figure 4-14 from [7] is a graphical representation of NLGPA.

Several developments of this method have followed ([7], [10]). It improves the non-linearity issue with GPA but shares similar disadvantages as explained above as the accurate ICM needs, measurement noise, etc…

Figure 4-14: NLGPA graphical representation [7]

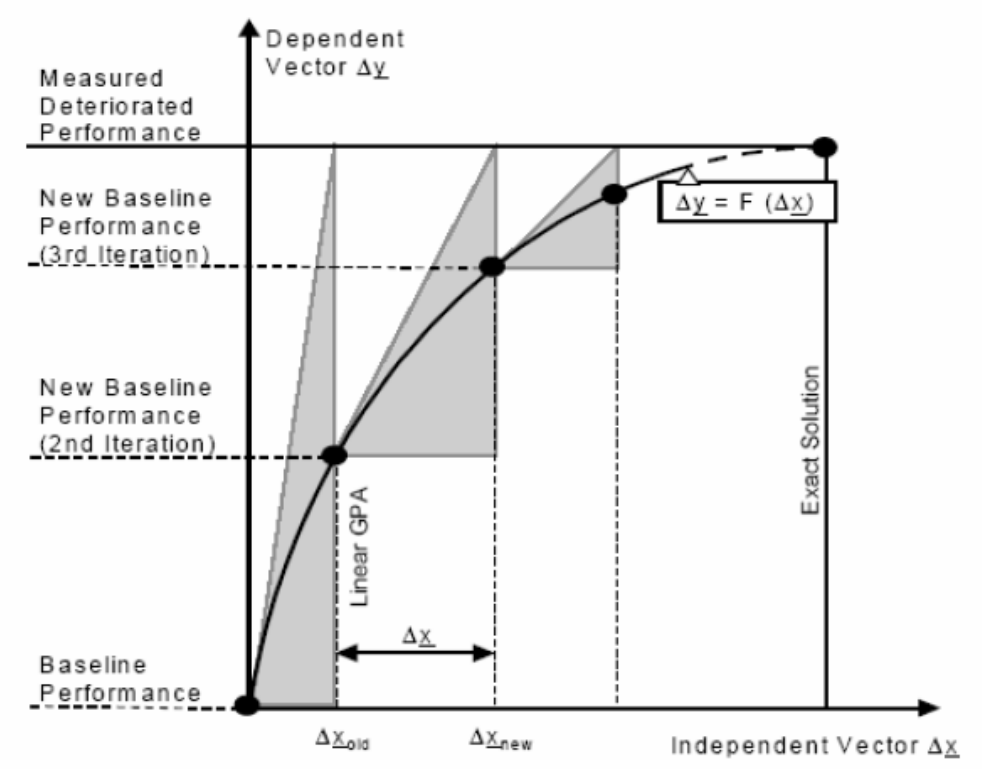

4.4.5 Artificial Neural Networks

An ANN is an information-processing paradigm inspired by the way the densely interconnected, parallel structure of the mammalian brain processes information ([11], [12], [13] and [10]). The human brain is composed of a huge number of neurons. Each neuron has three main components (Figure 4-15 [11]):

- Dendrites, in the shape of a dendritic tree, receive electrochemical stimulation from other neurons
- Soma, the central cell body
- Axon, allows the neuron to communicate to other neurons

The dendritic tree of a single neuron is connected to approximately one thousand other neurons. It receives inputs through those connections in the shape of electric charges. The dendritic tree performs a spatial and temporal summation of those charges. The aggregate input is passed to the soma. When the strength of the aggregate input is over a certain threshold, the neuron fires a signal through the axon. It is a signal of constant output communicated to other neurons via the interconnection between axon synaptic buttons and dendrites. The key idea is that the neuron receives input from other neurons and sends output to other neurons and cells. The latest estimate of the average number of neurons in a human brain is 86 bn and approximately 10^{14} synapses.

Figure 4-15: Neuron [11]

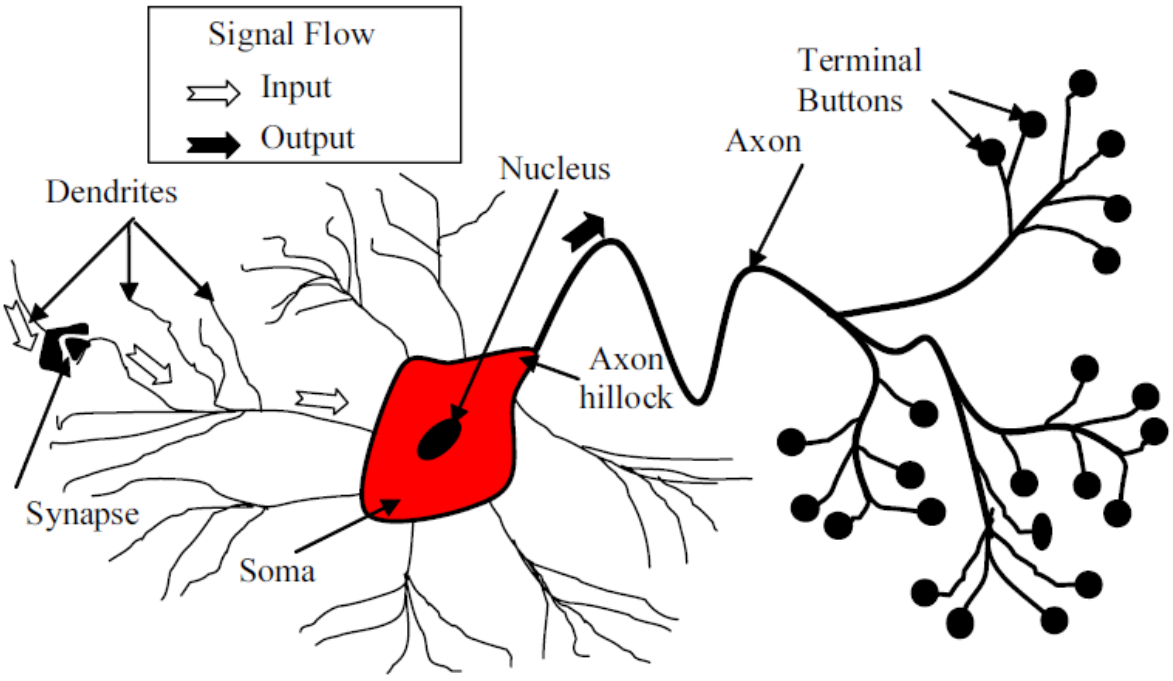

The human brain can learn by adjusting the connections between neurons. This capability plus the large parallel processing capability that the neuronal structure has, makes the human brain extremely flexible and capable. ANN tries to simulate this structure and connection method to take advantage of those two characteristics, processing capability and learning. It should be emphasized ANN are not designed to model the human brain.

An ANN is composed of a large number of highly interconnected processing elements analogous to neurons and tied together with weighted connections similar to synapses ([11]). It comprises weighted connections, adder and transfer function. ANN has to learn to be able to operate correctly. Learning typically occurs by example through training. Training consists in exposing the ANN to sets of input/output where the relationship is known. The training algorithm iteratively adjusts the connection weights to minimize the error in successive steps. A deeper description of ANN is done in Chapter 9.

Table 4-1: ANN characteristics

ANN strengths	ANN weaknesses
It can handle nonlinear relationships, as the ones amongst engine parameters	The optimal network structure for a problem is not known
It is tolerant to measurement noise or non-repeatability	Validation criteria is not well defined
It can operate with limited information	The criteria for selection of the best training algorithm for fast convergence is not understood
It can be applied on line as it converges very fast in recall mode	The rules for selecting the amount and type of data for training are minimal
	The convergence of the training algorithm is not guaranteed
	It may take long training times
	Requires data that might not be always available

The training sets of input/output will come from the engine model. A known fault will be implanted in the model and the simulation result will be used as input to the ANN, comparing results to the known fault to implement the required connection weights. This approach can be used as well to cover different ambient operating conditions.

Table 4-1 summarizes the advantages and disadvantages of ANN [11].

ANN have the advantage that only engine experimental knowledge is required for the training of neural nets and the computation time for diagnosis is very short once the neural nets are trained ([10]). In gas turbine diagnostic this experimental knowledge is difficult to attain so model generated data is used (reference Chapter 9).

4.4.6 Genetic algorithm

GA is a model based diagnostic approach and follows a search algorithm process. There are many different types of Genetic Algorithms able to perform optimization. They are based on the mechanics of natural selection and natural genetics. A “string” is the solution to a problem. Strings are collected together in “populations”. The string fitness is evaluated through an “objective function". It is defined as the difference between actual gas path measurement and estimated gas path measurement. The objective function is optimized through iterative process, until estimated component parameter $\hat{x}$ and real component parameter x are equal or near equal. The objective function must reach a minimum.

The potential strings are randomly selected to begin the search. An objective function is created for each string and fitness evaluated. A new population is created selecting the most fist strings. The GA algorithm then alters the composition of the “children” strings through genetic operators as cross over and mutation. A new iteration will find the fittest string until the search is stopped when certain parameter criteria are satisfied. The reproduction cycle can be found in Figure 4-16 from [7].

GA is a very flexible technique. It can cope with sensor bias and noise, but requires a long computational time to converge. A deeper of GA coverage for gas turbine diagnostic and sensor fault determination can be found in Zedda [54].

Figure 4-16: GA reproduction cycle [7]

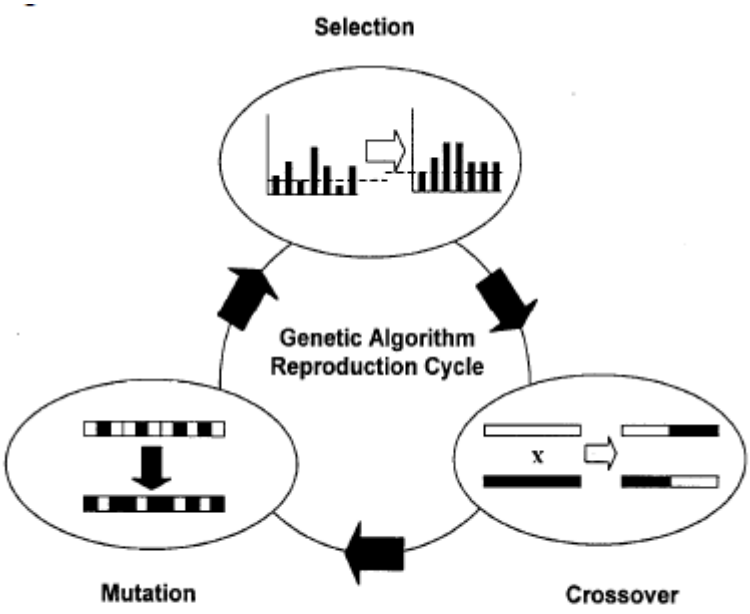

Figure 7.8 Genetic algorithm reproduction cycle

4.4.7 Fuzzy logic

It is an expert system made out of a “rule based” model. It tries to formalize the human capability for imprecise reasoning [7]. It involves (ref [10]):

- A “fuzzifier” maps crisp input numbers into fuzzy sets characterized by linguistic variables and membership functions.
- Fuzzy inference via an inference engine. The inference engine is made out of a rule library based on IF/THEN statements and a logic program based on AND/OR/NOT logic gates.
    - The inference engine maps fuzzy sets to fuzzy sets and determines the way in which the fuzzy sets are combined.
- A “defuzzifier” is sometimes needed to have a set of crisp numbers as output.

It is a very flexible technique, but model complexity is high, computational time is also high and it is difficult to determine the physical meaning of the results unless the underlying physical phenomena is well understood ([10]).

4.4.8 Comparison between techniques

The selection of one technique over others will be determined by the application. Each one has advantages and disadvantages summarized and compared in Table 4-2 below ([10]):

- Fault tree and fault matrix are simple, fast and easy to use, but are qualitative and cannot deal with more than one faulty component.
- LGPA is simple and can provide a quick solution to gas turbine diagnostics. It can detect, isolate and quantify multiple faults. But it requires a very accurate ICM, no sensor noise, uncorrelated measurements and a good choice of measurements to be accurate.
- NLGPA overcomes some of the LGPA problems but requires much longer computation time. It may have problems dealing with sensor noise and biases.
- ANN, GA and fuzzy logic can deal with sensor noise and bias and use real engine data. Once the NN, GA or rule library is created the diagnostic can be fast. But that step can take very long and is slow in computational time. These methods a more complicated than model based methods as LGPA and NLGPA.

Table 4-2: Comparison of diagnostics methods [10]

Diagnostic Methods		Earliest year of use	Model based	Model complexity	Computation speed	Coping with noise	Coping with bias
Linear model-based methods	LGPA	1967	Yes	Low	High	No	No
	Optimal estimates	1980	Yes	Fairly low	High	Yes	Yes
Non-linear model-based methods	NGPA	1992	Yes	Low	Fairly high	No	No
	Conventional optimization	1990	Yes	Medium	Low	Yes	Yes
ANN		1965	No	Fairly high	High	Yes	Yes
GA		1999	Yes	Fairly high	Low	Yes	Yes
Rule based expert systems		Early 1980	No	High	High	Yes	Yes
Rule based fuzzy expert systems		1997	No	High	Fairly high	Yes	Yes

4.5 Conclusions

After a review of Performance based diagnostic methods the reasons why ANN has been chosen for this project are:

- Data based methodology. The methodology can be implemented with real data, although in the project a model engine will be used.
- It can tackle nonlinear relationships, quite important when dealing with multiple shafts and combined fault scenarios.
- Its capability to deal with measurement noise and bias. The capability will not be used in this Thesis, but can be easily incorporated in the next development stages.
- Once trained it can be used as a standalone system and be integrated in a remote diagnostics system.
- It has a high computational speed once implemented.
- Standard commercial software tools can be used as MATLAB.
- It can be opaque to the operator who is typically only interested in the result.

Chapter 9 will go deeper into ANN and the selection of the network type considered most appropriate for this project.

5 GAS TURBINE PERFORMANCE MODEL

5.1 Introduction

This chapter will review the selected Aeroderivative Gas Turbine type and its Performance model using Cranfield's Web engine. The main objective of this Thesis is not the model, but the diagnostic tool and its suitability. The results of the model will be reviewed to ensure they match with Design Point characteristics and that Off Design makes sense. There has been no further refinement of the model in particular in off design cases. It can be the subject of future work, but requires more detailed engine information than currently available.

5.2 Selection of Gas Turbine

5.2.1 Background

Review of the literature has shown numerous papers on performance diagnostics related to off line water wash of single shaft or single shaft plus power turbine gas turbines. None has been found for a twin shaft machine where the low pressure shaft operates at a fixed speed, like the LM6000®. A reliable diagnostic tool to analyse the performance of an LM6000® type machine and determine when off line water wash is necessary can be very useful for operators. It is a fundamental part of a Maintenance program, with the benefits described in Chapter 2. It is desirable both from user and Original Equipment Manufacturer (OEM) perspective, in particular when a long term contractual service agreement exists. Paired with above reasons the author has extensive experience on this engine model.

5.2.2 The LM6000®

The LM6000® is manufactured by General Electric. It is a 2 shaft machine. The unit may have Variable or Fixed Inlet Guide Vanes into the 5 stage Low Pressure Compressor. After the LPC there is a gooseneck duct with Variable Bleed Vanes that help control the airflow. The 14th stage High Pressure Compressor has 5 stages of Variable Stator Vanes. The Compressor Rear Frame houses the combustor and it is different depending on the units' configuration. It can be a

Single Annular Combustor or Dry Low Emissions unit. After the combustor comes the 2 stage High Pressure Turbine and 5 stage Low Pressure Turbine. The Turbine Rear Frame connects the unit to an Exhaust Diffuser ([8]). Figure 5-1 is an image of the gas turbine.

Figure 5-1: LM6000®

(Courtesy of GE™ https://www.ge-distributedpower.com/news-media/download-center?slide=1)

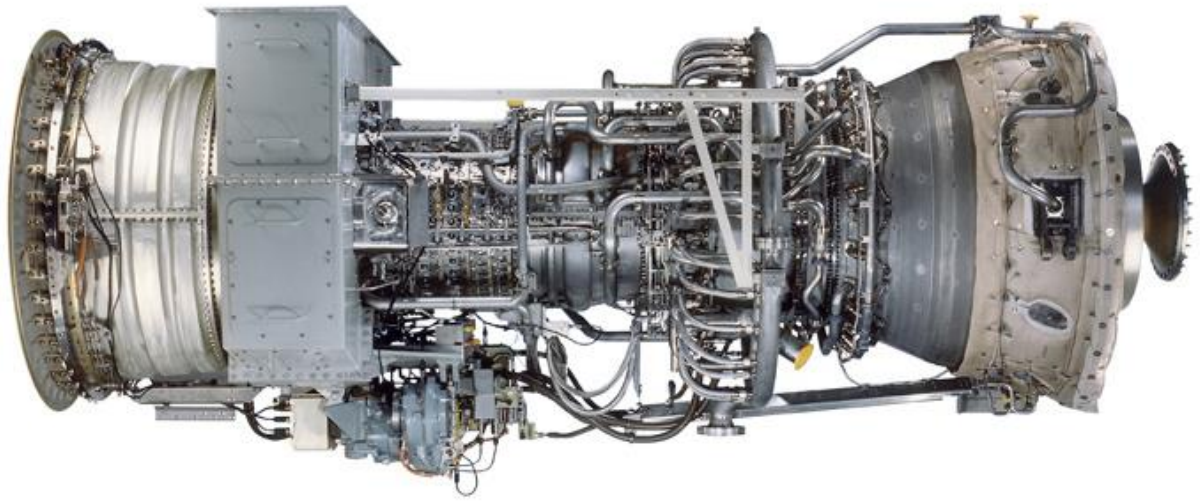

The unit can be installed in cold or hot end drive configurations, depending on which side of the gas turbine the load is connected. In the cold end drive configuration there is a radial inlet volute that connects to the FIGV/VIGV module. The exhaust is axial in this case. The hot end configuration exhaust is radial, and the inlet may vary based on plant needs (axial or radial).

The Low Pressure shaft runs at a constant 3600 rpm in 60 Hz applications. In 50 Hz applications this number may between 10 and 30 rpm ruled by the Reduction Gearbox (RGB) used to decrease the speed to the required 3000 rpm. It is also used in LNG plants for Mechanical Drive applications. In those applications LP shaft speed is variable.

It can use both gas and liquid fuels of several different types, in single or dual fuel configuration. Emissions can be controlled either by the injection of water or

steam into a SAC combustor, or by the use of Dry Low Emissions technology. DLE implies combustor staging with very fine control of air and fuel flows ([8]).

There is the possibility to use Sprint® as power augmentation both for SAC and DLE units, by injecting atomized water at LPC/HPC entry, improving unit's performance in hot ambient temperatures. There is also the option of power augmentation by injecting steam at HPC discharge called STIG® for SAC units, whenever excess of steam is available in the plant ([8]).

5.2.3 Selected Gas Turbine model

The LM6000® comes in many different configurations with varying degrees of complexity when it comes to modelling them. The author's opinion is the most reasonable approach is to start with the simplest configuration possible. That would probably be a natural gas fuelled SAC unit with FIGV and no emissions control.

5.3 Gas Turbine Performance Model

5.3.1 The need for a model

To train and validate an ANN vast amounts of accurate data in different conditions are required. There is no availability of enough real engine data, as it would mean implanting faults in it, so a mathematical model of the engine is built. Once the mathematical model is available all required engine simulations can be performed. The model is validated by comparing the design point values.

The Gas Turbine OEMs have similar mathematical models of varying degrees of complexity. The models are produced at the beginning of a Gas Turbine project and are updated constantly throughout the design process and life of the program. Both detailed design data and production test data are used for the updates.

5.3.2 The WebEngine

It is a Web based gas turbine performance simulation tool. At its core there is gas turbine performance simulation code, developed by the Department of Power and

Propulsion of Cranfield University, called Turbomatch. The WebEngine intended simulation capabilities are design point and off-design single runs/parametric analysis, engine library, engine model design, virtual engine sensors and power plant operating plan. Currently not all capabilities are available and that has impacted this Thesis negatively. Some approximations have been necessary (Chapter 9). A more detailed description of WebEngine can be found in reference ([14])

5.3.3 Gas Turbine WebEngine model

A gas turbine model was created by PhD student Asteris Apostolidis using the capabilities of Turbomatch and WebEngine as interface ([14]). The Design Point parameters were taken from reference [8]. Table 5-1 summarizes the characteristics of the engine.

Table 5-1: LM6000 Natural Gas dry ISO Performance Data

(Sea level, 15ºC, 0 inlet/exhaust losses, LHV=44194 kJ/kg @ 25ºC)

Power	43284	kW
Heat rate	8133	BTU/kW-hr
	8581	kJ/kW-hr
OPR	29:1	
LPC	2.4:1	
HPC	12:1	
Exhaust flow	125	kg/s
Exhaust temp	451	ºC
FIGV		
LPC	5 stages	
LP speed	3600	rpm
VBV	12 doors	
HPC	14 stages	
VSV	5 stages	
SAC		
HPT	2 stages	
LPT	5 stages	

The engine was simulated using the brick list below in Turbomatch nomenclature. Figure 5-2 is the engine model from the WebEngine design page.

1 - 2 Inlet

2 - 3 Low Pressure Compressor (LPC). The running speed is fixed.

3 - 4 Duct, connecting compressors

4- 5 High Pressure Compressor (HPC). Its speed can be used a "handle", although in this case it has been TET.

5 - 6 Duct. Some output airflow is diverted for High Pressure Turbine cooling. It will be an input of the appropriate brick.

Figure 5-2: Engine model from the WebEngine design page

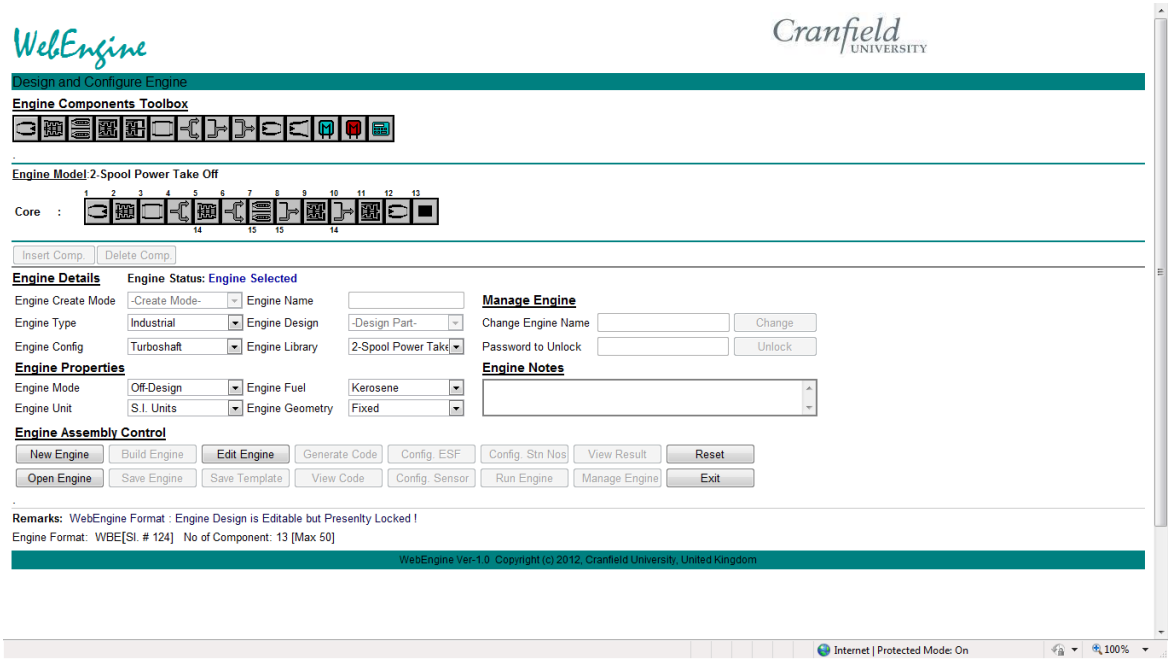

6 - 7 Combustor

7 - 8 Duct. High Pressure Turbine cooling flow is introduced here.

8 - 9 High Pressure Turbine. It is connected to High Pressure Compressor. Turbine Entry Temperature (TET) will be the “handle” used in all this Thesis model runs. It simulates better the real operation of the unit.

9 - 10 Duct, connecting HPT and LPT.

10 - 11 Low Pressure Turbine. Connected to Low Pressure Compressor, therefore it rotates at fixed speed.

11 - 12 Exhaust to ambient.

The results of the engine model run at Design Point and the data in Table 5-1 are compared in Table 5-2.

Table 5-2: Comparison between real engine rating and WebEngine model

	rating		Web Engine	diff
Power	43284	kW	43284	0.00%
SFC	0.194	kg/kW-hr	0.199	-2.31%
η	0.42		0.42	-0.16%
OPR	29.0		28.89	0.36%
LPC	2.4		2.39	0.50%
HPC	12.0		12.10	-0.83%
Exhaust flow	125	kg/s	127.39	-1.91%
Exhaust temp	451	ºC	450.61	0.09%

There is good accordance in most parameters. The difference in exhaust flow is because the reference data 125 kg/s has been used as inlet flow, not exhaust flow. This would not be acceptable if the engine model was used for a real case and would have to be adjusted.

The WebEngine currently can only run on liquid fuel. Reference [1] explains the impact of different CP between Gas and Liquid fuel in unit's performance. The estimate is SFC will decrease 1 to 2% and power output increase may increase 4 to 6%. The available data is for a Natural Gas Fuelled engine. No correction is done in the report for this circumstance. It would have to be considered if further refinement of the model data is sought.

The gas turbine model does not use Variable Geometry. The real Gas Turbine has VIGV, VBV doors in between the LPC and HPC and VSV in the HPC. If the objective of the project was the performance model of the gas turbine in Off Design conditions Variable Geometry would need to be modelled. The model will be used in its current configuration.

The final aim of this project is testing a methodology so all the above discrepancies are considered of no impact. If the methodology is deemed acceptable after the research, the Gas Turbine model block of the methodology can later be replaced by OEM cycle deck, where above limitations are not present.

The units are used in different modes:

- Peaker
- Mid merit
- Base load

When operating at part loads in droop mode, the unit's regulator is NPT (low pressure turbine speed) in order to maintain generator speed compatible to grid frequency. Base load is reached when a control limiting regulator appears. Limiting regulators are some unit's physical parameters that cannot be surpassed to protect the unit. Some of them are HPC Discharge Temperature (T3), Low pressure Turbine Inlet Temperature (T48), HPC Discharge Pressure (PS3) and Max Power. Turbomatch only has the Turbine Entry Temperature possibility to simulate based load. It is the one closer to T48 therefore TET will be used as handle. A field to explore is adding other physical handles to Turbomatch as T3.

5.4 Simulation of variable ambient conditions

The ambient temperature and pressure are varied. TET is the handle. Power (MW) and Specific Fuel Consumption are represented.

5.4.1 Ambient temperature simulation

Table 5-3 has the results of varying Tamb. Ambient temperature affects air properties. Air density decreases with increasing ambient temperature. The mass flow entering the engine is reduced with increasing ambient temperature, decreasing power.

Table 5-3: Performance variation with Tamb

ISA DEV	Power (MW)	SFC (kg/kW-hr)
-20	49.64	0.1939
-10	46.37	0.1962
0	43.28	0.1986
10	39.76	0.2026
20	36.60	0.2069
30	33.50	0.2117

Figures 5-3 and 5-4 are the same results in graphical format.

Figure 5-3: Power vs Tamb

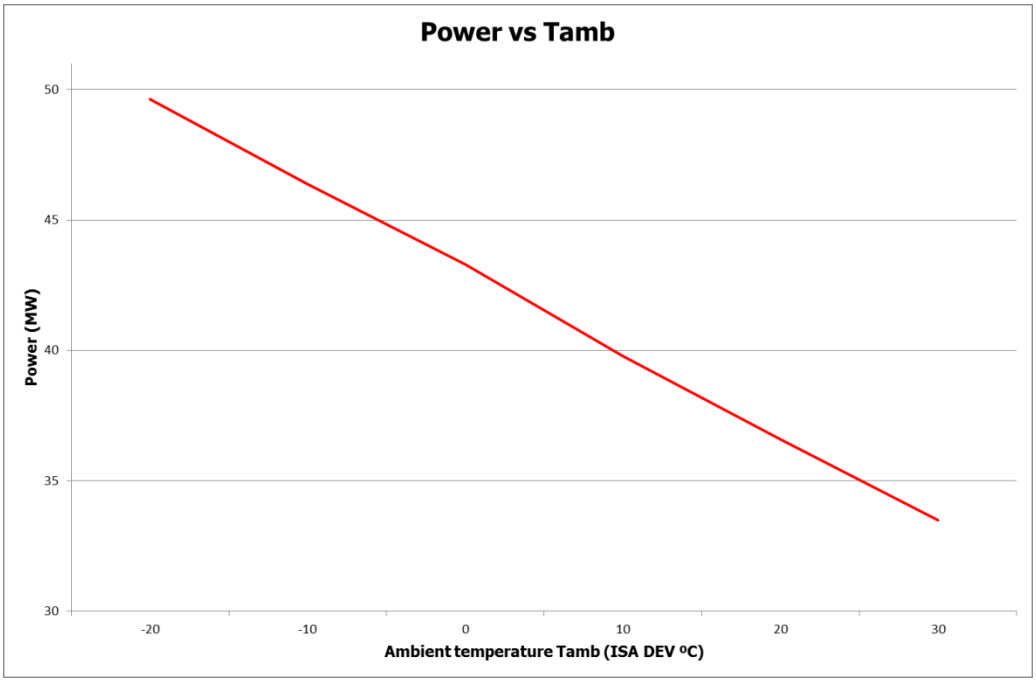

Compressor work is reduced with rising ambient temperature. It reduces the specific power output increasing fuel consumption. Also the pressure ratio and temperature ratio are reduced, decreasing engine efficiency and increasing fuel consumption.

Figure 5-4: SFC vs Tamb

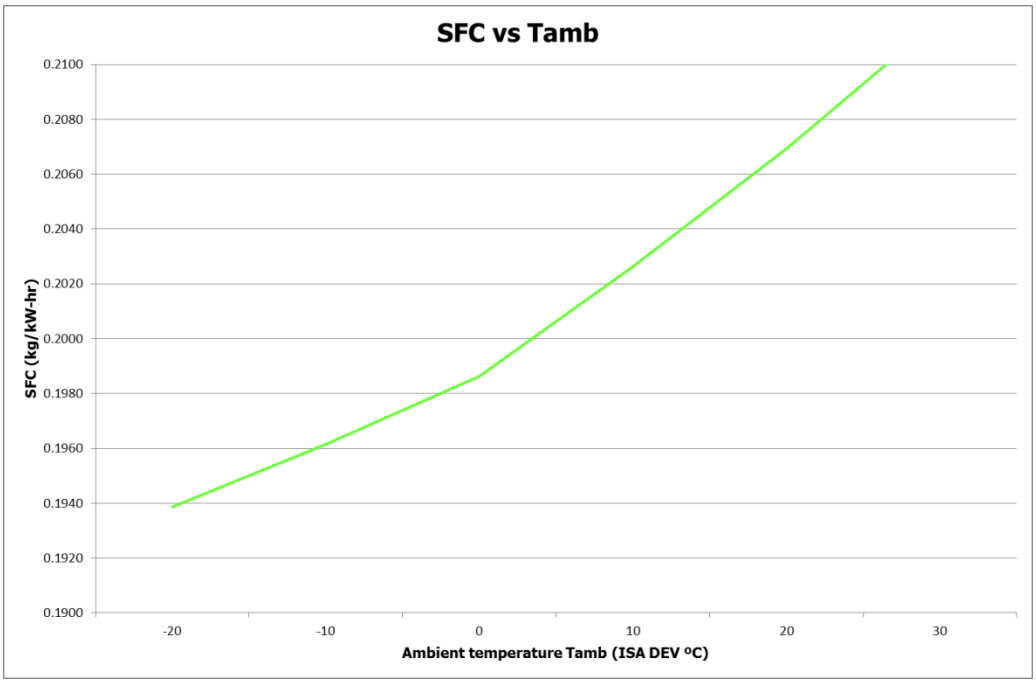

This WebEngine model has no VG, so the effect of the VG is not noted. At higher Tamb the Variable Bleed Vanes after the LPC will open to avoid surge, with higher power drop and SFC increase.

5.4.2 Altitude simulation

The variation of Power and Specific Fuel Consumption versus Site Altitude are contained in Table 5-4 and in graphical format in Figures 5-5 and 5-6. Turbomatch varies Tamb with Pamb to maintain ISA conditions when altitude is varied. It would be better if Pamb could be varied in WebEngine as an independent parameter.

Decreasing altitude decreases both air density and temperature. The reduction in density reduces the mass flow, therefore the power output. It is slightly offset by the reduction in temperature that Turbomatch applies. As the LP compressor runs at constant speed a reduction in ambient temperature means the corrected speed increases. Increased corrected speed means higher pressure and temperature ratios, thus improved thermal efficiency and SFC, as the graph shows.

Table 5-4: Performance variation with altitude

Altitude	Power (MW)	SFC (kg/kW-hr)
0	43.28	0.1986
250	42.50	0.1983
500	41.71	0.1980
1000	40.25	0.1969
1500	38.72	0.1963
2000	37.39	0.1948
2500	35.92	0.1943
3000	34.52	0.1934

Figure 5-5: Power vs Site Altitude

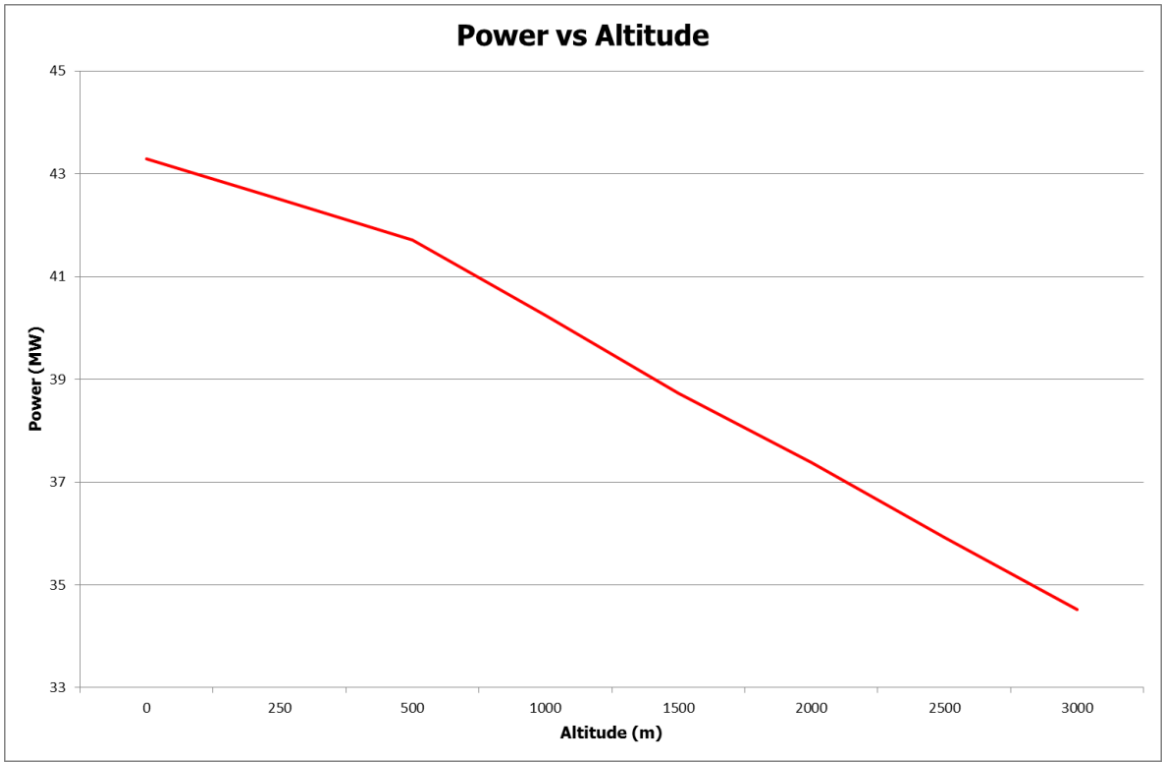

Figure 5-6: SFC vs Site Altitude

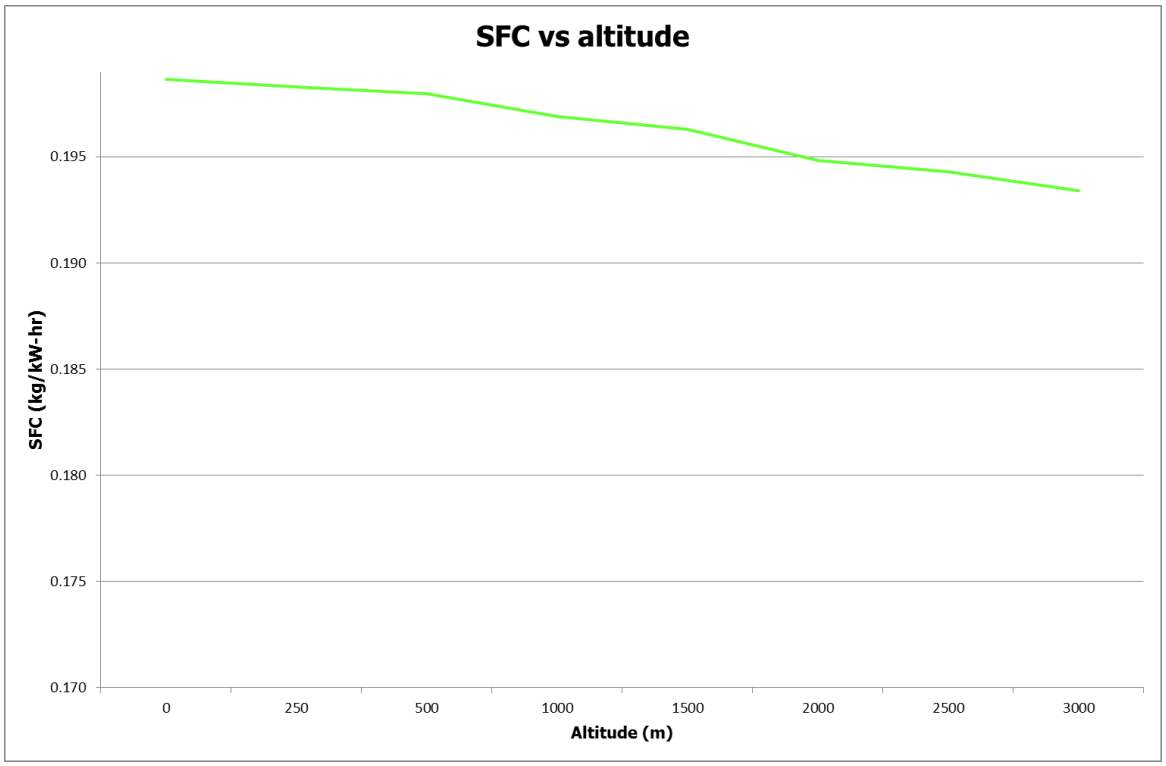

5.5 Conclusions

The model created is a working model enough to be used for the purpose of this Thesis. It misses variable geometry, the right control schedules etc… It is very difficult for a non OEM to model a full engine accurately outside of the design point due to lack of information considered proprietary by OEM.

As discussed in the Introduction the objective is not the model, but the diagnostic tool. If refined information is available, the model can be improved. Customers do have OEM cycle deck models with somehow reduced capabilities. They can be used as substitute for this WebEngine model.

6 DEGRADED PERFORMANCE

6.1 Introduction

Any gas turbine starts degrading the moment it is put into service. The causes for degradation are multiple. Some are related to normal operation wear and tear, but others are related to the environment. There is a performance penalty in degradation, both in output and fuel consumption. Figure 6-1 shows the typical degradation of a gas turbine ([18]). As it will be discussed later part of the degradation is recoverable, part of it is not. Degradation mechanisms are reviewed in this chapter.

Figure 6-1: Gas Turbine degradation sample [18]

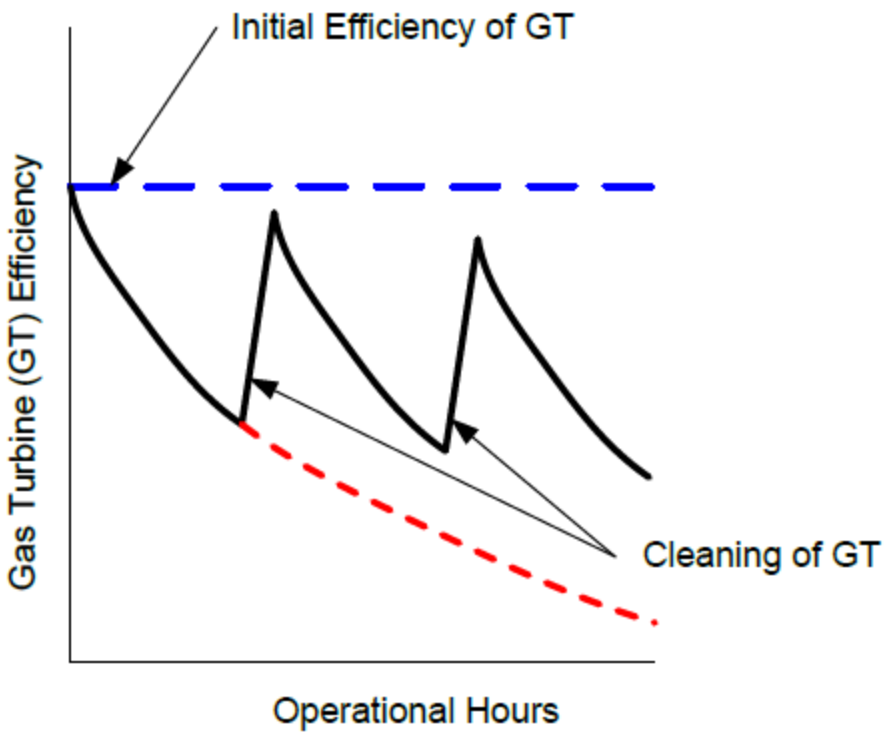

Once mechanisms have been reviewed the next step is modelling the degradation in the WebEngine model. The methodology is implementing faults in each module via the degradation of its health parameters (efficiency and flow). The results of fault implantation are then discussed.

6.2 Gas turbine degradation mechanisms

Gas turbine degradation can be classified in two main categories ([15]):

- Performance degradation
- Mechanical degradation

6.2.1 Mechanical degradation

Mechanical degradation is related to the deterioration of the gas turbine mechanical systems. Some examples are given below. It does not intend to be an exhaustive guide, just a description of the most usual encountered by the author. Mechanical degradation will impact gas turbine availability and reliability, and, in some cases, performance as well.

6.2.1.1 Bearings

Bearings are subject to normal wear and tear from the first minute of operation. Aeroderivative machines have antifriction bearings (roller and ball). In normal operation bearing elements wear and clearances open. These elements can also be subject of abnormal operation as lack of oil supply, oil contamination and sump pressurization air contamination. Lack of oil supply degrades the bearings rapidly because of high temperatures and no lubrication between parts. Contamination of any type (air or oil) may take longer to operate, but bearing life is compromised.

6.2.1.2 Seals

Seals wear throughout gas turbine operation and can be renewed at overhaul. Hot emergency shutdowns and restarts, fast ramps and contamination will open up seal clearances more than already done by normal operation. Engine operation and performance are impacted by open seal clearances. Oil and air leaks can develop, resulting in further deterioration of gas turbine parts as disks, frames, etc…

6.2.1.3 Combustors

Combustion is an aggressive process. High temperatures, combustion by-products as soot, combustion pressure instabilities (acoustics), all contribute to the degradation of combustors. Some methods of emissions control as steam or

water injection are also associated to degradation mechanisms. Water is a very aggressive media at the high pressures it has to be injected to go into the combustion chamber. It can rapidly deteriorate combustor coatings and base material. Contamination of any of the fluids entering the combustion chamber will result in early distress through corrosion, erosion or deposits that eventually will not allow normal operation.

6.2.1.4 Fuel nozzles

The interface between combustor and fuel nozzle can be an area of mechanical degradation. Depending on the detailed design of both, relative movement between combustor and fuel nozzle can deteriorate the interface surfaces of both. Also fuel or emissions suppression fluid (water, steam) contamination will accelerate the degradation of the fuel nozzles through plugging, erosion or even corrosion.

6.2.2 Performance degradation

Performance degradation is classified in two categories.

- Recoverable deterioration, which can be recovered by maintenance actions that do not require major intervention inside the gas turbine. It includes
    - Compressor fouling (on or off line washable)
    - Turbine fouling (off line washable)
    - Wear of externals that can be adjusted
- Non recoverable. A major intervention inside the gas turbine is required as a hot section repair or a major overhaul. Some types of fouling can be included in this section as it will be described later. Examples of this type of degradation are
    - Clearances on hot section blades
    - Rotating seals increased clearances
    - Compressor blades erosion and tip wear

Some authors include a third category, permanent ([15], [16]). In author's opinion the examples described as permanent are recoverable by standard maintenance actions, parts repair and substitution, although it might costly.

6.2.2.1 Fouling

Fouling can affect compressors and turbines. Particles present in the fluids entering the turbine may deposit on compressor and turbine blades. Between 50 to 60% of the total work produced in the turbine is consumed by the associated axial compressor ([17]) so degraded compressor performance will have a great impact on the overall plant's performance and revenues.

Compressor fouling can sometimes be recovered by on line, off line water washes or hand cleaning (reference Chapter 2 and [17], [22]).

Figure 6-2: Compressor blade fouling

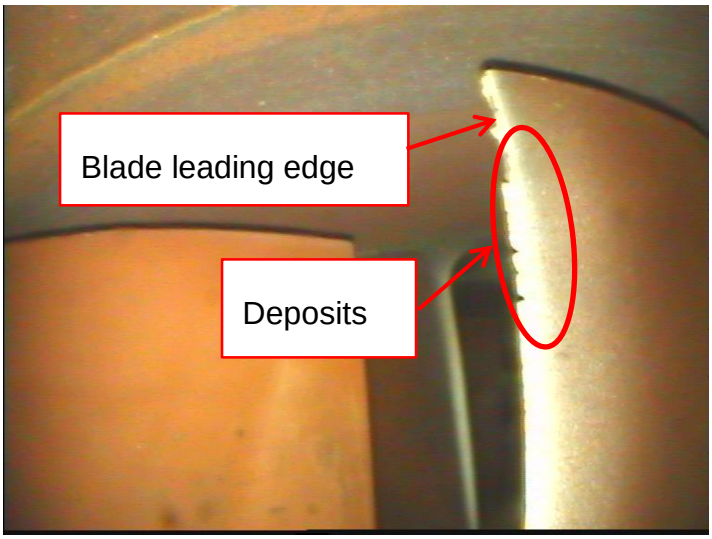

Figure 6-2, although blurry because it is a BSI picture, is a good example of compressor blade fouling. The leading edge is ragged because of the deposits. A normal off line water wash was enough to recover most of the performance of this compressor. High performance axial compressors have a large number of stages, high pressure ratios and high outlet temperatures. Fouling on the early stages of the compressor reduces the mass flow and has a larger impact on performance. The performance impact of the last stages is smaller ([17]). Figure 6-3 is a picture of a blade with baked deposits. This rotor was cleaned by hand when the effect of off line water wash proved negligible, regaining previous level of mass flow and efficiency. Hand cleaning has already been discussed in Chapter 2. A more detailed description of fouling mechanisms can be found in reference [19].

Figure 6-3: Blade with baked deposits

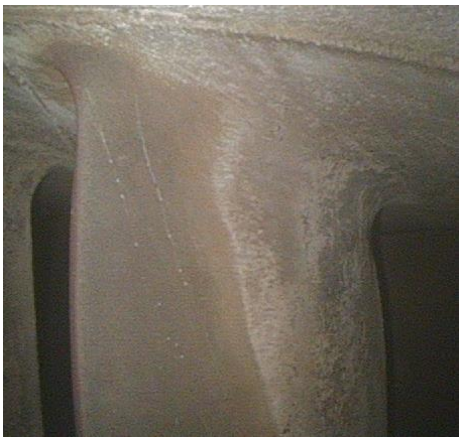

Turbine fouling occurs sometimes either related to air, fuel, and water or steam contamination. In this author's experience it is very difficult to remove and usually requires a major intervention and parts replacement. In minor cases steam injection via a boroscope port has proven successful. Figure 6-4 is a turbine contaminated by iron oxide powder present in the fuel after gas pipeline maintenance actions.

Figure 6-4: Contaminated High pressure turbine

6.2.2.2 Erosion

Erosion affects both compressors and turbines. Particles from 10 to 20 µm in the inlet air cause compressor blade erosion ([17]). High efficiency air filtering systems prevent the entry of most air borne particles of those sizes. Deficiencies

in filter house can lead to entry of enough particles to cause significant erosion ([18]).

The injection of atomized water into the axial compressor, like in fogging power augmentation systems, also causes erosion, primarily on the stages directly in front of the injection. Figure 6-5 shows the leading edge of the first stage of an axial compressor eroded by an inlet fogging system.

Figure 6-5: Eroded leading edge

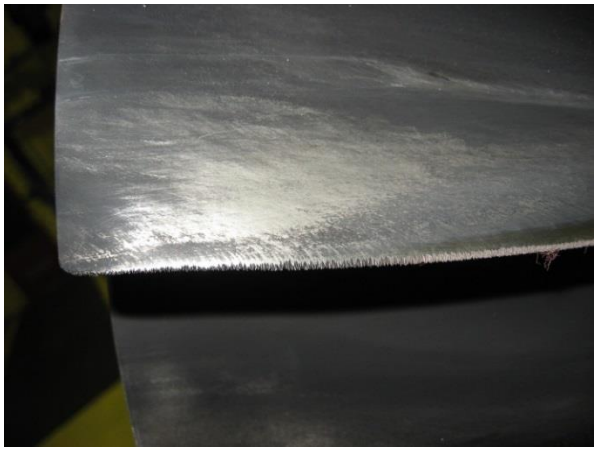

Turbine erosion is related to air, fuel, water or steam contaminants. It affects mostly the first stage of the high pressure turbine. Erosion removes the coating in coated blades, accelerating base material oxidation due to lack of the protective coating. Figure 6-6 is an example of coating removed by air contaminants.

6.2.2.3 Corrosion

Compressor corrosion is more likely to happen in marine environments. Cold parts will be attacked by sea salt (sodium chloride). It can be controlled via filtration ([18], [15]).

Turbine parts are subject to hot corrosion type I (“sulfidization”) ([20]) because of the high TET characteristic of Aeroderivative machines. It is driven by the presence of alkali metals like sodium in the air, steam or water combined with the sulphur in the fuel.

Figure 6-6: Turbine erosion

Hot corrosion type I attack takes place in the temperature range of 1500-1700F in the presence of condensed salt. This is characterized by sulphides found at the parent metal / attack zone interface. Na salts are the biggest driver of hot corrosion by the formation of Na_2SO_4 salts ([20]).

Figure 6-7: Hot corrosion

Figure 6-7 are first stage high pressure turbine blades affected by hot corrosion. The water injected for NO_x control had a high presence of Na. The blade is TBC coated, therefore not affected initially by hot corrosion. The blade tip cap is ground to dimension during manufacturing after coating and not recoated again, so the bare metal is present. The tip cap is considered sacrificial material in normal operation. It is the first area to be affected by hot corrosion attack. Once

the blade cooling passages are exposed as below, the blade cooling air flow is compromised and the blade is not considered serviceable.

6.2.2.4 Abrasion

Abrasion is caused when a rotating surface rubs on a stationary surface ([19]). Aeroderivative machines use abradable surfaces in compressor rotor and cases to allow for rubbing of blades and vanes during initial run. Honeycomb and others seal materials are used in the turbine area as well. Initial runs will remove some material of these surfaces, establishing proper operational tip clearances. The normal operation of the gas turbine plus other events, like hot shutdowns and restarts, remove further material.

The increased compressor tip clearances result in higher leakage flows with associated efficiency losses and reduction in surge margin ([19]). Turbine tip clearances reduce the efficiency of the turbine. The increase of clearance will not only reduce efficiency, but also increase the axial flow blockage. The consequence is the work extracted from the turbine is reduced and performance impacted.

6.2.2.5 Foreign Object Damage (FOD)

The ingestion of foreign object is a major source of distress for gas turbines. It can be controlled by careful maintenance practices and filtering systems. The compressor is normally affected, but liberated parts from it can also damage the turbines downstream. Figure 6-8 is an example of FOD.

Figure 6-8: FOD

6.3 Degraded Performance results

6.3.1 Fault implantation

Each engine model component can be characterized by its Isentropic Efficiency (η) and Mass Flow Capacity (Γ). Component faults are implanted by varying those two characteristics.

- Compressors

  Compressor fouling decreases efficiency and/or mass flow ([16]). Degraded performance simulation runs are done by decreasing Efficiency and Mass Flow Capacity up to -3% both in Low Pressure Compressor (LPC) and High Pressure Compressor (HPC).

- Turbines

  Turbine deterioration is due to the high environmental temperatures and potential impact of particles carried in the fluids entering the gas turbine, air, fuel and water when used. Tip clearances are increased, leading edges lose their optimal shape and nozzle area is increased ([28]). The effects are Efficiency decrease and Mass Flow Capacity increase. The ranges used for degraded performance runs are up to -3% Efficiency decrease and +3% Mass Flow Capacity increase.

6.3.2 Results

The WebEngine has the capability derived from Turbomatch to simulate engine's behaviour with implanted faults. In this Thesis the faults are implanted one at a time in each engine component, with TET as handle. The results for Power and SFC are shown in the figures below (Figures 6-9 and 6-10). Similar star diagrams for other parameters like PR, Mass Flow, HP Speed and Fuel Flow are in Appendix A, although some discussion of them is made later in this Chapter

6.3.2.1 General comments

- Efficiency degradation has a greater impact than Flow Capacity degradation for the same component. The only exception is the effect of LPC flow in Power discussed below.
- The Efficiency of the HP shaft components is critical. TET is the handle so the core cannot increase TET to accommodate for the efficiency loss of its components.
- LPT efficiency effect is quite marked and explained below.

6.3.2.2 Comments per component health parameter

- LPC efficiency

  LPC efficiency drop reduces Mass Flow, Fuel Flow and PR, so there is a reduction of Power and an increase of SFC. The effects are not too marked. At constant speed the compressor should move in a single corrected speed line. Therefore, the effects on Mass Flow and PR are small.
- LPC flow

  LPC flow capacity reduction has a marked effect on PR and Mass Flow reduction. The LPC speed is constant, so a reduction on its flow capacity has a significant impact in the engine's air flow. Fuel Flow also decreases as less air is passing through the engine. The result is a significant decrease in Power but less marked increase in SFC. The effect on HP Speed is negligible. The HP shaft matches to the new condition.

Figure 6-9: Power

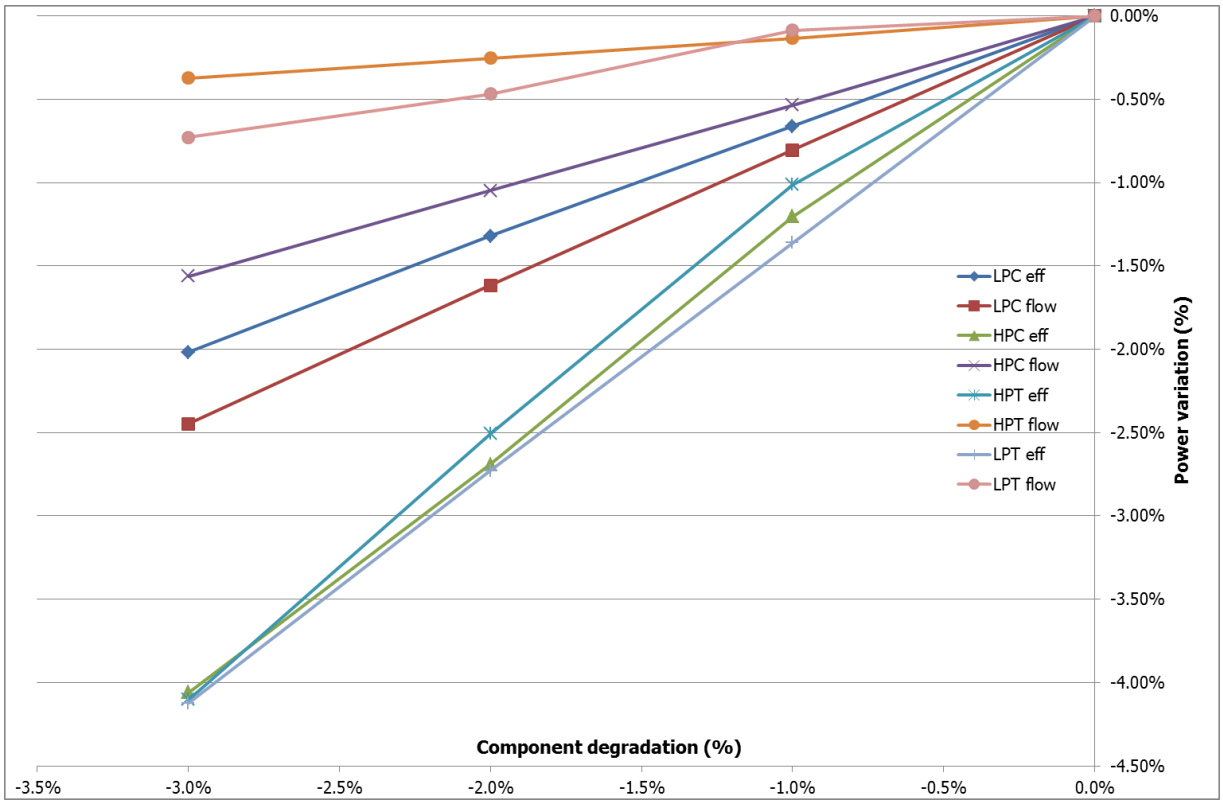

Figure 6-10: SFC

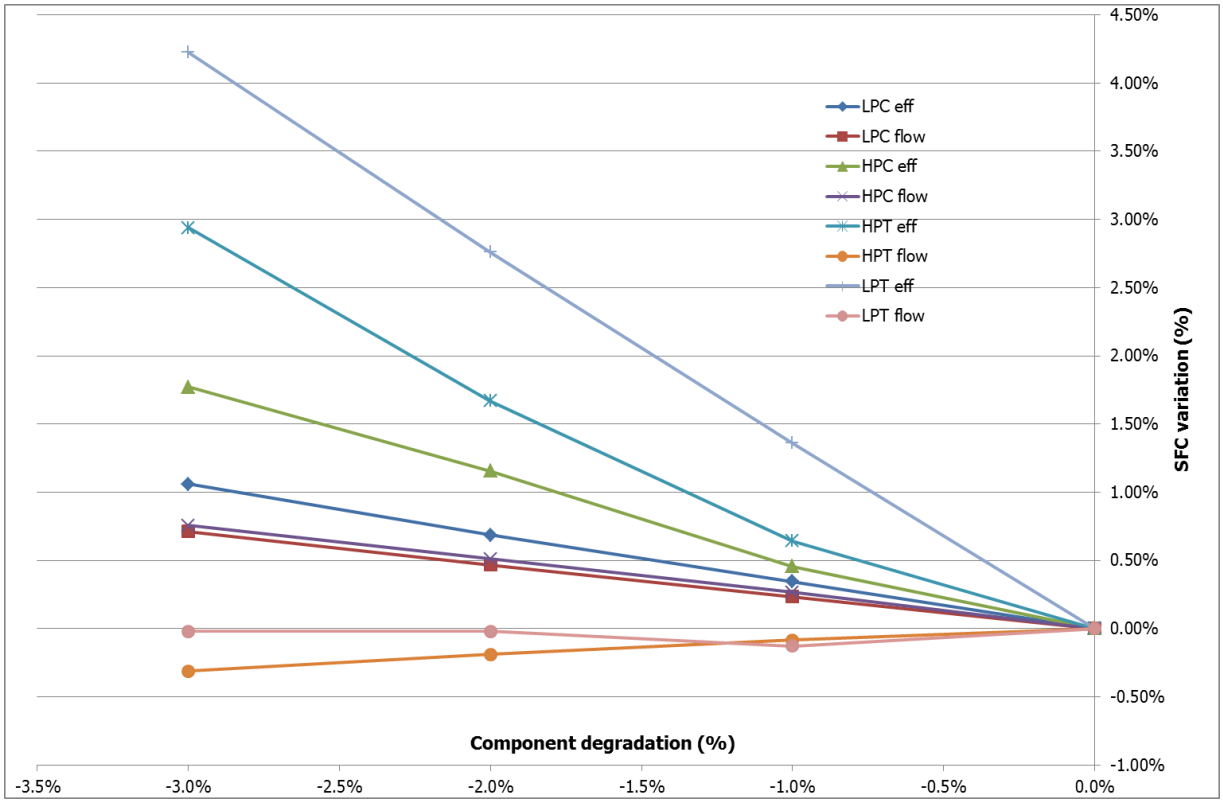

- HPC efficiency

  HPC efficiency decrease has a big impact in Mass Flow and Fuel Flow decrease. PR is as well decreased as HP Speed decreases significantly and the compressor moves to a different running point. The result is a marked decrease of Power and increase of SFC, the third largest. HP shaft accounts for approximately 60 % of the energy consumption therefore its efficiency is critical.

- HPC flow

  The reduction in HPC flow capacity means there is a small decrease in Mass Flow and Fuel Flow. But HP Speed increases and PR stays almost constant. The HP compressor matches to a new running point. The effect in Power and SFC is consequently small.

- HPT efficiency

  HPT efficiency reduction means a marked reduction of Mass Flow through the engine, Fuel Flow, HP Speed and PR. The HP shaft is mostly impacted by the reduction of work in the HPT. Once again as HP shaft consumes most of the energy in the gas turbine the SFC increase and Power reduction are very significant.

- HPT flow

  HPT flow capacity increase increases Mass Flow as the engine can accept more air. It increases as well HP Speed and PR, this one quite markedly. There is a small decrease of Fuel Flow. The combined effects almost cancel each other and mean a minor reduction of Power and a minor decrease of SFC.

- LPT Efficiency

  The reduction of LPT efficiency has a very marked effect on Power and SFC. It cannot be explained by the effect on PR, Mass Flow and Fuel Flow, as those affect mostly the core of the engine, the HP shaft. The engine runs on TET with a constant LP shaft speed. In these simulations only the LPT efficiency is modified, the rest stays equal. The LPC, at constant speed will operate in the same point. Mass Flow, driven by choked 1st stage HPT nozzle is not changed. PR and Fuel Flow are not changed. The

Power output of the units is the total Power production of the LP shaft minus the Power required to move the LP shaft and compress air in LPC. The reduced efficiency of the LPT reduces its capacity to produce Work, thus Power. If the LPC still requires the same Work the consequence is the total Power output of the unit is reduced. Fuel flow changes minimally so SFC has to increase.

- LPT flow

  The increase of LPT flow has a marked effect on Mass Flow, with minor effect in Fuel Flow and PR. The decrease of Mass Flow implies a decrease in Power. It is not too marked and, combined with the decrease in Fuel Flow, means a very minor decrease in SFC.

6.4 Conclusions

Degradation mechanisms have been reviewed and its impact in gas turbine performance and life detailed. The degraded performance of the model gas turbine has been simulated with the existing WebEngine model. The results are within expectation, although in author's opinion they might be optimistic. The real engine uses VBV to control LPC running line. When the unit degrades VBV's open, dumping high pressure air (at P25 = 2.4 bar aprox.). The impact on engine performance is exacerbated by this. It is not possible to compare OEM cycle deck model results with WebEngine results due to proprietary information issues.

7 OPTIMAL MEASUREMENT SELECTION

7.1 Introduction

The gas path instrumentation installed on the engine is critical to detect and evaluate the deterioration of the engine components. The combination installed during engine production may not be optimized to diagnose component faults. Installing additional sensors is costly and increases the chances of instrumentation faults, potentially affecting engine's reliability and availability. The selection of an optimal sensor suite, balancing diagnostic capabilities, reliability and cost is required. Several methods have been devised as LGPA ([9]), NLGPA ([28]) and Correlation between parameters ([21]). This project will use Provost's method described in reference [21].

7.2 Potential sensor suite

The list of potential engine sensors is in Table 7-1. It is cross referenced with WebEngine output parameters.

Table 7-1: Measurement set #1

Engine	Parameter	Web engine
P2	LPC inlet pressure	2*LPCin
P25	LPC exit pressure	3*LPCou
(P3)	HPC exit pressure	5*HPCou
PS3	HPC exit pr. Static	
	HPT inlet pressure	8*HPTin
P48	HPT exit pressure	9*HPTou
P8	LPT exit pressure	11*LPTou
XN25	HP shaft speed	HP PCN
MW	Generator power	Power
FF	Fuel flow	Fuel flow
T2	LPC inlet temperature	2*LPCou
T25	LPC exit temperature	3*LPCou
T3	HPC exit temperature	5*HPCou
	HPT inlet temperature	8*HPTin
T48	HPT exit temperature	9*HPTou
T8	LPT exit temperature	11*LPTou

P2 and T2 are equivalent to the ambient conditions because inlet losses will not be considered for this project although in reality there is a drop of pressure impacting performance. The condition of the inlet filtration, silencers, etc… is critical to maintain inlet losses at minimum.

The real engine has a static tap for PS3. In this report the analysis will be done for P3 (total) because it is the output of the WebEngine.

The exhaust conditions (P8 and T8) do not come with the engine itself. The user typically has sensors installed to measure them when the engine is used in a cogeneration or combined cycle. In simple cycle these sensors are not commonly used. Installing them is cheap and has no effect on engine's reliability or availability, as the engine can operate without them. The analysis below will show they can be beneficial for engine diagnostic.

There are Non gas path measurement parameters as Power (MW), High Pressure Shaft Speed (XN25) and Fuel Flow (FF). Those measurements are very useful for engine diagnose, as will be later seen. They are usually present in the engine and/or plant control systems.

Other derived parameters as SFC or heat rate (its industrial world "equivalent") are sometimes used. They provide no additional information over that provided by those measurements from which they derive.

Measurement Set #1 is the full sensor suite of table 7-1. It has 13 measurement parameters. The minimal number of measurements is equal to the number of health components 8 in this gas turbine, see below. The measurements sets discussed below will have 8 measurements each.

7.3 Engine component health parameters

As described in the previous chapter each of the engine components is described by two parameters, Isentropic Efficiency (η) and Mass Flow Capacity (Γ). The list of engine component health parameters is in Table 7-2.

Table 7-2: Engine component health parameters

Component	Parameter
LPC	Γ_{LPC}
	η_{LPC}
HPC	Γ_{HPC}
	η_{HPC}
HPT	Γ_{HPT}
	η_{HPT}
LPT	Γ_{LPT}
	η_{LPT}

7.4 Sensitivity analysis

Sensor sensitivity can be defined as the amount of change in a sensor measurement value due to a small change in engine component health parameters ([23], [24]). The diagnostic of an engine's health can only be done through the measurement of the sensors installed on it. Sensor sensitivity has to be considered when selecting engine sensor suite.

7.4.1 Exchange rate table

The analysis starts by the generation of an Exchange Rate Table (ERT). Each engine health parameter is varied 1% and the variation of each measurement parameter is calculated using equation below:

$$\Delta z = \frac{z_{new} - z_{ref}}{z_{ref}} \; x \; 100$$

Equation 7-1: Measurement parameter variation

The result is represented by a matrix of m x n format; m is the number of measurement parameters and n is the number engine health component parameters. In this case the matrix's size is 11x8.

There are two types of ERT ([25]):

- Design point ERT: This ERT shows the impact of a small change of engine component parameters on engine design point measurement parameters.

All other component parameters are maintained constant. The usual change is 1%.

- Synthesis ERT: They are utilized for off design analysis. One component is modified and no other components are redesigned. All components move or rematch to a different non-dimensional operating point. In consequence component performance parameter levels change, as well as cycle parameters.

Table 7-3: Exchange Rate Table

	LPC flow	HPC Flow	HPT flow	LPT flow	LPC eff	HPC eff	HPT eff	LPT eff
P25	-1.00%	0.77%	-0.31%	1.23%	0.50%	1.57%	2.11%	0.14%
P3	-0.72%	-0.10%	0.96%	-0.09%	-0.11%	-0.30%	-0.17%	-0.01%
P48	-0.66%	-0.20%	-0.02%	0.56%	-0.14%	-0.67%	-0.71%	0.07%
P8	0.06%	0.03%	0.04%	-0.22%	0.05%	-0.28%	-0.44%	0.04%
XN25	-0.02%	0.15%	0.23%	-0.89%	-0.15%	-1.13%	-1.52%	-0.10%
MW	-0.81%	-0.54%	-0.13%	-0.09%	-0.66%	-1.20%	-1.01%	-1.36%
FF	-0.57%	-0.27%	-0.22%	-0.21%	-0.32%	-0.75%	-0.38%	-0.02%
T25	-0.26%	0.20%	-0.08%	0.31%	0.37%	0.40%	0.53%	0.03%
T3	-0.13%	0.05%	0.30%	-0.14%	0.17%	0.29%	-0.24%	-0.01%
T48	0.01%	0.03%	-0.20%	0.18%	0.01%	-0.06%	0.30%	0.02%
T8	0.18%	0.09%	-0.21%	0.03%	0.05%	0.03%	0.41%	0.57%

In this case the ERT is a design point ERT, where one health parameter is modified by 1% and all the other are held constant at design point. The results are found in Table 7-3. Figure 7-1 is a graphical representation of the table.

7.5 Overall sensitivity

The next step is the calculation of overall sensitivity following references [25] and [23].

The overall sensitivity is the algebraic addition of each of the measurement parameters sensitivity from Table 7-3. The parameters are ranked based on the absolute value of the overall sensitivity. A group of 8 measurement sensors derives from it considering the highest absolute value measurements, named set #2.

Set #2: MW, P25, XN25, FF, P48, T25, T8, P8. Table 7-4 has the results and figure 7-2 its graphical representation.

Figure 7-1: ERT graphical representation

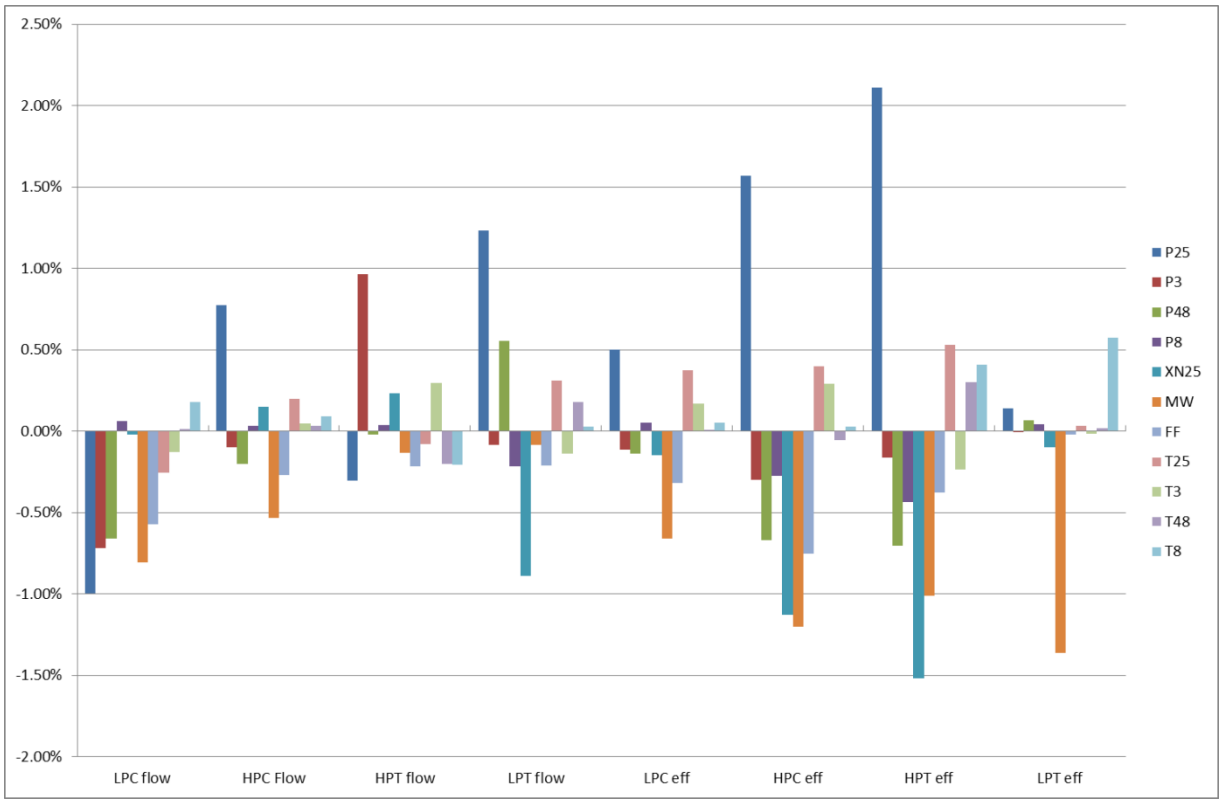

Table 7-4: Overall sensitivity results

Overall sensitivity		Rank	
P25	5.02%	MW	5.80%
P3	-0.53%	P25	5.02%
P48	-1.78%	XN25	3.43%
P8	-0.70%	FF	2.75%
XN25	-3.43%	P48	1.78%
MW	-5.80%	T25	1.51%
FF	-2.75%	T8	1.15%
T25	1.51%	P8	0.70%
T3	0.29%	P3	0.53%
T48	0.29%	T48	0.29%
T8	1.15%	T3	0.29%

Figure 7-2: Overall sensitivity

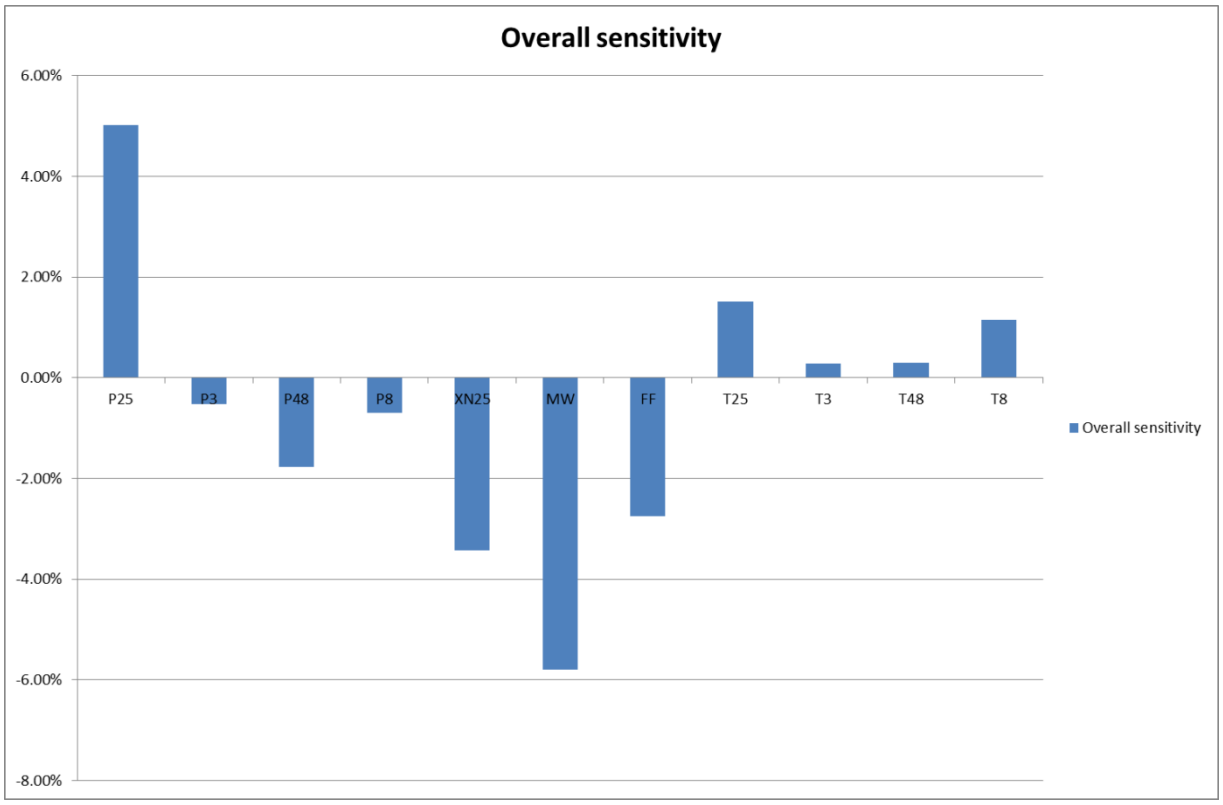

7.6 Ranking analysis

This step first evaluates the sensitivity of each measurement parameter to variations in each health parameter. It is done based on the absolute value of sensitivity, as the interest is focused on the effect of health parameter variation on the individual measurement parameter, not the sign of that variation. As an example variation on η_{LPC} has the biggest effect on MW -0.66% (reference ERT Table 7-3 above). The other measurement parameters can be organized in descending order MW, P25, T25, FF, T3, XN25, P48, P3, P8, T8, T48. This can be done for all health parameters and the results are in Table 7-5 (compressors) and Table 7-6 (turbines). The most sensitive eight for each case are highlighted in red.

Table 7-5: Ranking analysis by health parameter (compressors)

LPC flow		LPC eff		HPC Flow		HPC eff	
P25	1.00%	MW	0.66%	P25	0.77%	P25	1.57%
MW	0.81%	P25	0.50%	MW	0.54%	MW	1.20%
P3	0.72%	T25	0.37%	FF	0.27%	XN25	1.13%
P48	0.66%	FF	0.32%	P48	0.20%	FF	0.75%
FF	0.57%	T3	0.17%	T25	0.20%	P48	0.67%
T25	0.26%	XN25	0.15%	XN25	0.15%	T25	0.40%
T8	0.18%	P48	0.14%	P3	0.10%	P3	0.30%
T3	0.13%	P3	0.11%	T8	0.09%	T3	0.29%
P8	0.06%	P8	0.05%	T3	0.05%	P8	0.28%
XN25	0.02%	T8	0.05%	P8	0.03%	T48	0.06%
T48	0.01%	T48	0.01%	T48	0.03%	T8	0.03%

Table 7-6: Ranking analysis by health parameter (turbines)

HPT flow		HPT eff		LPT flow		LPT eff	
P3	0.96%	P25	2.11%	P25	1.23%	MW	1.36%
P25	0.31%	XN25	1.52%	XN25	0.89%	T8	0.57%
T3	0.30%	MW	1.01%	P48	0.56%	P25	0.14%
XN25	0.23%	P48	0.71%	T25	0.31%	XN25	0.10%
FF	0.22%	T25	0.53%	P8	0.22%	P48	0.07%
T8	0.21%	P8	0.44%	FF	0.21%	P8	0.04%
T48	0.20%	T8	0.41%	T48	0.18%	T25	0.03%
MW	0.13%	FF	0.38%	T3	0.14%	FF	0.02%
T25	0.08%	T48	0.30%	P3	0.09%	T48	0.02%
P8	0.04%	T3	0.24%	MW	0.09%	T3	0.01%
P48	0.02%	P3	0.17%	T8	0.03%	P3	0.01%

The same procedure can be applied at component level (i.e. LPC, HPC, HPT & LPT, Table 7-7) and engine level (Table 7-8). The measurement parameters are ranked adding the absolute sensitivity values at component level and then at engine level. The result is a measurement set called number set #3.

Set #3: P25, MW, XN25, P48, FF, P3, T25, T8.

Table 7-7: Ranking analysis at component level

LPC		HPC		LPT		HPT	
P25	1,49%	P25	2,34%	P25	2,42%	P25	1,37%
MW	1,47%	MW	1,74%	XN25	1,75%	P3	0,09%
FF	0,89%	XN25	1,28%	MW	1,15%	P48	0,62%
P3	0,83%	FF	1,03%	P3	1,13%	P8	0,26%
P48	0,80%	P48	0,87%	P48	0,73%	XN25	0,99%
T25	0,63%	T25	0,59%	T8	0,61%	MW	1,45%
T3	0,30%	P3	0,40%	T25	0,61%	FF	0,23%
T8	0,23%	T3	0,34%	FF	0,59%	T25	0,35%
XN25	0,17%	P8	0,31%	T3	0,53%	T3	0,15%
P8	0,11%	T8	0,12%	T48	0,50%	T48	0,20%
T48	0,02%	T48	0,09%	P8	0,47%	T8	0,60%

Table 7-8: Ranking analysis at component level

Engine level	
P25	7.62%
MW	5.80%
XN25	4.19%
P48	3.02%
FF	2.75%
P3	2.45%
T25	2.18%
T8	1.56%
T3	1.33%
P8	1.15%
T48	0.81%

7.7 Correlation analysis

7.7.1 Correlation between measurements

A gas path measurement may respond in a similar way to other measurements to changes in all component health parameters. The selection of two measurements with similar behaviour may result in unnecessary measurement redundancy. If the minimum number of gas path measurements are selected this may result in lack of enough information for a proper diagnostic. Reference [21] proposes a method based on a multidimensional “Component Change Space”.

Each component is represented by an axis perpendicular to the other component axes.

The “Component Change Space” will contain measurement vectors for each of the gas path measurements. The vectors are defined by the rows in ERT (table 7-3).

It is not possible to represent an 8-dimensional space. An example is done in a 2-dimensional space. If only η_{LPC} and η_{HPC} are considered, P25, P3 and P8 measurement vectors coordinates are:

P25 (0.50,1.57)

P3 (-0.11,-0.30)

P8 (0.05,-0.28)

They are represented in Figure 7-3. Measurement vectors P25 and P3 and nearly parallel, P8 is not. Parallel measurement vectors indicate similar response to component health parameters change. Using P25 and P3 it will be difficult to detect η_{LPC} from η_{HPC} change. The angle between vectors needs to be evaluated.

Figure 7-3: Component Change Space example

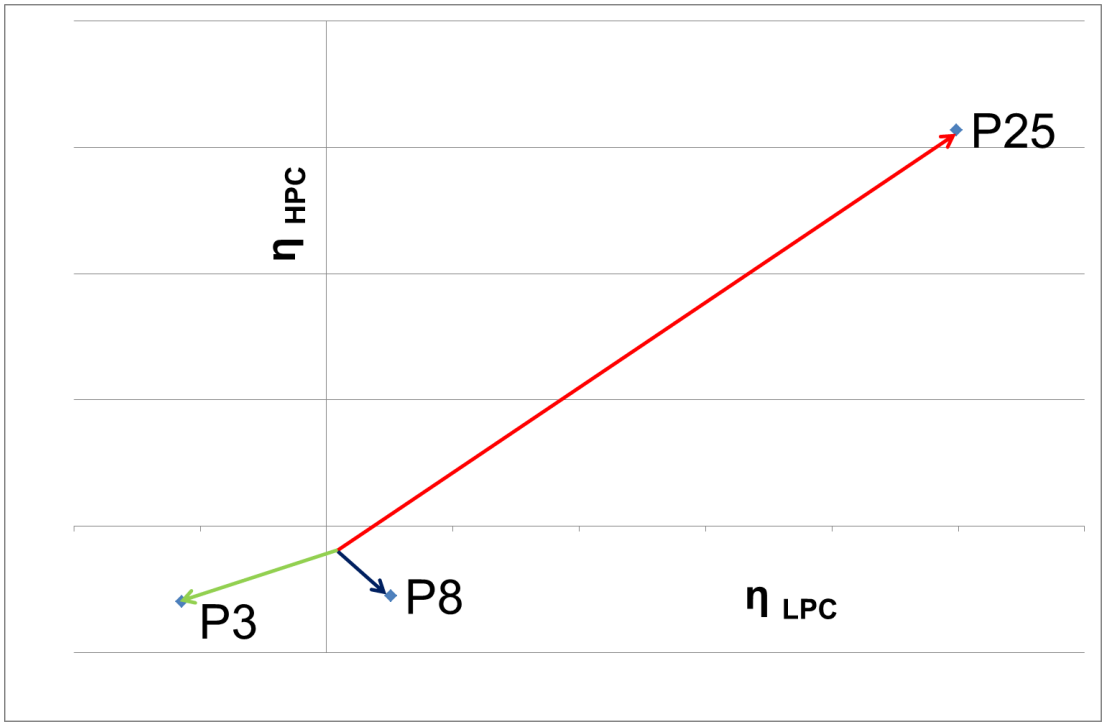

The procedure is:

- Normalize the rows of the ERT, by dividing each element by the square root of the sum of squares of that row. The result is ERT_n.
- Multiple ERT_n by $ERT_n{}^T$, transpose of ERT_n. If the rows of a matrix are considered vector coordinates this operation gives the cosine of the angle between rows. The result is a symmetrical matrix with the diagonal components all 1 called Measurement Correlation Matrix MCM = ERT_n by $ERT_n{}^T$. MCM elements will vary from 1 to -1.
    - 1 indicates both measurements change in the same direction. This is a perfect positive correlation. The amount of change is not indicated.
    - 0 indicates the measurement pair does not behave in the same way to component changes
    - -1 indicates both measurements change in opposite direction. This is a perfect negative correlation. The amount of change is not indicated.

Criteria to determine the significant correlations are required. Reference [21] uses the following:

- Below 0.7 no correlation is considered
- 0.7 to 0.8 indicates some correlation, it will be called low.
- 0.8 to 0.9 a high degree of correlation
- 0.9 to 1 a very high degree of correlation and gas path measurements can be considered redundant.

Table 7-9 shows the MCM results and correlations above 0.7.

Table 7-9: MCM and gas path measurement correlations

Correlation criteria	
Very high	0.9 to 1
High	0.8 to 0.9
Low	0.7 to 0.8

	P25	P3	P48	P8	XN25	MW	FF	T25	T3	T48	T8
P25	1.000										
P3	-0.157	1.000									
P48	-0.330	0.452	1.000								
P8	-0.894	0.214	0.425	1.000							
XN25	-0.894	0.338	0.473	0.969	1.000						
MW	-0.547	0.373	0.668	0.463	0.615	1.000					
FF	-0.536	0.397	0.748	0.536	0.654	0.798	1.000				
T25	0.961	-0.167	-0.327	-0.794	-0.838	-0.576	-0.565	1.000			
T3	-0.031	0.466	-0.082	0.208	0.180	-0.115	-0.252	0.060	1.000		
T48	0.643	-0.494	-0.160	-0.681	-0.690	-0.292	-0.180	0.595	-0.766	1.000	
T8	0.406	-0.441	-0.389	-0.367	-0.483	-0.783	-0.334	0.388	-0.415	0.591	1.000

- Very high correlations
  - XN25 and P8
  - T25 and P25
- High correlations
  - P8 and P25
  - XN25 and P25
  - T25 and XN25
- Low correlation
  - FF and P48
  - FF and MW

Summarizing to determine the gas path measurement selected based on correlation analysis

- P25 is correlated in different degrees to P8, XN25 and T25.
- P3 is not correlated to any other
- P48 is correlated to FF
- P8 is correlated to XN25 and P25
- XN25 is correlated to P25, P8 and T25
- MW is correlated to FF
- FF is correlated to P48 and MW
- T25 is correlated to P25 and XN25

- T3 and T48 are correlated
- T8 is not correlated

Therefore the path measurement set is selected as follows.

- P3 and T8, are not correlated to anybody
- XN25, it is correlated to P25, P8 and T25, which in turn show correlation amongst them. It is installed on the engine and required for engine control
- MW and FF, although correlated, are part of normal installation
- T3 and T48, although correlated are required for engine control.

The measurement set #4 is P3, T8, XN25, MW, FF, T3 and T48, based on gas path measurement correlations. An additional parameter is required to complete a full measurement set. T25 is selected as it will be installed in the engine by default.

Set #4: P3, T8, XN25, MW, FF, T3, T48, T25

7.7.2 Correlation between component health parameters

The same analysis can be done between component health parameters. Using the same “Component Change Space” methodology the correlation between health parameters can be analysed. A Component Exchange Rate Table (CERT, Table 7-10) is created by transposing ERT. It is then normalized by row ($CERT_n$), transposed ($CERT_n^T$), the normalized matrix and its transposed are then multiplied. The result is called Component Correlation Matrix CCM = $CERT_n$ x $CERT_n^T$.

Table 7-10: Component Exchange Rate Table CERT

	P25	P3	P48	P8	XN25	MW	FF	T25	T3	T48	T8
LPC flow	-1.00	-0.72	-0.66	0.06	-0.02	-0.81	-0.57	-0.26	-0.13	0.01	0.18
HPC Flow	0.77	-0.10	-0.20	0.03	0.15	-0.54	-0.27	0.20	0.05	0.03	0.09
HPT flow	-0.31	0.96	-0.02	0.04	0.23	-0.13	-0.22	-0.08	0.30	-0.20	-0.21
LPT flow	1.23	-0.09	0.56	-0.22	-0.89	-0.09	-0.21	0.31	-0.14	0.18	0.03
LPC eff	0.50	-0.11	-0.14	0.05	-0.15	-0.66	-0.32	0.37	0.17	0.01	0.05
HPC eff	1.57	-0.30	-0.67	-0.28	-1.13	-1.20	-0.75	0.40	0.29	-0.06	0.03
HPT eff	2.11	-0.17	-0.71	-0.44	-1.52	-1.01	-0.38	0.53	-0.24	0.30	0.41
LPT eff	0.14	-0.01	0.07	0.04	-0.10	-1.36	-0.02	0.03	-0.01	0.02	0.57

The same criteria as in MCM case is applied to CCM. CCM is Table 7-11.

Table 7-11: Component Correlation Matrix CCM

Correlation criteria	
Very high	0.9 to 1
High	0.8 to 0.9
Low	0.7 to 0.8

	LPC flow	HPC Flow	HPT flow	LPT flow	LPC eff	HPC eff	HPT eff	LPT eff
LPC flow	1.000							
HPC Flow	-0.009	1.000						
HPT flow	-0.099	-0.158	1.000					
LPT flow	-0.471	0.496	-0.378	1.000				
LPC eff	0.164	0.888	-0.108	0.522	1.000			
HPC eff	0.081	0.800	-0.216	0.686	0.886	1.000		
HPT eff	-0.097	0.737	-0.342	0.795	0.765	0.935	1.000	
LPT eff	0.398	0.564	-0.009	0.175	0.682	0.510	0.448	1.000

- Very high correlations
  - HPC efficiency (η_{HPC}) and HPT efficiency (η_{HPT}).
- High correlations
  - HPC flow (Γ_{HPC}) with LPC efficiency (η_{LPC}) and HPC efficiency (η_{HPC}).
  - LPC efficiency (η_{LPC}) and HPC efficiency (η_{HPC}).
- Low correlations
  - HPT efficiency (η_{HPT}) with HPC flow (Γ_{HPC}), LPT flow (Γ_{LPT}) and LPC efficiency (η_{LPC}).

The very high correlation in between HPC efficiency (η_{HPC}) and HPT efficiency (η_{HPT}) indicates it will be difficult to discriminate between them without the use of additional parameters.

7.8 Observability analysis

A steady state system is said to be observable if all system states can be uniquely determined from the system outputs ([21]). In this case the system states are the component health parameters, and the system outputs the gas path measurements. M. J. Provost in reference [21] uses a method to determine the observability of a system based on two references quoted in his thesis. This project will follow the same procedure.

The combination of two component changes may be highly correlated to change in other component. The aim of observability analysis is to detect which combinations of component changes are not detectable with the available measurement set.

Figure 7-4 is a graphical example taken from reference [21]. There are no correlations between component changes A to B, B to C or A to C. The angles between them are large. But if A and B component changes are combined, the result in dotted line, has a very small angle with component C, thus is very highly correlated.

Similar to the correlation analysis this cannot be represented with a larger number of dimensions. So a mathematical method is devised ([21], [23]).

An Observability Matrix (OBSM) is calculated from Exchange Rate Table. OBSM = ERT^{T}_{n} x ERT_{n}. ERT_{n} is row normalized Exchange Rate Table and ERT^{T}_{n} is its transpose.

Figure 7-4: Example of correlated component changes [21]

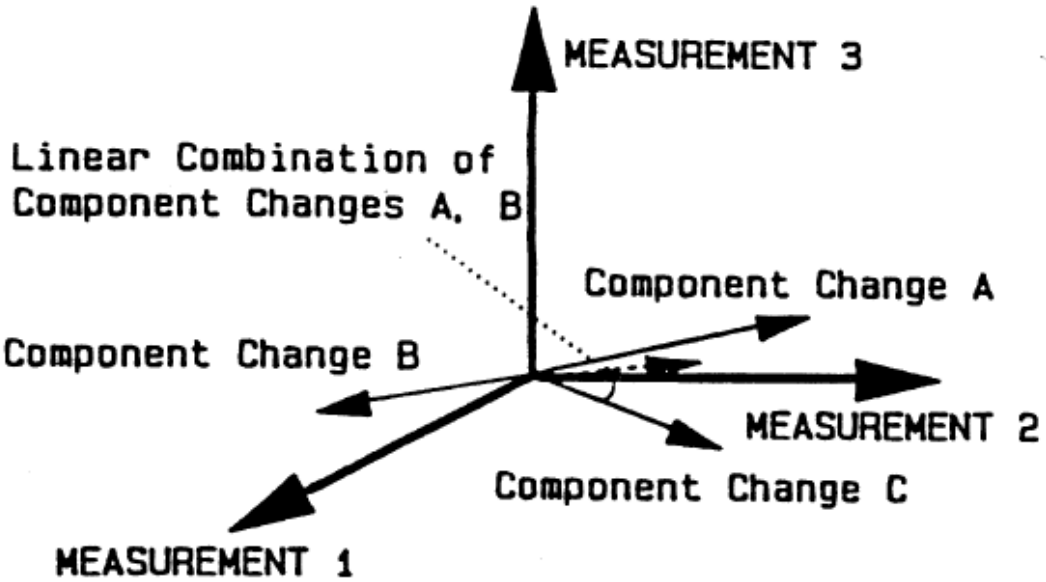

An Eigenvector is obtained for each row of OBSM from the equation

OBSM x [X] – λ [I][X] = 0

[X] measurement vector

λ Eigenvalue, for each one there is an Eigenvector that satisfies the equation

[I] Identity matrix of the same dimension as OBSM

The number of Eigenvectors will be equal to the number of component changes (states). Each Eigenvector will have associated an Eigenvalue that expresses the level of observability of the system in the direction of the associated vector.

A Measurement Delta Matrix (MDM) is calculated from MDM = ERT x Eigenvectors. This procedure is done for each measurement set. The magnitude of the Eigenvalues will determine the observability of a state (component change). The criteria used is

- Eigenvalue ≥ 1 → Highly observable state
- Eigenvalue ≥ 0.1 → Normal observable state
- Eigenvalue ≥ 0.01 → Low observable state

7.8.1 Measurement set #1

The Observability Matrix (OBSM1) is calculated from $OBSM1 = ERT1_n{}^T \times ERT1_n$, and it is shown in Table 7-12. In this case, as all gas path measurements are part of the set, ERT1 = ERT.

Table 7-12: Observability Matrix OBSM1 = ERT1n T x ERT1n

	LPC flow	HPC Flow	HPT flow	LPT flow	LPC eff	HPC eff	HPT eff	LPT eff
P25	-1.00	0.77	-0.31	1.23	0.50	1.57	2.11	0.14
P3	-0.72	-0.10	0.96	-0.09	-0.11	-0.30	-0.17	-0.01
P48	-0.66	-0.20	-0.02	0.56	-0.14	-0.67	-0.71	0.07
P8	0.06	0.03	0.04	-0.22	0.05	-0.28	-0.44	0.04
XN25	-0.02	0.15	0.23	-0.89	-0.15	-1.13	-1.52	-0.10
MW	-0.81	-0.54	-0.13	-0.09	-0.66	-1.20	-1.01	-1.36
FF	-0.57	-0.27	-0.22	-0.21	-0.32	-0.75	-0.38	-0.02
T25	-0.26	0.20	-0.08	0.31	0.37	0.40	0.53	0.03
T3	-0.13	0.05	0.30	-0.14	0.17	0.29	-0.24	-0.01
T48	0.01	0.03	-0.20	0.18	0.01	-0.06	0.30	0.02
T8	0.18	0.09	-0.21	0.03	0.05	0.03	0.41	0.57

The final result is in Table 7-13. There are:

- 3 High observable states

- 4 Normal observable states
- 1 Low observable state

Table 7-13: Observability results for set #1

			OBSM1					
Eigenvalues1	5.91	2.05	1.58	0.73	0.38	0.20	0.13	0.03
Eigenvectors1								
LPC flow	0.14	0.00	0.80	-0.28	0.10	0.39	0.30	-0.07
HPC Flow	0.15	0.14	0.09	0.11	-0.25	-0.32	0.48	0.74
HPT flow	-0.19	0.62	-0.24	0.23	0.47	0.31	0.38	-0.03
LPT flow	0.29	-0.26	-0.42	-0.02	-0.37	0.69	0.23	0.06
LPC eff	0.17	0.29	0.02	0.12	-0.51	-0.28	0.36	-0.64
HPC eff	0.48	0.63	0.00	-0.26	-0.15	0.10	-0.51	0.14
HPT eff	0.74	-0.23	-0.15	0.04	0.53	-0.24	0.17	-0.12
LPT eff	0.17	-0.03	0.30	0.88	-0.06	0.18	-0.26	0.03
MDM1								
P25	2.81	0.24	-1.44	0.12	-0.29	-0.33	-0.06	0.38
P3	-0.62	0.43	-0.76	0.46	0.45	0.03	0.17	-0.01
P48	-0.82	-0.49	-0.66	0.34	-0.44	0.34	-0.02	0.01
P8	-0.49	0.02	0.21	0.10	-0.12	-0.05	0.07	-0.01
XN25	-1.99	-0.01	0.51	0.23	-0.15	-0.33	0.24	0.17
MW	-1.87	-0.80	-0.90	-0.86	0.09	-0.18	-0.01	-0.01
FF	-0.84	-0.59	-0.30	0.21	0.06	-0.25	-0.22	-0.03
T25	0.75	0.13	-0.36	0.06	-0.20	-0.16	0.07	-0.06
T3	-0.12	0.51	-0.08	0.04	-0.09	-0.03	-0.06	-0.01
T48	0.30	-0.27	-0.05	-0.01	-0.01	-0.02	0.06	-0.01
T8	0.51	-0.20	0.30	0.43	0.04	-0.01	-0.06	0.00

7.8.2 Measurement set #2

This measurement set has the following parameters

Set #2: MW, P25, XN25, FF, P48, T25, T8, P8

Therefore ERT2 becomes (Table 7-14)

Table 7-14: ERT2

	LPC flow	HPC Flow	HPT flow	LPT flow	LPC eff	HPC eff	HPT eff	LPT eff
P25	-1.00	0.77	-0.31	1.23	0.50	1.57	2.11	0.14
P48	-0.66	-0.20	-0.02	0.56	-0.14	-0.67	-0.71	0.07
P8	0.06	0.03	0.04	-0.22	0.05	-0.28	-0.44	0.04
XN25	-0.02	0.15	0.23	-0.89	-0.15	-1.13	-1.52	-0.10
MW	-0.81	-0.54	-0.13	-0.09	-0.66	-1.20	-1.01	-1.36
FF	-0.57	-0.27	-0.22	-0.21	-0.32	-0.75	-0.38	-0.02
T25	-0.26	0.20	-0.08	0.31	0.37	0.40	0.53	0.03
T8	0.18	0.09	-0.21	0.03	0.05	0.03	0.41	0.57

Following the same procedure as in Measurement set #1 case the results for Measurement set #2 are in Table 7-15. There are

- 2 High observable states
- 3 Normal observable states
- 3 Low observable states

Table 7-15: Observability results for set #2

			OBSM2					
Eigenvalues2	5.27	1.34	0.79	0.35	0.19	0.03	0.02	0.00
Eigenvectors2								
LPC flow	0.10	0.73	-0.23	-0.14	-0.42	-0.34	0.30	0.03
HPC Flow	0.16	0.13	-0.01	0.41	0.38	0.35	0.72	-0.01
HPT flow	-0.05	0.09	-0.32	0.25	-0.21	0.40	-0.24	0.75
LPT flow	0.25	-0.51	0.14	0.31	-0.67	-0.16	0.29	0.03
LPC eff	0.20	0.08	-0.03	0.61	0.32	-0.62	-0.27	0.12
HPC eff	0.57	0.05	-0.43	0.13	-0.10	0.33	-0.32	-0.50
HPT eff	0.71	-0.12	0.11	-0.48	0.23	-0.10	0.08	0.42
LPT eff	0.18	0.39	0.79	0.17	-0.16	0.26	-0.25	-0.02
MDM2								
P25	2.86	-1.36	0.16	0.28	0.40	0.31	0.18	-0.06
P48	-0.86	-0.73	0.51	0.36	-0.32	0.01	0.01	0.00
P8	-0.49	0.22	0.04	0.16	0.06	-0.03	0.00	-0.02
XN25	-1.98	0.55	0.04	0.33	0.35	0.15	0.10	0.05
MW	-1.97	-1.16	-0.44	-0.47	0.11	-0.19	0.20	0.00
FF	-0.91	-0.40	0.45	-0.26	0.22	0.03	-0.08	-0.01
T25	0.77	-0.33	0.03	0.22	0.18	-0.08	-0.02	0.01
T8	0.47	0.29	0.51	-0.10	0.00	-0.03	0.04	0.00

7.8.3 Measurement set #3

The parameters included are

Set #3: P25, MW, XN25, P48, FF, P3, T25, T8

ERT3 is shown in Table 7-16.

Table 7-16: ERT3

	LPC flow	HPC Flow	HPT flow	LPT flow	LPC eff	HPC eff	HPT eff	LPT eff
P25	-1.00	0.77	-0.31	1.23	0.50	1.57	2.11	0.14
P3	-0.72	-0.10	0.96	-0.09	-0.11	-0.30	-0.17	-0.01
P48	-0.66	-0.20	-0.02	0.56	-0.14	-0.67	-0.71	0.07
XN25	-0.02	0.15	0.23	-0.89	-0.15	-1.13	-1.52	-0.10
MW	-0.81	-0.54	-0.13	-0.09	-0.66	-1.20	-1.01	-1.36
FF	-0.57	-0.27	-0.22	-0.21	-0.32	-0.75	-0.38	-0.02
T25	-0.26	0.20	-0.08	0.31	0.37	0.40	0.53	0.03
T8	0.18	0.09	-0.21	0.03	0.05	0.03	0.41	0.57

The results of the analysis with this different set are shown in Table 7-17. There are

- 2 High observable states
- 4 Normal observable states
- 2 Low observable states

Table 7-17: Observability results for set #3

			OBSM3					
Eigenvalues3	4.76	1.37	0.80	0.64	0.25	0.15	0.02	0.01
Eigenvectors3								
LPC flow	0.21	-0.81	-0.21	-0.07	0.22	0.29	0.07	0.34
HPC Flow	0.20	-0.01	-0.06	0.09	0.17	-0.59	-0.66	0.37
HPT flow	-0.12	0.24	-0.51	0.74	0.11	0.24	0.03	0.20
LPT flow	0.19	0.45	0.20	-0.28	0.62	0.41	-0.07	0.27
LPC eff	0.25	0.07	-0.08	0.04	0.33	-0.56	0.71	0.08
HPC eff	0.57	0.04	-0.44	-0.07	0.13	0.06	-0.19	-0.65
HPT eff	0.65	0.19	0.11	0.06	-0.60	0.15	0.12	0.37
LPT eff	0.23	-0.20	0.67	0.59	0.20	0.05	-0.04	-0.26
MDM3								
P25	2.64	1.75	0.16	-0.32	-0.22	-0.19	-0.38	-0.02
P3	-0.62	0.72	-0.24	0.78	-0.10	0.07	0.01	0.02
P48	-0.93	0.60	0.54	-0.11	0.47	0.09	-0.01	0.00
XN25	-1.87	-0.66	-0.02	0.36	0.18	-0.61	-0.10	0.04
MW	-2.10	0.58	-0.19	-0.87	-0.38	0.10	0.00	0.19
FF	-0.95	0.20	0.50	-0.08	-0.31	-0.07	0.02	-0.07
T25	0.73	0.46	0.02	-0.07	0.03	-0.19	0.08	0.01
T8	0.51	-0.22	0.48	0.19	-0.06	0.02	0.00	0.04

7.8.4 Measurement set #4

Measurement set #4 has the below list of parameters.

Set #4: P3, T8, XN25, MW, FF, T3, T48, T25

Table 7-18 has ERT4.

Table 7-18: ERT4

	LPC flow	HPC Flow	HPT flow	LPT flow	LPC eff	HPC eff	HPT eff	LPT eff
P3	-0.72	-0.10	0.96	-0.09	-0.11	-0.30	-0.17	-0.01
XN25	-0.02	0.15	0.23	-0.89	-0.15	-1.13	-1.52	-0.10
MW	-0.81	-0.54	-0.13	-0.09	-0.66	-1.20	-1.01	-1.36
FF	-0.57	-0.27	-0.22	-0.21	-0.32	-0.75	-0.38	-0.02
T25	-0.26	0.20	-0.08	0.31	0.37	0.40	0.53	0.03
T3	-0.13	0.05	0.30	-0.14	0.17	0.29	-0.24	-0.01
T48	0.01	0.03	-0.20	0.18	0.01	-0.06	0.30	0.02
T8	0.18	0.09	-0.21	0.03	0.05	0.03	0.41	0.57

The calculations are in Table 7-19.

There are

- 2 High observable states
- 3 Normal observable states
- 3 Low observable states

Table 7-19: Observability results for Set #4

					OBSM4			
Eigenvalues4	4.16	1.91	0.96	0.66	0.22	0.09	0.00	0.00
				Eigenvectors4				
LPC flow	0.25	-0.07	-0.72	-0.32	0.48	0.21	0.18	-0.06
HPC Flow	0.15	0.14	-0.09	0.02	-0.22	0.67	-0.62	0.25
HPT flow	-0.29	0.62	0.17	0.32	0.59	0.22	0.08	-0.03
LPT flow	0.31	-0.12	0.38	-0.17	0.22	0.10	0.32	0.74
LPC eff	0.20	0.34	0.03	-0.05	-0.48	0.40	0.62	-0.24
HPC eff	0.38	0.66	-0.05	-0.34	-0.09	-0.49	-0.22	0.09
HPT eff	0.69	-0.17	0.36	0.20	0.27	0.06	-0.14	-0.48
LPT eff	0.28	0.04	-0.40	0.78	-0.13	-0.20	0.11	0.29
				MDM4				
P3	-0.75	0.43	0.62	0.62	0.27	0.07	0.00	0.00
XN25	-1.86	-0.28	-0.76	0.24	-0.32	0.48	0.00	0.00
MW	-1.94	-0.99	0.79	-0.61	-0.03	-0.04	0.00	0.00
FF	-0.80	-0.65	0.22	0.32	-0.27	-0.15	0.00	0.00
T25	0.68	0.26	0.44	-0.01	-0.22	0.07	0.00	0.00
T3	-0.18	0.50	0.00	0.00	-0.10	-0.03	0.00	0.00
T48	0.32	-0.23	0.13	0.00	0.00	0.04	0.00	0.00
T8	0.59	-0.14	-0.24	0.39	-0.04	-0.03	0.00	0.00

7.9 Selection of Measurement Set

7.9.1 Methodology

Several measurement sets have been evaluated in the preceding pages. The next step is testing the capability of those measurement sets to detect engine component faults. Four simulation scenarios of potential engine degradation cases are chosen and run in the WebEngine model. The fault cases are in Table 7-20.

- FC1 is a case of LPC fouling.

- FC2 simulates HPC fouling. It can happen with the use of on line water wash. The contamination is removed from the LPC but sticks on to the HPC.
- FC3 is centered on the HPT. It simulates an HPT approaching its expected life.
- FC4 both compressors are mildly fouled compared with other fault cases.

Figure 7-5 is a graphical representation of the variation of measurement parameters between Design Point (DP) and each Fault Case (FC).

Table 7-20: Fault cases

	Implanted faults
FC 1	η_{LPC} = -3%
	Γ_{LPC} = -5%
FC 2	η_{HPC} = -3%
	Γ_{HPC} = -5%
FC 3	η_{HPT} = -2%
	Γ_{HPT} = 2%
FC 4	η_{LPC} = -1%
	Γ_{LPC} = -2%
	η_{HPC} = -1%
	Γ_{HPC} = -2%

Figure 7-5: Variation of measurement parameters

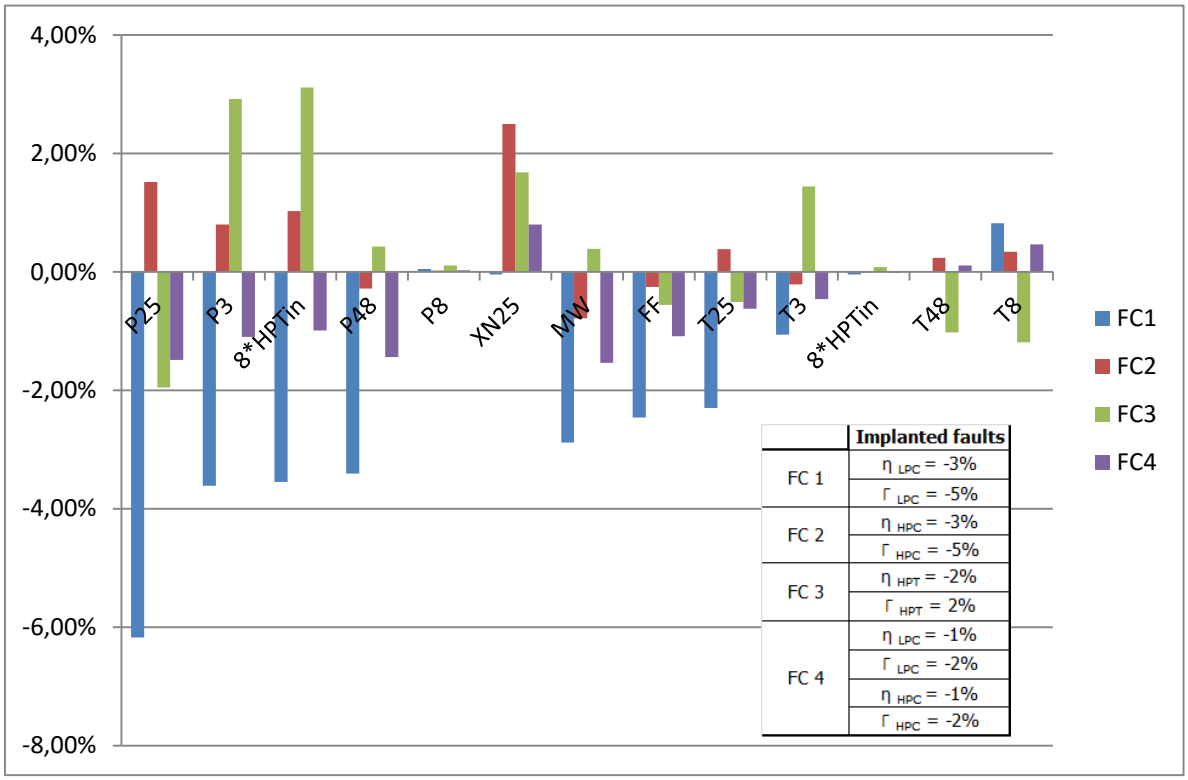

The cases are analysed using LGPA. The simplicity of the process is the reason why LGPA is preferred. The steps that applied to each fault case and measurement set are ([7], [28]):

- Calculate the ICM for each measurement set using the WebEngine. The ERT has already been calculated in Chapter 6. The ICM for each measurement set is the ERT minus the rows of those instruments that are not present in the set. Table 7-21 is an example of ICM for Set #3:

Table 7-21: ICM3

	LPC flow	HPC Flow	HPT flow	LPT flow	LPC eff	HPC eff	HPT eff	LPT eff
P25	-1.00	0.77	-0.31	1.23	0.50	1.57	2.11	0.14
P3	-0.72	-0.10	0.96	-0.09	-0.11	-0.30	-0.17	-0.01
P48	-0.66	-0.20	-0.02	0.56	-0.14	-0.67	-0.71	0.07
XN25	-0.02	0.15	0.23	-0.89	-0.15	-1.13	-1.52	-0.10
MW	-0.81	-0.54	-0.13	-0.09	-0.66	-1.20	-1.01	-1.36
FF	-0.57	-0.27	-0.22	-0.21	-0.32	-0.75	-0.38	-0.02
T25	-0.26	0.20	-0.08	0.31	0.37	0.40	0.53	0.03
T8	0.18	0.09	-0.21	0.03	0.05	0.03	0.41	0.57

- Calculate the Fault Coefficient Matrix (FCM), the inverse of ICM. Table 7-22 is the FCM for set number 3

Table 7-22: FCM3

-0.29	0.00	0.01	0.00	0.74	-1.73	0.00	1.76
1.02	-0.02	0.01	1.42	0.77	-1.79	-1.19	1.83
-0.13	0.96	0.00	-0.01	0.36	-1.19	-0.03	0.85
0.05	0.04	1.00	-0.14	0.62	-1.65	-0.22	1.28
-1.03	0.01	0.00	-0.01	0.01	-0.02	4.02	0.03
0.37	-0.54	0.00	-0.39	-1.60	1.82	-1.60	-3.80
-0.13	0.52	-0.61	-0.15	1.01	-0.78	0.85	2.38
0.04	0.00	0.38	-0.09	-0.89	0.93	-0.68	-0.35

- The deviation of measurement parameters vector is the difference between measurement parameter vector of the new and clean engine z_{DPm} and the measurement parameter vector of the Fault Case z_{FCm}.

$$\Delta z_{FCm} = \frac{z_{FCm} - z_{DPm}}{z_{DPm}}$$

Equation 7-2: Deviation of measurement parameter vector

Where FC is the Fault Case number, m is the measurement set number and DP is Design Point.

- The health component deviation vector of the Fault Case Δx_{FCm} is calculated but the following equation

$$\Delta x_{FCm} = FCM_m \times \Delta z_{FCm}$$

- The Root Mean Square (RMS) error of estimation is calculated for each Fault Case and measurement set. The measurement set that portraits the fault with the least RMS is the considered the most suitable for that particular Fault Case.

$$RMS_{FCm} = \sqrt{\frac{(\Delta x_{NOMm} - \Delta x_{FCm})^2}{M}}$$

Equation 7-3: Root Mean Square error

Where M is the number of parameters, 8 in this case.

The results of Chapter 6 and above are then combined to select the most suitable measurement set.

7.9.2 Results

A sample of the results is shown for FC4 (Compressors fouling) and set #3: P25, MW, XN25, P48, FF, P3, T25, T8.

Tables 7-21 and 7-22 are ICM3 and FCM3. The difference between measurement parameter vector of the new and clean engine z_{DP} and the measurement parameter vector of the Fault Case z_{FC}, is Δz_{43} (Table 7-23):

$$\Delta z_{43} = \frac{z_{43} - z_{DP3}}{z_{DP3}}$$

Equation 7-4: Fault case 4 deviation

Table 7-23: Deviation of Measurement Parameter Vector for FC 4 (%)

Δz_{34}	
P25	-1.5
P3	-1.1
P48	-1.4
XN25	0.8
MW	-1.5
FF	-1.1
T25	-0.6
T8	0.5

The health component deviation vector Δx_{FCm} calculated as per Equation 7-5 is in Table 7-24:

$$\Delta x_{43} = FCM_3 \times \Delta z_{43}$$

Equation 7-5: Fault case 4 health component deviation

Table 7-24: Health Component Deviation Vector for FC4 (%)

Δx_{34}	
LPC flow	1.99
HPC Flow	1.97
HPT flow	0.29
LPT flow	-0.08
LPC eff	-0.96
HPC eff	-0.57
HPT eff	0.26
LPT eff	-0.07

The RMS for this Fault Case and measurement set:

$$RMS_{43} = \sqrt{\frac{(\Delta x_{NOM3} - \Delta x_{43})^2}{8}} = 0.02$$

Table 7-25 summarizes RMS for each Measurement Set and Fault Case:

Table 7-25: Summary of FC and MS

			RMS		
	Implanted faults	**Set #1**	**Set #2**	**Set #3**	**Set #4**
FC 1	η_{LPC} = -3%		0.04	0.05	0.22
	Γ_{LPC} = -5%				
FC 2	η_{HPC} = -3%		0.06	0.04	0.23
	Γ_{HPC} = -5%				
FC 3	η_{HPT} = -2%		0.03	0.01	0.96
	Γ_{HPT} = 2%				
FC 4	η_{LPC} = -1%		0.04	0.02	0.07
	Γ_{LPC} = -2%				
	η_{HPC} = -1%				
	Γ_{HPC} = -2%				

7.10 Conclusion

The first consideration to select the most appropriate measurement set is what the aim of the diagnostic is. This project objective is to build a water wash diagnostic tool to support day to day operation of a unit. The most common issue in day to day plant operation related to performance is determining the condition of unit's compressors, when to perform off line water washes. Additionally for CBM the condition of the HPT will be critical to determine the schedule for Hot Section Repair, so the capability of a diagnostic tool to discriminate HPT deterioration should be considered, although it is not the subject of this Thesis.

Measurement set #3 (P25, P3, P48, XN25, MW, FF, T25, T8) has the lowest error in terms of RMS for 3 Fault Cases. In particular it has the lowest error for FC#4 that simulates a mildly compressor fouling. It also has good results for FC#1 heavy LPC fouling, FC#2 HPC heavy fouling and FC#3 HPT deterioration. This makes it the most attractive set in terms of detecting fouling condition, required to determine off line water wash need.

Reviewing the preceding results, set #3 has good Overall Sensitivity, as it is similar to set #2 replacing P8 by P3, both with similar order of magnitude sensitivity. Set #3 is derived from the Ranking Analysis at engine level. The

Observability Analysis determines set #3 is the second best after the set #1 the full instrumentation suite.

Based on all above set #3 is the selected one to be used in the rest of the project,

Set #3: P25, MW, XN25, P48, FF, P3, T25, T8

An engine with only set#3 instruments will not be viable as this set does not have T3 and T48, required for engine control. It is valid to minimize diagnostic measurements, but not for operation.

8 LINEAR GAS PATH ANALYSIS APPLICATION

8.1 Introduction

Linear Gas Path Analysis has been described in Chapter 4. Although it has drawbacks, its simplicity and speed make it very attractive for real life solutions. Once an accurate Influence Coefficient matrix (ICM) is available, it only requires standard applications in an average personal computer as Microsoft Excel. The availability of ICM is probably its biggest drawback from user's perspective. It needs good engine baseline data (new and clean, with no faulty sensor). With that in hand OEM can adapt its simulation program to reproduce as accurate as possible the individual engine modifying health parameters. ICM can be created by implanting faults in the model of the real engine (ref. Chapters 6 and 7).

LGPA results will be analysed trying to determine its suitability detecting Gas Turbine off line water wash need in line with the Thesis aim.

8.2 Compressor fouling cases

The author through real life has experienced mild fouling cases that can be solved via off line water wash typically impacts Γ_{LPC} (LPC flow) and η_{HPC} (HPC efficiency). As rule of thumb a power loss around 2 MW from baseline in similar conditions is considered a good threshold for off line water wash, but this value is highly site dependent and will be used here only as a guideline.

An example comes from an engine where via analysis it had been evaluated to be fouled. Off line water wash recovered and average of 12% (three different dates, Figure 8-1) in ISO corrected power. In depth analysis showed the significant variation had been on the two health parameters here discussed:

$$\Delta \Gamma_{LPC} = +1.7\%$$

$$\Delta \eta_{HPC} = +2.2\%$$

The Web Engine allows determining the combination of Γ_{LPC} and η_{HPC} that will give a power decrease of 2 MW from Design Point selected as baseline (Table 8-1). The ambient conditions will not be varied due to issues with WebEngine

explained in Chapter 9. Similarly, other modules will not be degraded. For a deeper analysis η_{HPT} should be considered as well, simulating the degradation of the gas turbine. This project will be limited to variation versus design point at constant ambient conditions derived from compressor fouling. Further gas turbine degradation will also have impact on η_{LPC} and Γ_{HPC}.

Figure 8-1: Real engine water wash case

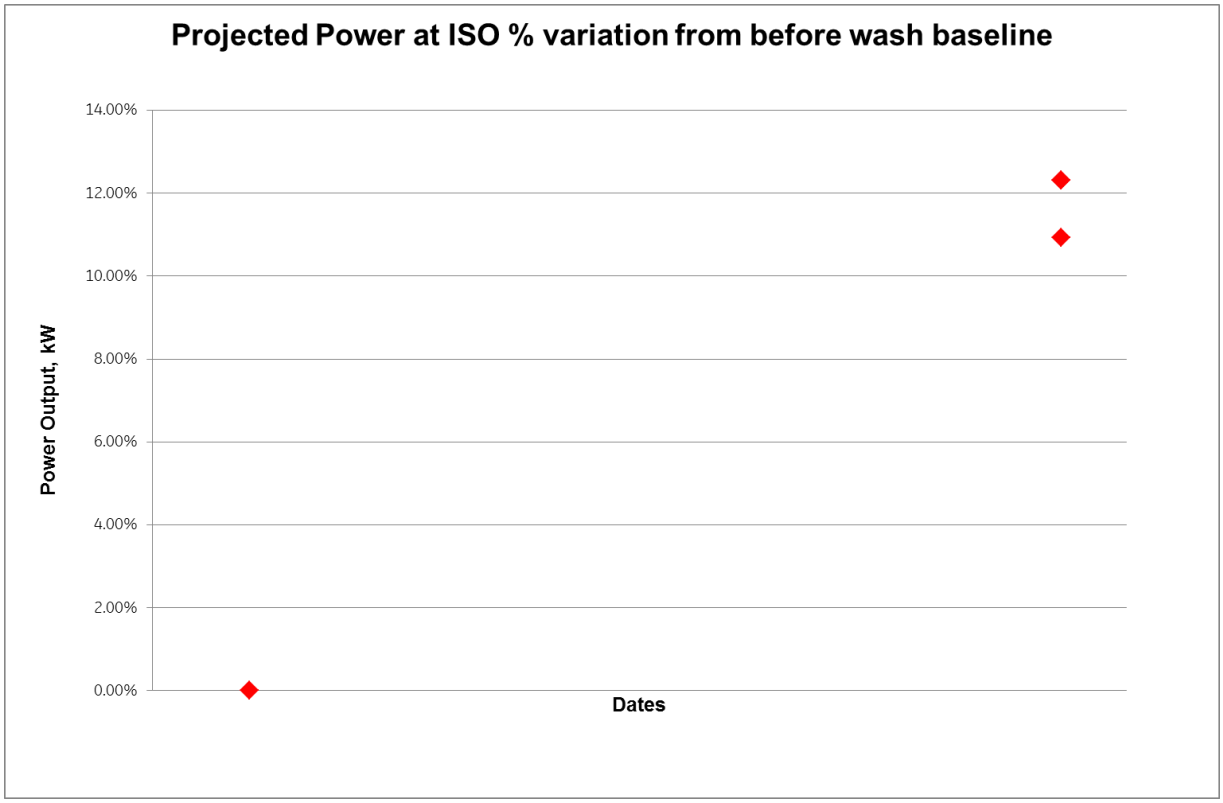

The resulting range of Γ_{LPC} is [0, -6] (%). In the author experience this is large. Most likely the differences are related to the off design behaviour of the model versus the real engine.

The calculated range for η_{HPC} is [0,-3.5] (%). A rule of thumb in this engine model is a decrease of η_{HPC} = -3% the unit can be considered in risk of stall during a transient manoeuvre.

Notwithstanding real life experience both ranges will be used to test the process.

Table 8-1: Combination of ΓLPC and ηHPC for ∆Power = -2MW

				MW (diff vs DP)				
		Γ_{LPC} (%)						
		0	-1	-2	-3	-4	-5	-6
η_{HPC} (%)	0	0.00	-0.35	-0.70	-1.06	-1.43	-1.81	-2.13
	-0.5	-0.26	-0.60	-0.94	-1.30	-1.47	-1.91	
	-1	-0.52	-0.85	-1.20	-1.55	-1.92	-2.05	
	-1.5	-0.78	-1.11	-1.45	-1.80	-2.16		
	-2	-1.16	-1.46	-1.71	-2.06			
	-2.5	-1.46	-1.75	-2.04				
	-3	-1.76	-2.05					
	-3.5	-2.11						

8.3 Influence Coefficient Matrix (ICM)

The basis for ICM is the Exchange Rate Table (ERT, Table 7-3) calculated in Chapter 7. The gas turbine is supposed to be instrumented with Measurement set #3 (P25, MW, XN25, P48, FF, P3, T25, T8) from Chapter 7. The specific measurements can be selected from the full engine suite (reference Table 7-1) for compressor fouling diagnostic purposes. Its ICM, called ICM3, is in Table 8-2.

Table 8-2: Influence Coefficient Matrix for set #3

	LPC flow	HPC Flow	HPT flow	LPT flow	LPC eff	HPC eff	HPT eff	LPT eff
P25	-1.00	0.77	-0.31	1.23	0.50	1.57	2.11	0.14
P3	-0.72	-0.10	0.96	-0.09	-0.11	-0.30	-0.17	-0.01
P48	-0.66	-0.20	-0.02	0.56	-0.14	-0.67	-0.71	0.07
XN25	-0.02	0.15	0.23	-0.89	-0.15	-1.13	-1.52	-0.10
MW	-0.81	-0.54	-0.13	-0.09	-0.66	-1.20	-1.01	-1.36
FF	-0.57	-0.27	-0.22	-0.21	-0.32	-0.75	-0.38	-0.02
T25	-0.26	0.20	-0.08	0.31	0.37	0.40	0.53	0.03
T8	0.18	0.09	-0.21	0.03	0.05	0.03	0.41	0.57

8.4 Linear Gas Path Analysis (LGPA)

Refreshing from Chapter 4, the relationship between the deviation of engine measurable parameter deltas (also called dependent parameters) and the deviation of non-measurable component parameter (also called independent or health parameters) deltas at certain engine operating conditions, is expressed with a linear Influence Coefficient Matrix (ICM) ([7], [9] and [10]):

$$\Delta z_3 = ICM3 \times \Delta x_3$$

The deviation of engine component parameters can be calculated with a Fault Coefficient Matrix (FCM) (or diagnostic matrix), which is the inverse of the influence coefficient matrix:

$$\Delta x_3 = ICM3^{-1} \times \Delta z_3$$

The degraded measurable parameters are generated implanting known degradation values to component characteristics. The degradation of health parameters used in this case are a combination of Γ_{LPC} = [0, -6%] and η_{HPC} = [0,-3.5%]. Γ_{LPC} is varied in 1% steps and η_{HPC} in 0.5% steps as per Table 8-1.

Web Engine provides the engine measurable parameters for each degraded case. The measurement parameter deviation vector $\boldsymbol{\Delta z_3}$ is calculated using the equation below (subscript 3 because measurement set #3 is used), DP being Design Point condition and fault the results for the implanted fault condition:

$$\Delta \boldsymbol{z_3} = \frac{\boldsymbol{z_{3fault} - z_{3DP}}}{\boldsymbol{z_{3DP}}} \, x \, 100$$

The case (Γ_{LPC}, η_{HPC}) = (-1, -3) is used as example. The results for $\Delta \boldsymbol{z_3}$ are in Table 8-3.

Table 8-3: Results for ∆z3 for (ΓLPC, ηHPC) = (-1, -3)

	DP	(-1, -3)	$\Delta \boldsymbol{z_3}$
P25	2.39	2.49	-4.47%
P3	28.89	28.34	1.94%
P48	6.78	6.62	2.35%
XN25	1	0.9612	3.88%
MW	43284000	41236444	4.73%
FF	2.388	2.320	2.87%
T25	381.56	385.79	-1.11%
T8	723.76	727.36	-0.50%

The LGPA derived value of health parameter vector $\boldsymbol{\Delta x_3}$ for the above deviation of engine measurement can be calculated using equation:

$$\Delta \boldsymbol{x_3} = \mathrm{FCM} \times \Delta \boldsymbol{z_3}$$

The results for the sample case are in Table 8-4:

Calc Δx_3 – Calculated deviation of health parameters using Web Engine derived deviation of measured parameters and LPGA

Impl Δx_3 – Implanted deviation of health parameters, implanted fault, for the sample case (Γ_{LPC}, η_{HPC}) = (-1, -3)

Impl – Calc – Is the Error

Table 8-4: LGPA estimation of health parameters and error for sample case

	Calc Δx_3	Impl Δx_3	Impl - Calc
Γ_{LPC}	-0.0102	-0.01	0.02%
Γ_{HPC}	-0.0015	0	0.15%
Γ_{HPT}	0.0028	0	-0.28%
Γ_{LPT}	-0.0054	0	0.54%
η_{LPC}	0.0006	0	-0.06%
η_{HPC}	-0.0292	-0.03	-0.08%
η_{HPT}	-0.0002	0	0.02%
η_{LPT}	-0.0024	0	0.24%

To keep consistency with previous error calculations for fault cases Root Mean Square Error for the Γ_{LPC}, η_{HPC}) = (-1, -3) deviation is calculated:

$RMS_{(-1,-3)}$ = 0.68%

The above results are derived for all implanted fault combinations of Table 8-1 and resulting RMS for each case is shown in Table 8-5.

Table 8-5: LGPA RMS for each fault case

RMS in %		Γ_{LPC} (%)						
		0	-1	-2	-3	-4	-5	-6
η_{HPC} (%)	0	DP	0.00	0.03	0.08	0.17	0.3	0.56
	-0.5	0.02	0.12	0.25	0.38	0.29	0.44	
	-1	0	0.12	0.24	0.37	0.52	0.45	
	-1.5	0.03	0.1	0.22	0.35	0.49		
	-2	0.45	0.43	0.2	0.33			
	-2.5	0.58	0.54	0.53				
	-3	0.73	0.68					
	-3.5	1.16						

The table shows that RMS error grows as the deviation from Design Point gets bigger. This is related to the relative weight of nonlinear effects. Gas turbines are highly nonlinear.

The RMS error result, although interesting, does not show clearly whether LPGA could be used with confidence determining whether to water wash or not. The evaluation of all LGPA estimated health parameters for each case would be a better indication, in particular Γ_{LPC} and η_{HPC}. The results for non-faulty health parameters should be close to zero, and in orders of magnitude smaller than the implanted faults. The health parameters where the faults have been implanted have to show results in line with implanted faults.

8.4.1 Health parameter LGPA calculated values for fault cases

The following figures show LGPA calculated health parameter value for the ranges of variation of Γ_{LPC} and η_{HPC}. The review of 34 cases will be cumbersome so some cases will be used as examples. The remaining results are plotted in Appendix B. There are a couple of general conclusions:

- For large Γ_{LPC} deviations LGPA tends to overestimate it.
- As Γ_{LPC} deviation increases η_{HPC} deviation is underestimated.

The cases in Figure 8-2 have no variation on Γ_{LPC}, all variation is in η_{HPC}. It could be the situation of a gas turbine subject to frequent on line water washes, with no off line water wash scheduled. In that case dirt removed from the front stages may accumulate in the back stages of the compressor ([17]). The subject unit configuration is more prone to this effect due to the combined lengths of LPC and HPC.

Small changes in η_{HPC} are properly detected. Once the change becomes larger LGPA determines variation on other components health parameters as Γ_{HPT} of enough magnitude to be of concern. An increase in Γ_{HPT} is explained by erosion.

Figure 8-2: ΓLPC = 0% & ηHPC [0,-3.5]

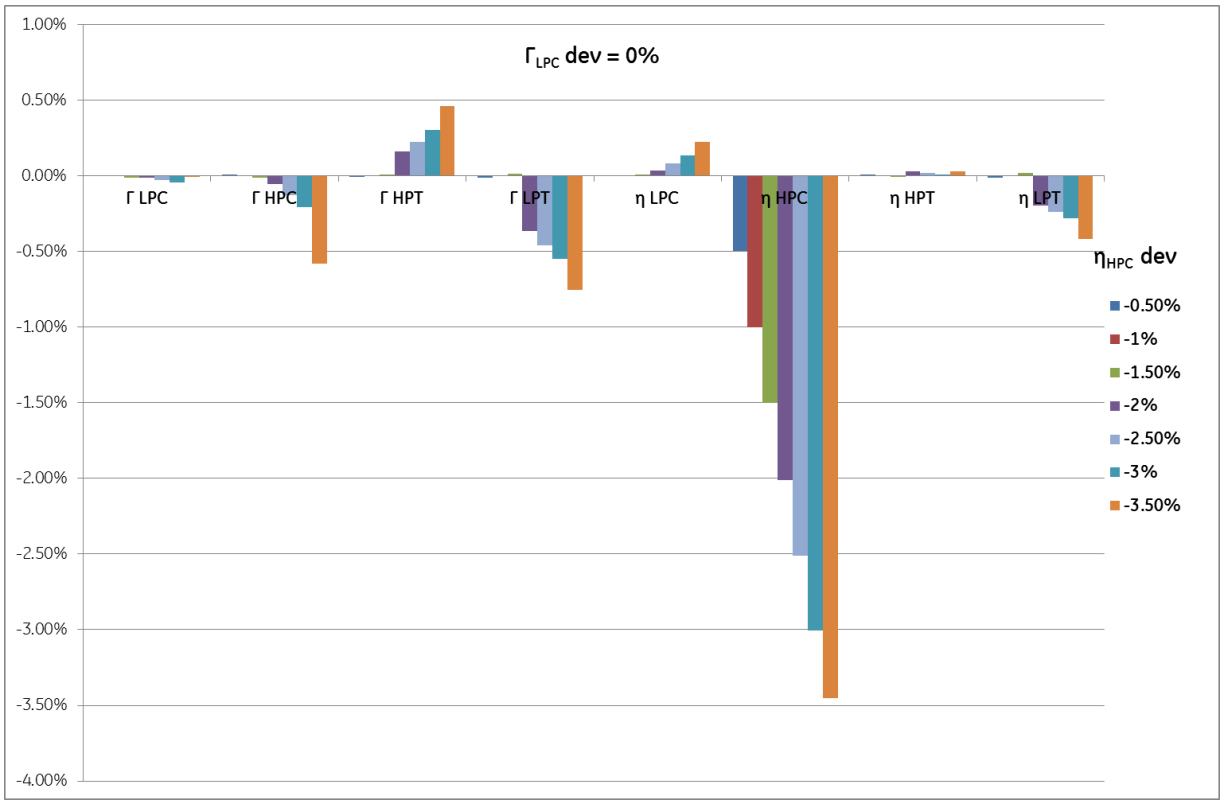

Let's take a look at other example, Γ_{LPC} = -2% and η_{HPC} [0,-2.5] (Figure 8-3). It can be described as an engine where LPC fouling has reached a stable level, maintained via on line water wash, while dirt is accumulating in HPC last stages ([17]).

Once more significant effects appear on other health parameters as η_{HPC} degrades further. But, if those are discounted and acknowledged, a sensible water wash decision may be taken based on this analysis. With power loss increasing, stable Γ_{LPC} degradation and diminishing η_{HPC}, there should be enough indications to schedule an off line water wash.

Let's review two of cases where the HPC has a constant level of η_{HPC}. The first one is η_{HPC} = 0% & Γ_{LPC} = [0,-6%] (Figure 8-4). It simulates an engine on initial stages of fouling, no on line water wash applied, dirt depositing on LPC initial stages. In real life a level above of Γ_{LPC} = -4% with no impact of fouling in HPC is

difficult to imagine, but it will be kept in the simulation as example. LGPA results show a very good detection level, with no confusion possible with other effects.

Last case is η_{HPC} = -2% & Γ_{LPC} = [0,-3%] (Figure 8-5). Now the stable level is on η_{HPC}, the unit has a dirty HPC and is fouling on LPC. It can be due to a rapid fouling of LPC with no on line water wash applied.

Once again LGPA results are good enough to determine water wash, as long as results on other component health parameters are ignored.

Figure 8-3: ΓLPC = -2% ηHPC [0,-2.5]

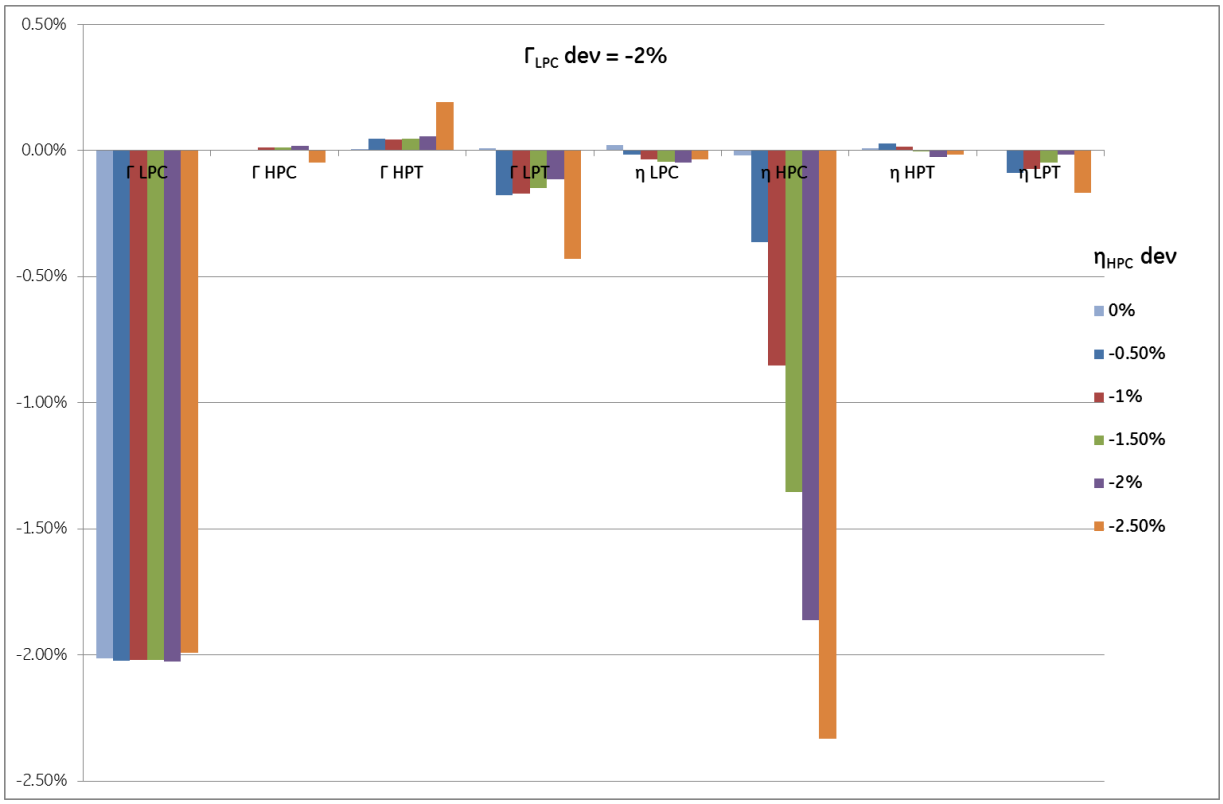

Figure 8-4: ηHPC = 0% & ΓLPC = [0,-6%]

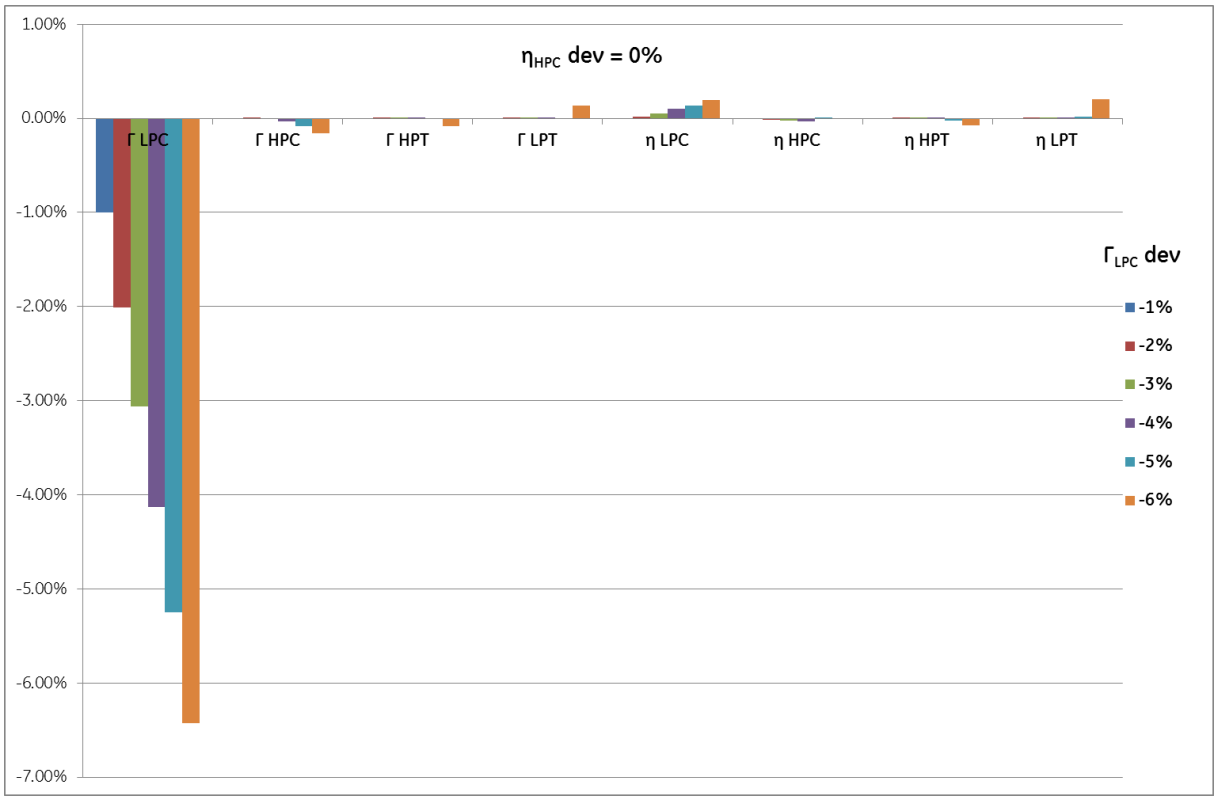

Figure 8-5: ηHPC = -2% & ΓLPC = [0,-3%]

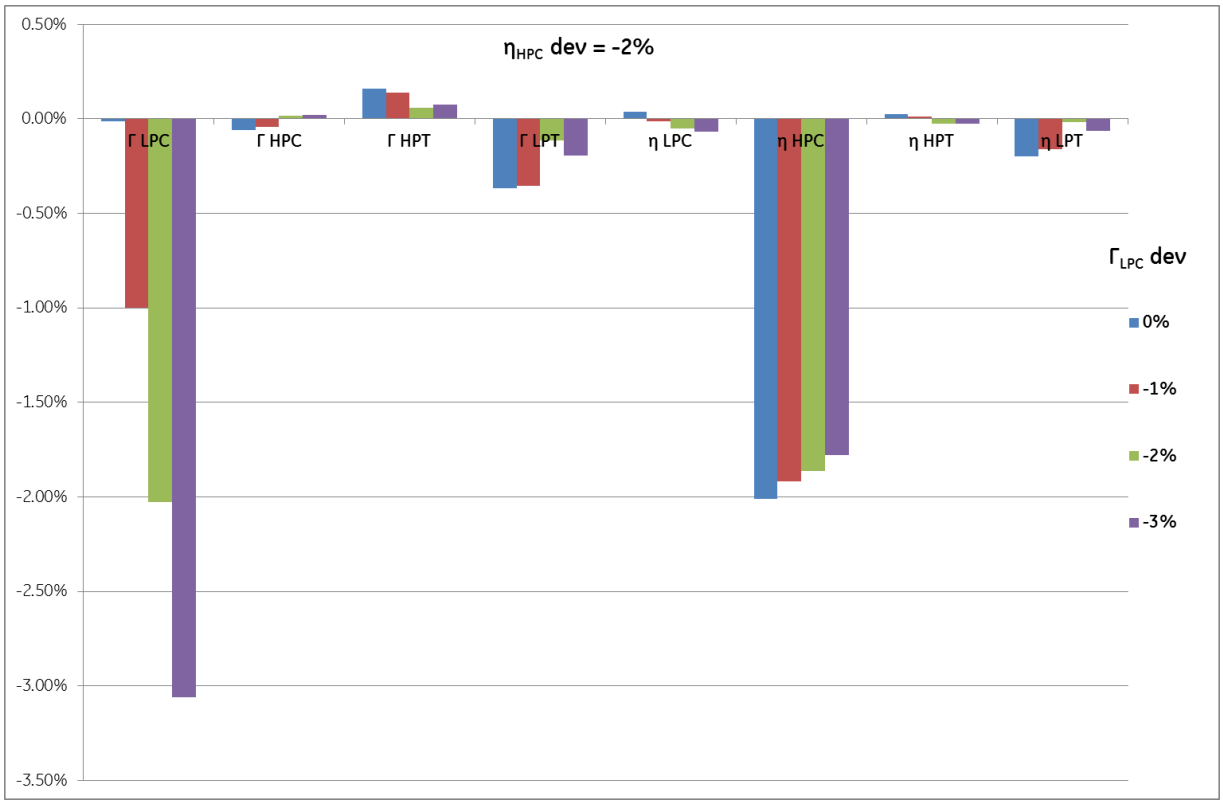

8.5 Conclusions

The presented results show LGPA could be used as a tool to determine when to wash, as long as some precautions are taken:

- An accurate ICM is required; therefore the standard Cycle Deck engine simulation cannot be used. It can be adapted and simulate the real engine. This is done by careful analysis of baseline data and adjustment of health parameters values.
- Health parameter values should be considered indicative especially when they grow, as the bigger they get the larger is the difference between implanted fault and LGPA estimation.
- Further work will need to be done incorporating combined faults on other parameters discussed above (η_{LPC}, Γ_{HPC}, η_{HPT}).

9 ANN TOOL

9.1 Introduction

A general description of ANN was done in Chapter 4. This chapter will go deeper into ANN, types, training, and other characteristics. A network will be built to investigate its use as a tool to help determining when to water wash. The criteria will be its ability to quantify the levels of degradation of two engine health parameters (Γ_{LPC} (LPC flow) and η_{HPC} (HPC efficiency)) as already introduced in Chapter 8. The results will be compared with LGPA results with the same “real” test data.

9.2 Artificial Neural Networks background

9.2.1 The Neuron Mathematical model

The physical neuron receives inputs through the dendritic tree connection in the shape of electrical signals (reference Figure 4-15, Ch. 4). The tree performs a summation of all inputs and the aggregate passes to the soma. If the strength of the aggregate is over a certain threshold, the neuron fires a signal through the axon. This output signal is communicated to other neurons via the interconnection between axon synaptic buttons and dendrites.

The mathematical model of the neuron is inspired on this way of working. Figure 9-1 is a mathematical model of a single neuron [31].

Figure 9-1: Mathematical model of single neuron

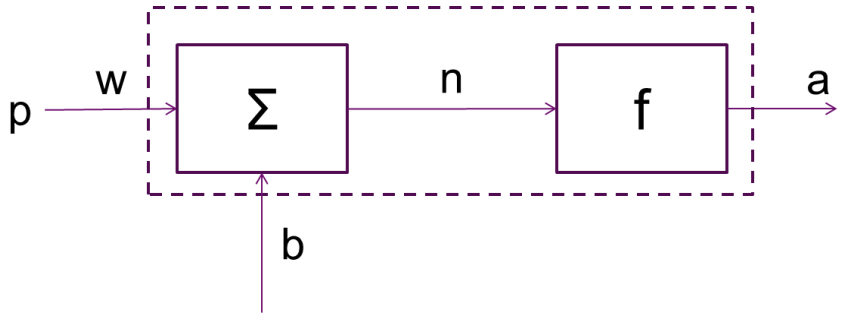

The mathematical relationships between input and output are:

$$n = p * w + b$$

$$a = f(p * w + b)$$

Equation 9-1: Neuron mathematical relationships

Where:

p = the input signal

w = synaptic weight (weight of input signal)

b = neuron bias

n = induced local field or activation potential

f = transfer or activation function

a = neuron output

The neuron does a linear sum of the product of the synaptic and input signal with the bias. The value is then passed through a transfer/activation function that limits the amplitude of the output. The type of transfer function will be dependent on the system being modelled and the requirements of the desired output. The weights characterize the neuron connections and store the knowledge. The adjustment of the weights is the learning or training process of the network. Training is typically done by exposing the network to a set of known input/output data. The training algorithm adjusts the weights iteratively.

Figure 9-2: Multi-input and multi-layered NN [59]

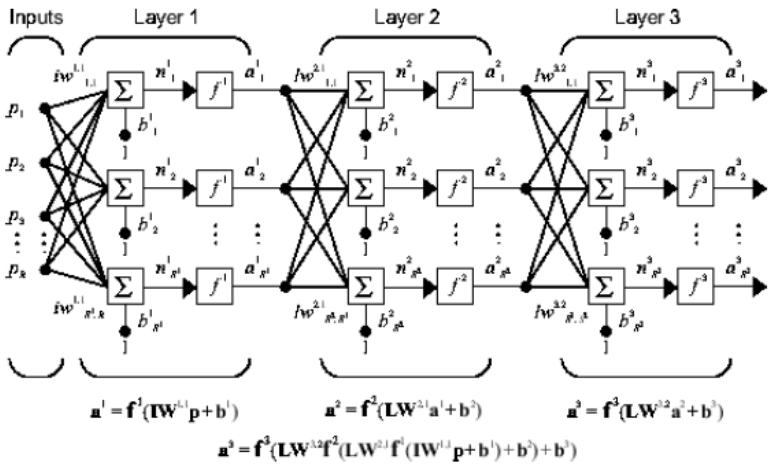

Practical networks are multi-input and multi-layered thus the variables in the relationships above take the shape of vectors ***a***, ***p*** and ***b***, and ***w*** is a matrix of weights (Figure 9-2, [59]).

9.2.2 Types of ANN architectures

There are many types of ANN architectures depending on the number of layers, types of transfer functions, training procedure or the way the information is processed ([59]). Focusing on how is information processed, there are two types, feedforward networks and recurrent networks. In the former the information passes ahead through the network, whereas in the later there is at least a feedback loop. Recurrent networks are more difficult to train, present convergence and local minima problems and are not typically used in gas turbine diagnostic tools ([59]). They will not be discussed further and the chapter will focus on feedforward network architectures.

9.2.2.1 The Perceptron

The network comprises a single input layer where binary input patterns are fed. The output is binary as well (Figure 9-3, [31]). The output layer number of neurons can vary. They were first introduced by Rosenblatt and have limited computational and non-linearity capabilities, so they are not used in gas turbine diagnostics.

Figure 9-3: The Perceptron [31]

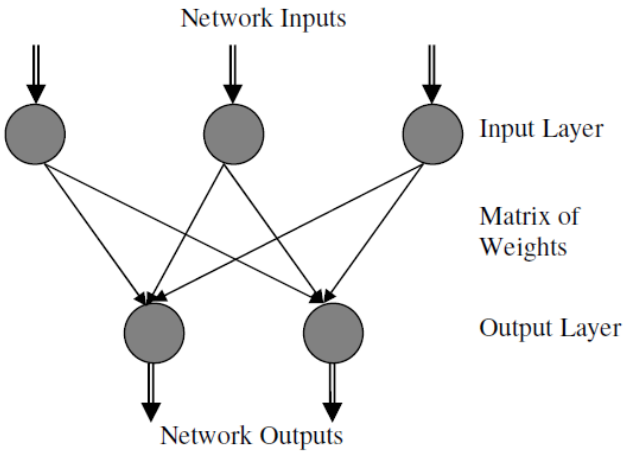

9.2.2.2 Multilayer Perceptron (MLP). The FFBP and AANN Neural Networks

MLP are an extended form of the Perceptron, with one or more hidden layers between input and output layer (Figure 9-4, [31]). They are also called Multilayer Feedforward Neural Networks (MLFFNN). They have shown a recognized ability in pattern recognition and function fitting, and are widely used in gas turbine diagnostics ([31]). The most common types are Feed Forward Back-Propagation (FFBP) and Auto-Associative Neural Networks (AANN). MLFFNN are used for input to output mapping, as curve fitting or pattern recognition.

In general MLP cannot perform outside the range trained. The number of hidden layers, number of neurons per layer and training method are important decisions impacting the ability of the network to be trained and perform the desired task.

Figure 9-4: 2 hidden layer MLP for gas turbine diagnostic [31]

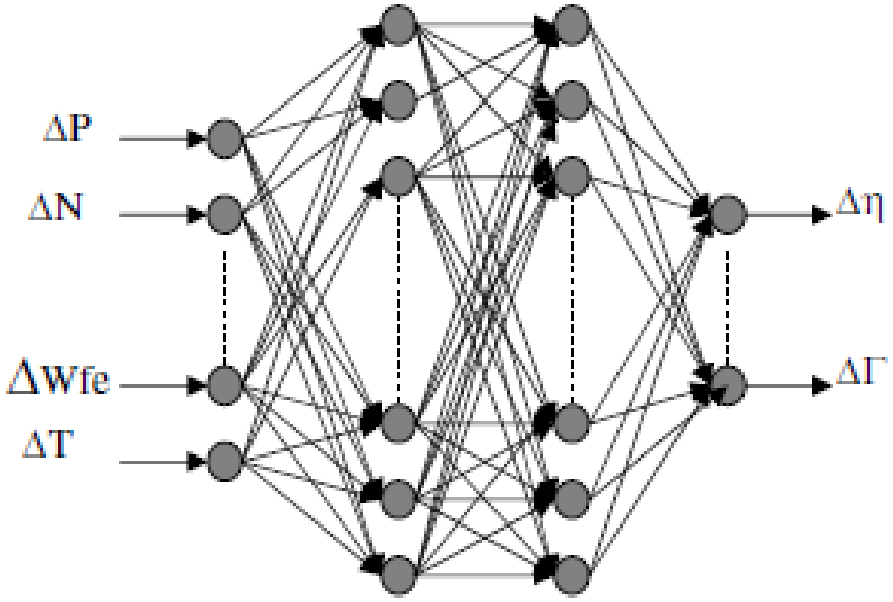

9.2.2.3 Radial Basis Function (RBF)

RBF is another variant of the MLFFNN, with usually two computational layers (Figure 9-5, [31]). The first computational layer is made of “radbas” functions where the output is a function of the distance between the input and the “center” of the basis function. Radbas functions can be Gaussian, multiquadratic, inverse-multiquadratic or Cauchy ([31]). The further the input from the center value, the

smaller the neuron output. In the second layer there is a linear sum of weights for the outputs of the first layer that are now the inputs. Reference [31] states they are used in function approximation, pattern classification, the modelling of dynamic systems and time series, but were discontinued in gas turbine diagnostics due to poor generalization capabilities.

Figure 9-5: RBF network with 1 output [31]

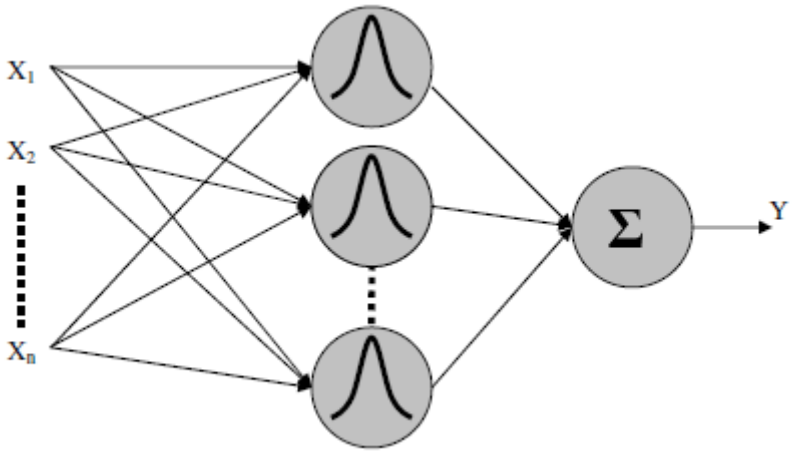

9.2.2.4 Probabilistic Neural Network (PNN)

PNN is a special case of RBF used for pattern classification, which utilizes supervised training to develop statistical distribution functions in the middle layer. It has three layers (Figure 9-6, [31]). The input layer has a many neurons as parameters needed to classify the objects. The middle layer has as many elements as the training set has input vectors. When in recall mode the distribution functions developed during training are used to determine the probability of a given pattern being a member of a class, with the criteria of the closeness of the input vector to the distribution function of that class. The output layer is a summation layer with as many elements as classes to be recognized.

Figure 9-6: Probabilistic Neural Network (PNN) [31]

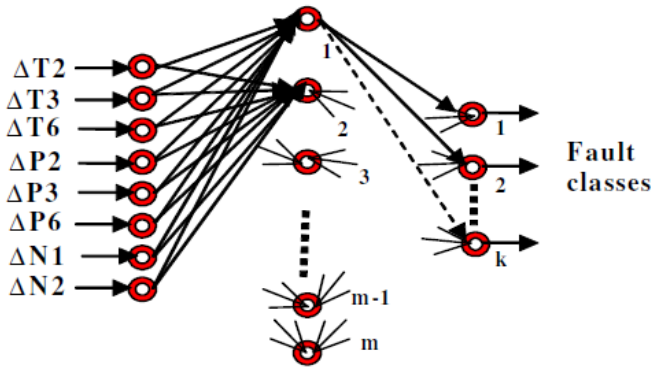

Training of PNN is simple and they work well in classification tasks. The major drawback is the middle pattern layer can be big depending on the need of distinction between categories. Also they are computationally slow in recall mode.

9.2.2.5 Self-Organizing Map Network (SOM)

The main characteristic of this type of network is a middle layer where neurons organize themselves spatially according to certain input values. It is called the "feature map" (Figure 9-7, [31]). The training method is unsupervised (more in next paragraph). These networks are considered feedforward (from input layer to map) and recurrent as the feature map neurons organize themselves. They are applied to pattern classification, optimization and simulation.

Figure 9-7: Self-Organizing Map Network (SOM) [31]

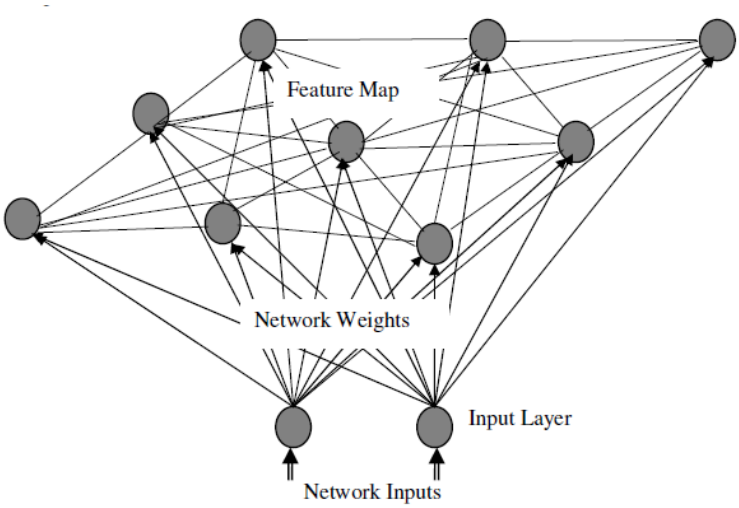

9.2.3 Network Transfer functions

The transfer or activation function limits the amplitude of the neuron's output. There are three categories: hard limit, linear and sigmoid transfer functions. Figure 9-8 from [31] shows graphically each one of them.

The hard limit or step transfer function (fig 9-8 (a)) is used in classification networks and can be written as (*n* and *a* as per Figure 9-1):

$$a = 0 \text{ if } n<0$$

$$a = 1 \text{ if } n\geq 0$$

Linear transfer functions provide linear outputs for net inputs, both with a direct variation (fig 9-8 (b)). It is used in output layer of multilayer networks. It is not used in hidden layers of gas turbine diagnostic as the parameter relationships are highly nonlinear.

The sigmoid transfer function takes the net input *n* ranging from minus to plus infinity and limits the output *a* into a range of:

[0,1] for Log-sigmoid transfer function (fig 9-8 (c))

[-1,1] for Tan-sigmoid transfer function (fig 9-8 (d))

Figure 9-8: Transfer functions [31]

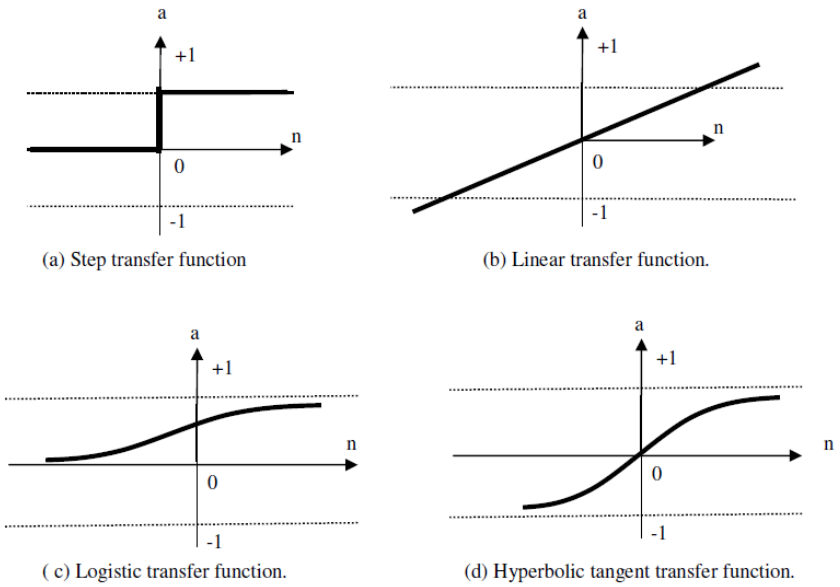

(a) Step transfer function

(b) Linear transfer function.

(c) Logistic transfer function.

(d) Hyperbolic tangent transfer function.

The Log-sigmoid (logistic) transfer function is referred as the nonsymmetrical and has the following mathematical expression, where $\boldsymbol{n}_j$ is the weighted sum of all inputs plus the bias, and $\boldsymbol{a}_j$ is the output.

$$\boldsymbol{a}_j = logsig(\boldsymbol{n}_j) = \frac{1}{1 + e^{-\boldsymbol{n}_j}}$$

Equation 9-2: Log-sigmoid

The Tan-sigmoid (hyperbolic tangent) is symmetrical and its mathematical expression is:

$$\boldsymbol{a}_j = tansig(n_j) = \frac{e^{\boldsymbol{n}_j} - e^{-\boldsymbol{n}_j}}{e^{\boldsymbol{n}_j} + e^{-\boldsymbol{n}_j}}$$

Equation 9-3: Tan-sigmoid

Sigmoid transfer functions are differentiable and well adapted to nonlinear environments, therefore they are commonly used in the hidden layers or multilayer neural networks used in gas turbine diagnostics.

9.2.4 Network Training methods

Similar to human brain ANN have to learn so they can perform their expected task effectively. Learning means adjusting weights and biases by an optimum amount to minimize error. The process is known as network training. It is an iterative process with initial weights chosen randomly. After every iteration the network learns more about the environment adjusts the weights and ideally should be able to produce a more accurate output when exposed to an input.

9.2.4.1 Training style

There are two styles, incremental (or sequential) and batch training. In incremental training the weights and biases are adjusted each time the network is presented with an input. In batch training adjustment is done once all inputs are introduced for every iteration. Iterations are called epochs. For most problems batch training is faster and produces smaller errors ([59]).

Training can be either supervised or unsupervised. Through training the designer will learn if the network will produce the expected outputs. If it does not then the

design needs to be reviewed, as number of layers, neurons per layer, connections, transfer function and initial weights.

9.2.4.2 Supervised training

It is similar to leaning with a teacher. The network uses training samples, which are inputs coupled with their corresponding outputs called targets. The output of each iteration is compared with the desired targets and weights and biases are adjusted via a backpropagation algorithm, called the training algorithm. Figure 9-9 is a scheme of the process.

9.2.4.3 Unsupervised training

It is learning with no teacher. The neurons train themselves with no outside participation. The learning process searches for trends in the input signals an makes adaptations according to the function of the network ([31]). The basis for learning is either cooperation or competition between clusters or individual processing elements. Further can be found in reference [59].

Figure 9-9: Supervised training process

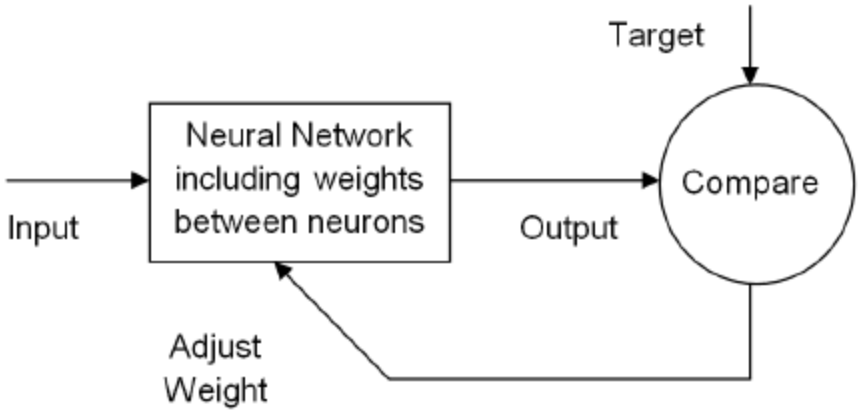

9.2.5 Training algorithms

Training algorithms are used to adjust weights and biases. They are usually based on partial differential equations. Each one has its advantages and disadvantages. It is outside the scope of this thesis to discuss them in detail, further can be found in references [31] and [60].

The most common of them is the back-propagation algorithm used in MLFFNN. It does two sweeps through the network. One sweep is forward, from inputs to outputs and one backward from the output to the input layer. In the backward sweep errors are propagated back. The typical error function is the Mean Square Error (MSE), although other error functions can be used:

$$MSE = \frac{1}{N}\sum_{i=1}^{N}(t_i - n_i)^2$$

Equation 9-4: Mean Square Error

Where

n_i training inputs

t_i target outputs

The theory states MSE should get smaller in each iteration. Weights and biases are adjusted comparing with a desired level of error and learning rate until minimized.

The back-propagation algorithm has been improved by other techniques as Scaled Conjugate Gradient (*scg*), Levenberg-Marquardt (*lm*) or BFGS Quasi-Newton, amongst others (reference [31] and [60]).

9.2.6 Network Generalization, Overfitting and Underfitting

In the supervised training scheme, the network is trained using known inputs and target outputs, but must retain its performance when presented with inputs never seen before to be really useful. The ability to retain performance when presented with inputs never seen before is called generalization. To check for generalization capabilities of a network the training samples are divided into three categories, training, validation and testing samples. The training samples are input into the network and error is adjusted using them. The decrease of training error indicates the network is learning (Figure 9-10, [31]).

The validation set is used to check generalization capabilities of the network. The validation error is calculated in every iteration (epoch) and when it starts rising

the network training is stopped. MATLAB stops by default when the validation error rises for 6 epochs.

The optimal epoch occurs when the network reaches a certain performance level, for example the criteria used by MATLAB above. Underfitting occurs to the left of the optimal epoch. It means the network parameters have not been trained enough and the network will not represent properly the problem features. Overfitting is the opposite but with similar result. The network parameters have gone through excessive training and have “memorized” the examples, losing the ability to generalize. The test samples are then used to determine the true capability of the network to perform the required task.

Figure 9-10: Network overfitting and underfitting [31]

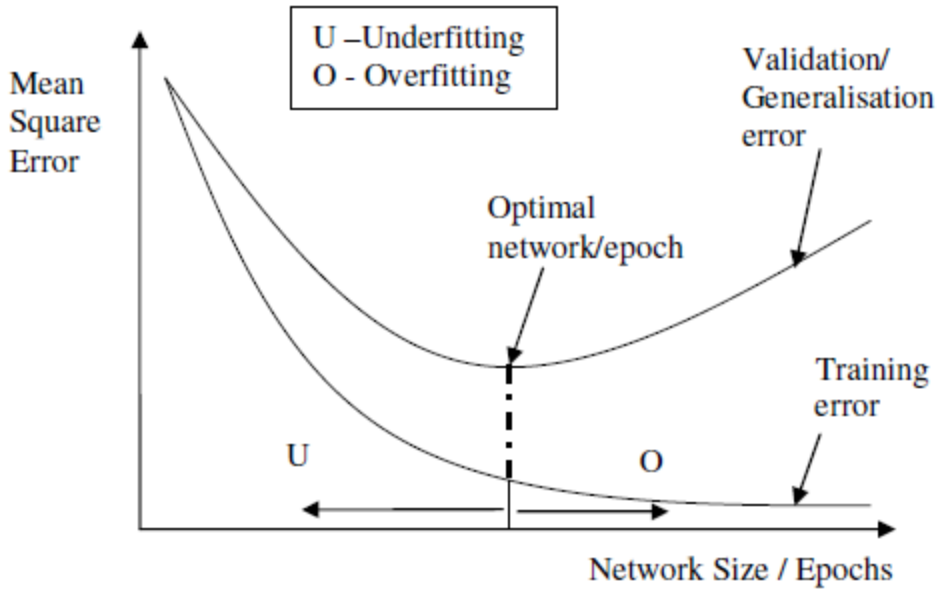

9.3 Artificial Neural Network tool in the estimation of water wash need

9.3.1 Methodology

The aim of this research is creating a tool based on ANN that can help in the determination of the need for a water wash. It is done through the quantification of two health parameter faults Γ_{LPC} (LPC flow) and η_{HPC} (HPC efficiency). Literature research identifies a FFBPN (Feedforward Back-Propagation Network)

as the best option for these kind of diagnostic problem ([11], [12], [31], and [58]), so it was the one used here.

The network was created in MATLAB, starting from a standard Neural Net Fitting Application from MATLAB Graphical User Interface (GUI). A script was generated and used as basis. The commands were modified in order to test the different options used during the network adjustment. Appendix D has the script used showing a two hidden layer network.

The type of MATLAB feedforward network used was *fitnet* a specialized function fitting neural network. The input layer has eight neurons, one per measurement parameter considered. Different hidden layer configurations were tested as explained below. The output layer has two neurons, one per health parameter evaluated.

The network was trained, validated and tested with a set of data. The generation of this data is explained in detail in the next paragraph, as some difficulties were experienced. Once a network was configured it was finally tested with a different set of randomly generated health parameters, called the “real” data set. The intention of this step was simulating real life conditions where the network would be “seeing” data sets never experienced during training.

9.3.2 Training data

Data is required to train, validate and test the network. Ideally it would be real engine data with known implanted faults, but that data is very difficult, if not impossible, to get. Access to a real gas turbine to be able to implant required faults is an unrealistic prospect. The way around is to use an engine model, where faults can be implanted and degraded engine behaviour simulated, as WebEngine in this case. The fault implanting process is the same as in Chapter 6.

Once chosen how to generate the required data, the next step is which data in particular, what level of degradation in which health parameters. The idea to concentrate in Γ_{LPC} (LPC flow) and η_{HPC} (HPC efficiency) was discussed in Chapter 8. Of course this can be challenged and other parameters added as η_{LPC}

and Γ_{HPC}. It was discussed in previous chapters that based on experience fouling typically first impacts LPC flow and HPC efficiency. Although during the tests large variations of these parameters are used, in reality the conditions that would drive to those levels of degradation will most likely be unrecoverable through normal water wash (baking, compressor length), as explained in Chapters 2 and 8.

The training set range was determined by looking at the sensitivity of the model to implanted faults based on the easiest parameter a customer can follow, power. Customers claim they can detect between 0.15 and 0.3 MW power loss (author's experience) with standard plant instrumentation. Through WebEngine and the cases from Chapter 8 it was determined that amount of power output change can happen when the variation of health parameters analysed is $-0.5\% < \Delta\Gamma_{LPC} < -1\%$ and $-0.25\% > \Delta\eta_{HPC} > -0.5\%$. Here the author bumped into an unexpected problem also impacting LGPA analysis. WebEngine was not properly configured to run parametric studies, crashing continuously. It was agreed with Project Director to use previously collected cases and apply linear interpolation when data was not available. That limited the capability to generate training cases and influenced the final results as will be discussed later.

The cases used were (Table 9-1).

$0\% > \Gamma_{LPC} > -11\%$ in -0.5% steps

$0\% > \eta_{HPC} > -7\%$ in -0.5% steps

ISA temperature and pressure

That means a total of 345 cases, which is not a large number but considered sufficient. If the capability to run cases automatically had been available author would have added Tamb and Pamb variation, aiming to simulate reality better.

9.3.2.1 Training cases linear interpolation

WebEngine data was available for cases with $0\% > \Gamma_{LPC} \geq -6\%$ and $0\% > \eta_{HPC} \geq -3.5\%$ and its combinations. The rest had to be generated by linear interpolation, thus cases where $\Gamma_{LPC} < -6\%$ and $\eta_{HPC} < -3.5\%$ were interpolated twice. In summary only

31.3% of the cases were WebEngine simulated, data for the rest came out of linear interpolation. The situation is explained in Table 9-1.

The linear fit tool used was the function LINEST from Excel. Other options were tested as well like polynomial approximation. The results were not satisfactory. Discussion can be found in Appendix C “Training cases linear interpolation”.

The data used were column vectors made out of Measurement set #3 parameters (P25, MW, XN25, P48, FF, P3, T25, T8). The values were normalized to have inputs between -1 and 1. The normalization was done using the data at Design Point as reference:

$$p_{ij} = \frac{x_{ij} - x_{dpi}}{x_{dpi}}$$

Equation 9-5: Normalization for ANN

Where $i \in (1, 8)$ being 8 the number of measured parameters, and $j \in (1, 345)$ 345 being the number training cases (Table 9-1).

Table 9-1: ANN training cases and linear interpolation

9.3.3 Create and configure the network

The network was created in MATLAB, starting from a standard Neural Net Fitting Application from MATLAB Graphical User Interface (GUI). A script was generated and used as basis. The commands were modified in order to test the different options used during the network adjustment. Appendix D has a sample script and how commands were modified.

The number of hidden layers and neurons per layer were modified to configure several test networks (Table 9-2). The output layer was always a linear transfer function (*purlin*), and the hidden layers a Tan-sigmoid (*tansig*) transfer function. Figure 9-11 is a sample of network configuration showing all characteristic here described.

Table 9-2: Network configurations tested

# neurons per layers			
Input	**L1**	**L2**	**Output**
8	10		2
	20		
	50		
	10	10	
	20	10	
		20	
	50	10	
		20	
		50	

The MATLAB software has several training algorithms available. For this tool two were tested, Levenberg-Marquardt (*trainlm*) and Scaled Conjugated Gradient (*trainscg*). The intention was to compare results in regards to speed and error. For the sake of testing Gradient Descent algorithm (*traingd*) was also used, but the performance was significantly slower and with much bigger errors from the first network configuration, so testing with it was not pursued.

Figure 9-11: Sample 2 hidden layer 8-50-20-2 network configuration

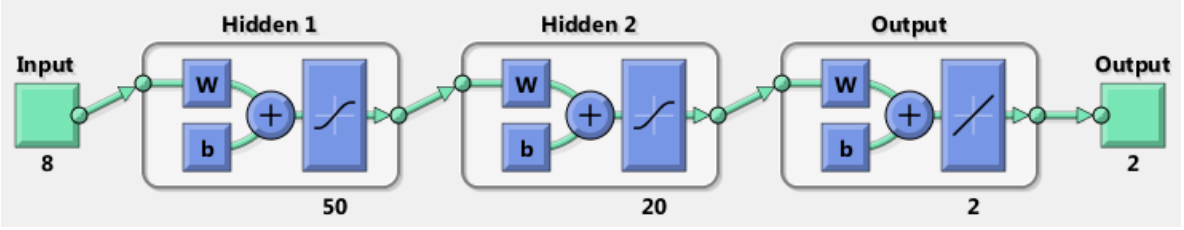

9.3.4 "Real" data test

MATLAB uses 15% of the training samples to test the network once trained and validated (Appendix D), but the author considered the network should be tested

by using a set of random input data not in the main training set. The intention was simulating the exposure of the network once trained and validated to “real” engine data. Health parameter pairs were chosen and the associated measurement vectors were created with WebEngine or through the linear interpolation described in Appendix C. Table 9-3 shows the “real” data test cases and highlighted in yellow those cases where the input vector was created through linear interpolation. Only one of the cases had been previously seen by the network during training ([Γ_{LPC}, η_{HPC}] = [0, -6.5]). All tested networks were exposed to the set of “real” data, and the output compared to the known input values (Appendix E).

Table 9-3: “Real” data for testing

Γ_{LPC}	-1.7	-2.4	-1.9	-4.5	0	-6	-9.75	-9.75
η_{HPC}	-2.3	-2.7	-1.7	-5.75	-6.5	-6.75	0	-6.5

9.3.5 Results

As discussed above several network configuration and two training algorithms were tested. The results were compared in terms of time to train, validate and test, MSE, number of epochs and error level in “real” data test cases (refer to Table E-1). A summary is shown in Table 9-4.

All MSE for *lm* trained networks were well within acceptable. For *scg* trained networks the error worsened in between 2 to 3 orders of magnitude, so they were discarded. When testing “real” engine test cases *scg* trained networks the error also increased significantly (Table E-1 in Appendix E for the complete list of results).

Training time was not a big issue as the largest was 38 s (8-50-50-2 *lm*). In general when the number of neurons increased same did the time to train, validate and test. Variation was so small in absolute terms that time was not considered selection criteria. It may have been major criteria years ago, when computing power was much smaller it was major criteria, or if the network requirements in terms of data had been much larger. For this particular case the increases were irrelevant and well within bearable values.

Table 9-4: ANN summary results

lay/neu	tra. alg.	tr. time(s)	Epoch	MSE
10	lm	2	176	2.96E-04
20		4	217	3.91E-05
50		9	160	1.50E-05
10_10		3	149	1.01E-04
20_10		7	181	5.12E-05
20_20		9	118	3.61E-05
50_10		6	36	1.80E-05
50_20		19	43	4.95E-05
50_50		38	22	8.02E-05
20	scg	1	93	1.26E-02
50		1	129	1.17E-02
20_20		1	123	1.07E-02
50_20		1	100	1.26E-02

Three networks were chosen for further analysis, one from single hidden layer and another two each one with different number of neurons in hidden layer (8-20-2, 8-20-10-2 and 8-50-20-2 all trained with *lm* algorithm). The choice was done looking at the error values with the “real” data test cases (Table E1 in Appendix E). They showed smaller average error values, although once again author would highlight the differences were not significant in real terms. Table 9-5 extracts these error values from Table E-1.

Table 9-5: Chosen network configurations “real” test case errors

			"Real" test cases (Γ_{LPC} / η_{HPC})									
tra. alg.	type	health p.	-1.7/-2.3	-2.4/-2.7	-1.9/-1.7	-4.5/-5.75	0/-6.5	-6/-6.75	-9.75/0	-9.75/-6.5	average	std. Dev
lm	20	Γ_{LPC}	0.07%	-0.28%	-0.04%	0.08%	0.00%	0.03%	0.05%	0.01%	0.004%	0.001
		η_{HPC}	0.17%	-0.02%	-0.26%	-0.01%	0.06%	0.01%	0.23%	-0.01%		
	20_20	Γ_{LPC}	-0.04%	-0.02%	-0.12%	0.04%	-0.12%	-0.02%	-0.05%	0.02%	0.033%	0.002
		η_{HPC}	0.06%	0.28%	0.61%	-0.03%	-0.02%	0.04%	-0.12%	0.02%		
	50_20	Γ_{LPC}	0.19%	0.10%	-0.01%	-0.01%	0.02%	-0.87%	-0.04%	-0.01%	0.001%	0.003
		η_{HPC}	-0.18%	0.12%	-0.11%	0.00%	0.00%	0.10%	0.72%	0.01%		

Probably a better indicator of tool capabilities are the absolute values that come out from testing with the “real” test cases. When compared with the health parameters implanted faults they give a clearer picture of tool results. Table E-2 has the complete set and Table 9-6 is an extract for the configurations considered. Both tables show extremely good results for *lm* trained networks. Any of them, if results were replicated when extended to more cases and other health

parameters, would be more than good enough for diagnostic. Further work has to be done in this direction to prove the validity of the approach in a more realistic scenario (refer to Chapter 10 Recommendations).

Table 9-6: "Real" test case results for chosen configurations

			"Real" test cases (Γ_{LPC} / η_{HPC})							
tra. alg.	lay/neur	health p.	-1.7/-2.3	-2.4/-2.7	-1.9/-1.7	-4.5/-5.75	0/-6.5	-6/-6.75	-9.75/0	-9.75/-6.5
lm	20	Γ_{LPC}	-1.70	-2.39	-1.90	-4.50	0.00	-6.00	-9.75	-9.75
		η_{HPC}	-2.30	-2.70	-1.70	-5.75	-6.50	-6.75	0.00	-6.50
	20_20	Γ_{LPC}	-1.70	-2.40	-1.90	-4.50	0.00	-6.00	-9.74	-9.75
		η_{HPC}	-2.30	-2.71	-1.71	-5.75	-6.50	-6.75	0.00	-6.50
	50_20	Γ_{LPC}	-1.70	-2.40	-1.90	-4.50	0.00	-5.95	-9.75	-9.75
		η_{HPC}	-2.30	-2.70	-1.70	-5.75	-6.50	-6.76	0.01	-6.50

Figure 9-12: Summary 8-50-20-2 network configuration and behaviour during training

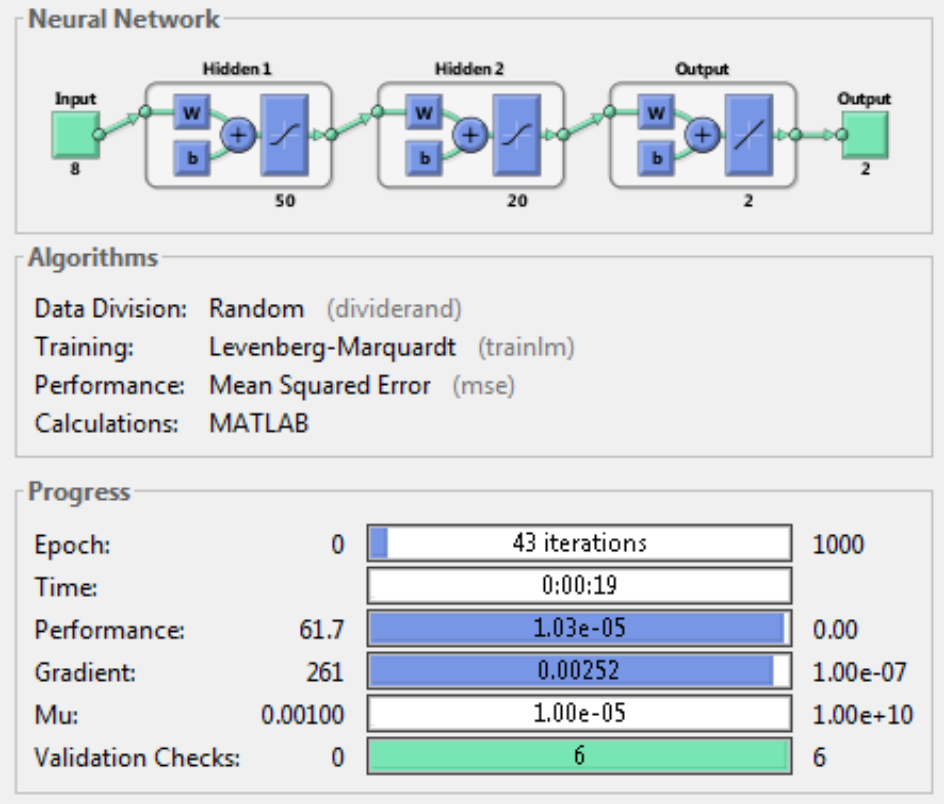

Combining all above the best choice was considered 8-50-20-2 *lm* network. Training time was small, MSE one of the lowest and in "real" test cases it showed slightly better overall results than the others aside from case [Γ_{LPC}, η_{HPC}] = [-6, -

6.75]. When looking at the absolute value of network calculated $\Gamma_{LPCresult}$ =-5.95% vs -6% the error is truly insignificant in real life terms. Figure 9-12 is a summary of the network configuration and behaviour during training.

Other items were also reviewed for this network as the variation of MSE during training, validation and testing (Figure 9-13). Training error was constantly going down, validation error started growing after 30 epochs, but test error did grow significantly, showing there was no overfitting (Figure 9-10).

The regression plot (Figure 9.14) describes the relationship between network outputs and targets; the closer it is to unity the better. In this case is R=1 for training and validation and 1 as well for test, in all indicating a too good performance driven by most likely by the fact the number of training cases was not large and only almost 70% were the result of linear interpolation. Although this compromises the results of this particular exercise it does not question the overall procedure. Had there been more capability to generate WebEngine cases the regression results might have been different, but the process would have been the same.

Figure 9-13: MSE variation (8-50-20-2)

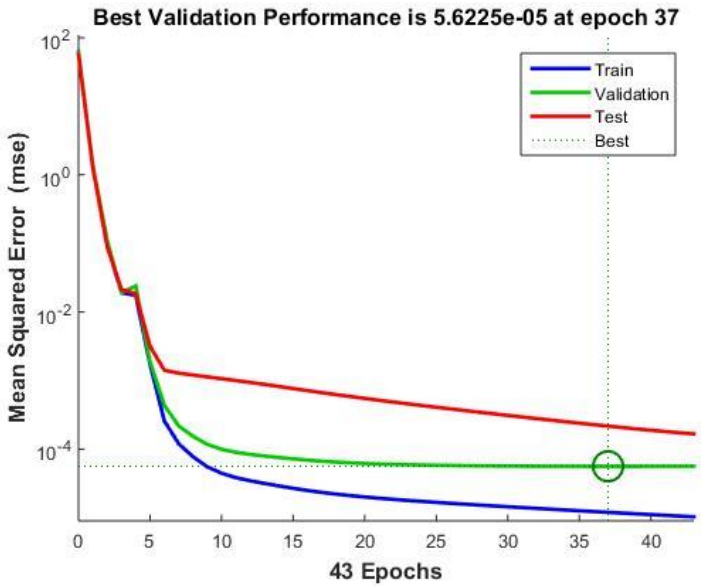

Figure 9-14: Regression plots (8-50-20-2)

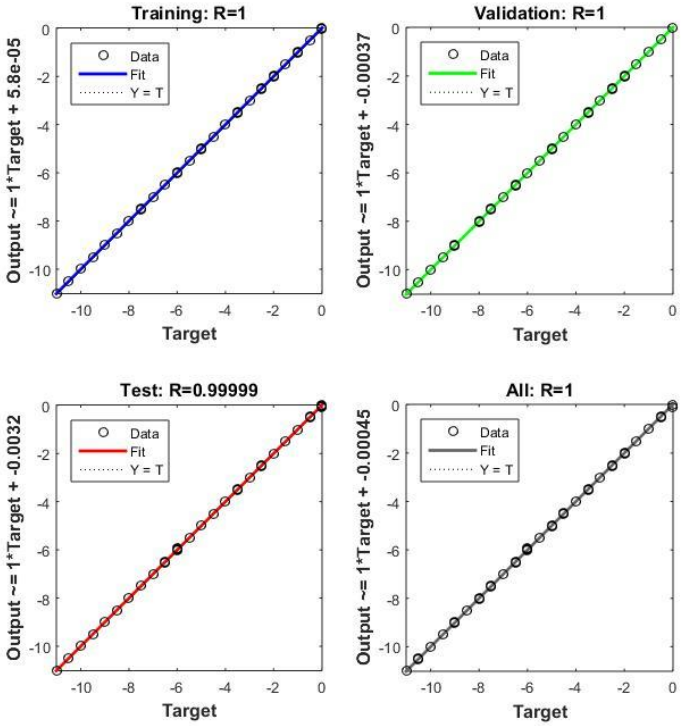

9.3.6 ISA temperature variation test

It is a known fact ANN do not respond properly to cases outside the boundaries where they have been trained. WebEngine difficulties prevented from creating training cases with ISA temperature and pressure variation, so the network has only been trained at ISO conditions. A test was done with 8-50-20-2 *lm* network running four ISA temperature variation cases just to try the response. The results were disastrous. Table 9-7 is a summary. The tool failed miserably, proving that further work needs to be done in expanding the envelope, as will be discussed in recommendations.

Table 9-7: ISA Temp. Variation test cases result

			ISA temp. deviation test cases (Γ_{LPC} / η_{HPC})			
			ISA T +10		ISA T -10	
tra. alg.	lay/neur	health p.	0/0	-2.3/-1.7	0/0	-3.85/-1.4
lm	50_20	Γ_{LPC}	-4.63	-4.82	5.92	3.64
		η_{HPC}	-10.93	-11.22	8.08	7.57

9.4 Comparison of results with LGPA

A comparison of results between 8-50-20-2 *lm* network results and LGPA was done using “real” data test cases. The summary is Table 9-8. It should be highlighted the bigger degradation cases could not be compared as using interpolated data in LGPA would not be correct. For lower degradation ANN proved to be more accurate evaluating the behaviour of η_{HPC}, with no significant difference in Γ_{LPC}.

Table 9-8: Comparison of 8-50-20-2 *lm* network and LGPA

CASE	-1.7/-2.3	-2.4/-2.7	-1.9/-1.7
50_20	-1.70	-2.40	-1.90
	-2.30	-2.70	-1.70
LGPA	-1.70	-2.40	-1.92
	-2.16	-2.49	-1.56

9.5 Conclusions

ANN has proven the capability to quantify the level of degradation of two health parameters Γ_{LPC} (LPC flow) and η_{HPC} (HPC efficiency) necessary for the decision of whether to water wash or not. Although difficulties generating data have compromised the results of this exercise, the outcome has proven the process can be used, although will require further generalization. How the results can be used and the outcome improved will be discussed in the next chapter. Comparison was done with LGPA results, ANN demonstrating better performance.

10 CONCLUSIONS AND RECOMMENDATIONS

10.1 Conclusions

The objective of this thesis was the selection and application of a Gas Turbine Performance Diagnostic Technique for a Twin Shaft Aeroderivative Gas Turbine in order to determine the need of Off-Line Water wash. Before reaching that stage other topics were covered, as review of gas turbine maintenance philosophies and instrumentation to have a better overview of the specifics of Aeroderivative Gas Turbines. Within maintenance review special attention was paid to water wash.

The overview of diagnostic methods focused on Performance Based Diagnostic methods, aiming to select the most suitable for the kind of diagnostic required. The conclusion was ANN was the most suitable method and within the reach of the Thesis scope.

A model of the engine had to be created as none was available when the project started. With the help of PhD student Asteris Apostolidis the model was created and tested via WebEngine. The results were encouraging both in design point and off design conditions although WebEngine presented some difficulties.

Once the model was available a full analysis of the Optimal Measurement set could be done applying standard methods. The test of LGPA as a potential water wash determination tool was a spinoff of this study.

The next step was the development and testing of an ANN tool. Difficulties were encountered in the creation of training case due to WebEngine limitations. An alternative technique was used, which had impact on the results, but not on the process and the suitability of the diagnostic tool. As discussed in Chapter 9 the data interpolated was in an area where degradation of Γ_{LPC} (LPC flow) and η_{HPC} (HPC efficiency), was way above what will be typically acceptable, as it will not be recoverable via normal off line water wash. The results of ANN were truly encouraging. It showed very good data approximation.

The objectives of this Thesis have been covered at the same time allowing the author to deepen his understanding of Performance Based Diagnostic methods. The skeleton of a valid tool has been laid, with attractive results. Further work is discussed in the next paragraph.

10.2 Recommendations

This Thesis has come short of finalizing a fully working tool to determine the need for on line water wash. Further areas of work can be:

- Improve the WebEngine based model of the engine with the addition of variable geometry and modifications so it matches off design behaviour closer. This is a difficult task without available data from real engines.
- Finalize WebEngine capabilities.
- If the possibility to generate more data becomes available further tests can be done on ANN with ΔT_{amb} and ΔP_{amb} training data.
- Include other parameters as η_{LPC} (LPC efficiency), Γ_{HPC} (HPC flow) and η_{HPT} (HPT efficiency) so the behaviour of the real engine is simulated better.
- Expand the investigation into the use of Dynamic ANN ([59]) in the prediction of health parameter degradation therefore engine degradation.

The final aim of all this work is a viable tool easy to use by the operator and directly connected to both the plant data acquisition and control system and the RM&D system. The schematic of how can this be achieved is outlined below, assuming OEM participation.

- New and clean engine data should be gathered in the initial hours of operation.
- The OEM cycle deck engine model can be personalized for that particular engine, adjusting health parameters so the engine's behaviour is best simulated. This can also be done with any other engine model program as WebEngine.
- Once the model is personalized training cases can be created as required.
- Based on the work above several ANN can be configured, trained and tested, choosing the most suitable.

- The selected ANN can be used within a water wash schedule determination program discussed below.

It was highlighted in Chapter 2 water wash (off line and on line) schedule is very site dependent. A proposal for a program using the developed tool is below:

- From new and clean engine start on line water wash schedule (i.e. daily) evaluating its effects with ANN tool as well as standard techniques as power output, pressure ratio, etc…
- Incorporate off line schedule. The initial schedule is best conservative, as it has been highlighted if fouling progresses too far, dirt maybe difficult to remove with no manual hand clean.
- Different schedules of off line and on line should be tested carefully.
- Above schedules will determine the threshold of the chosen parameters defining the need for water wash.
- Once threshold is selected it can be easily combined with the output of ANN, and if linked with a RM&D system for continuous monitoring.
- The output of this monitoring can be fed via mobile communications to plant engineers, as for example a message highlighting the need for off line water wash is approaching.

The program described does not intend to be exhaustive, just outline further potential development. References [17], [55] and [57] are good starting points for this potential program development. The engine will deteriorate with operation and focusing on just two health parameters will become more and more unrealistic. The above proposal can be thought as the starting point of a deeper investigation into the use of Performance Based Diagnostic methods for this engine model.

REFERENCES

[1] Gas Turbine Performance; Walsh P.P., Fletcher P.; Blackwell Science Ltd. & ASME, 2nd Ed., 2000

[2] Gas Turbine Theory; Saravanamutto H.I.H.; Pearson Prentice Hall, 6th ed., 2008

[3] Gas Turbine Performance Simulation; Pachidis V.A.; Thermal Power MSc Course Notes, Cranfield, 2011

[4] Performance Prediction and Simulation of Gas Turbine Engine Operation; RTO-TR-044, April 2002, Chapter 2

[5] Gas turbine performance prognostic for condition-based maintenance; Li Y.G.; Nilkitsaranont, P.; Applied Energy 86, 2009, pp. 2152–2161

[6] Systematic measurement selections for gas path diagnostics of industrial gas turbines; Jasmani M.S.; MSc Thesis, Cranfield, 2009

[7] Gas Turbine Diagnostics MSc course notes (Ed. 1.4); Li Y.G.; Cranfield, 2011

[8] GE Aeroderivative Gas Turbines – Design and Operating Features; Baader G.H.; GE Power Systems, 2000

[9] Parameter selection for multiple fault diagnostics of gas turbine engines; Urban L.A.; ASME Paper 74-GT-62, J. Eng. Power, Apr 1975, pp. 225-230

[10] Performance-analysis-based gas turbine diagnostics: a review; Li Y.G.; Proc Instn Mech Engrs Vol 216 Part A: J Power and Energy, 2002, pp. 363-377

[11] Artificial Neural Networks in Fault Diagnosis: A Gas Turbine Scenario; Ogaji S.; Singh R.; Computational Intelligence in Fault Diagnosis, Vasile Palade, Cosmin Danut Bocaniala and Lakhmi Jain (Eds), Springer-Verlag, 2006, pp. 179-207

[12] Development of an Industrial Gas Turbine Component and Sensor Fault Diagnostic System using Artificial Neural Networks; Burke J.B.; MSc Thesis, Cranfield, 2011

[13] Gas turbine gas path diagnostics using classification and approximation neural networks; Onyeche N.C.; MSc Thesis, Cranfield, 2010

[14] WebEngine - a web-based gas turbine performance simulation tool, Apostolidis A.; Sampath S.; Laskaridis P.; Singh R.; Proceedings of ASME Turbo Expo 2013 GT2013, ASME, 2013

[15] Gas turbine Performance Deterioration; Meher-Homji C.B., Chaker M.A., Motiwalla H.M.; Proceedings of the Thirtieth Turbomachinery Symposium, Turbomachinery Laboratory, ppp. 139 – 175, Texas A&M University, College Station, Texas, 2001

[16] Analysis of gas turbine compressor fouling and washing on line; Vigueras M. O.; PhD thesis Cranfield, 2007

[17] Gas Turbine Axial Compressor Fouling and Washing; Meher-Homji C. B. and Bromley A.; 33rd Turbomachinery Symposium edition, Texas A&M University, 2004

[18] Guideline for gas turbine inlet air filtration systems; Wilcox M., Baldwin R., Garcia-Hernandez A., Brun K.; Gas Machinery Research Council Southwest Research Institute®, 2010

[19] Gas Turbine Tutorial, Maintenance and operating practices effects on degradation and life; Kurz R., Brun K.; Proceedings of the 36th Turbomachinery Symposium, 2007, pp 173 to 185

[20] The Superalloys, fundamentals and applications; Reed R.C.; Cambridge University Press, 2006, pp. 165 – 169

[21] The use of optimal estimation techniques in the analysis of gas turbines; Provost M.J.; Cranfield, PhD Thesis, 1995

[22] Aeroderivatives Engines Performance Material Training PSE Europe (GE Internal); Adhami W.; Chavez P.; Trejo A.; GE internal, 2009

[23] Gas Path Analysis Methods For A Turboshaft Aeroengine; Manickam R.; Cranfield, MSc Thesis Academic Year: 2009 – 2010

[24] Gas Turbine Performance and Diagnostics for Oil & Gas Applications: Experimental Study of Compressor Fouling and On-line Washing; Cottin C.; Cranfield, MSc Thesis, Sep 2012

[25] Assessment of the effectiveness of gas path diagnostics schemes; Mathiudakis K.; Kamboukos Ph.; Journal of Engineering for Gas Turbines and Power, Vol 126, Jan 2006, pp. 57 – 63

[26] An investigation of ANN for a gas path deterioration analysis applied to the GE 6B Frame engine; Al-Mahrooqi T.; Cranfield, MSc Thesis, 2002

[27] The application of Neural Networks to diagnostics of an industrial gas turbine; Ghoreyshi M.; Cranfield, MSc Thesis, 2003

[28] Parameter selection for diagnosing a gas-turbine's performance-deterioration; Ogaji S., Sampath S., Singh R., Probert, S.D.; Applied Energy 73 (2002), pp. 25–46

[29] Neural Network for detection of gas turbine sensor faults using multiple operating performance analysis; Ismail I.; Cranfield, MSc Thesis, 1999

[30] Industrial gas turbines: performance and operability; Razak A.M.Y.; Cambridge: Woodhead, 2007

[31] Advanced Gas-path Fault Diagnostics for Stationary Gas Turbines; Ogaji, S.O.T.; Cranfield; PhD Thesis, 2003

[32] The world's first industrial gas turbine set – GT Neuchâtel; ASME Historical Landmark #135 brochure

[33] The Jet Engine; Rolls Royce Technical Publications, 2004

[34] The Development of Jet and Turbine Aero Engines; Gunston B.; PSL 1995

[35] The History of the Industrial Gas Turbine (Part 1 The First Fifty Years 1940-1990); Hunt R.J.; IDGTE Paper 532 Version 2, 2011

[36] Aeroderivative Gas Turbines for LNG Liquefaction Plants; Meher-Homji C.B., Messersmith D., Hattenbach T., Rockwell J., Weyermann H., Masani K.;

Proceedings of ASME Turbo Expo 2008 Power for Land, Sea, and Air, June 9-13, Berlin, Germany, 2008

[37] Artificial Neural Networks, an introduction; Priddy K., Keller P.E.; Tutorial Texts in Optical Engineering TT68; SPIE—The International Society for Optical Engineering, Washington, 2005

[38] Instrumentation and control. Fundamental and applications; Nachtigal C.L. (Ed.); Wiley Series in Mech .Eng. Practice, John Wiley & Sons, Inc 1990

[39] Measurement Uncertainty Analysis: Methods and Applications; Dieck R.H.; ISA, 1992

[40] ASME PCT22-2005 Gas Turbine Performance Test Codes; ASME, 2006

[41] BS ISO 2314:2009 Gas turbines - Acceptance tests; British Standard, 2009

[42] Evaluation of measurement data — Guide to the expression of uncertainty in measurement; Joint Committee for Guides in Metrology (JCGM), BPIM, 2008

[43] Gas Turbine Engineering Handbook 3rd edition; Boyce M.P.; Gulf Professional Publishing, Burlington, 2006

[44] Machinery Vibration Analysis and Predictive Maintenance; Girdhar P., Scheffer C. (ed); IDC Technologies, 2004

[45] Condition-Based Maintenance for Gas Turbines Plants; Romesis C., Li Y.

[46] Fundamentals of Maintenance (Thermal Power Plant Performance Analysis); Souza G., Carazas F.; Springer – Verlag London Ltd, 2012

[47] Risk-Based Inspection and Maintenance (RBIM) of Power Plants (Thermal Power Plant Performance Analysis); Khan F., Haddara M., Khalifa M.; Springer – Verlag London Ltd, 2012

[48] Fast, Flexible Power Aeroderivative Product and Service Solutions (GEA18249b); GE Power and Water®; downloaded March 2015

[49] The Industrial Trent 60 Gas Turbine; Siemens; downloaded March 2015

[50] Marine Gas Turbine Health Monitoring a New Approach; Walker J., Summerfield A.; 87-GT-245; Gas Turbine Conference and Exhibition, Anaheim, California, 1987

[51] Turbine Oil Condition Monitoring (Technical Training Guide); Mobil; downloaded October 2010

[52] Performance Diagnostics And Creep Life Study Of Aeroderivative Gas Turbine In Marine Application; Kumar S.; MSc Thesis, Cranfield, 2011

[53] Measurement and Control Basics; Hughes T.A.; Resources for Measurement and Control Series, Instrument Society of America, 1988

[54] Gas Turbine Engine and Sensor Fault Diagnosis; Zedda M.; PhD Thesis; Cranfield, 1999

[55] Determining compressor wash programmes for fouled gas turbines; Sánchez D., Chacartegui R., Becerra J.A., Sánchez T.; Journal of Power and Energy 223, Institution of Mechanical Engineers, 2009

[56] Gas Turbine Compressor Washing: Historical, Developments, Trends, and Main Design Parameters, for Online Systems; Mund F., Pilidis P.; Journal of Gas Turbine Engineering and Power Vol 128, ASME, April, 2006

[57] A Prognostic Modeling Approach for Predicting Recurring Maintenance for Shipboard Propulsion Systems; Kacprzynski G., Gumina M., Roemer M., Caguiat D., Galie T., Mc Groarty J.; ASME 2001-GT-0218; ASME, 2001

[58] Gas turbine performance and diagnostics investigating the applicability of artifical neural network during compressor fouling; Sinanis A.; MSc Thesis, Cranfield, 2013

[59] MATLAB Neural Network Toolbox™ User's Guide; Hudson M., Hagan M.T., Demuth H.B.; The MathWorks Inc, 2015

[60] Neural Network Design; Hagan M.T., Demuth H.B., Beale M.H.; PWS Publishing, Boston, 1996

APPENDICES

Appendix A DEGRADED PERFORMANCE RESULTS

A.1 Degraded Performance Results Graphs

Graphical results for main performance are shown below. Discussion of results is done in Chapter 6

Table A-1: List of degraded performance simulation graphs

Figures	
A2-1	Power
A2-2	SFC
A2-3	PR
A2-4	Mass Flow
A2-5	HP Speed
A2-6	Fuel Flow

Figure A-1: Power

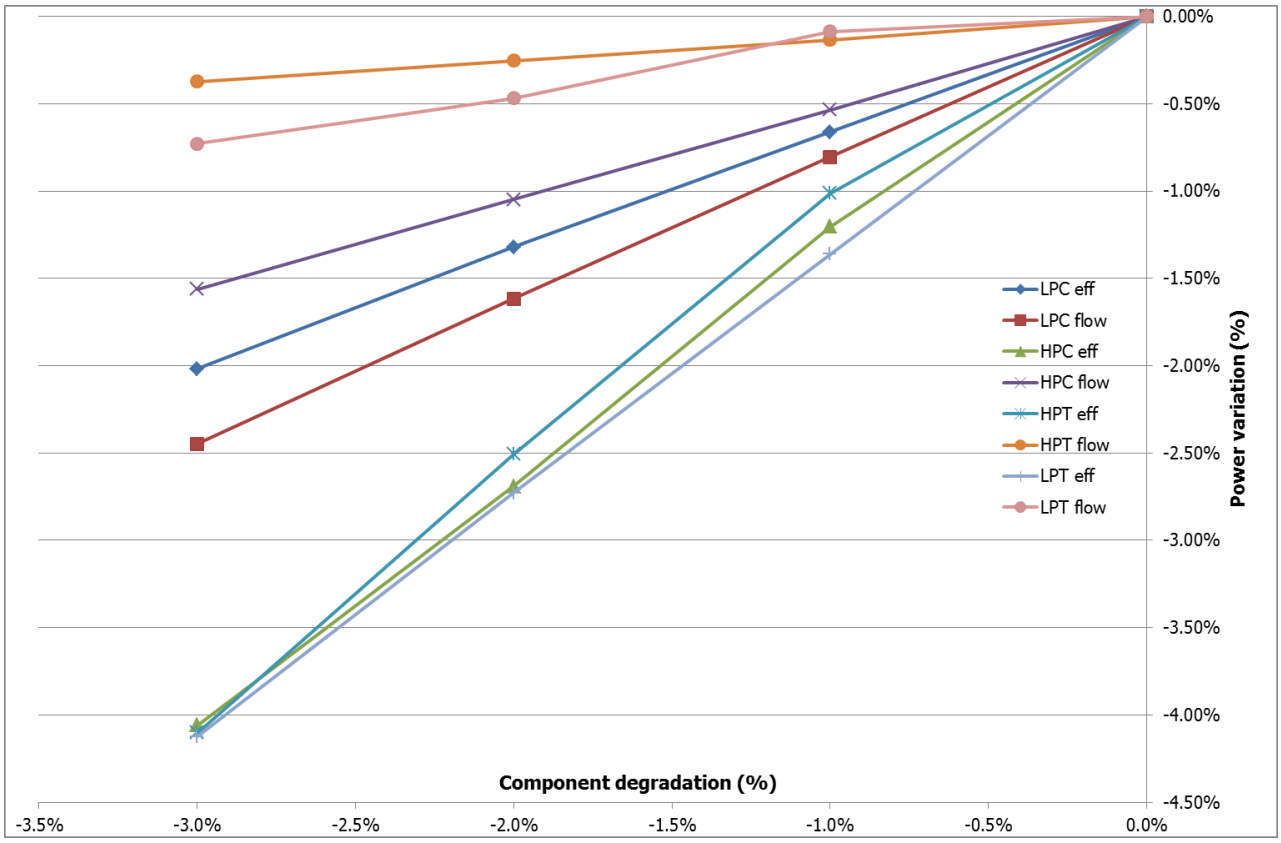

Figure A-2: SFC

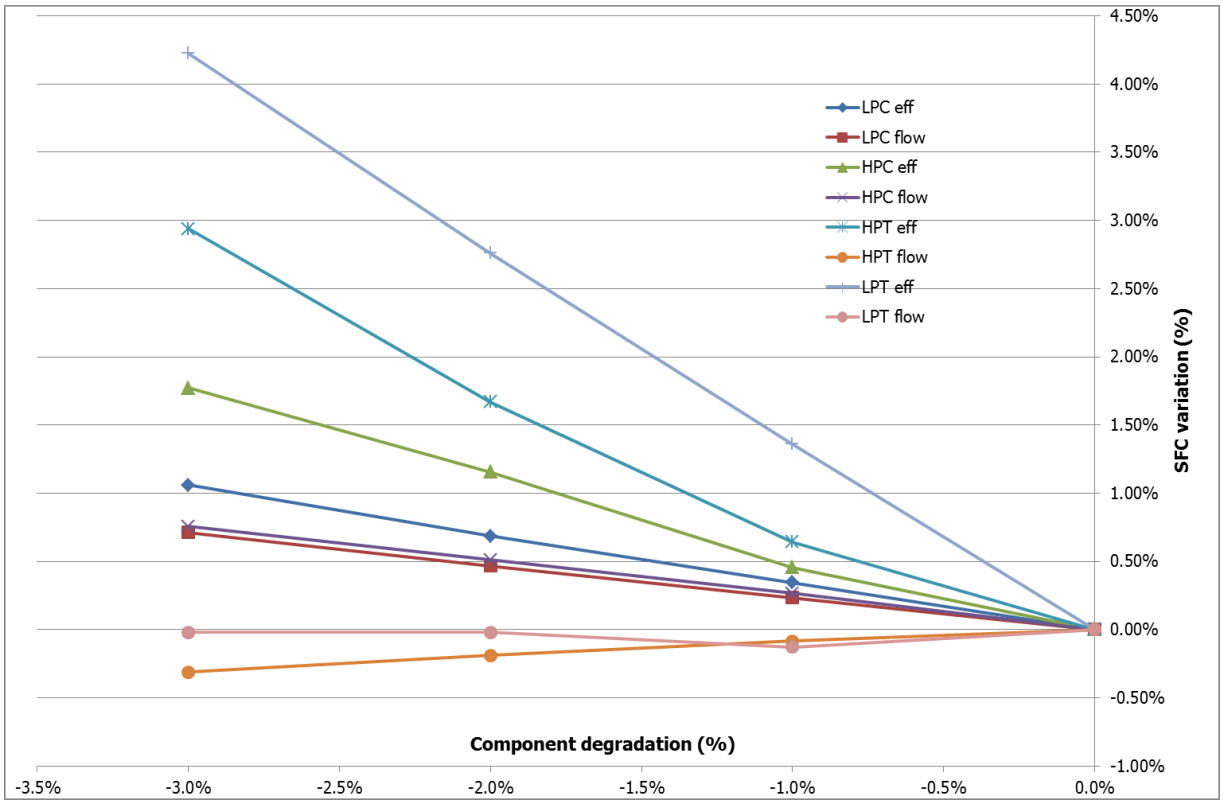

Figure A-3: PR

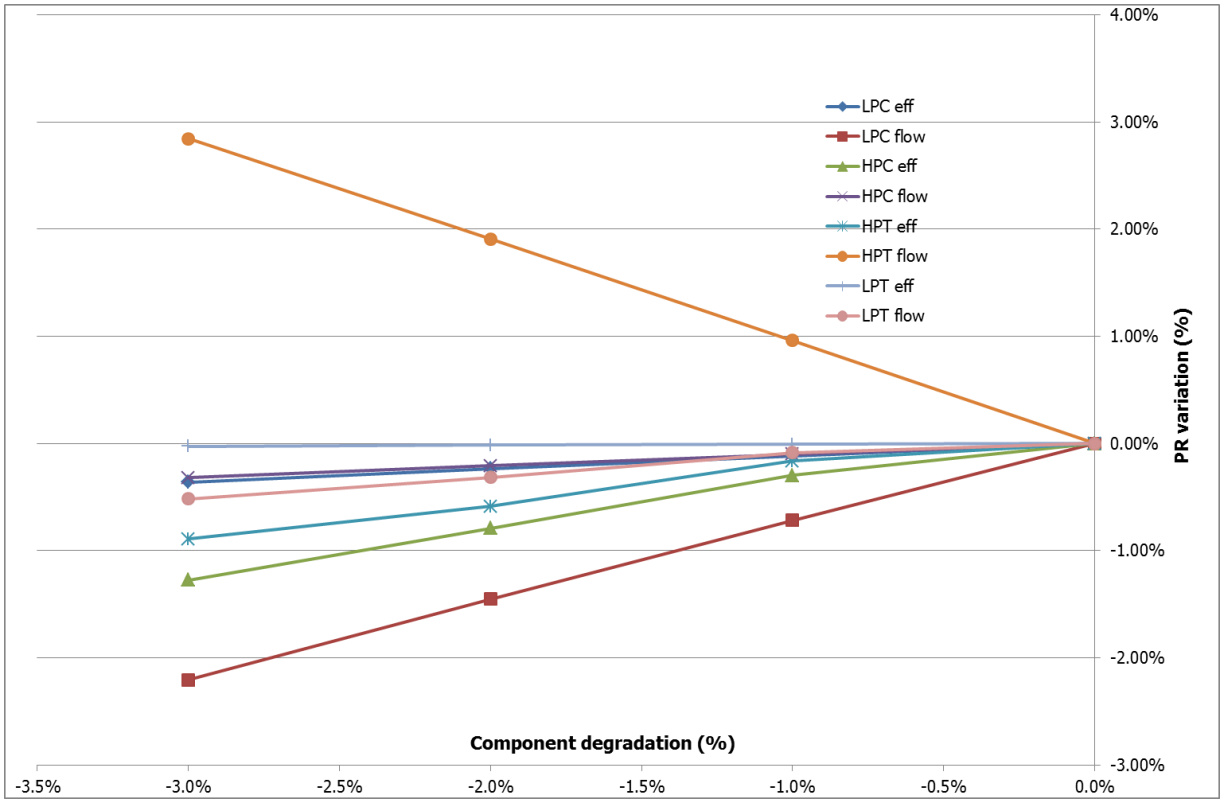

Figure A-4: Mass Flow

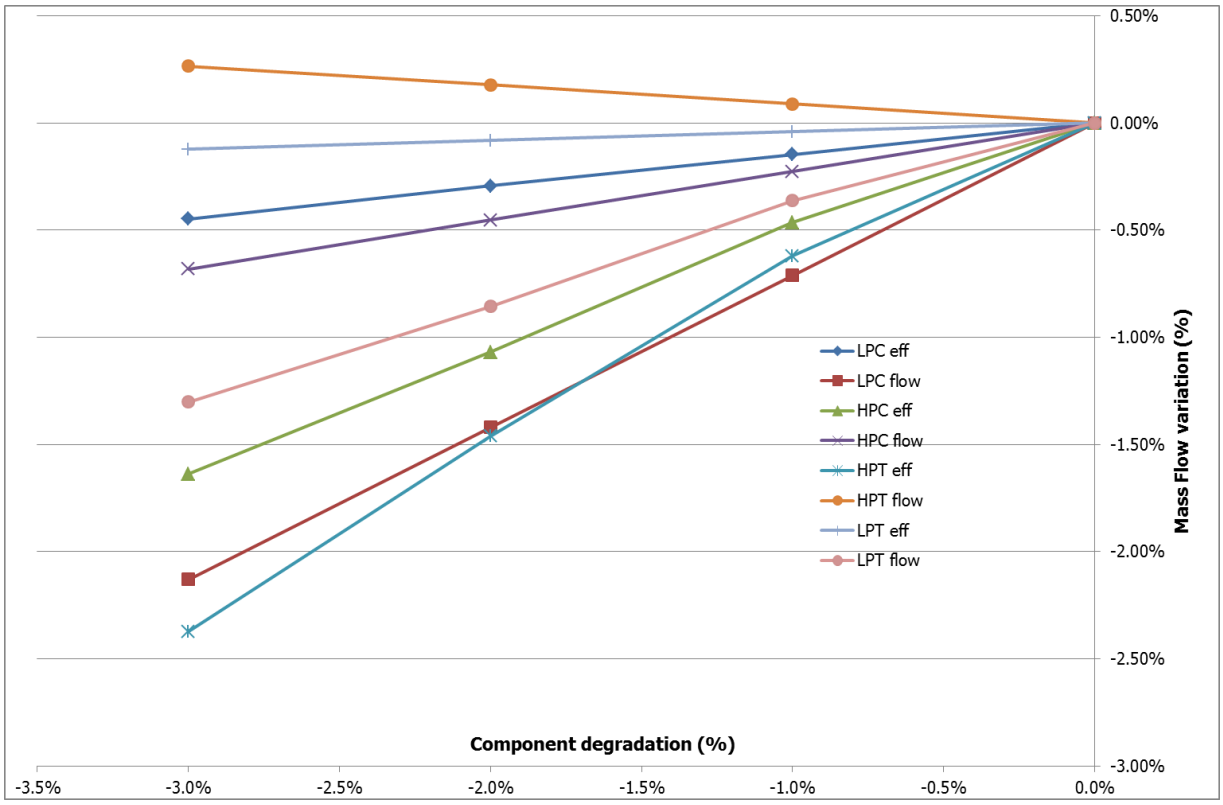

Figure A-5: HP Speed

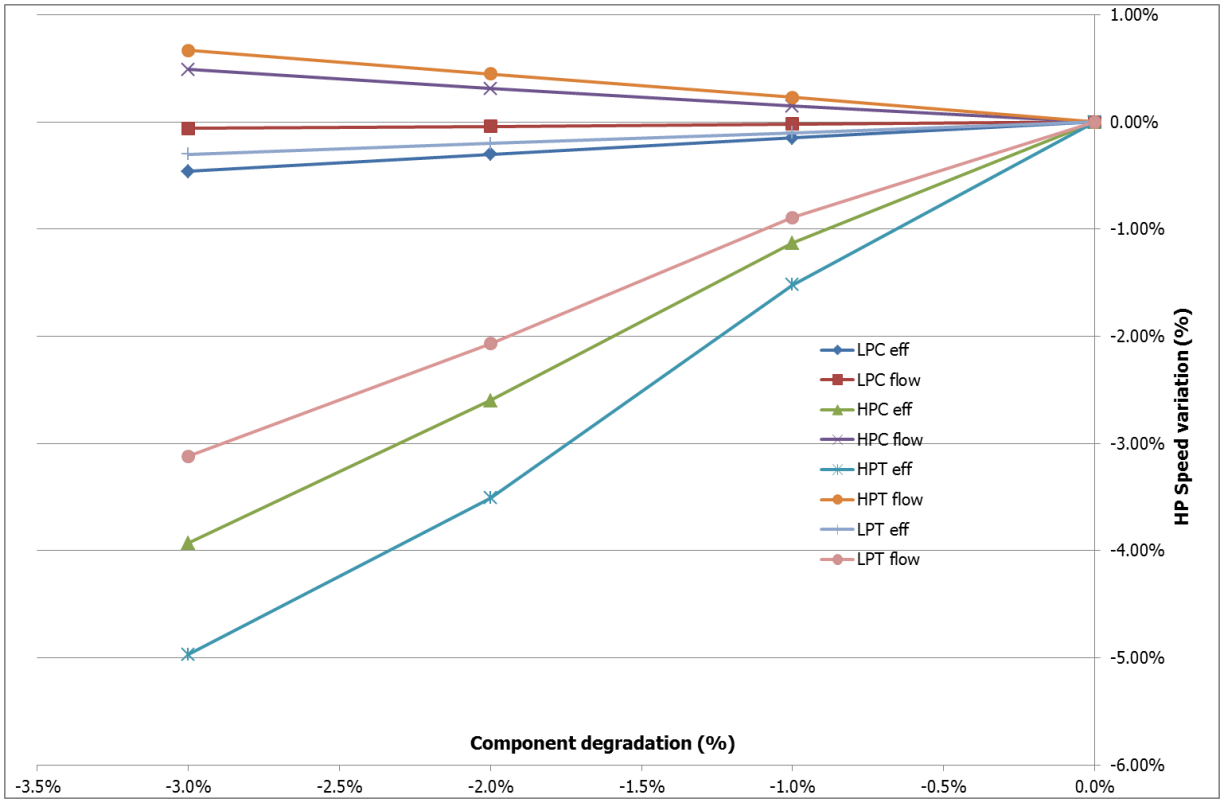

Figure A-6: Fuel Flow

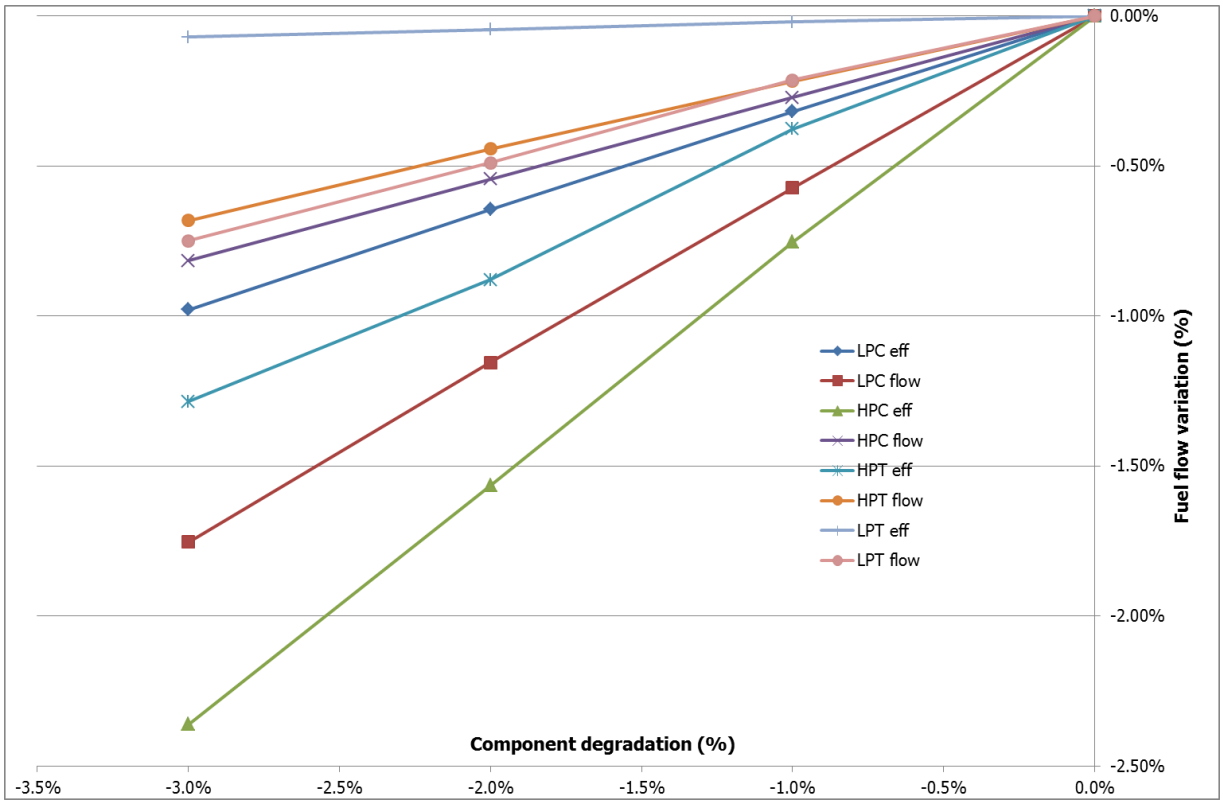

Appendix B LGPA FOULING CASES

This appendix has the graphical results of all the cases from Chapter 8. The following figures show LGPA calculated health parameter value for the ranges of variation of Γ_{LPC} and η_{HPC}. Table below summarizes the cases and the amount of power loss each one represents as per Web Engine results (same as Table 8-1).

Table B-1: Combination of ΓLPC and ηHPC for ΔPower=-2 MW

		MW (diff vs DP)						
		Γ LPC (%)						
		0	-1	-2	-3	-4	-5	-6
η HPC (%)	0	0.00	-0.35	-0.70	-1.06	-1.43	-1.81	-2.13
	-0.5	-0.26	-0.60	-0.94	-1.30	-1.47	-1.91	
	-1	-0.52	-0.85	-1.20	-1.55	-1.92	-2.05	
	-1.5	-0.78	-1.11	-1.45	-1.80	-2.16		
	-2	-1.16	-1.46	-1.71	-2.06			
	-2.5	-1.46	-1.75	-2.04				
	-3	-1.76	-2.05					
	-3.5	-2.11						

Γ_{LPC} [0, -6%]

Figure B-1: ΓLPC = 0% & ηHPC = [0,-3.5%]

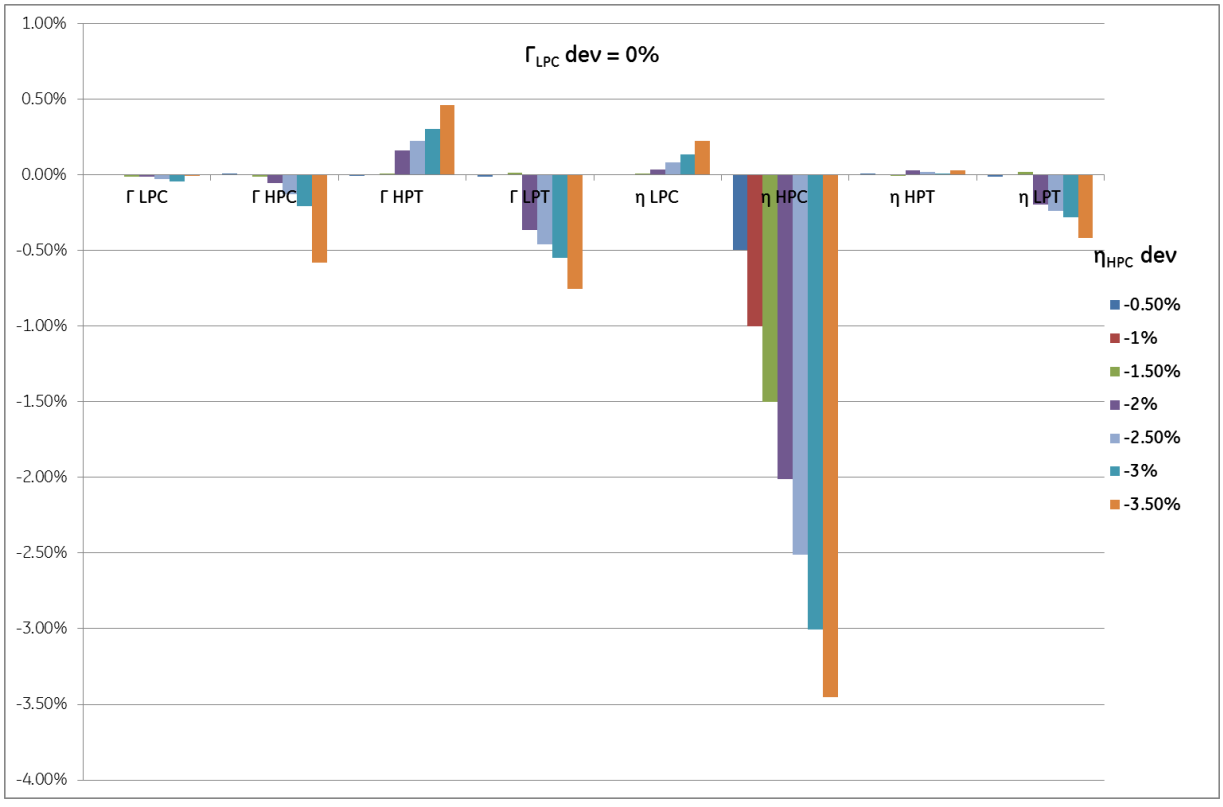

Figure B-2: ΓLPC = -1% & ηHPC = [0,-3%]

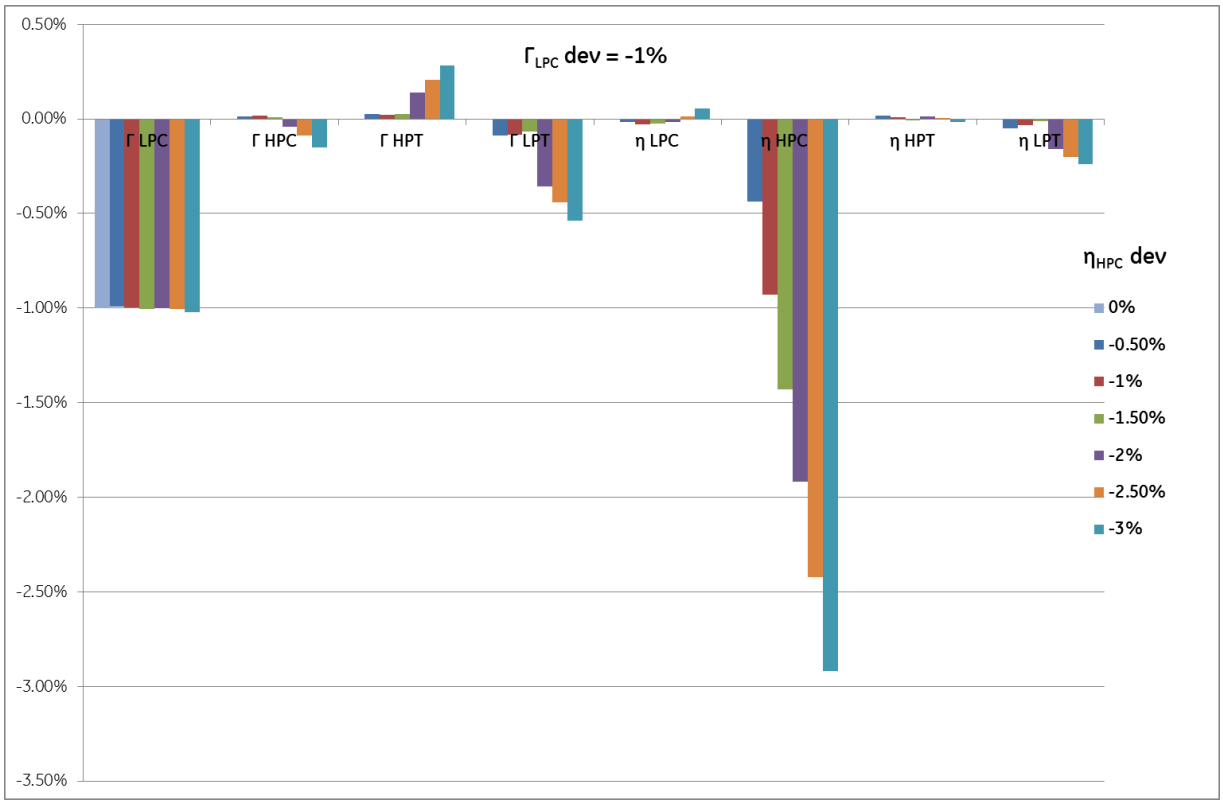

Figure B-3: ΓLPC = -2% & ηHPC = [0,-2.5%]

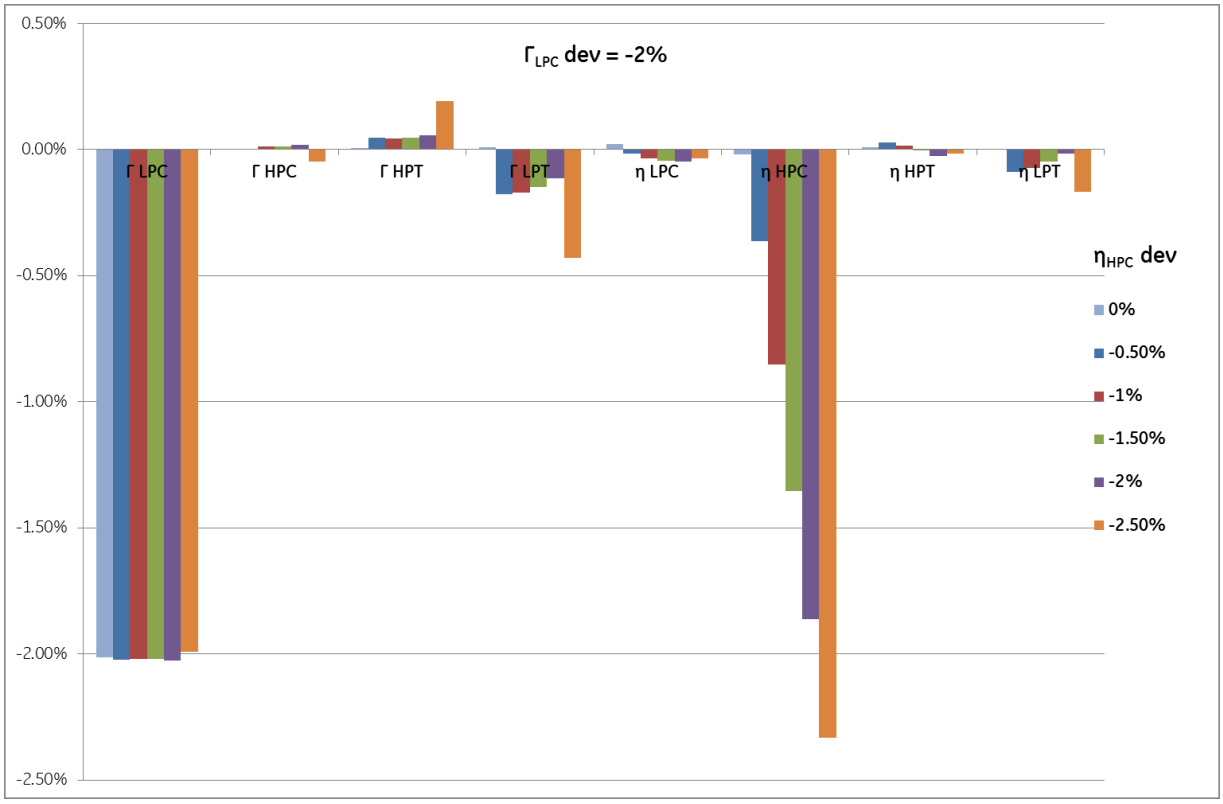

Figure B-4: ΓLPC = -3% & ηHPC = [0,-2%]

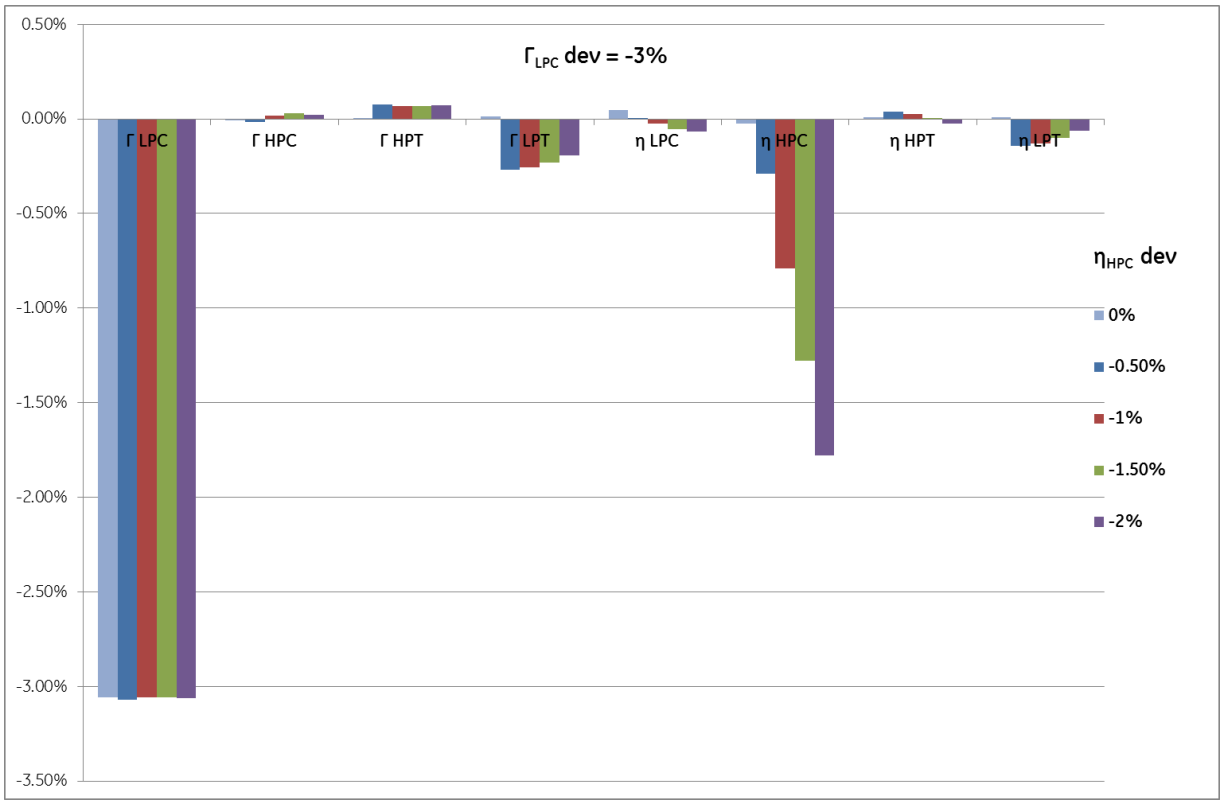

Figure B-5: ΓLPC = -4% & ηHPC = [0,-1.5%]

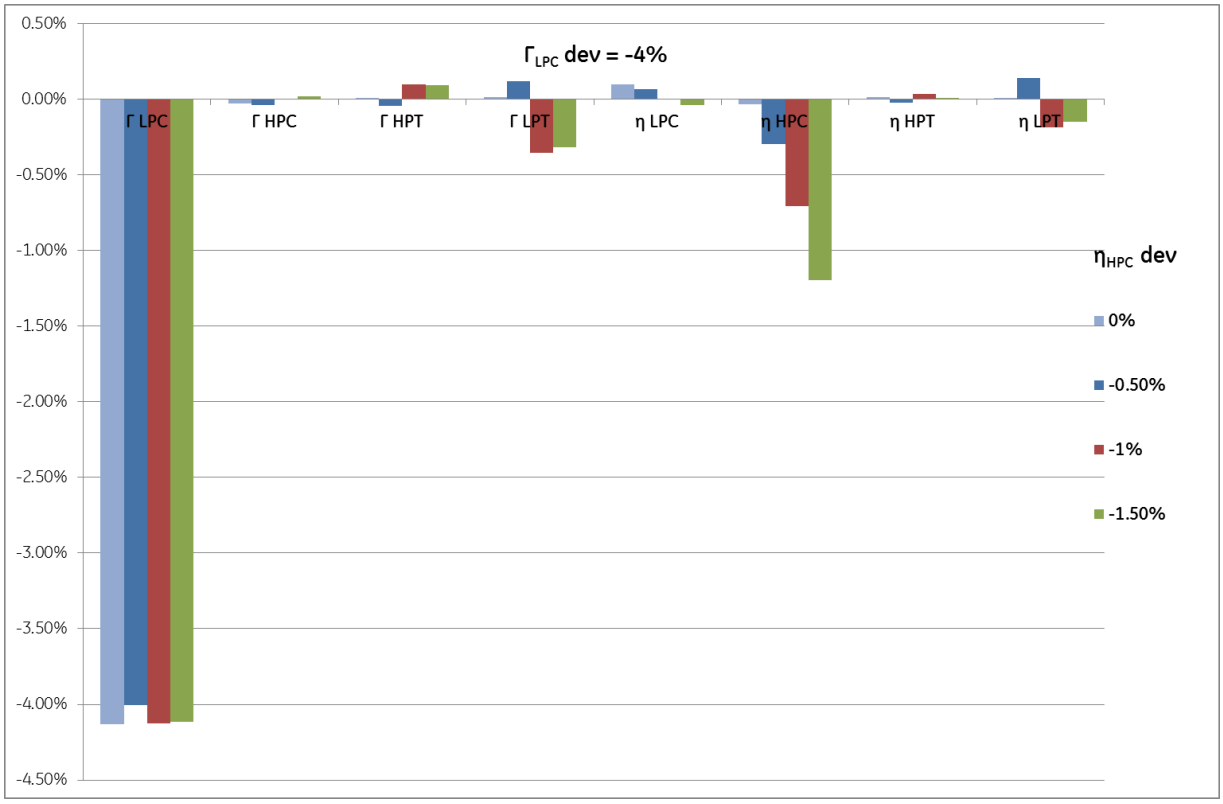

Figure B-6: ΓLPC = -5% & ηHPC = [0,-1%]

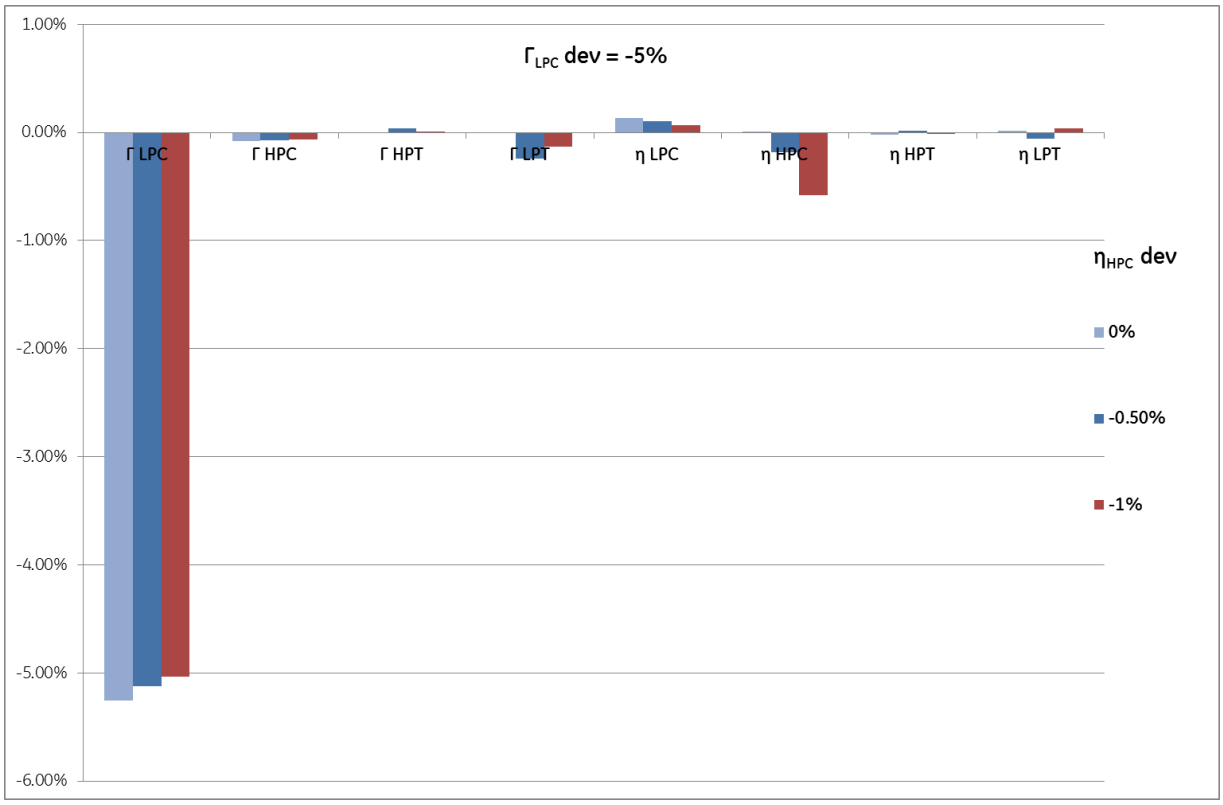

Figure B-7: ΓLPC = -6% & ηHPC = 0%

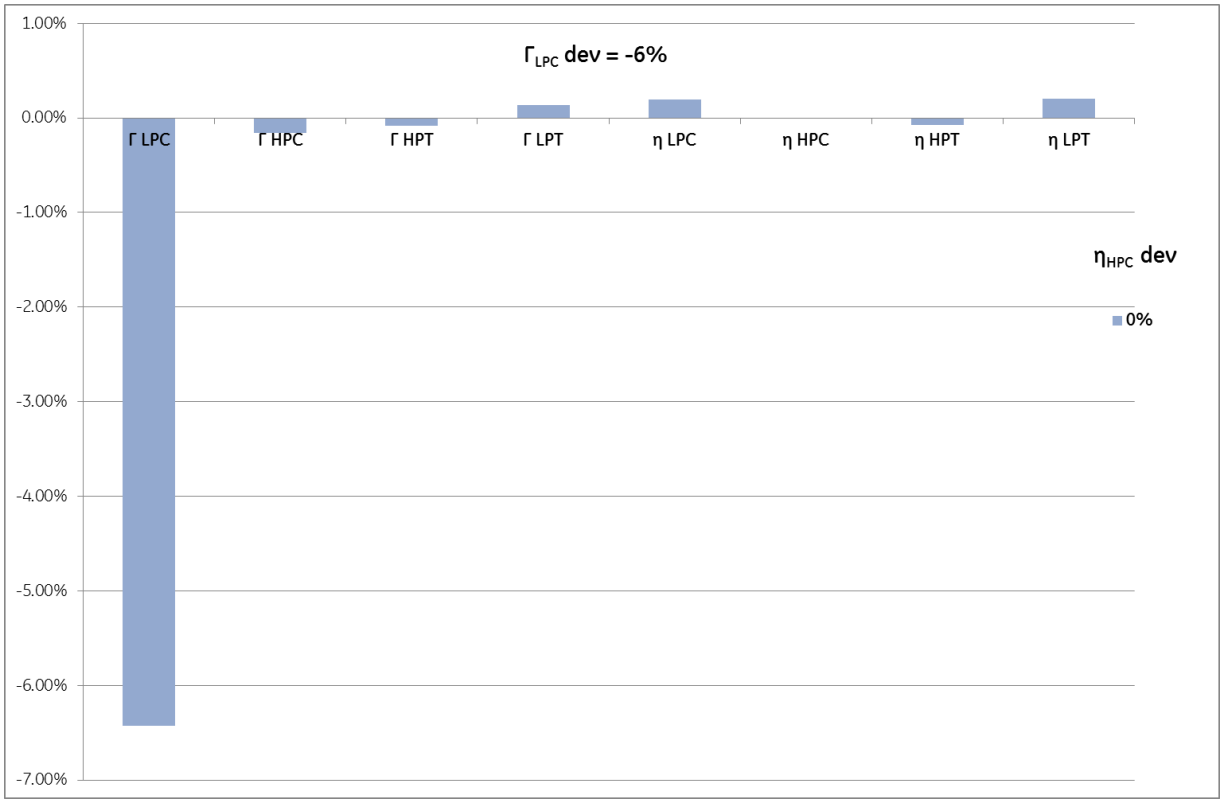

η_{HPC} = [0,-3.5%]

Figure B-8: ηHPC = 0% & ΓLPC = [0,-6%]

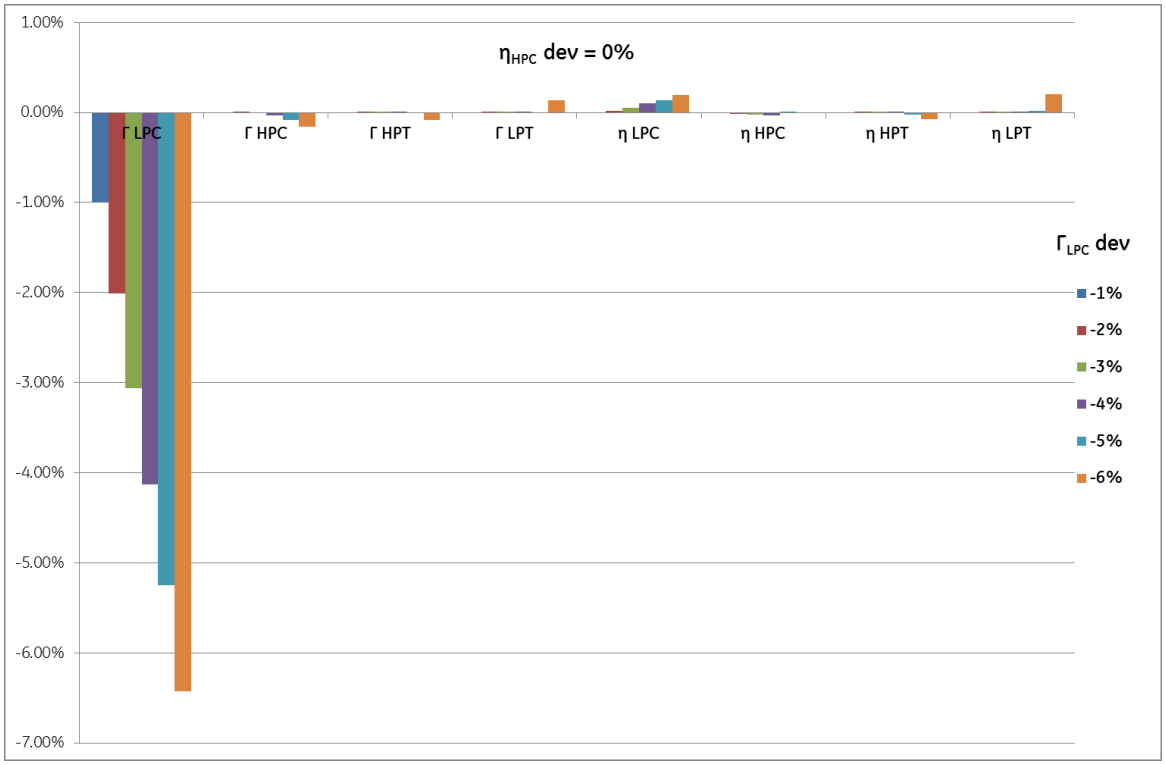

Figure B-9: ηHPC = -0.5% & ΓLPC = [0,-5%]

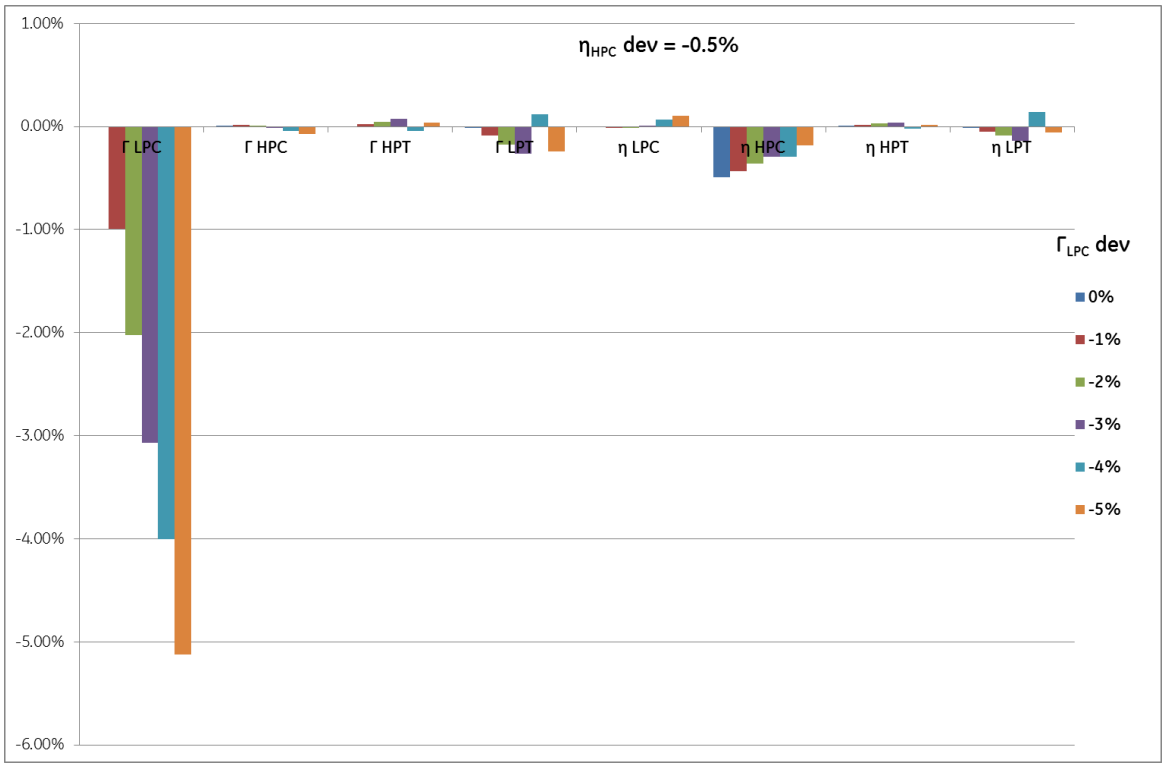

Figure B-10: ηHPC = -1% & ΓLPC = [0,-5%]

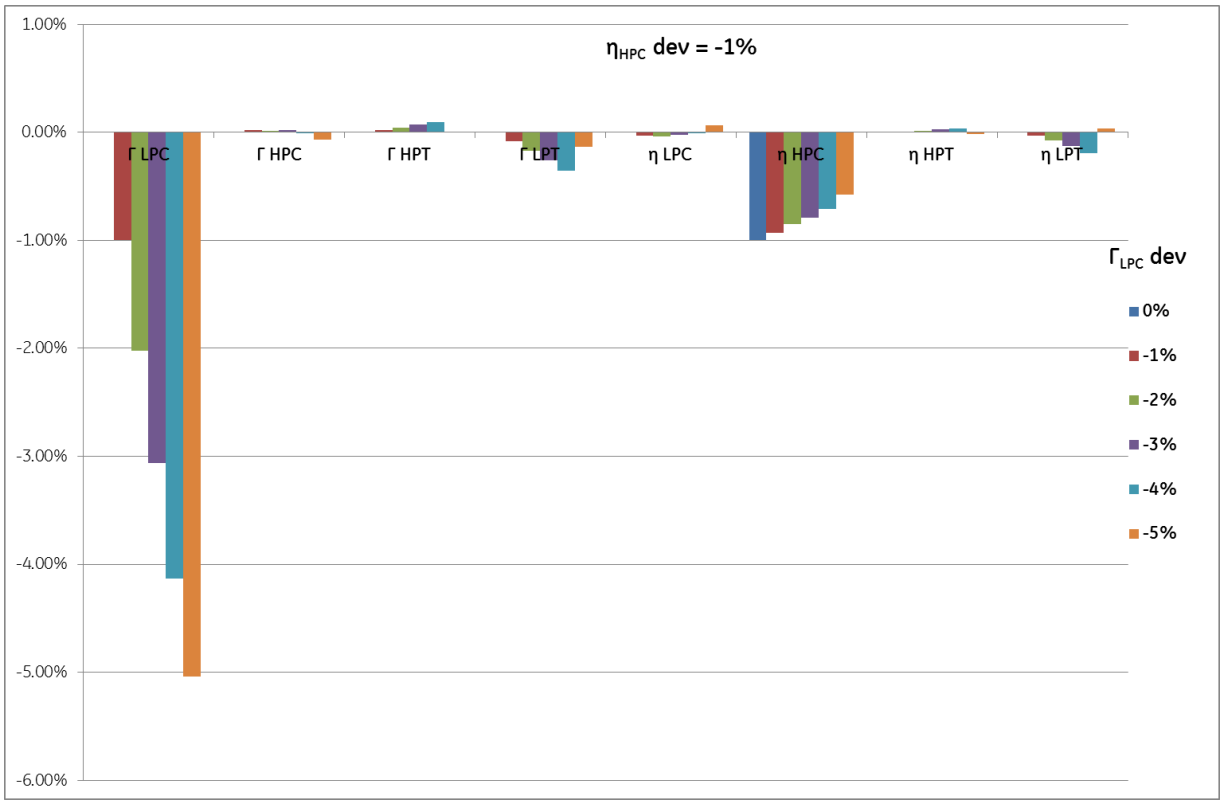

Figure B-11: ηHPC = -1.5% & ΓLPC = [0,-4%]

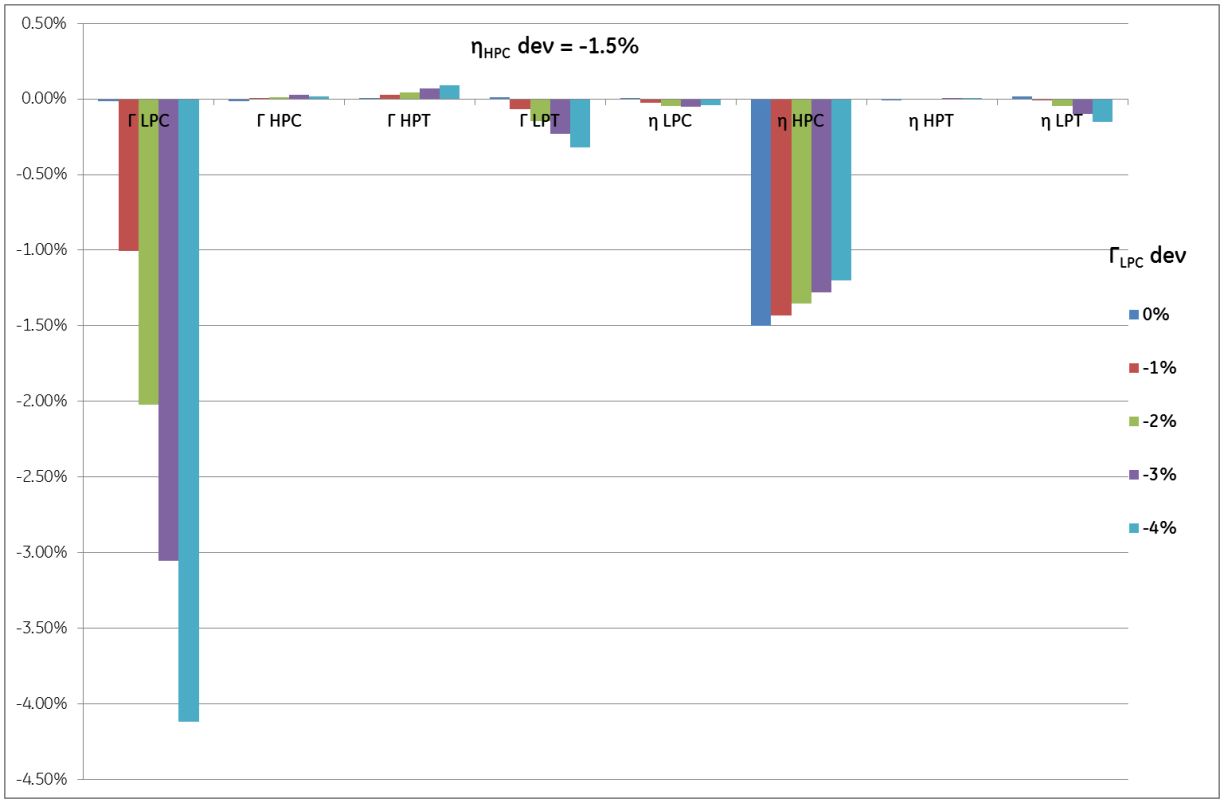

Figure B-12: ηHPC = -2% & ΓLPC = [0,-3%]

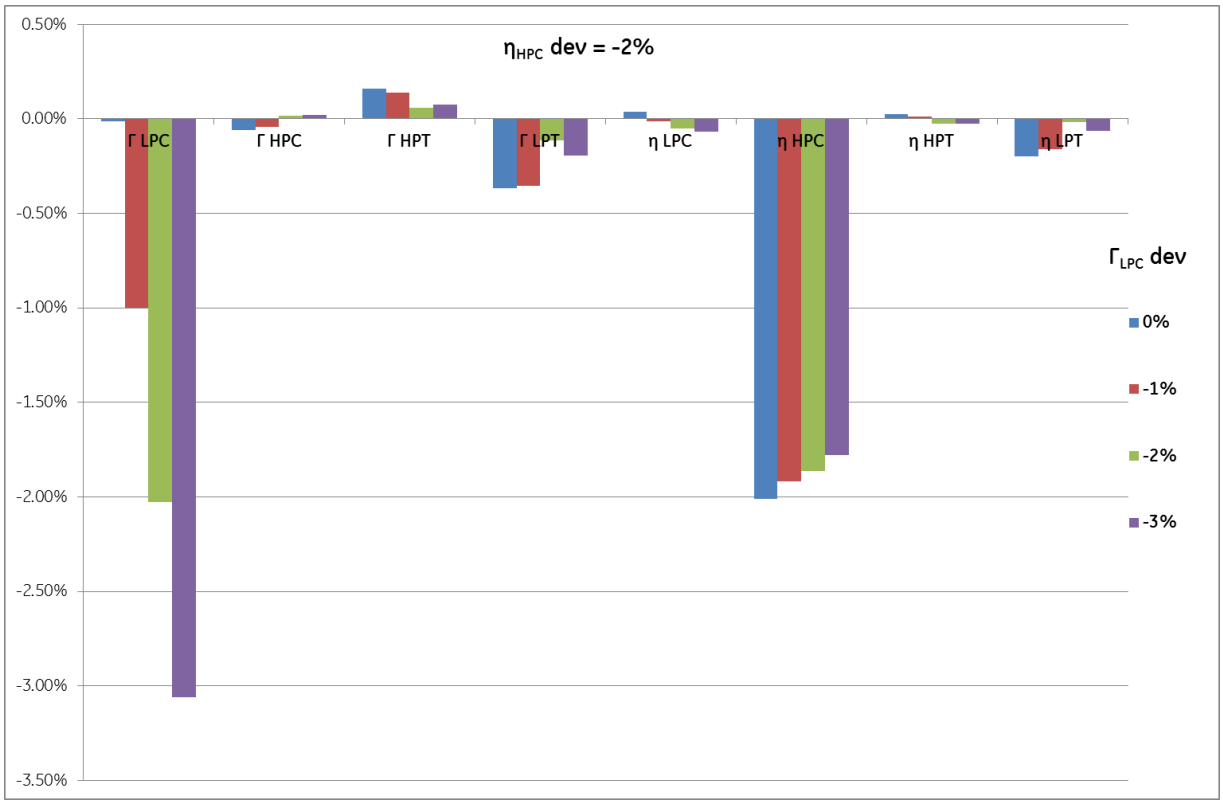

Figure B-13: ηHPC = -2.5% & ΓLPC = [0,-2%]

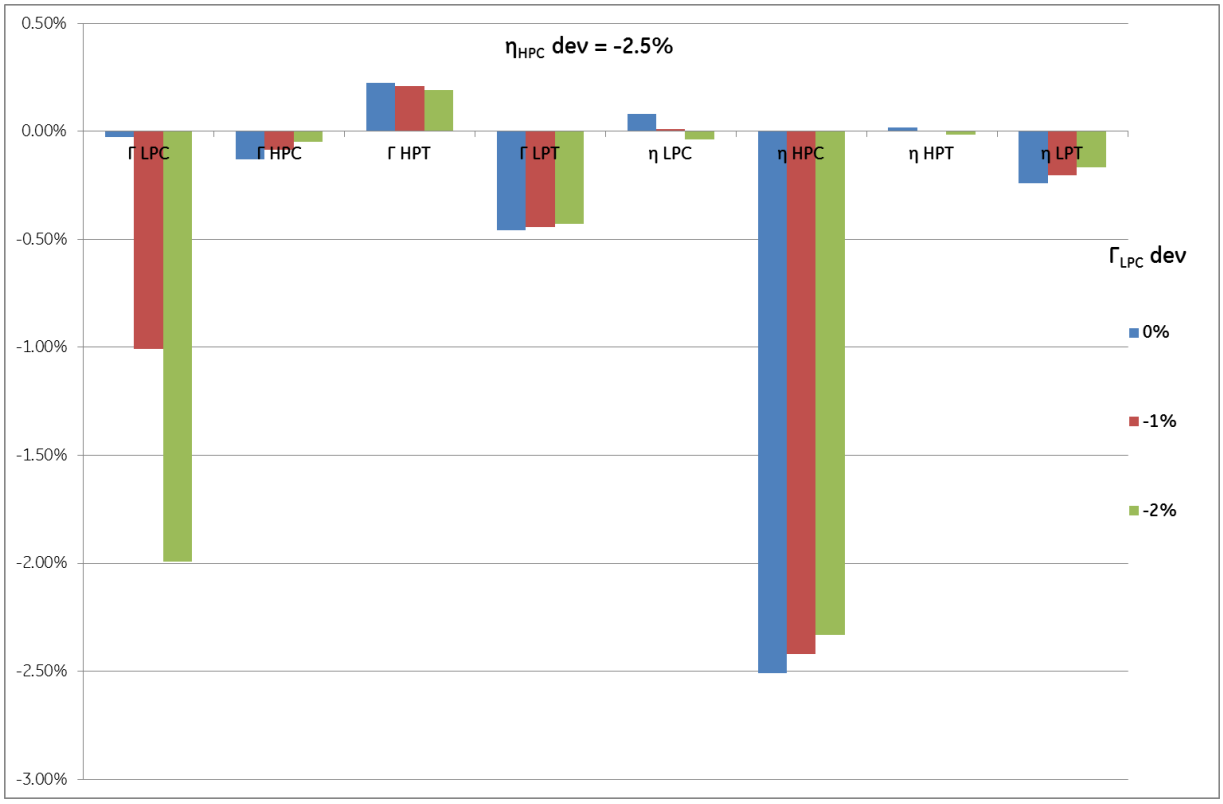

Figure B-14: ηHPC = -3% & ΓLPC = [0,-1%]

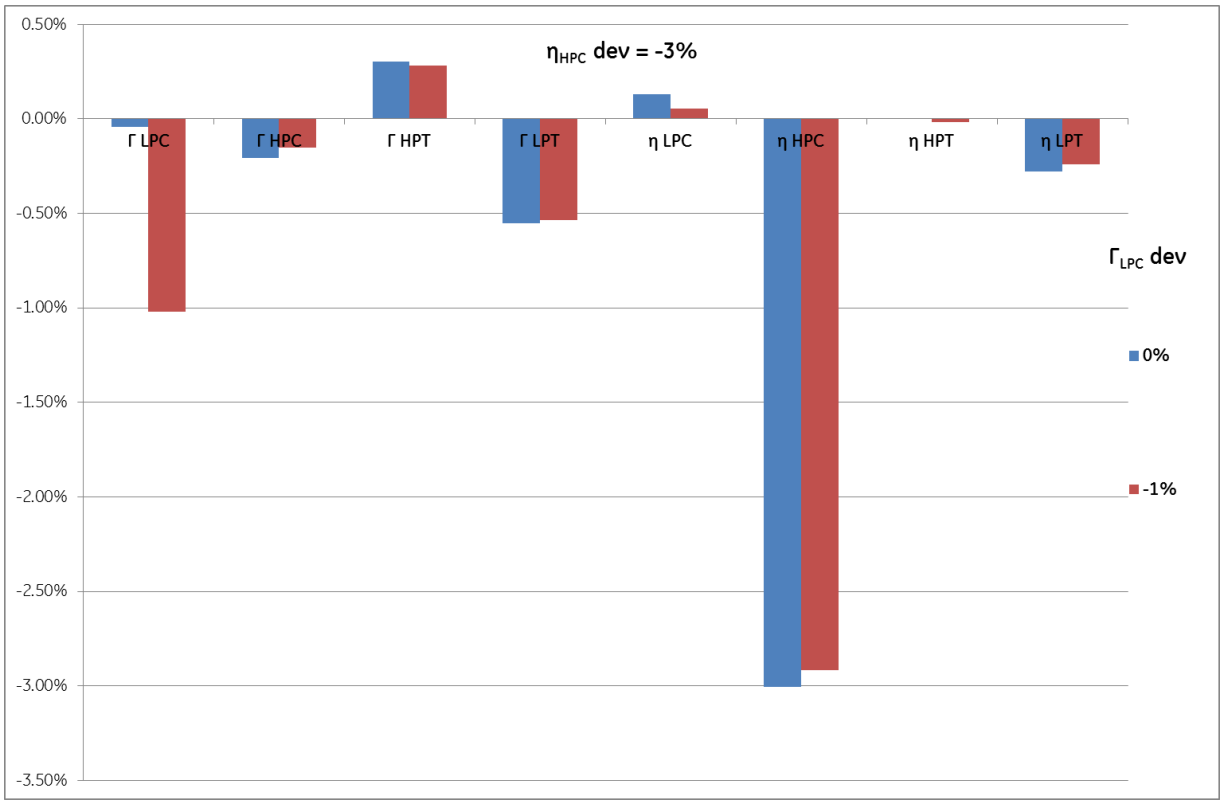

Figure B-15: ηHPC = -3% & ΓLPC = [0,-1%]

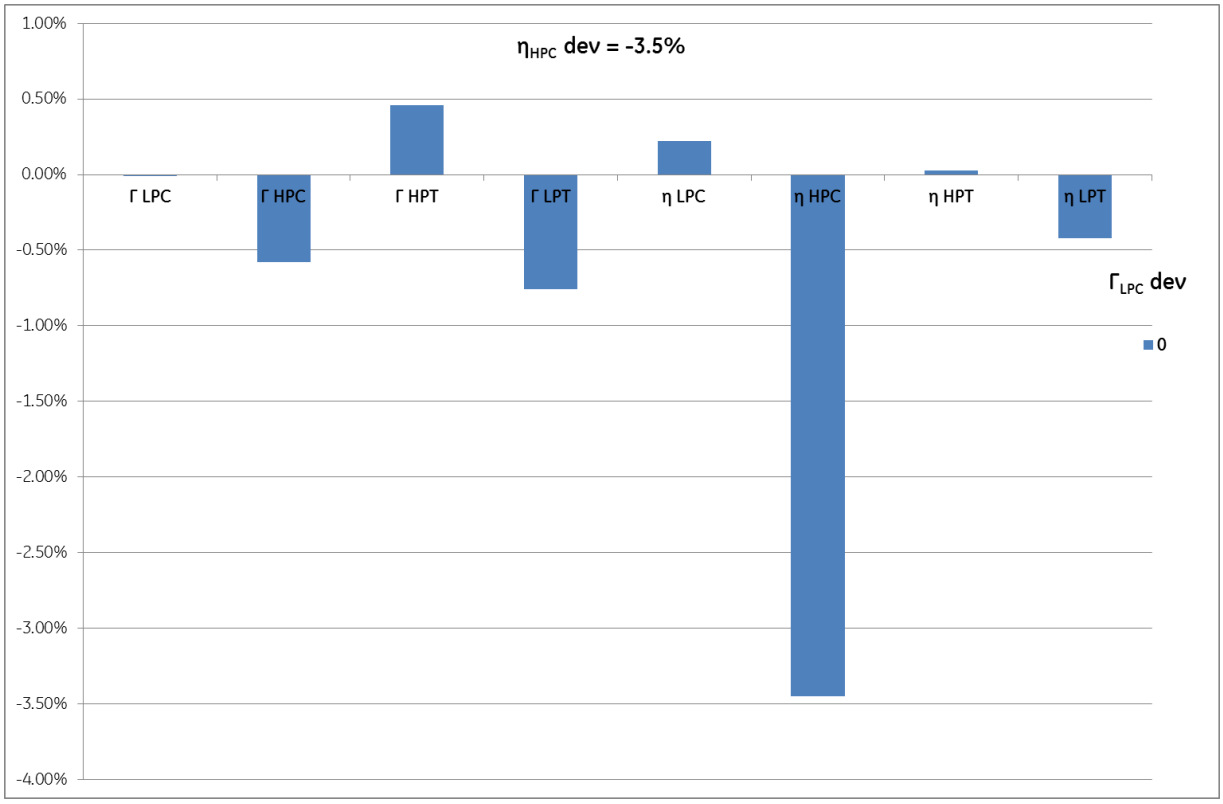

Appendix C TRAINING CASES LINEAR INTERPOLATION

C.1 Linear interpolation vs polynomial

Table C-1 (equal to Table 9-1) shows the training cases and the linear interpolation that was applied, as explained in Chapter 9.

Table C-1: ANN training cases and linear interpolation

Linear interpolation tool used was the function LINEST from Excel. Other options were tested as well, like polynomial approximation. The tests were done on parameter T8 (exhaust temperature) for the cases Γ_{LPC}= 0 and 0%>η_{HPC}>-7%.

As it can be seen from Figures A4-1 to A4-4 apparently the best fit was a 6th grade polynomial. When results were compared with a WebEngine generated [Γ_{LPC}, η_{HPC}] = [0,-7%] the situation changed completely (Table C-2). Only T8 is presented.

Table C-2: T8 approximations

T8 (ºC)	
Webegine	732.64
Linear	723.24
5th grade	723.75
6th grade	723.75

Therefore linear fit was to calculate all missing parameters. For [Γ_{LPC}, η_{HPC}] = [0,-7%] the error is calculated assuming WebEngine result as the golden rule (Table C-3).

Table C-3: Error by linear interpolation for case [ΓLPC, ηHPC] = [0,-7%]

	P25	P3	P48	XN25	MW	FF	T25	T8
Webengine	2.77	27.74	6.49	0.9164	38743428	2.245	395.45	732.64
Linearization	2.71	28.00	6.52	0.9081	39097925	2.257	394.14	730.41
Error	-0.02	0.01	0.00	-0.91%	0.91%	0.53%	-0.33%	-0.31%

Figure C-1: Linear fit

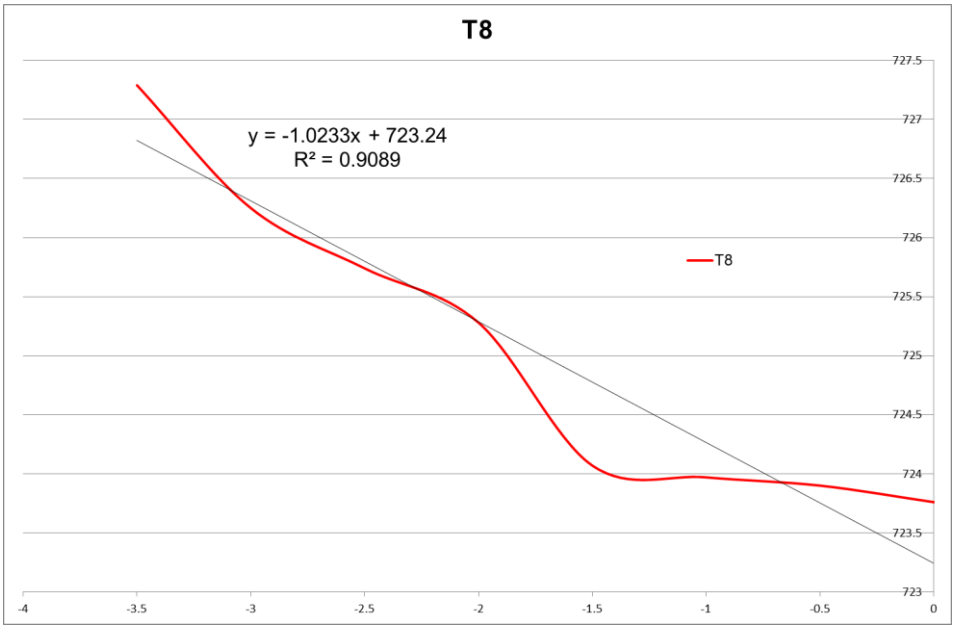

Figure C-2: Quadratic fit

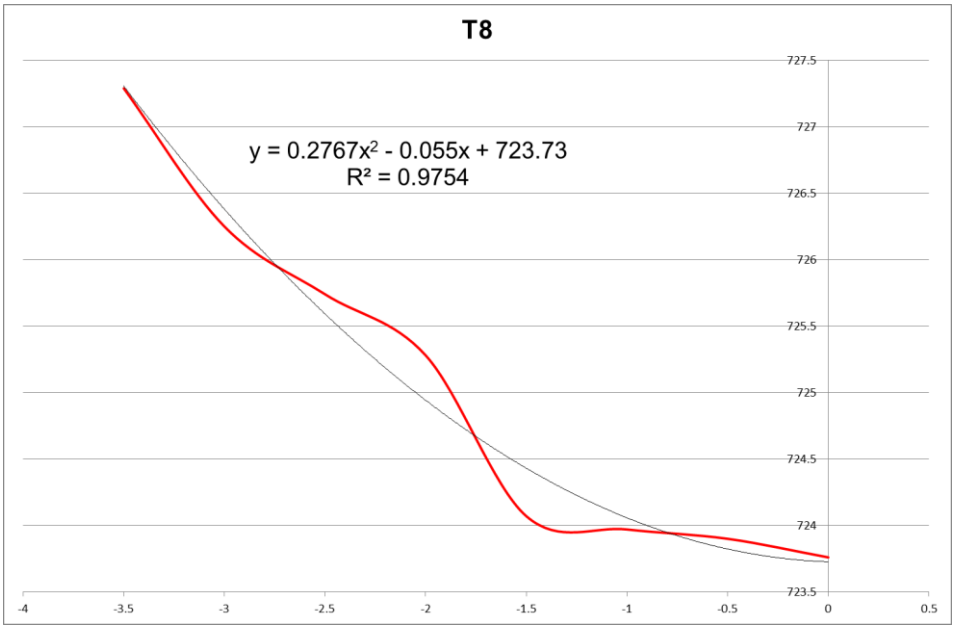

Figure C-3: Fifth grade polynomial fit

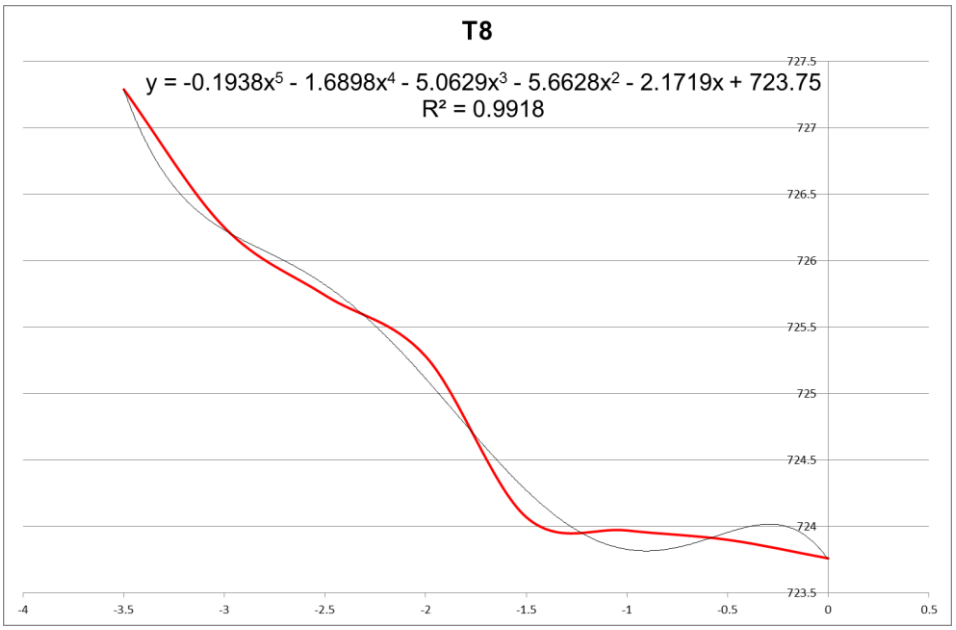

Figure C-4: Sixth grade polynomial fit

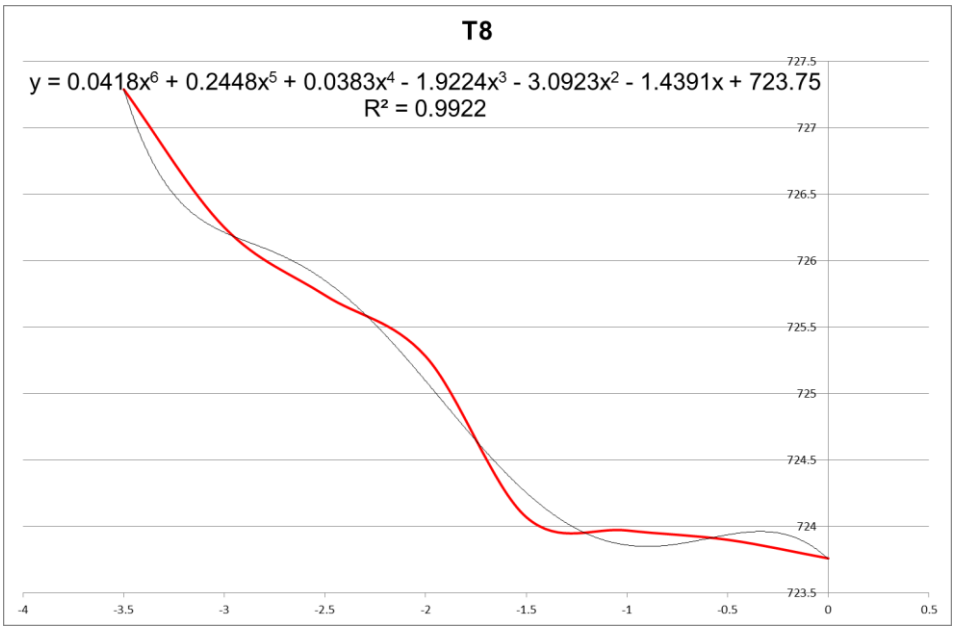

Appendix D MATLAB SCRIPT

The script used was the following

```
%   Inputvector - input data.
%   Targetvector - target data.

x = Inputvector;     %   8x345   training cases
t = Targetvector;    %   2x345   target cases
T = testcases;       %   8x8     Real test cases

trainFcn = 'trainlm';  % Levenberg-Marquardt backpropagation.
                       % Others are 'trainscg', 'trainbr', 'traingd'

% Create a Fitting Network
% Transfer functions 'tansig', 'logsig', 'purlin'
hiddenLayerSize= [30,30];
net = fitnet(hiddenLayerSize,trainFcn);
net.layers{1}.transferFcn = 'tansig';
net.layers{2}.transferFcn = 'tansig';

% Setup Division of Data for Training, Validation, Testing
net.divideParam.trainRatio = 70/100;
net.divideParam.valRatio = 15/100;
net.divideParam.testRatio = 15/100;

% Initialize weights
net=init(net);
% Train the Network
[net,tr] = train(net,x,t);
```

```
% Test the Network
y = net(x);
e = gsubtract(t,y);
performance = perform(net,t,y)

% Run the real test cases
testnet=sim(net,testcases);
save testnet3030.txt testnet -ASCII; % Save the result for each run
testnet
% View the Network
% view(net)
```

The script shown has two layers of 30 neurons each that will be changed for different configuration test. The transfer functions are Tan-sigmoid (‘tansig’) for the two hidden layers and Linear for the output layer (‘purlin’). Training algorithm in this case is Levenberg-Marquardt (*lm*). The input vectors are divided 70% for training, 15% for validation and 15% for testing, a split used all across the network tests. There is additional testing done by using some “real” data examples (reference Chapter 9).

Appendix E REAL TEST CASE RESULTS

Table E-1 shows the results of the "real" test cases errors in each one of the tested networks. The error is defined as

$$error\ (\%) = \frac{(x_{network} - x_{simulated})}{x_{simulated}} * 100$$

Where

$x_{simulated}$ is the value of degradation used to create the WebEngine test cases

$x_{network}$ is the result of each network

Table E-1: Results of "real" engine test cases error

			"Real" test cases (Γ_{LPC} / η_{HPC})									
tra. alg.	lay/neur	health p.	-1.7/-2.3	-2.4/-2.7	-1.9/-1.7	-4.5/-5.75	0/-6.5	-6/-6.75	-9.75/0	-9.75/-6.5	average	std. Dev
lm	10	Γ_{LPC}	-0.65%	-0.83%	1.20%	1.14%	-0.53%	-0.09%	-0.20%	0.02%	0.037%	0.007
		η_{HPC}	0.63%	0.50%	0.71%	0.41%	-0.11%	-0.12%	-1.48%	-0.03%		
	20	Γ_{LPC}	0.07%	-0.28%	-0.04%	0.08%	0.00%	0.03%	0.05%	0.01%	0.004%	0.001
		η_{HPC}	0.17%	-0.02%	-0.26%	-0.01%	0.06%	0.01%	0.23%	-0.01%		
	50	Γ_{LPC}	0.31%	0.08%	0.22%	-0.03%	-0.90%	-0.05%	0.01%	-0.03%	-0.022%	0.003
		η_{HPC}	-0.12%	0.33%	-0.27%	-0.02%	-0.03%	-0.01%	0.16%	0.00%		
	10_10	Γ_{LPC}	-0.64%	-0.30%	0.53%	0.35%	-0.81%	0.07%	0.03%	0.00%	-0.035%	0.003
		η_{HPC}	0.18%	0.12%	0.12%	-0.08%	-0.15%	0.04%	0.04%	-0.07%		
	20_10	Γ_{LPC}	0.26%	0.24%	0.08%	0.17%	0.25%	-0.01%	0.01%	0.02%	0.077%	0.001
		η_{HPC}	-0.08%	0.14%	0.05%	-0.03%	0.01%	0.03%	0.07%	0.03%		
	20_20	Γ_{LPC}	-0.04%	-0.02%	-0.12%	0.04%	-0.12%	-0.02%	-0.05%	0.02%	0.033%	0.002
		η_{HPC}	0.06%	0.28%	0.61%	-0.03%	-0.02%	0.04%	-0.12%	0.02%		
	50_10	Γ_{LPC}	-0.11%	-0.07%	-0.10%	-0.07%	-0.60%	0.03%	-0.03%	-0.02%	-0.073%	0.001
		η_{HPC}	-0.02%	0.01%	-0.01%	-0.03%	-0.01%	-0.02%	-0.14%	0.01%		
	50_20	Γ_{LPC}	0.19%	0.10%	-0.01%	-0.01%	0.02%	-0.87%	-0.04%	-0.01%	0.001%	0.003
		η_{HPC}	-0.18%	0.12%	-0.11%	0.00%	0.00%	0.10%	0.72%	0.01%		
	50_50	Γ_{LPC}	-0.21%	0.00%	-0.05%	0.00%	-4.02%	0.27%	0.02%	0.00%	-0.219%	0.010
		η_{HPC}	0.14%	0.11%	0.28%	0.04%	-0.17%	-0.05%	0.16%	0.00%		
scg	20	Γ_{LPC}	-0.05%	-1.70%	-0.60%	2.20%	13.26%	-2.94%	0.88%	0.13%	-2.412%	0.121
		η_{HPC}	2.23%	0.44%	-1.36%	0.10%	-2.21%	-2.51%	-46.98%	0.52%		
	50	Γ_{LPC}	5.74%	1.67%	-0.11%	1.93%	8.58%	-5.56%	1.81%	-0.33%	0.258%	0.066
		η_{HPC}	4.21%	7.49%	6.52%	-1.31%	-3.23%	-3.96%	-20.37%	1.06%		
	20_20	Γ_{LPC}	3.05%	1.93%	-2.91%	2.44%	1.31%	-4.10%	1.44%	-0.24%	-0.746%	0.052
		η_{HPC}	2.54%	3.86%	-0.97%	1.39%	-0.77%	-2.16%	-19.16%	0.43%		
	50_20	Γ_{LPC}	-3.62%	-0.25%	-6.20%	0.24%	-4.56%	0.26%	1.95%	-0.20%	-2.539%	0.071
		η_{HPC}	3.80%	5.16%	-10.23%	1.65%	-0.88%	-1.18%	-25.98%	-0.59%		

Table E-2 has the output values of the network for the "real" test cases.

Table E-2: "Real" test cases network output values

			"Real" test cases (Γ_{LPC} / η_{HPC})							
tra. alg.	lay/neur	health p.	-1.7/-2.3	-2.4/-2.7	-1.9/-1.7	-4.5/-5.75	0/-6.5	-6/-6.75	-9.75/0	-9.75/-6.5
lm	10	Γ_{LPC}	-1.69	-2.38	-1.92	-4.55	-0.01	-5.99	-9.73	-9.75
		η_{HPC}	-2.31	-2.71	-1.71	-5.77	-6.49	-6.74	-0.01	-6.50
	20	Γ_{LPC}	-1.70	-2.39	-1.90	-4.50	0.00	-6.00	-9.75	-9.75
		η_{HPC}	-2.30	-2.70	-1.70	-5.75	-6.50	-6.75	0.00	-6.50
	50	Γ_{LPC}	-1.71	-2.40	-1.90	-4.50	-0.01	-6.00	-9.75	-9.75
		η_{HPC}	-2.30	-2.71	-1.70	-5.75	-6.50	-6.75	0.00	-6.50
	10_10	Γ_{LPC}	-1.69	-2.39	-1.91	-4.52	-0.01	-6.00	-9.75	-9.75
		η_{HPC}	-2.30	-2.70	-1.70	-5.75	-6.49	-6.75	0.00	-6.50
	20_10	Γ_{LPC}	-1.70	-2.41	-1.90	-4.51	0.00	-6.00	-9.75	-9.75
		η_{HPC}	-2.30	-2.70	-1.70	-5.75	-6.50	-6.75	0.00	-6.50
	20_20	Γ_{LPC}	-1.70	-2.40	-1.90	-4.50	0.00	-6.00	-9.74	-9.75
		η_{HPC}	-2.30	-2.71	-1.71	-5.75	-6.50	-6.75	0.00	-6.50
	50_10	Γ_{LPC}	-1.70	-2.40	-1.90	-4.50	-0.01	-6.00	-9.75	-9.75
		η_{HPC}	-2.30	-2.70	-1.70	-5.75	-6.50	-6.75	0.00	-6.50
	50_20	Γ_{LPC}	-1.70	-2.40	-1.90	-4.50	0.00	-5.95	-9.75	-9.75
		η_{HPC}	-2.30	-2.70	-1.70	-5.75	-6.50	-6.76	0.01	-6.50
	50_50	Γ_{LPC}	-1.70	-2.40	-1.90	-4.50	-0.04	-6.02	-9.75	-9.75
		η_{HPC}	-2.30	-2.70	-1.70	-5.75	-6.49	-6.75	0.00	-6.50
scg	20	Γ_{LPC}	-1.70	-2.36	-1.89	-4.60	0.13	-5.82	-9.84	-9.76
		η_{HPC}	-2.35	-2.71	-1.68	-5.76	-6.36	-6.58	-0.47	-6.53
	50	Γ_{LPC}	-1.80	-2.44	-1.90	-4.59	0.09	-5.67	-9.93	-9.72
		η_{HPC}	-2.40	-2.90	-1.81	-5.67	-6.29	-6.48	-0.20	-6.57
	20_20	Γ_{LPC}	-1.75	-2.45	-1.84	-4.61	0.01	-5.75	-9.89	-9.73
		η_{HPC}	-2.36	-2.80	-1.68	-5.83	-6.45	-6.60	-0.19	-6.53
	50_20	Γ_{LPC}	-1.64	-2.39	-1.78	-4.51	-0.05	-6.02	-9.94	-9.73
		η_{HPC}	-2.39	-2.84	-1.53	-5.84	-6.44	-6.67	-0.26	-6.46

Some highlights

- Results for network trained with *lm* algorithm were in general very good, with low error values.
- Error values tended to be bigger for those simulated values were the linear interpolation of the input vector had not been used.
- The absolute values in Table E-2 are very good and enough for a diagnostic tool
- Networks trained with *scg* algorithm had worse results, especially on low values as in case [Γ_{LPC}, η_{HPC}] = [-9.75, 0] were the relative error evaluating η_{HPC} was almost 47% and absolute value difference was -0.47% vs -0%

test case. Because of the low value of degradation, it implies it would not be a bad situation, but the performance of other network configurations in similar cases is much better.